



<https://theses.gla.ac.uk/>

Theses Digitisation:

<https://www.gla.ac.uk/myglasgow/research/enlighten/theses/digitisation/>

This is a digitised version of the original print thesis.

Copyright and moral rights for this work are retained by the author

A copy can be downloaded for personal non-commercial research or study, without prior permission or charge

This work cannot be reproduced or quoted extensively from without first obtaining permission in writing from the author

The content must not be changed in any way or sold commercially in any format or medium without the formal permission of the author

When referring to this work, full bibliographic details including the author, title, awarding institution and date of the thesis must be given

Enlighten: Theses

<https://theses.gla.ac.uk/>  
[research-enlighten@glasgow.ac.uk](mailto:research-enlighten@glasgow.ac.uk)

# **The Role of Dystroglycan in Cell Adhesion**

Yun-Ju Chen

Ph.D



University of Glasgow

Division of Biochemistry and Molecular Biology

Faculty of Biomedical and Life Science

December 2003

ProQuest Number: 10391035

All rights reserved

INFORMATION TO ALL USERS

The quality of this reproduction is dependent upon the quality of the copy submitted.

In the unlikely event that the author did not send a complete manuscript and there are missing pages, these will be noted. Also, if material had to be removed, a note will indicate the deletion.



ProQuest 10391035

Published by ProQuest LLC (2017). Copyright of the Dissertation is held by the Author.

All rights reserved.

This work is protected against unauthorized copying under Title 17, United States Code  
Microform Edition © ProQuest LLC.

ProQuest LLC.  
789 East Eisenhower Parkway  
P.O. Box 1346  
Ann Arbor, MI 48106 – 1346



GLASGOW  
UNIVERSITY  
LIBRARY:

13197

COPY 2

## Abstract

Dystroglycan is a heterodimeric transmembrane glycoprotein protein of  $\alpha$  and  $\beta$  subunits that links the extracellular matrix to the cytoskeleton. Recent data tend to suggest that the role of dystroglycan in non-muscle cells is for cell adhesion, and cytoskeleton reorganisation signalling. To study the relationship between dystroglycan signalling and ERK signalling in focal adhesions, an YFP-ERK construct was expressed in REF52 cells. YFP-ERK was expressed with ERK activity and formed adhesion-like structures in the REF52 cells, however, no ERK activity was detected in the adhesion-like structures in the REF52 cells. To determine the function of dystroglycan for adhesion or cytoskeleton organisation in non-muscle cells, a GFP-tagged full-length dystroglycan ( $\alpha\beta$ DG-GFP) or its deletion mutants was expressed in REF52 cells. Expression of  $\alpha\beta$ DG-GFP markedly altered cell phenotype on a laminin or fibronectin substrate, resulting in the induction of actin-rich filopodia. The  $\beta$ -dystroglycan cytoplasmic domain is determined as the mediator for the dystroglycan-dependent filopodia formation mediated partly by integrin signalling. The dystroglycan deletion mutants lacking  $\alpha$ -dystroglycan failed to target to the plasma membrane. Expression of an alkaline phosphate-tagged  $\beta$ -dystroglycan cytoplasmic domain construct (AP-c $\beta$ ), which targeted the  $\beta$ -dystroglycan cytoplasmic domain to the membrane without the  $\alpha$ -dystroglycan, was sufficient to induce the filopodia phenotype, indicating that with the proper membrane localisation,  $\beta$ -dystroglycan can regulate filopodia formation independently of  $\alpha$ -dystroglycan. However,  $\alpha$ -dystroglycan might be necessary for  $\beta$ -dystroglycan to target to the plasma membrane. These distinct morphologies strongly implied that  $\beta$ -dystroglycan mediates Cdc42 regulated cytoskeleton reorganisation. By cotransfecting dominant negative Cdc42 (Cdc42N17) or constitutively activated Cdc42 (V12Cdc42) constructs with  $\alpha\beta$ DG-GFP or the mutants, Cdc42 was determined to be a mediator for dystroglycan-dependent filopodia formation. Therefore a signalling cycle of dystroglycan-Cdc42-PAK-czrin-dystroglycan is identified. With this signalling cycle, dystroglycan plays a role in inducing actin filopodia formation and, at the same time, might also inhibit focal adhesion and stress fibre formation.

<i>Table of Contents</i>	<i>ii</i>
<i>Table of Figures</i>	<i>viii</i>
<i>Acknowledgement</i>	<i>xi</i>
<i>Abbreviations</i>	<i>xii</i>

## Table of Contents

<b>Chapter1</b>	
<b><u>Introduction</u></b>	<b>1</b>
<b>1.1 Background</b>	<b>2</b>
<b>1.2 Structure of dystroglycan</b>	<b>5</b>
1.2.1 $\alpha$ -Dystroglycan	5
1.2.2 $\beta$ -Dystroglycan	8
<b>1.3 Functions of dystroglycan in muscle and non-muscle cells</b>	<b>12</b>
1.3.1 Function of dystroglycan in muscle cells	12
1.3.1.1 <i>Role of dystroglycan in muscular dystrophies</i>	12
1.3.1.2 <i>Role of dystroglycan in neuromuscular junction</i>	15
1.3.2 Functions of dystroglycan in nonmuscle cells	16
1.3.2.1 <i>Role of dystroglycan in Nervous system</i>	16
1.3.2.2 <i>Role of dystroglycan in morphogenesis</i>	17
1.3.2.3 <i>Early embryonic tissues</i>	18
1.3.2.4 <i>Dystroglycan and adhesion</i>	18
<b>1.4 Signalling role of dystroglycan</b>	<b>19</b>
<b>1.5 Focal adhesion signalling</b>	<b>22</b>
1.5.1 Focal adhesions	22
1.5.2 Integrin mediated focal adhesion signalling pathways	24
1.5.2.1 <i>The FAK pathway</i>	24
1.5.2.2 <i>The Fyn/Shc pathway</i>	26
1.5.3 Focal adhesions and cytoskeleton signalling	27
1.5.3.1 <i>Activation of Rho GTPases and Rho Kinase</i>	27
1.5.3.2 <i>Adhesion dependent Rho activation</i>	29
<b><u>1.6 Aims of the study</u></b>	<b>33</b>

## Chapter 2

### Methods and materials

---

36

<b>2.1 Materials</b>	<b>37</b>
2.1.1 Chemicals, reagents and Kits	37
2.1.2 Media and general buffers	37
2.1.3 Plasmid and clones	37
2.1.4 Cell lines	37
2.1.5 Antisera	37
2.1.6 Oligos	37
<b>2.2 Molecular biology methods</b>	<b>37</b>
2.2.1 Bacterial strain	37
2.2.2 Growth of bacteria	38
2.2.3 Transformation of DH5a	38
2.2.3.1 <i>preparation of calcium competent cells</i>	38
2.2.3.2 <i>Transformation of calcium competent cells</i>	38
2.2.4 Preparation of plasmid DNA	39
2.2.4.1 <i>Small-scale preparation of plasmid DNA by spin column</i>	39
2.2.4.2 <i>Large-scale preparation of plasmid DNA for transfection</i>	39
2.2.5 Spectrophotometric quantification of DNA	39
2.2.6 Restriction digestion of DNA	39
2.2.7 Agarose gel electrophoresis	40
<b>2.3 Cell culture</b>	<b>40</b>
2.3.1 Growth of cell lines	40
2.3.2 Transfection and cotransfection	40
2.3.3 Harvesting cells in RIPA buffer	41
2.3.4 EGF treatment	41
2.3.5 UO126 treatment	41
<b>2.4 Protein Biochemistry methods</b>	<b>41</b>
2.4.1 Quantification of protein concentration	41
2.4.2 SDS polyacrylamide gel electrophoresis (SDS-PAGE)	42
2.4.3 Immunoprecipitation	42
2.4.4 Western blotting	43
2.4.5 Antibody binding and detection (Alkaline phosphatase development)	43



<b>2.5 Protein immunofluorescence assay</b>	<b>43</b>
2.5.1 Immunofluorescent staining of transfected cells	43
2.5.2 Actin morphology	44
2.5.3 Development of the expression of AP-dystroglycan construct	44
2.5.4 Fluorescent microscopy	44
<b>2.6 Construction of dystroglycan mutants</b>	<b>45</b>
2.6.1 PCR mutagenesis	45
2.6.2 Purification of PCR products	46
2.6.3 Ligation of DNA	46
2.6.4 Colony screening by PCR	46
<b>2.7 Cell Adhesion assay</b>	<b>47</b>
2.7.1 Coating of coverslips	47
2.7.2 Adhesion time course of transfected REF52	47
2.7.3 Substrate dependent assay of dystroglycan transfected REF52	47
<b>2.8 ERK kinase activity assay</b>	<b>48</b>
2.8.1 Preparation of ERK kinase assay sample	48
2.8.2 Myelin Basic Protein (MBP) ERK kinase activity assay	48

---

## **Chapter 3**

### **Expression of YFP –ERK construct in REF52 cells** **50**

---

<b>3.1 Introduction</b>	<b>51</b>
3.1.1 ERK cascade	51
3.1.2 Aim of the experiment	52
<b>3.2 Result</b>	<b>55</b>
3.2.1 Expression of YFP-ERK in REF52	55
3.2.2 Western blotting assay of YFP-ERK activity	55
3.2.3 Effects of UO126 on YFP-ERK in REF52 cells	58
3.2.4 MBP kinase activity assay of YFP-ERK	58
3.2.5 Adhesion time course	60
3.2.6 Localisation of ERK at focal adhesion sites in REF 52 cells	63
3.2.7 Activity of ERK at focal adhesion sites in REF52	63

<b>3.3 Discussion</b>	<b>67</b>
3.3.1 Regulation of expression and activation of YFP-ERK	67
3.3.2 Translocation of YFP-ERK	68
3.3.3 Localisation of YFP-ERK at focal adhesion sites	69

---

## **Chapter4**

### **Expression of GFP-tagged dystroglycan and dystroglycan function domain deletion mutants**

**71**

<b>4.1 Introduction</b>	<b>72</b>
<b>4.2 Result</b>	<b>73</b>
4.2.1 Construction of GFP-tagged dystroglycan and functional domain deletion mutants	73
4.2.2 Examination of GFP-tagged dystroglycan construct ( $\alpha\beta$ DG-GFP) in REF52 cells	73
4.2.2.1 <i>Expression of <math>\alpha\beta</math>DG-GFP in REF52 cells</i>	73
4.2.2.2 <i>Filopodia formation of <math>\alpha\beta</math>DG-GFP transfected REF52 cells on laminin</i>	76
4.2.2.3 <i>Examination of utrophin in <math>\alpha\beta</math>DG-GFP transfected REF52 cells</i>	78
4.2.3 Expression of $c\beta$ deletion mutant construct ( $\alpha\beta\Delta c\beta$ -GFP) in REF52 cells	81
4.2.4 Substrate effects on dystroglycan dependent filopodia formation	83
4.2.5 Expression of $c\beta$ dystroglycan construct ( $c\beta$ DG-GFP) in REF52 cells	86
4.2.6 Expression of $\beta$ dystroglycan ( $\beta$ DG-GFP) construct in REF52 cells	88
4.2.7 Expression of $\alpha$ -dystroglycan deletion mutant construct ( $\alpha\beta\Delta\alpha$ DG-GFP) in REF52 cells	91
4.2.8 Expression of $e\beta$ dystroglycan deletion mutant ( $\alpha\beta\Delta e\beta$ -GFP) in REF52 cells	94
4.2.9 Expression of alkaline phosphatase conjugated $\beta$ -dystroglycan (AP- $\beta$ DG) construct in REF52 cells	97
<b>4.3 Discussion</b>	<b>101</b>
4.3.1 Spatial importance for $\beta$ -dystroglycan cytoplasmic domain	

in induction of a formation	101
4.3.2 Role of $\beta$ -dystroglycan C-terminal tail PPPY motif in dystroglycan dependent filopodia formation	103
4.3.3 Dystroglycan functional domains in its post-translational processing	105
4.3.3.1 <i>Glycosylation of dystroglycan in biosynthesis</i>	105
4.3.3.2 <i>Hypothesis for dystroglycan trafficking</i>	108

---

## Chapter 5

### **Dystroglycan dependent activation of Rho GTPases and the organisation of the actin cytoskeleton**

**113**

<b>5.1 Introduction</b>	<b>114</b>
5.1.1 Cdc42 dependent actin dynamics of the cell cortex	114
5.1.2 Model of Cdc42 dependent filopodia formation	115
5.1.3 Cdc42 activity assay in $\alpha\beta$ DG-GFP transfected cells	118
<b>5.2 Result</b>	<b>120</b>
5.2.1 Morphological similarity of V12Cdc42 transfected cells with $\alpha\beta$ DG-GFP transfected cells	120
5.2.2 Effects of coexpression of dominant negative Rho GTPases constructs on $\alpha\beta$ DG-GFP transfected REF52 cells	120
5.2.3 Coexpression of constitutively activated Cdc42 construct and $\alpha\beta$ DGDc $\beta$ -GFP in REF52 cells	124
5.2.4 Coexpression of constitutively activated Cdc42 construct and $\alpha\beta$ DG-GFP in REF52 cells	127
5.2.5 Focal adhesions in $\alpha\beta$ DG-GFP transfected cells	127
<b>5.3 Discussion</b>	<b>130</b>
5.3.1 Cdc42 mediates dystroglycan in dependent filopodia formation	130
5.3.2 Mediators between dystroglycan and Cdc42	131
5.3.3 Regulation of dystroglycan dependent filopodia formation through the mediators	135
5.3.3.1 <i>Role of PAK</i>	135
5.3.3.2 <i>Role of ezrin</i>	137
5.3.4 Role of dystroglycan in adhesion and filopodia formation	139

---

## **Chapter 6**

### **Summary**

**144**

---

### **Appendices**

**148**

---

Appendix I	Chemicals, reagents and kits	149
Appendix II	Media and general buffers	151
Appendix III	Plasmids and clones	153
Appendix IV	Cell lines	155
Appendix V	Antibodies	156
Appendix VI	PCR primers	158
Appendix VII	PCR reaction conditions	159
Appendix VIII	Plasmid transfection conditions	160

---

### **References**

**161**

---

## Table of figures and tables

Figure 1.1 Schematic representation of the arrangement of dystrophin Glycoprotein complex (DGC) of muscle cells and dystroglycan of non-muscle cells	4
Figure 1.2 Processing of the dystroglycan propeptide	6
Figure 1.3 A representation of $\alpha$ - and $\beta$ -dystroglycan and binding partners at the cell surface	9
Figure 1.4 Structure of the dystrophin- $\beta$ -dystroglycan complex	11
Figure 1.5 Direct cell growth signaling by integrins-mediated focal adhesions	25
Figure 1.6 Activity cycle of Rho GTPases and cytoskeleton morphology induced by active Rac, Rho or Cdc42	28
Figure 1.7 Mechanisms for Rho-induced stress-fibre formation through the activation of Rho kinase	30
Figure 1.8 Multiple signaling pathways control focal adhesion assembly by coordinately regulating the activation of the small GTP-binding protein RhoA	32
Figure 3.1 RTK induced ERK cascade in mammalian cells	53
Figure 3.2 Overexpression of YFP-ERK construct in REF52 cells	56
Figure 3.3 Expression and inhibition YFP-ERK in REF52 cells	57
Figure 3.4 UO126 treatment of YFP-MAPK overexpressed REF52 cells	59
Figure 3.5 MBP-ERK activity assay in YFP-ERK transfected REF52 cells	61
Figure 3.6 Adhesion timecourse of YFP-ERK transfected REF52 cells	62
Figure 3.7 Colocalisation of YFP-ERK and talin in the adhesion sites in REF52 cells	64
Figure 3.8 Phospho-specific ERK antiserum staining of focal adhesions in YFP-ERK transfected REF52 cells	66
Figure 4.1 Construction of dystroglycan-GFP and dystroglycan functional domain deletion mutants	74
Figure 4.2 Expression of DG-GFP construct in REF52 cells	75
Figure 4.3 Expression of $\alpha\beta$ DG-GFP in REF52 on laminin	77
Figure 4.4 Quantification of the filopodia formation in $\alpha\beta$ DG-GFP transfected cells on laminin	79

Figure 4.5 Expression of utrophin in dystroglycan overexpressed REF52 cells	80
Figure 4.6 Expression of dystroglycan GFP in utrophin null cells	82
Figure 4.7 Expression of $\beta$ dystroglycan cytoplasmic domain deletion mutant, $\alpha\beta\Delta c\beta$ -GFP	84
Figure 4.8 Formation of filopodia in $\alpha\beta$ DG-GFP transfected cells on extracellular substrates	85
Figure 4.9 Substrate effects on dystroglycan mutants transfected cells	87
Figure 4.10 Expression of dystroglycan cytoplasmic domain $c\beta$ -GFP	89
Figure 4.11 Expression of $\beta$ dystroglycan, $\beta$ DG-GFP, in REF52 cells	90
Figure 4.12 Expression of dystroglycan $\alpha$ subunit deletion mutant $\Delta\alpha$ -GFP	92
Figure 4.13 Expression of $\beta$ -dystroglycan extracellular domain deletion mutant, $\Delta e\beta$ DG-GFP, in REF52 cells	95
Figure 4.14 Expression of $\alpha$ DG-GFP in REF 52 cells	96
Figure 4.15 Expression of alkaline phosphatase tagged $\beta$ dystroglycan construct (AP- $\beta$ DG) in REF52 cells	98
Figure 4.16 Model of posttranslational modification route of dystroglycan	111
Figure 5.1 Model of Cdc42-dependent lamellipodia formation and filopodia organisation	116
Figure 5.2 Actin phenotypes of constitutively Rho GTPases constructs transfected cells and $\alpha\beta$ DG-GFP transfected cell	121
Figure 5.3 Coexpressing of $\alpha\beta$ DG-GFP with dominant negative Rho GTPase constructs in REF52 cells	122
Figure 5.4 Quantification of the effect of dominant negative Rho GTPase constructs coexpressing with $\alpha\beta$ DG-GFP with in REF52 cells	123
Figure 5.5 Coexpression of constitutively activated Cdc42 construct with dystroglycan mutants	125
Figure 5.6 Quantification of the coexpression of constitutively activated Cdc42 construct with dystroglycan mutants	126
Figure 5.7 Immunostaining of talin in $\alpha\beta$ DG-GFP transfected REF52 cells	129
Figure 5.8 The sequence of dystroglycan juxtamembrane region and ezrin association sequence in the membrane protein	132
Figure 5.9 Signalling of dystroglycan induced formation of membrane protrusions	136
Figure 5.10 Hypothesis of the regulation of dystroglycan-dependent filopodia formation	140
Table 1.1 Dystroglycan and muscular dystrophies	14

Table 1.2	Evidence of ERK-mediated non-mitogenetic regulation	34
Table 4.1	Localisation and filopodia formation of GFP-tagged dystroglycan and dystroglycan mutants transfected REF 52	100

## Acknowledgements

My thanks go first to Dr S. J. Winder for giving me the opportunity to this project, and supervising me for these years. His support throughout makes my research life far away from home being warmer.

Secondly, I would like to thank all the members of the lab, past and present, for practical advice, helping hands, and for tea & birthday cakes.

Finally, I would like to say thanks to my good friends, Xenia and Marios, for listening to my endless complaint during the writing up period. And, of course, thanks to my parents and three sisters for their support and encouragement.



## Abbreviations

AChR	Acetylcholine receptor
AP	Alkaline phosphate
APS	Ammonium persulphate
BCIP	5-Bromo-4-Chloro-3'-Indolyphosphate p-Toluidine Salt
BSA	Bovine serum albumin
CAPS	3-(Cyclohexylamino)-1-propansulfonsyre
CMD	Congenital muscular dystrophy
CNS	Central nervous system
DEP2	Dystrophin-related protein 2
DG	Dystroglycan
DGC	Dystroglycan-glycoprotein complex
DMD	Duchenne muscular dystrophy
DMEM	Dulbecco's Modification of Eagle's Medium
ECM	Extracellular matrix
EDTA	Ethylenediamine Tetra-Acetic Acid
EGF	Epidermal Growth Factor
EGTA	Ethylene Glycol-bis Tetra-Acetic Acid
ERK	Extracellular regulated kinase
ERM	Ezrin-redixin- moesin
FBS	Fetal bovine serum
FCMD	Fukuyama congenital muscular dystrophy
FKRP	Fukutin-related protein
FN	Fibronectin
GAP	GTP-activating proteins
GEF	Guanosine exchange factors
GFP	Green fluorescent protien
JNK	Jun N-terminal kinase
KSR-1	Kinase suppressor of Ras
LG domain	Laminin $\alpha$ G domain

LGMD	Limb-Girdle Muscular Dystrophy
LN	Laminin
LPA	Lysophosphatidic acid
MAPK	Mitogen-activated protein kinase
MBP	Myelin basic protein
MEB	Muscle-eye-brain disease
MLC	Myosin light chain
MLCK	Myosin light chain kinase
MLCP	Myosin light chain phosphatase
MP-1	MEK Partner-1
MuSK	Muscle-specific kinase
NBT	Nitroblue tetrazolium chloride
NMJ	Nuromuscular junction
NOS	Nitric oxide synthase
PAGE	Polyacrylamide gel electrophoresis
PAK	p21 activated kinase
PBS	Phosphate-buffered saline
PCR	Polymerase chain reaction
PDGF	Platelet-Derived Growth Factor
PIX	PAK interacting exchange factor
PKC	Protein kinase C
PLL	Poly-L-lysine
PNS	Peripheral nervous system
RhoGDI	Rho guanine nucleotide disassociation protein
RIPA buffer	Radio immunoprecipitation buffer
ROK	Rho kinase
RTK	Receptor tyrosine kinase
SDS	Sodium dodecyl sulfate
SOS	Son of sevenless
TEMED	Tetramethylethylenediamine
WASP	Wiscott-Aldrich syndrome protein

WWS

Walker-Warburg Syndrome

YFP

Yellow fluorescent protein

**Chapter 1**  
**Introduction**

## 1.1 Background

Dystroglycan is a transmembrane heterodimer complex of  $\alpha$  and  $\beta$  subunits that links the extracellular matrix to the cytoskeleton and was originally isolated from skeletal muscle as a component of the dystrophin-glycoprotein complex (DGC) (Ibraghimov-Beskrovnaya, *et al.*, 1992). DGC has been determined to be disrupted or missing as a cause of Duchenne muscular dystrophy (DMD) (Arahata *et al.*, 1988). The DGC in skeletal muscle is expressed throughout the sarcolemma. The membrane presented DGC has been shown to interact with the extracellular matrix (ECM) and associate with dystrophin, which directly associates with the actin cytoskeleton. In addition to dystroglycan, the DGC comprises sarcoglycans, sarcospan, syntrophins, caveolin, and dystrobrevin. Thus, by interacting with ECM proteins and dystrophin, the DGC forms a physical linkage between ECM and cytoskeleton (Ervasti and Campbell, 1991).

Dystroglycan is central to the DGC and has been shown to directly interact with ECM proteins and dystrophin. In muscle cells, dystroglycan binds to the extracellular proteins laminin1 and laminin2 and anchors to dystrophin, which associates with actin in the cytoskeleton, forming a physical link between the cytoskeleton and extracellular matrix of the membrane (Fig 1.1, A) (Ervasti and Campbell, 1991; Ervasti and Campbell, 1993). The dramatic reduction of dystroglycan in patients affected by DMD and in dystrophin deficient *mdx* mice (Siciński *et al.*, 1989) supports the hypothesis that the dystrophin-dystroglycan complex may play a structural role in maintaining the stability of the sarcolemmal membrane (Ervasti, *et al.*, 1990; Menke and Jockusch, 1991; Ervasti and Campbell, 1993).

Beyond muscle cells, dystroglycan has been shown to be expressed in many non-muscle tissues and cell types, indicating that functions of dystroglycan are not restricted to muscle tissues (Fig1.1 B). However, instead of full-length dystrophin, alternative products from the dystrophin locus containing the dystroglycan interaction domain are found to be expressed in non-muscle cells and associate with dystroglycan (James *et al.*, 1996). These include products of the same gene by using alternative promoters and

related proteins encoded by different genes (reviewed in Sadoulate-Puccio and Kunkel, 1996). Utrophin is the most closely related to dystrophin, and associates with a complex similar to that in DGC in most of the non-muscle cells (James, *et al.*, 1996), and also at neuromuscular junctions (NMJ) in muscle (Mastumura *et al.*, 1992). Loss-of-function studies have clearly shown that dystroglycan is required for branching epithelial morphogenesis (Durbcej *et al.*, 1995), neuronal development (Tian *et al.*, 1996; Mastumura *et al.*, 1997), embryonic basement membrane (Reichert's membrane) formation (Williamson *et al.*, 1997) and neuromuscular junction formation (Gee *et al.*, 1994). Interestingly, these cellular or developmental events are all adhesion-mediated. This suggests that in non-muscle tissues, dystroglycan performs a function in receiving adhesion-mediated signals, and regulating cell proliferation and survival signalling.

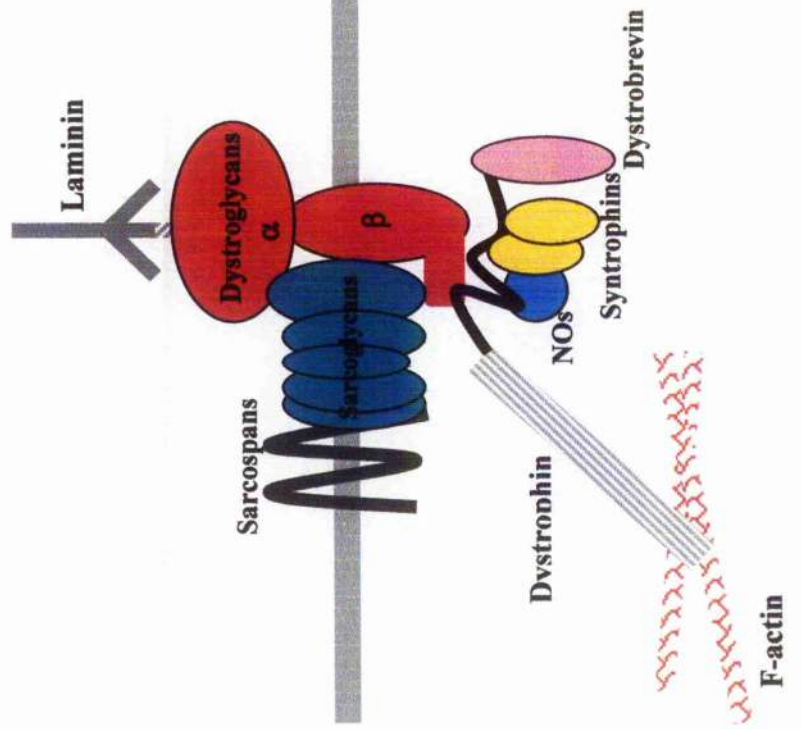
Dystroglycan has been shown to colocalise with focal adhesion structural proteins, indicating dystroglycan might be involved in the assembly of focal adhesions (Belkin and Smalheiser, 1996). The transmembrane portion of dystroglycan has been shown to associate with dystrophin homologues linking to the actin cytoskeleton, and has been shown to associate with the SH3 domain of the Grb2 adaptor protein (Jung *et al.*, 1995). This implies that both actin cytoskeleton organisation and activation of Grb2-mediated signalling might be in response to the expression of dystroglycan. Additionally, it has been shown that a tyrosine residue in the PPPY motif in the C-terminal tail of  $\beta$ -dystroglycan is phosphorylated in an adhesion-dependent manner. This tyrosine phosphorylation in the PPPY motif can regulate the binding affinity of dystroglycan to dystrophin/utrophin (James *et al.*, 2000) or the recruitment of some SH2 domain containing proteins, including Src, Fyn, Csk, Nck and SCH (Sotgia *et al.*, 2001), which are involved in integrin dependent focal adhesion signalling. Thus, dystroglycan seems to be a transmembrane laminin receptor that plays a role in regulating focal adhesion signalling and cytoskeleton reorganisation. The adhesion role of  $\alpha$ -dystroglycan binding to the ligands in non-muscle cells has been described (reviewed in Durbcej *et al.*, 1995) whereas the signalling role of  $\beta$ -dystroglycan has remained unclear. This study is to investigate the function of dystroglycan, especially  $\beta$ -dystroglycan, in mediating adhesion signalling and regulating actin cytoskeleton organisation in non-muscle cells.

**Figure 1.1 Schematic representation of the arrangement of dystrophin glycoprotein complex (DGC) of muscle cells and dystroglycan of non-muscle cells**

In skeletal muscle (A), the dystrophin-glycoprotein complex (DGC), in addition to dystrophin, contains the dystroglycans  $\alpha$  and  $\beta$ , the sarcoglycans, sarcospan, syntrophin and dystrobrevin. Neuronal NO synthase (NOs) is associated with syntrophin. Dystrophin in the DGC associates with transmembrane dystroglycan and F-actin cytoskeleton via its C-terminal and its N-terminal, respectively. Dystroglycan, which interacts with extracellular matrix laminin and agrin (not shown), and associates with dystrophin, is considered crucial in maintaining the stability of muscle cells. Dystroglycan is expressed in non-muscle cells as well. In non-muscle cells (B), dystroglycan interacts with laminin and associates with utrophin or other dystrophin isoforms, completing the linkage between extracellular matrix and actin cytoskeleton.

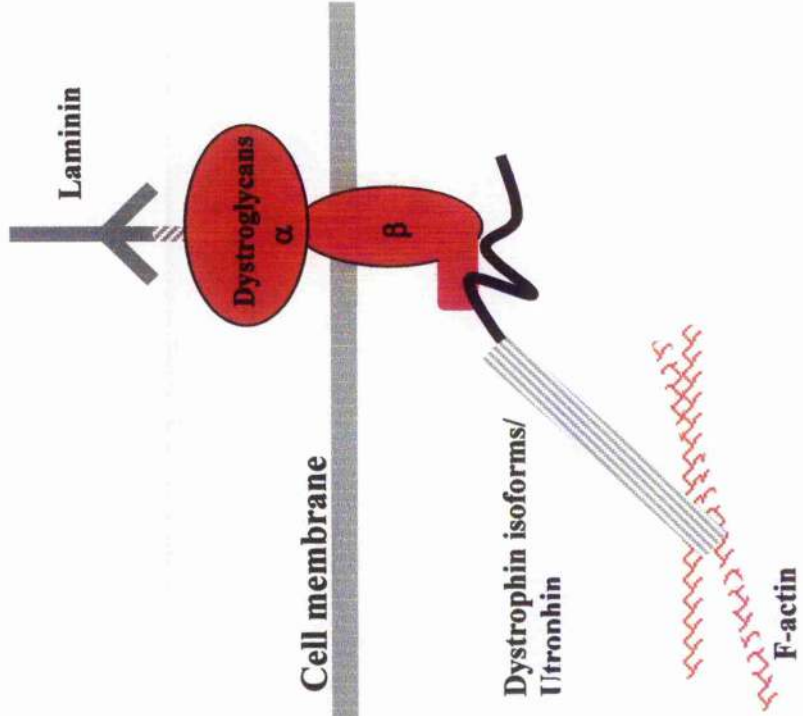
**A**

**Sarcolemma**



**B**

**Non-muscle cells**





## 1.2 Structure of dystroglycan

Dystroglycan contains  $\alpha$  and  $\beta$  subunits.  $\alpha$ -dystroglycan is a highly glycosylated peripheral membrane protein and  $\beta$ -dystroglycan is membrane spanning protein. A highly conserved gene encoding  $\alpha$ - and  $\beta$ - dystroglycan has been found in several vertebrate species (Henry and Campbell, 1996). The dystroglycan gene, *DAG1*, comprises two exons, which are transcribed into a single mRNA product for  $\alpha$ - and  $\beta$ - dystroglycan (Ibraghimov-Beskrovnaya *et al.*, 1993).  $\alpha$ - and  $\beta$ - dystroglycan encoded by a single mRNA is translated into a single dystroglycan precursor. The dystroglycan precursor undergoes proteolytic cleavage at amino acid residue 653 and, posttranslational glycosylation to generate mature  $\alpha$ - and  $\beta$ - dystroglycan subunits (Ibraghimov-Beskrovnaya *et al.*, 1992). Both O-linked and N-linked glycosylation are found in dystroglycan. The mechanism of the proteolytic cleavage of dystroglycan is still unclear. However, it has been identified that neither the O-linked nor the N-linked glycosylation affects the proteolytic cleavage of dystroglycan (Holt *et al.*, 2000). The primary structure of  $\alpha/\beta$  dystroglycan precursor, and mature  $\alpha$  and  $\beta$  dystroglycan are shown in figure 1.2A and B. The  $\alpha$ - and  $\beta$ -dystroglycan presented on the plasma membrane is shown in figure 1.3.

### 1.2.1 $\alpha$ -Dystroglycan

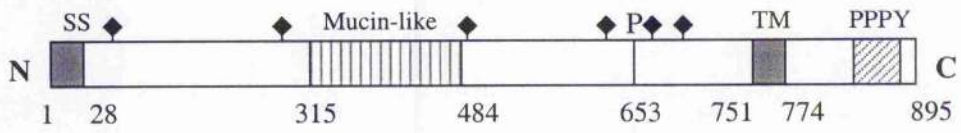
A 28 amino acid signal sequence (SS) is present at the N-terminal of the  $\alpha/\beta$  dystroglycan precursor, allowing the precursor to insert the ER membrane system. The sequence of mature  $\alpha$ -dystroglycan starts from amino acid 29.  $\alpha$ -dystroglycan contains both N-linked and O-linked carbohydrates. The sialylated O-linked oligosaccharides of  $\alpha$ -dystroglycan are concentrated at the region between amino residues 315 and 484 (Durbeej, *et al.*, 1998). Studies of  $\alpha$ -dystroglycan structures using rotary shadowed electron microscopy suggested  $\alpha$ -dystroglycan has a dumbbell-like structure; two globular domains connected by a rod-like mucin domain in the central region (Fig 1.2 C; left).

### **Figure 1.2 Processing of the dystroglycan propeptide**

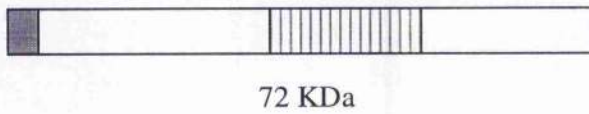
(Adapted from Winder, 2001)

(A) The product of the DAG1 gene,  $\alpha/\beta$ -dystroglycan, is synthesized as a single 895 amino-acid propeptide with signal sequence (SS), mucin-like region, and a transmembrane region (TM). Positions of WW domain interaction motifs PPPY are shown. The propeptide is glycosylated with both N-linked (  $\uparrow$  ) and O-linked (mucin-like) oligo-carbohydrate chains, and is post-translationally cleaved by an unknown protease at residue 653 (P) to generate mature  $\alpha$ - and  $\beta$ -dystroglycan (B). (C) Electron microscopy (EM) analysis reveals  $\alpha$ -dystroglycan has a dumbbell shape. Carbohydrate side chains are shown schematically as circles for O-linked glycosylation, and branches for N-linked glycosylation and glycosaminoglycan chains;  $\beta$ -dystroglycan is shown inserted in a lipid bilayer with its C-terminus on the intracellular side. Over 50% of the mass of mature  $\alpha$ - and  $\beta$ -dystroglycan comprises carbohydrate moieties.

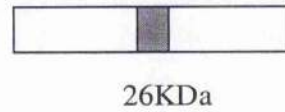
**A**  $\alpha/\beta$ -dystroglycan propeptide



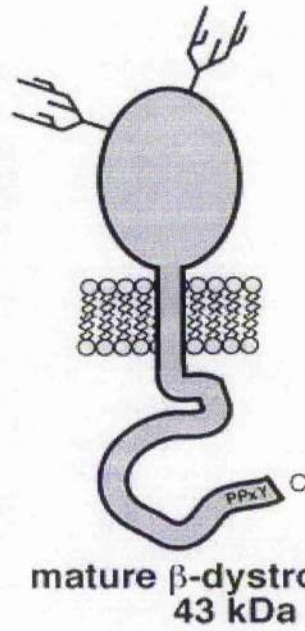
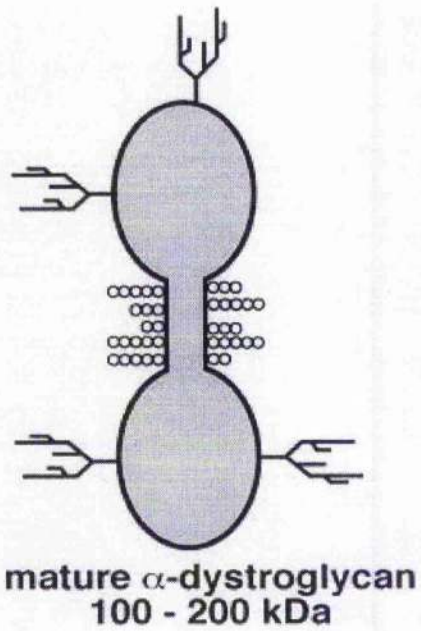
**B**  $\alpha$ -dystroglycan



$\beta$ -dystroglycan



**C**



(Adapted from Winder, 2001)

$\alpha$ -dystroglycan has been identified as a receptor for laminins (Ervasti and Campbell, 1991; Ervasti and Campbell, 1993). Laminin is an ECM protein which is abundant in basal lamina. All laminins are heterotrimers composed of individual  $\alpha$ ,  $\beta$ , and  $\gamma$  subunits. Laminins assemble into trimers by forming a long coiled-coil interaction in the COOH-terminal half of the protein, designated as the long arm. There are currently five laminin alpha chains, three beta chains, and three gamma chains that are found in at least 11 different heterotrimer combinations in vivo (Miner *et al.*, 1998). The unique carboxy terminal laminin globular (LG) modules at the C-terminal of laminin bind several cell surface integrins.  $\alpha 1$  and  $\alpha 2$  LG modules, which are present in laminin1 ( $\alpha 1\beta 1\gamma 1$ ) and laminin2 ( $\alpha 2\beta 1\gamma 1$ ), have been shown to bind to  $\alpha$ -dystroglycan with very high affinity (Andac *et al.*, 1999).

The mucin-like region of  $\alpha$ -dystroglycan has been identified as being critical for dystroglycan binding to LG modules (Yamada *et al.*, 1996a). The binding mechanism between  $\alpha$ -dystroglycan mucin-like region and LG domain has recently been studied. For example, the  $\alpha$ -dystroglycan-laminin interaction is known to be calcium-dependent and requires O-mannosyl-GlcNac glycosylation (Chiba *et al.*, 1997) or sialic acid residues (Ervasti *et al.*, 1997) on  $\alpha$ -dystroglycan. The  $\text{Ca}^{2+}$  ions in each of the LG module structures, and an extensive positively charged surface surrounded by  $\text{Ca}^{2+}$  ions, are proposed as the site of  $\alpha$ -dystroglycan interaction. Furthermore, the binding of heparin to the positively charged surface of the LG module can efficiently inhibit the interaction with  $\alpha$ -dystroglycan (Ervasti and Campbell, 1993). Thus, the mechanism of  $\alpha$ -dystroglycan binding to LG modules may involve the coordination of the missing calcium ligand by negatively charged carbohydrate group of  $\alpha$ -dystroglycan mucin-like domain and positively charged surface of the LG modules (Tisi *et al.*, 2000).

In addition to laminin1 and 2, it has been shown that agrin (Hoch, 1999), perlecan (Iozzo, 1998) and biglycan (Bowe *et al.*, 2000) are also the ligands of  $\alpha$ -dystroglycan. Microbes such as arena viruses and *M. leprae* (Rambukkana *et al.*, 1998) have been

shown to recognise  $\alpha$ -dystroglycan as an infection receptor (Fig 1.3). However, the precise biological functions of these binding to  $\alpha$ -dystroglycan remains unclear.

The primary sequence of  $\alpha$ -dystroglycan predicts a molecular mass of 72 KDa; however,  $\alpha$ -dystroglycan is 156KDa in skeletal muscle (Ervasti and Campbell, 1993), 140KDa in cardiac muscle (James *et al.*, 1997) and 120KDa in brain and peripheral nerves (Yamada *et al.*, 1994). Therefore,  $\alpha$ -dystroglycan may undergo significant posttranslational modifications in a tissue-specific manner and these specific modifications possibly affect functions of dystroglycan. On the cell surface,  $\alpha$ -dystroglycan is anchored to the extracellular domain of  $\beta$ -dystroglycan by a non-covalent interaction. The association site of  $\alpha$ -dystroglycan recognised by  $\beta$ -dystroglycan has recently been mapped to the amino acid sequence 550-585 (Bozzi *et al.*, 2001).

### 1.2.2 $\beta$ -Dystroglycan

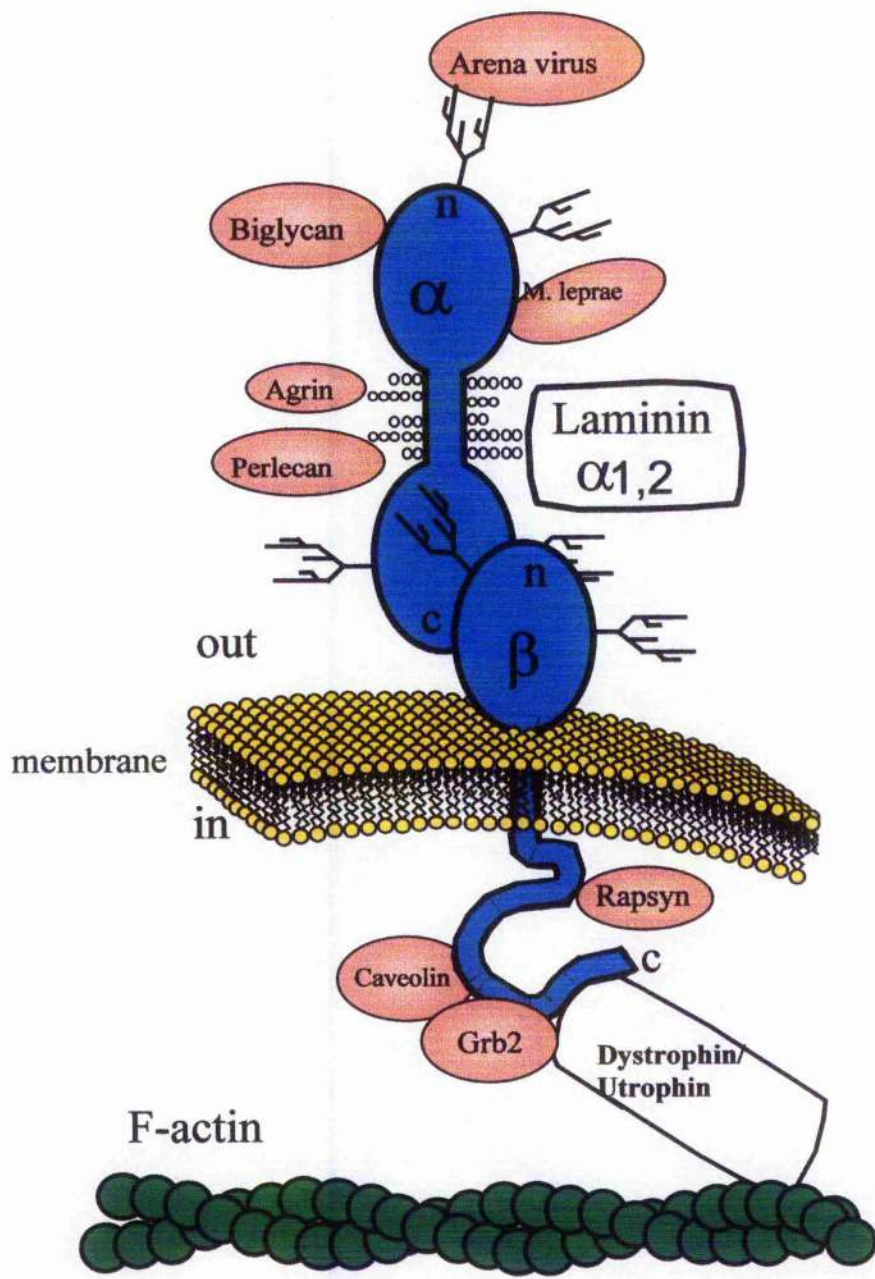
$\beta$ -Dystroglycan is a 43KDa transmembrane glycoprotein with an N-terminal extracellular domain, a transmembrane region and a C-terminal cytoplasmic tail (Fig 1.2 C; right) (Ibraghimov-Beskrovnaya *et al.*, 1992). The amino acid sequences of  $\beta$ -dystroglycan are strikingly similar between different species. In particular, there is a 100% conservation of the carboxy-terminal dystrophin binding sites and a 93% conservation of the central Pro-Thr rich regions (Branaccio *et al.*, 1995). The N-terminal extracellular domain of  $\beta$ -dystroglycan is the glycosylated portion of  $\beta$ -dystroglycan. The association region for  $\alpha$ -dystroglycan on  $\beta$ -dystroglycan has been mapped to amino acid sequence 654-750 (Di Stasio *et al.*, 1999).

$\beta$ -dystroglycan associates with dystrophin or dystrophin homologues fulfilling the connection role of linking the extracellular matrix to the F-actin cytoskeleton (Fig 1.3). The binding site of dystrophin or dystrophin homologues in  $\beta$ -dystroglycan has been localized to a proline-rich region at the extreme C-terminus of the cytoplasmic tail. This region contains the proline-rich motif (PPxY or PY motif, where P denotes proline,

**Figure 1.3 A representation of  $\alpha$ - and  $\beta$ -dystroglycan and binding partners at the cell surface**

(Adapted from Winder, 2001)

The extracellular  $\alpha$ -dystroglycan ( $\alpha$ ) and transmembrane  $\beta$ -dystroglycan ( $\beta$ ) are shown in blue. Agrin, perlecan and laminin isoforms bind to the  $\alpha$ -dystroglycan mucin-like region via their laminin G domain (LG) modules. Arenaviruses require  $\alpha$ -dystroglycan to be glycosylated for binding to occur. Biglycan binds unglycosylated regions of the  $\alpha$ -dystroglycan N-terminus. *Mycobacterium leprae* binds  $\alpha$ -dystroglycan in a laminin-dependent manner. Rapsyn associates with membrane-proximal residues in the  $\beta$ -dystroglycan cytoplasmic tail, and Grb2 binds via a SH3-dependent interaction to  $\beta$ -dystroglycan C-terminus tail. Dystrophin or utrophin (or isoforms) bind the C-terminal 12 amino acids of  $\beta$ -dystroglycan via the WW domain motif PPPY; the utrophin and dystrophin N-termini binds to F-actin. Caveolin associates with  $\beta$ -dystroglycan also at the PPPY motif.



(Adapted from Winder, 2001)

Y represents tyrosine, and x denotes any amino acid), which is a consensus site for binding dystrophin in muscle cells or utrophin in most of the non-muscle cells (Chen *et al.*, 1995). Either dystrophin or utrophin interacts with the cytoplasmic domain of  $\beta$ -dystroglycan through a cluster of domains in the C-terminal cysteine-rich region of dystrophin or utrophin. The cysteine-rich region of utrophin/dystrophin comprises three recognized modules, a WW domain, a pair of EF hands and a ZZ domain (Sudol, 1996). The WW domain is a protein-protein interaction domain which resembles SH3 (Src Homology) domain. The WW domain is necessary, but not sufficient for binding of dystrophin/utrophin to  $\beta$ -dystroglycan (Jung *et al.*, 1995; Suzuki *et al.*, 1994). The EF hands and the ZZ domain play a role in increasing the binding strength of WW domain to  $\beta$ -dystroglycan (James *et al.*, 2000).

Two potential PY motifs are present in the cytoplasmic domain of  $\beta$ -dystroglycan. However, except for the C-terminal tail PPPY motif, which is the binding motif of dystrophin/utrophin WW domain, no interactions with the other PY motif of  $\beta$ -dystroglycan have been reported. It has been shown that tyrosine phosphorylation at Y892 of the C-terminal tail PPPY motif causes significant reduction of the binding affinity of  $\beta$ -dystroglycan to WW domain of dystrophin/utrophin (James *et al.*, 2000), suggesting the interaction between dystroglycan and dystrophin/utrophin WW domain is regulated by tyrosine phosphorylation of the PPPY motif.

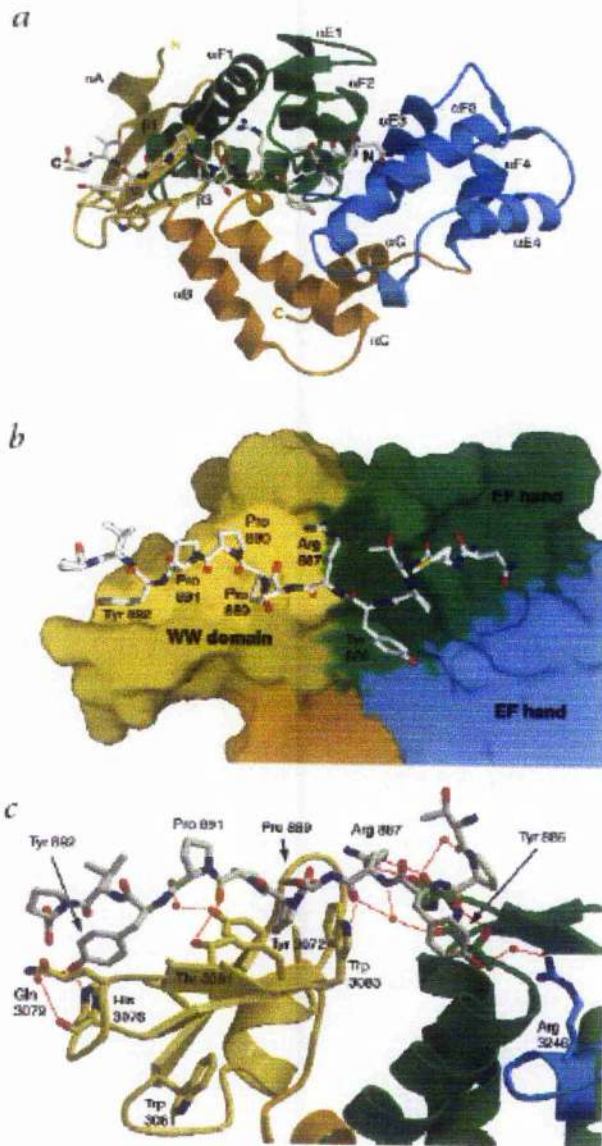
An atomic structure of  $\beta$ -dystroglycan C-terminus PPPY motif and dystrophin/utrophin N-terminal WW domain has recently been solved (Huang, *et al.*, 2000) (Fig 1.4). The PPPY motif with its adjacent amino acids, KNMTPYRSPPPYVPP, corresponding to 880-895 of  $\beta$ -dystroglycan is involved in the binding the WW domain of dystrophin/utrophin. First, the three proline residues at the PPPY motif, form a single turn of a left-handed poly-proline II helix that is recognised by the WW domain. Second, the first two proline residues (residue 889 and 890) in the motif insert into a concave hydrophobic surface formed by Tyr 3072 and Trp 3038 in the WW domain are stacked against Tyr 3072 and Trp 3080 respectively. The tyrosine residue in PPPY motif (Y892) is then located in the hydrophobic pocket formed by Ile 3074, Gln3079



### **Figure 1.4 Structure of the dystrophin- $\beta$ -dystroglycan complex**

(Huang *et al.*, 2000)

(A) Ribbon diagram showing the overall organization of the dystroglycan binding region of dystrophin. The WW domain is colored yellow, the first EF-hand domain green, the second EF-hand domain blue, and additional helices gold. The  $\beta$ -dystroglycan peptide (white) extends across the first EF-hand and the WW domain. Elements of secondary structure, the N- and C-termini of the protein, and peptide are labeled. (B) Molecular surface of the dystrophin  $\beta$ -dystroglycan binding region, colored as in (A). Peptide residues Pro 889–Tyr 892 constitute the PPxY motif. Those in the PPxY motif form a single turn of polyproline II helix. (C) Detailed view of dystrophin- $\beta$ -dystroglycan recognition. The peptide makes six hydrogen bonds (thin red lines) directly to the dystrophin- $\beta$  dystroglycan binding region, and an additional six through bridging water molecules (red spheres).



(Huang *et al.*, 2000)

and His 3076 of dystrophin (or utrophin) WW domain. The hydroxyl group hydrogen of Y892 bonds with His 3076. Additionally, Arg 887 of  $\beta$ -dystroglycan C-terminal tail forms a hydrogen bond with Trp 3083 in WW domain. Interestingly, beyond the WW domain, Arg 887 also forms hydrogen bonds with first EF-hand of dystrophin/utrophin, also Pro885 and Tyr886 of  $\beta$ -dystroglycan contact Thr3188 in the EF-hand. This additional interaction not only stabilises the binding between  $\beta$ -dystroglycan and dystrophin/utrophin, but also provides the  $\beta$ -dystroglycan C-terminal tail with a high specificity.

This study helps to explain why the EF hand is necessary for the interaction between PPPY motif of  $\beta$ -dystroglycan and WW domain of dystrophin/utrophin. Indeed, the other proline rich motif of  $\beta$ -dystroglycan cytoplasmic domain, APLPPPEYPNQS, corresponding to residues 824-835 does not bind to the WW domain of dystrophin/utrophin. The WW domain present in YAP (YES Kinase Associated protein) which binds to PPXY motif cannot recognise the PPPY binding motif at the C-terminal tail of  $\beta$ -dystroglycan either (Chen and Sudol, 1995). Tyrosine phosphorylation at Tyr892 in  $\beta$ -dystroglycan C-terminal tail PPPY motif disrupts the hydrogen bonded formation between Y892 of PPPY and His 3076 of WW, and has been shown to result in reduced binding affinity to dystrophin/utrophin WW domain (Isley *et al.*, 2000; James *et al.*, 2000). These phenomena showed that binding of  $\beta$ -dystroglycan C-terminal tail PPPY motif with dystrophin/utrophin WW domain is a highly specific but dynamic interaction that is responsible for regulation of the connection between  $\beta$ -dystroglycan and the actin cytoskeleton.

### **1.3 Functions of dystroglycan in muscle and non-muscle cells**

#### **1.3.1 Function of dystroglycan in muscle cells**

##### ***1.3.1.1 Role of dystroglycan in muscular dystrophies***

In skeletal muscle, dystroglycan with sarcoglycans, syntrophins, sarcospan, caveolin, and dystrobrevin are expressed throughout the sarcolemma, forming a large membrane

protein complex associating with dystrophin called the dystrophin-glycoprotein complex (DGC) (Ervasti and Campbell, 1991) (Fig1.1A). The DGC links to actin filaments, which connect to Z-lines of myofibrils, via dystrophin and forms a physical linkage between the sarcolemma and myofibrils (reviewed in Spence *et al.*, 2002). In this linkage, dystroglycan directly associates with dystrophin and acts as a membrane receptor for laminin 1 and 2 and plays a central role in connecting the extracellular matrix, actin cytoskeleton and myofibrils in skeletal muscle. The studies of dystroglycan started from the investigation into Duchenne muscular dystrophy (DMD) and the milder Becker muscular dystrophy (BMD). DMD is caused by mutations at DMD locus leading to a total lack of dystrophin in muscle cells (Hoffman *et al.*, 1988). Interestingly, dystroglycan has been found to be greatly reduced in DMD patients as well as in dystrophin deficient *mdx* mice, revealing that dystroglycan plays an important role as well as dystrophin in completing the physical linkage between extracellular matrix and cytoskeleton, thereby maintaining the stability of skeletal muscle (Sicinski *et al.*, 1989). The mutations of dystrophin appear to cause the secondary reduction of dystroglycan. However, no primary mutations in dystroglycan have been identified in any human disease. Additionally, disruption of DAG1 gene in mice results in embryonic lethality. Therefore, despite the important role of dystroglycan in linking extracellular matrix to cytoskeleton in muscle cells, no direct evidence has been shown that primary mutations of dystroglycan can lead to muscular dystrophies. Recently, a series of studies suggested that a variety of muscular dystrophies are caused by disruption of the interaction between  $\alpha$ -dystroglycan and laminin (Table 1.1). In Fukuyama congenital muscular dystrophy (FCMD), Muscle-eye-brain (MEB) disease, and Walker-Warburg Syndrome (WWS) patients, dystroglycan has been found expressed as a less glycosylated form. Similar abnormal reduction of dystroglycan in glycosylation has been found in myodystrophy (*myd*) mice as well. Defects in laminin  $\alpha$ 2, which is the ligand of  $\alpha$ -dystroglycan, has been found in patients with congenital muscular dystrophy (CMD). These studies all support the idea that dystroglycan, or the interaction between dystroglycan and its extracellular matrix ligands, plays a very

**Table 1.1 Dystroglycan and muscular dystrophies**

<b>Disease</b>	<b>Primary affected</b>	<b>Dystroglycan</b>	<b>Reference</b>
Duchenne muscular dystrophy (DMD)	dystrophin	reduced	Ervasti <i>et al.</i> , 1990
Becker muscular Dystrophies (BMD)	dystrophin	reduced	Hoffman <i>et al.</i> , 1988
Congenital muscular dystrophy (CMD)	laminin $\alpha 2$	N.D.	Helbling <i>et al.</i> , 1995
Limb Girdle muscular dystrophy_2D (LGMD-2D)	$\alpha$ sarcoglycan	reduced	Roberds <i>et al.</i> , 1993
Limb Girdle muscular dystrophy_2F (LGMD-2F)	$\delta$ sarcoglycan	reduced	Nigro <i>et al.</i> , 1996
Limb Girdle muscular dystrophy 21 (LGMD 21)	homology to fukutin	reduced	Brockington, <i>et al.</i> , 2001
Muscle- eye-brain disease (MEB)	homology to fukutin	missing	Michele <i>et al.</i> , 2002 Kano <i>et al.</i> , 2002
Fukuyama congenital muscular disease (FCMD)	fukutin	missing	Michele <i>et al.</i> , 2002 Hayashi <i>et al.</i> , 2001
Walker-Warburg syndrome (WWS)	homology to o-mannosyltransferase	missing	Beltran -Valero De Bernabe <i>et al.</i> , 2002

N.D. Not determined.

important role in maintaining the stability of muscle cells. Expression levels of dystroglycan have been shown to be reduced in several types of Limb girdle muscular dystrophies (LGMDs), including LGMD2C, LGMD2D, LGMD2E, LGMD2F, which are defective in expression of sarcoglycans. As mentioned above, dystroglycan reduction is also a consequence of loss of function of dystrophin; thus, expression or processing of dystroglycan seems to be affected by other members of the DGC. Despite playing a central role in forming the ECM-cytoskeleton linkage, dystroglycan might be necessary but not sufficient for maintaining the stability of muscle cells.

### *1.3.1.2 Role of dystroglycan in neuromuscular junctions*

The neuromuscular junction (NMJ) is the contact region between motor neurones and the sarcolemma that is responsible for transmitting the electrical stimulus for muscle contraction. During the development of the NMJ, acetylcholine receptor (AChR) clustering at the motor end plate on the sarcolemma has been shown to be triggered by proteins released from the axonal terminal of the motor neuron. The protein agrin has been found to be crucial for AChR clustering on the motor end plate (reviewed in Burden, 1998). In 1994, agrin was found to be a binding ligand of  $\alpha$ -dystroglycan, implying that dystroglycan might be the agrin receptor involved in the formation of NMJ (Gee *et al.*, 1994). However, subsequent studies revealed that dystroglycan binds to inactive muscle agrin isoforms more tightly than to active neuronal agrin isoforms (Sugiyama *et al.*, 1994; Campanelli *et al.*, 1994). Additionally, the dystroglycan binding domain of agrin is physically separable from the part that induces the AChRs clusters in cultured myotubes (Campanelli *et al.*, 1994). Moreover, utrophin knockout *mdx* mice, which also have reduced levels of dystroglycan, still show normal AChR clustering during NMJ formation (Deconick, *et al.*, 1997; Grady *et al.*, 1997). The finding that muscle-specific kinase (MuSK) is a target for agrin-mediated signalling diminished the role of dystroglycan in clustering AChRs (reviewed in Ruegg and Bixby, 1997). MuSK is a receptor tyrosine kinase (RTK) that appears to trigger the agrin-mediated AChR clustering (reviewed in Ruegg and Bixby, 1997). Tyrosine phosphorylation of MuSK has been shown to be triggered by agrin, but agrin itself is not a ligand that directly binds to MuSK (Glass *et al.*, 1996). The interaction between agrin and MuSK is still

unknown, but it is now clear that binding of agrin to  $\alpha$ -dystroglycan is not necessary for the agrin-mediated aggregation of AChRs. Rapsyn has been identified as an intracellular membrane peripheral protein that directly binds to MuSK and is necessary for agrin-mediated AChRs clustering (Apel *et al.*, 1997). Interestingly, studies in *Torpedo californica* have shown that rapsyn binds directly to the  $\beta$ -dystroglycan juxtamembrane portion (Cartaud *et al.*, 1998) (Fig 1.3). The physiological role of dystroglycan in synapse formation is now still unclear, but it is considered that dystroglycan may function more as a structural, rather than signalling component of postsynaptic apparatus assembly (reviewed in Durbeej *et al.*, 1998).

### ***1.3.2 Functions of dystroglycan in nonmuscle cells***

In addition to muscle cells, dystroglycan is also found expressed in many tissues and cell types, suggesting that dystroglycan function is not restricted to muscle cells.  $\alpha$ -dystroglycan in non-muscle cells has been shown to interact with extracellular laminin as it does in muscle cells (Ervasti and Campbell, 1993). However, instead of full-length dystrophin, various dystrophin isoforms have been identified as the binding proteins linking dystroglycan to the actin cytoskeleton. Utrophin, which is the dystrophin homologue most related to dystrophin, has been also been shown to be expressed in most non-muscle cells where it associates with dystroglycan (James *et al.*, 1996).

#### ***1.3.2.1 Role of dystroglycan in the central nervous system***

In the central nervous system (CNS), dystroglycan is expressed in the brain in many different cell types (reviewed in Durbeej, *et al.*, 1998). For example, in the cerebellum, dystroglycan is expressed in Purkinje cells and binds to the laminin  $\alpha 2$  chain at the glial-vascular interface, suggesting a role for dystroglycan in maintaining the blood-brain barrier (Tian *et al.*, 1996). Histochemical staining showed that dystroglycan in the CNS colocalises with utrophin or Dp71 (Schofield *et al.*, 1995; Gorecki, 1995). Dystroglycan is also present in the peripheral nervous system (PNS) in Schwann cells. It has been shown that  $\alpha$ -dystroglycan in PNS is a receptor for both laminin  $\alpha 2$  chain and agrin, which are expressed in the surrounding matrix of Schwann cells (Yamada *et*

*al.*, 1996b). In the *dy* mouse that shows a deficiency in laminin  $\alpha 2$  chain expression, there are myelination defects, implicating dystroglycan in myelinogenesis (Mastumura *et al.*, 1997). Both utrophin and Dp116 were found to associate with dystroglycan in Schwann cells (Love, *et al.*, 1989; Yamada *et al.*, 1994). Recently, a third member of the dystrophin family, dystrophin-related protein 2 (DRP2) has been identified to associate with dystroglycan and L-peraxin, which is a PDZ domain containing protein, forming a protein complex specific to Schwann cells (Dixon *et al.*, 1997; Sherman *et al.*, 2001). In the absence of peraxin, DRP2 is mislocalised. Disruption of DRP2-dystroglycan complex led to hypermyelination and destabilisation of Schwann cells in peraxin knockout mice (Sherman *et al.*, 2001). Thus, the dystroglycan-DRP2 complex, which associates with extracellular laminin and intracellular peraxin might play a role in the termination stage of Schwann cells myelinogenesis (Sherman *et al.*, 2001).

#### **1.3.2.2 Role of dystroglycan in morphogenesis**

It has been revealed that dystroglycan is abundant at the basal side of most epithelial cells facing the basement membrane in both embryonic and mature tissues (Durbeej *et al.*, 1995; reviewed in Durbeej *et al.*, 1998b). In addition, there is dystroglycan expression at sites of cell-cell contacts both in vitro and in vivo (Belkin *et al.*, 1996). The intracellular binding partners of  $\beta$ -dystroglycan in epithelial cells may include utrophin, Dp117 and Dp140 (Durbeej *et al.*, 1997). Antibody perturbation experiments have shown that dystroglycan might be required for kidney epithelial morphogenesis (Durbeej *et al.*, 1995). Likewise, antibody perturbation experiments suggest a role for dystroglycan in salivary gland morphogenesis (Durbeej, *et al.*, 1998a). Additionally, dystroglycan has been shown to bind to E3 fragment, containing LG domain, of laminin 1 (Brancaccio *et al.*, 1995), which also has been implicated in branching epithelial morphogenesis and basement membrane formation of kidney as well as salivary gland (Sorokin *et al.*, 1992; Kadoya *et al.*, 1995). Moreover, the role of dystroglycan in the formation of NMJ in muscle development has been described (1.3.1.2). Thus, dystroglycan appears to play an important role in the morphogenesis both in epithelial cells and muscle tissues.



### ***1.3.2.3 Early embryonic tissues***

The disruption of the dystroglycan gene (*DAG1*) in mice led to embryonic lethality at around day 6.5; the mutant failed to progress beyond the early egg cylinder stage. This lethality is due to failure of the formation of Reichert's membrane, which is an early basement membrane produced by extra-embryonic tissues (Williamson *et al.*, 1997). Detailed analysis of the embryoid bodies isolated from dystroglycan-deficient animals has shown that components of basement membrane, including laminin, perlecan, and collagen type IV cannot bind to the surface of dystroglycan-deficient cells (Williamson *et al.*, 1997; Henry and Campbell, 1998). These results strongly suggested that dystroglycan is necessary for nucleating the assembly of a primary laminin matrix, which then serves as a scaffold for the assembly of the remaining components of the extracellular matrix. In accordance with this, muscular dystrophies might also be a consequence of a failure to assemble the muscle basal lamina properly (Meier and Ruegg, 2000).

### ***1.3.2.4 Dystroglycan and adhesion***

The evidence that dystroglycan is involved in morphogenesis, myelinogenesis and embryogenesis all suggested a role for dystroglycan in adhesion in non-muscle tissues. The role of dystroglycan in adhesion became clearer when dystroglycan was identified as playing an important role in assembling the extracellular matrix during development. The central role of dystroglycan as a linkage between the extracellular matrix and the cytoskeleton clearly defines dystroglycan as an adhesion molecule. Furthermore, it was also shown that utrophin associates with dystroglycan at the cell membrane where it is localized to cell-cell (Belkin and Burridge, 1995a; Belkin and Burridge, 1995b) and cell-matrix adhesion structures (focal adhesions) (Belkin and Smallheriscr, 1996; James *et al.*, 1996). Hence, despite the mechanism of adhesion mediated by dystroglycan remaining unclear, dystroglycan now is widely considered an adhesion molecule in non-muscle cells.

## 1.4 Signalling role of dystroglycan

In studies of dystroglycan in non-muscle cells, a great deal of emphasis was placed on  $\alpha$ -dystroglycan and its role in development (reviewed in Durbeej, *et al.*, 1998a). The fact that dystroglycan interacts with laminin via its carbohydrate moiety has raised the possibility that “dystroglycan-activated” signalling could participate in the adhesion signalling in non-muscle cells. A signalling role for the DGC has been described in muscle cells. Firstly, neuronal nitric oxide synthase (nNOS) has been identified to associate with DGC via  $\alpha$ -dystrobrevin. Dystrobrevin associates with dystrophin and syntrophins. In DGC, this association affected the recruitment of nNOS to the sarcolemma via syntrophin (Grozdanovic *et al.*, 1996), implying that DGC members plays a role in regulating nNOS signalling pathways. Secondly, as mentioned above, dystroglycan in skeletal muscle could be necessary for the AChR clustering signalling in development of NMJ.

More direct evidence of dystroglycan mediating signalling has been shown in the studies of  $\beta$ -dystroglycan. The 12kDa C-terminal cytoplasmic domain of  $\beta$ -dystroglycan contains more than 20% proline residues, containing four potential SH3 binding motifs (PxxP) and two WW domain binding motifs (xPPxY), giving it the potential to be the signal transduction region of dystroglycan.  $\beta$ -dystroglycan has been shown to directly interact with Grb2, an adapter protein involved in signal transduction and cytoskeletal organization (Jung *et al.*, 1995). Grb2 contains SH2 and SH3 domains which can interact with proteins containing phosphotyrosine or proline-rich domains. The same study also showed that Grb2 interacts with  $\beta$ -dystroglycan via its SH3 domain (Fig 1.3). Fractionation of the extracts from bovine brain synaptosomes using a laminin-affinity column revealed that in addition to  $\alpha/\beta$  dystroglycan and Grb2, focal adhesion kinase (FAK) was also detected in the laminin binding complex. This study showed that FAK has no direct association with  $\beta$ -dystroglycan but was co-immunoprecipitated with Grb2, suggesting that the adaptor protein Grb2 may mediate FAK- $\beta$ -dystroglycan interaction (Cavaldesi *et al.*, 1999). This finding raised the exciting possibility that  $\beta$ -

dystroglycan might be able to regulate signalling molecules such as FAK through the Grb2 adaptor. However, to date, no signalling pathway mediated by  $\beta$ -dystroglycan-Grb2-FAK has been reported.

Despite the functions of dystroglycan in non-muscle cells remaining unclear, adhesion-dependent dystroglycan tyrosine phosphorylation has been demonstrated (James *et al.*, 2000, Iisley *et al.*, 2001). The phosphorylation site was determined as Y892 in the  $\beta$ -dystroglycan WW domain binding motif, PPPY. In HeLa cells, the tyrosine phosphorylation at Y892 of  $\beta$ -dystroglycan triggered by adhesion led to the reduction in binding affinity of  $\beta$ -dystroglycan to dystrophin/utrophin WW domain, suggesting that the interaction between dystroglycan and utrophin/dystrophin WW domain could be regulated by adhesion-dependent tyrosine phosphorylation of the  $\beta$ -dystroglycan PPPY motif (James *et al.*, 2000). Characterisation of  $\beta$ -dystroglycan-Grb2 interaction *in vitro* has determined that the 20 amino acid sequence, containing the PPPY motif, at the C-terminal tail of  $\beta$ -dystroglycan is responsible for its ability to bind to the N-terminal SH3 domain of Grb2. Interestingly, the interaction between dystroglycan PPPY motif and Grb2 N-terminal SH3 domain was significantly inhibited in the presence of dystrophin, indicating that both dystrophin/utrophin WW domain and Grb2 SH3 domain appeared to associate with  $\beta$ -dystroglycan PPPY motif. This implies that a competitive regulation of utrophin/dystrophin WW domain or Grb2 SH3 domain binding to  $\beta$ -dystroglycan might take place (Russo *et al.*, 2000).

In addition to WW domain of utrophin/dystrophin and the N-terminal SH3 domain of Grb2, caveolin has also been identified to interact with  $\beta$ -dystroglycan. In skeletal muscle, caveolin-3 is localized to the sarcolemma, coinciding with dystrophin (McNally *et al.*, 1998). Caveolins are believed to play a role in the formation of the caveolae. Caveolins are small membrane invaginations on the surface of cells that participate in membrane trafficking (including endocytosis and pinocytosis). They act as scaffolding proteins organizing and concentrating caveolin-interacting proteins and lipids in caveolae microdomains (reviewed in Schlegel and Lisanti, 2001). The number and size of caveolae are abnormal in DMD-patients (McNally *et al.*, 1998). In muscle cells,

caveolin-3 has been shown to directly interact with nNOS, and binding results in the loss of NOS activity (reviewed in Garcia-Cardena et al., 1997). The association between  $\beta$ -dystroglycan and caveolin was mapped in the WW-like domain on caveolin and the PPPY motif on  $\beta$ -dystroglycan (Sotgia *et al.*, 2000). While tyrosine phosphorylation at Y892 on  $\beta$ -dystroglycan inhibits the binding affinity of the PPPY motif to dystrophin/utrophin WW domain, it does not affect the interaction between the PPPY and caveolin (Sotgia *et al.*, 2000). However, the binding of dystrophin to  $\beta$ -dystroglycan appeared to be interrupted in the presence of caveolin, revealing that caveolin also competes for the PPPY motif binding site on  $\beta$ -dystroglycan with WW domain (Sotgia *et al.*, 2000). In addition to being triggered by adhesion, the phosphorylation of  $\beta$ -dystroglycan at Y892 has been shown to be elevated by a v-Src transformed state (Sotgia *et al.*, 2001). Surprisingly, some SH2 containing proteins including Fyn, Csk, Nck, SHC, and v-Src itself appeared to be recruited to interact with PPPY containing region on  $\beta$ -dystroglycan in response to the tyrosine phosphorylation at Y892 (Sotgia *et al.*, 2001). The function of this regulation and recruitment is unclear, but these results strongly suggest that  $\beta$ -dystroglycan plays a role as an adhesion signalling molecule.

Altogether, the role of dystroglycan in myelinogenesis, morphogenesis and embryogenesis, even in maintaining muscle stability could be explained by its role as an adhesion molecule. WW domain, caveolin and Grb2 SH3 domain appeared to compete for the PPPY binding motif in  $\beta$ -dystroglycan. The adhesion-dependent tyrosine phosphorylation at Y892 in PPPY motif of  $\beta$ -dystroglycan seems to play an important role in regulating the binding of  $\beta$ -dystroglycan to various signalling molecules. Therefore, dystroglycan is doubtless a signalling molecule.  $\alpha$ -dystroglycan is responsible for recognition and assembly of an extracellular matrix network, while  $\beta$ -dystroglycan, which provides an anchor for  $\alpha$ -dystroglycan, might act as an important adhesion signalling mediator. Studies conducted in this thesis are to investigate the role of dystroglycan in cell adhesion signalling.

## 1.5 Focal adhesion signalling

### 1.5.1 Focal adhesions

Evidence has shown that  $\beta$ -dystroglycan might play a role in regulating cell-matrix adhesion signalling. Adhesion between a cell and its surrounding extracellular matrix (ECM) controls complex biological processes such as development, wound healing, immune response, and tissue function. Adhesion triggers signals regulating cell growth and differentiation. Cell attachment to the ECM is primarily mediated by integrins, a widely expressed family of cell surface adhesion receptors (Hynes, 1992). In addition to anchoring cells, integrins transmit signals that direct cell migration, proliferation, and differentiation (Ruoslahti and Reed, 1994). After binding to ECM proteins, integrins cluster together to form focal adhesions - complexes of intracellular signalling and structural proteins. These specialized sites of attachment provide not only a structural link between the internal actin cytoskeleton and the ECM but also function as a locus of signal transduction activity that control cellular response (reviewed in Jockusch *et al.*, 1995).

Numerous proteins have been identified in focal adhesions, some of which play a predominantly structural role (e.g.  $\alpha$ -actinin, talin, vinculin, paxillin) while others are involved in signal transduction pathways (e.g. FAK, Src). At the cytoplasmic face of focal adhesion sites, bundles of actin filaments (stress fibres; see below) are anchored to the cytoplasmic domain of integrins through the multi-molecular complex of junctional proteins. Focal adhesion complexes are highly dynamic structures, continuously assembling and disassembling in the processes of cells. For example, during cell migration, new focal adhesion complexes, containing newly recruited focal adhesion structural and signalling proteins, assemble rapidly at the leading edge, and, at the same time, disassemble at the retracting tail of the cells (reviewed in Burridge and Chrzanowska-Wodnicka, 1996). The signalling events that occur with integrin-mediated focal adhesion include the phosphorylation of FAK, Src-mediated tyrosine phosphorylation of adhesion proteins and stimulation of the mitogen activated protein kinase (MAP kinase) cascade.

Integrins are the important cell-matrix receptors that regulate the assembly of focal adhesion complex. Integrins are a family of heterodimeric transmembrane cell adhesion receptors which are of crucial importance in interacting with extracellular matrix proteins and promoting a variety of cellular functions such as cell growth, migration, proliferation and cytoskeleton reorganization (reviewed in Giancotti and Ruoslahti, 1999). Each integrin contains  $\alpha$  and  $\beta$  subunits; each subunit has a large extracellular domain, a single trans-membrane region and a short cytoplasmic domain (except for  $\beta 4$  subunit). The differential association of more than 18  $\alpha$ -integrins and 8  $\beta$ -integrins subunits give rise to more than 20 different  $\alpha/\beta$ -integrin heterodimers (Hynes, 1992; Ruoslahti, 1991). Integrin dimers are expressed in specific tissues or cell types and have different specificity for extracellular ligands such as laminin or fibronectin. The binding affinity of integrins with their ligands can be regulated either by the extracellular factors or by intracellular processes so called inside-out signalling (Hughes *et al.*, 1997).

Integrins have been implicated in two major types of activities: adhesion of cells to their substrate and transmission of signals from the external environment to the cell interior. The  $\alpha\beta$  pairings specify the ligand binding abilities for integrin heterodimers. Large ECM proteins such as collagen, laminin, vitronectin, and fibronectin can be recognised by integrins. However, some short peptide sequences within the larger proteins, for example, RGD (Arg-Gly-Asp) sequence found in fibronectin and vitronectin, were found to be sufficient for recognition by integrins (Ruoslahti, 1996). The cytoplasmic tails of integrins are generally short and always devoid of enzymatic features. Hence, integrins transduce signals by associating with adapter proteins that connect the integrin to the cytoskeleton, such as cytoplasmic kinase, and transmembrane growth factor receptors. Integrin signalling and assembly of the cytoskeleton are then intimately linked. As integrins bind to the ECM, they become clustered in the plane of the cell membrane and associate with a cytoskeletal and signalling complex that promotes the assembly of actin filaments. The reorganization of actin filaments into larger stress fibres in turn causes more integrin clustering, thus enhancing the matrix binding and organization by integrins in a positive feedback system. As a result, ECM proteins, integrins, and cytoskeletal proteins assemble into aggregates on each side of the

membrane (reviewed in Giancotti and Ruoslahti, 1999). These well-developed aggregates can be detected by immunofluorescence microscopy and are known as focal adhesions. In this manner, integrins, like dystroglycan, serve as integrators of the ECM and cytoskeleton.

### **1.5.2 Integrin mediated focal adhesion signalling pathways**

In integrin-dependent focal adhesion complex activation, integrins activate various protein tyrosine kinases, including focal adhesion kinase (FAK), Src family kinases, Abl, and a serine-threonine kinase, integrin-linked kinase (ILK) (Wary *et al.*, 1996; Lawis *et al.*, 1996). Adhesion processes of cells also appear to activate the ERK1/2 cascade (section 3.1.1), which regulates the activation of transcription factors and promote the expression of molecules for cell proliferation and cell growth (Assoian, 1997; Renshaw *et al.*, 1997; Schwartz, 1997). Integrin engagement to ECM along with focal adhesion assembly is able to activate the ERK1/2 cascade that is involved in the regulation of cell survival (reviewed in Howe *et al.*, 1998). Two sets of signalling pathways induced by integrin engagement have been shown to be involved in the assembly of focal adhesion complexes in cells, the FAK pathway and the Fyn/Shc pathway (Juliano, 2002).

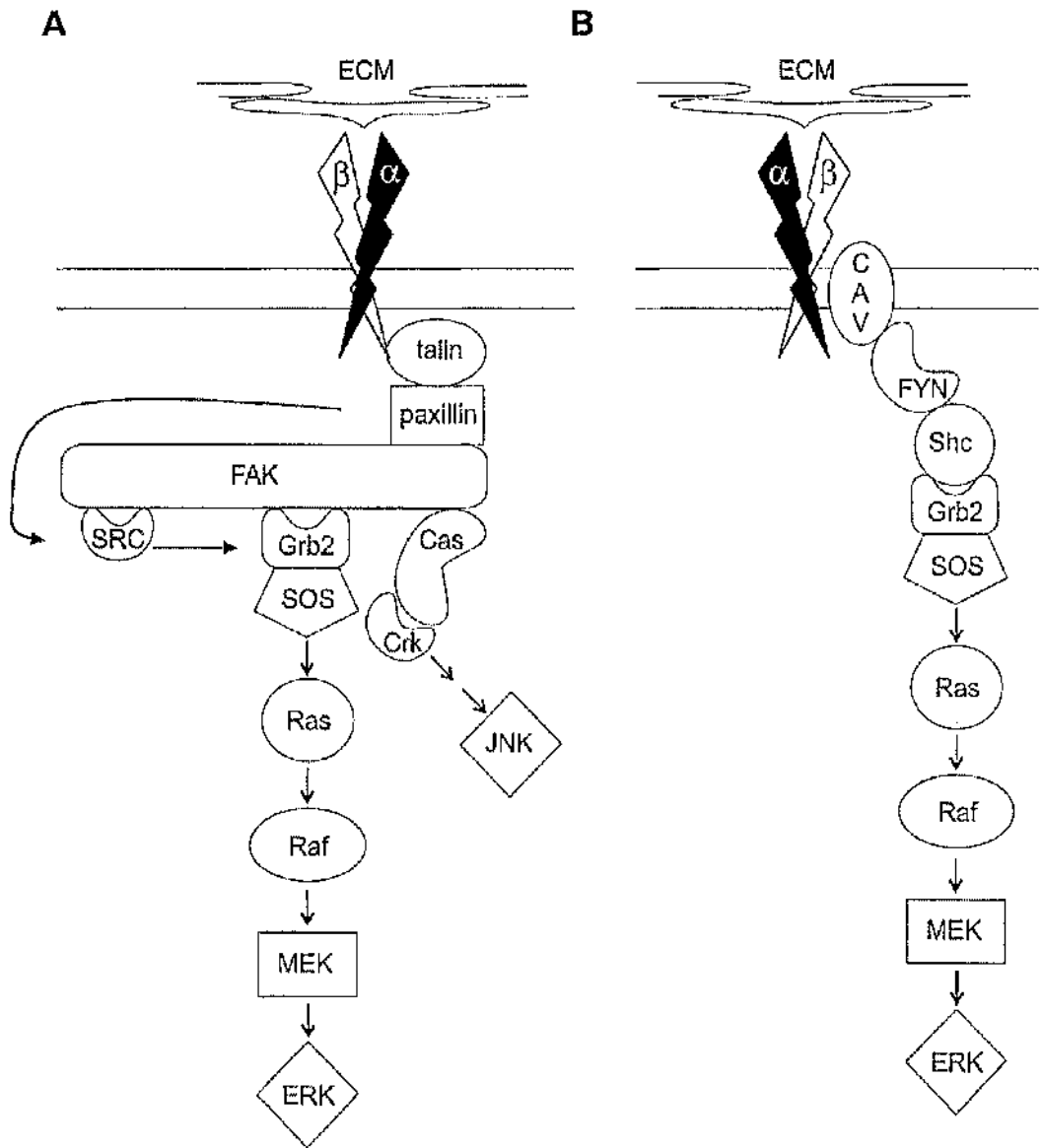
#### **1.5.2.1 The FAK pathway**

The integrin-dependent pathways involving FAK and Src-family kinases have been studied in some detail. The FAK pathway is activated by most integrins (Fig 1.5 A). The activation of FAK is not well understood, but it is coupled to the assembly or disassembly of focal adhesions. FAK may be recruited to nascent focal adhesions because it interacts, either directly or through the cytoskeletal proteins talin and paxillin, with the cytoplasmic tail of integrin  $\beta$  subunits (Miyanoto, *et al.*, 1995). Upon activation, FAK autophosphorylates Tyr397 and is recruited to focal adhesions, thereby creates a binding site for the Src homology 2 (SH2) domain of Src or Fyn (Schaller *et al.*, 1994; Schlaepfer, *et al.*, 1994). The Src kinase then phosphorylates a number of focal adhesion components. The major targets include paxillin, tensin, and Cas, a

**Figure 1.5 Direct cell growth signaling by integrins-mediated focal adhesions**

Two models are shown depicting how integrins may directly stimulate the ERK cascade. (A) Integrin engagement causes recruitment and activation of FAK and its autophosphorylation. This creates a binding site for the Src tyrosine kinase, which then further phosphorylates FAK. This allows the Grb2 SOS complex to bind, thus triggering Ras activation and subsequent activation of Raf, MEK, and ERK. A second pathway leads from p130 Cas and Crk to c-Jun kinase activation. (B) Certain integrins (but not all) associate with Fyn and Shc via caveolin. The phosphorylation of Shc by the Fyn tyrosine kinase allows recruitment of Grb2-SOS and activation of the cascade.





(Adapted from Juliano, 2002)

docking protein that recruits the adapter protein Crk, which can stimulate the JNK pathway (Vuori, et al., 1996; Schlaepfer, et al., 1997). Active Src phosphorylates FAK at Tyr925, creating a binding site for the complex of the adapter Grb2 and Ras guanosine-triphosphate exchange factor Sos (Son of sevenless) (Schlaepfer, et al., 1994). Paxillin is a multi-domain adaptor protein that shown to associate with SH3 domain of Src (Turner, 2000). Activation of FAK leads to the recruitment and activation of Src in focal adhesions (reviewed in Schaller, 2001) that subsequently interacts with paxillin and activates Grb2-Sos. Hence, by the activation of FAK in response to integrin engagement, paxillin, Src, Grb2-Sos are activated and recruited to focal adhesions. Association of active Src with paxillin and FAK then activates Grb2-Sos followed by exchange of Ras-GDP to Ras-GTP, which subsequently activates the downstream ERK cascade (reviewed in Howe *et al.*, 1998). Whereas FAK is phosphorylated on tyrosine residues upon assembly of focal adhesions, it becomes phosphorylated on serine residues and disassociates from Src and Cas during mitosis (via activation of JNK) (Yamakita *et al.*, 1999). These events may loosen cell-substrate contacts and allow cells to divide and move apart.

#### *1.5.2.2 The Fyn/Shc pathway*

In addition to activating FAK, some  $\beta 1$  and  $\alpha_v$  integrins also activate the tyrosine kinase Fyn and, through it, the adapter protein Shc (Fig1.5 B) (Wary *et al.*, 1996). In this pathway, caveolin-1 appears to function as a membrane adapter, which couples the integrin  $\alpha$  subunit to Fyn. This function of caveolin-1 is consistent with its ability to bind cholesterol and glycosphingolipids and organize specialized plasma membrane "rafts," which are enriched in the Src-family kinases such as Fyn, Yes, and Lck (reviewed in Harder and Simons, 1997). Upon integrin binding to ECM, Fyn becomes activated, and its SH3 domain interacts with a proline-rich site in Shc. Shc is then phosphorylated by Fyn at Tyr317 and combines with the Grb2-SOS complex (Wary *et al.*, 1996), thereby stimulating the ERK cascade. Although most integrins interact with caveolin-1 and Fyn, only a subset of integrins can activate Fyn and thereby recruit Shc (Wary *et al.*, 1998). Yes and Lck are known to be enriched in rafts and may mediate the activation of Shc when Fyn is not expressed (Wei, *et al.*, 1999).

It is likely that both FAK and Shc contribute to the activation of the Ras-extracellular signal-regulated kinase (ERK) MAPK cascade when Shc-linked integrins bind to ECM (Giancotti and Ruoslahti, 1999). The relative contribution of each pathway may depend on the cell type and perhaps also on how far the adhesion process has progressed. In many cell types, Shc appears to be responsible for the initial high-level activation of ERK upon cell adhesion. FAK, which is activated more slowly, may sustain the ERK activation (Howe and Juliano, 1998; Pozzi, et al., 1998). The integrins that do not activate Shc are weak activators of ERK and cell proliferation (Howe and Juliano, 1998; Mainiero *et al.*, 1997). The ability of integrins to activate ERK may be especially important when the concentration of growth factors available to the cell is limited. In this setting, proliferation is likely to require co-stimulation of ERK through integrins and growth factor receptors.

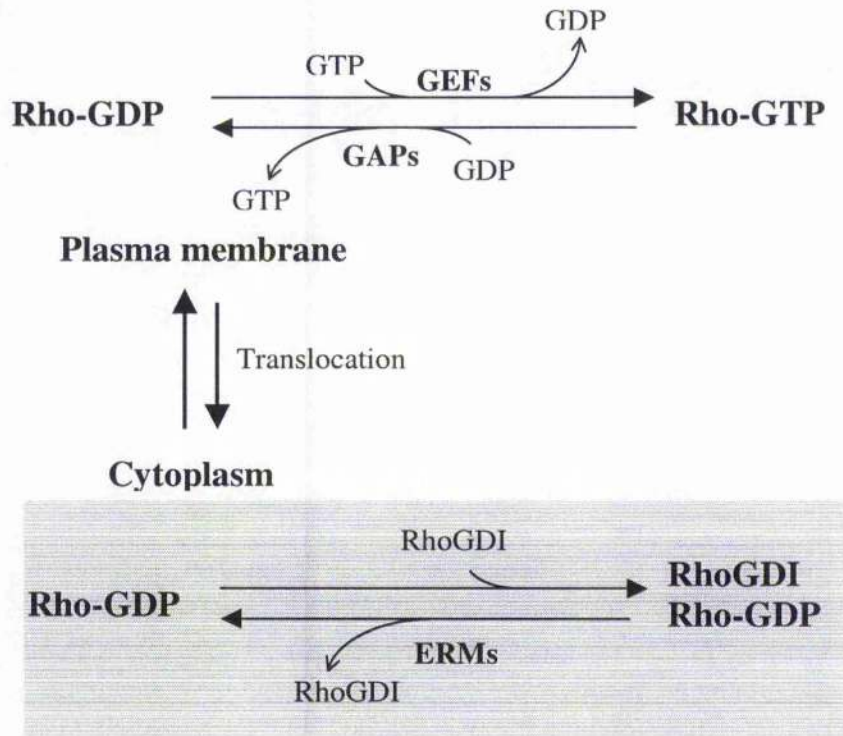
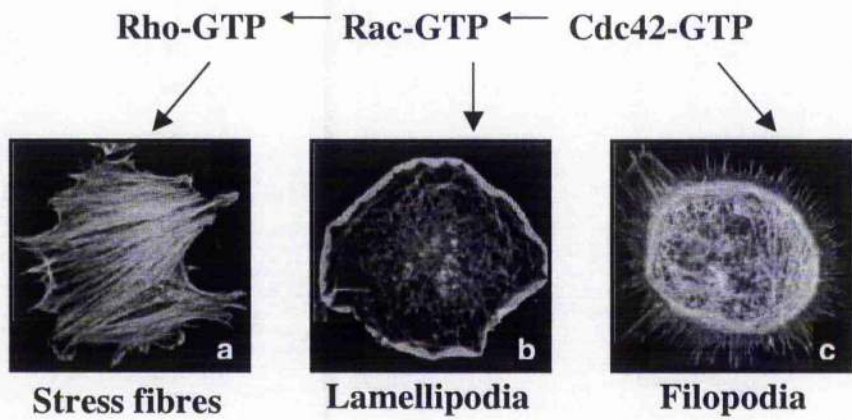
### **1.5.3 Focal adhesions and cytoskeleton signalling**

#### ***1.5.3.1 Activation of Rho GTPases and Rho Kinase***

In addition to regulating cell growth and survival signalling, focal adhesion signalling has also been shown to be involved in the formation of actin stress fibres. It has been indicated that integrin engagement can regulate the organisation of the cytoskeleton through regulating the activation of Rho GTPases (Hall, 1998). The Rho GTPases, which are a group of small GTPases belonging to the Ras superfamily, have been identified as important regulators for modulating actin organisation (reviewed in van Aelst and Dsouza-Schorey, 1997). Like other members of the Ras superfamily of proteins, the Rho GTPases acts as a molecular switches cycling between an active GTP-bound and inactive GDP-bound form (reviewed in Nobes and Hall, 1994). Guanine nucleotide exchange factors (GEFs) facilitate the exchange of GDP for GTP, and GTPase-activating proteins (GAPs) increase the rate of GTP hydrolysis of Rho GTPases (Fig 1.6 A). In resting cells, inactive GDP-bound Rho GTPases are found in the cytoplasm as a complex with Rho guanine nucleotide disassociation protein (RhoGDI) which inhibits GDP/GTP exchange. GDP-bound Rho GTPases released from GDI are translocated and activated during Rho GTPase dependent events (Takai, *et al.*, 1995)

**Figure 1.6 Activity cycle of Rho GTPases and cytoskeleton morphology induced by active Rac, Rho or Cdc42**

(A) At the plasma membrane, Rho GTPases cycle between active GTP bound form and inactive GDP bound form. Guanine exchange factors (GEFs) facilitate the exchange of GDP for GTP, and GTP-activating proteins (GAPs) increase the hydrolysis rate of RhoGTPases. In resting cells, inactive GDP bound Rho GTPases form a complex with Rho guanine dissociation inhibitor (RhoGDI) in the cytoplasm, thereby inhibiting the GDP/GTP exchange rate of GDP bound Rho GTPases (**grey panel**). ERM (ezrin/radixin/moesin) proteins interacting with RhoGDI leads to the disassociation of GDI from GDP bound Rho GTPases, thereby enabling the GDP bound Rho GTPases to translocate and couple to the GDP/GTP exchange cycle in the plasma membrane. (B) The actin cytoskeleton morphology triggered by activation of Rho GTPases. (a) Activation of Rho induces an increase in the number of stress fibres. (b) Activation of Rac induces cells to form peripheral lamellipodia. (c) Activation of Cdc42 induces the formation of numerous actin-rich filopodia in the periphery extended from the cell body.

**A****B**

(Hall, 1998)

(Fig 1.6 A, grey panel). The mechanism by which GDP-bound Rho GTPases are released from RhoGDI is still unclear. However, it has been shown that ERM (ezrin / radixin/ moesin) proteins might play a role in disassociating GDI from GDP-bound Rho GTPases, thereby releasing GTP bound Rho GTPases and increase the GDP/GTP exchange rate of Rho GTPases and the organisation of cytoskeleton (Takahashi *et al.*, 1997). Over 30 members of the Rho family are known in mammals (reviewed in Bishop and Hall, 2000). The members of Rho family GTPase, Rho, Rac and Cdc42, are shown to be responsible for the formation of specific actin cytoskeletal structures (reviewed in Hall, 1998) (Fig 1.6 B). The activation of Rho leads to the assembly of stress fibres (Fig 1.6 B, a) and formation of focal adhesion complexes (Ridley and Hall, 1992). Rac activation induces the formation of an actin meshwork at the cell periphery, producing lamellipodia (Fig 1.6 B, b) (Ridley *et al.*, 1992). Activation of Cdc42 in cells has been shown to lead to the formation of actin-rich membrane protrusions and microspikes, such as microvilli and filopodia (Kozma *et al.*, 1995) (Fig 1.6 B, c)

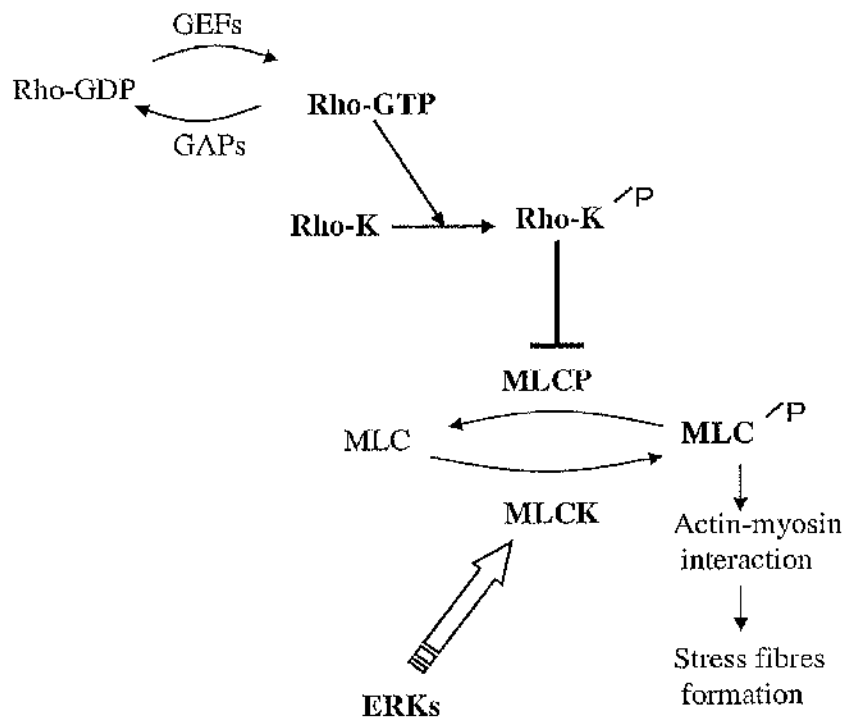
Rho activation results in the formation of focal adhesions and the contractile bundles of actin and myosin promoting the formation of stress fibres (Fig 1.7) (Ridley and Hall, 1992). Induction of these structures is known to be mediated by Serine/threonine kinases, which are downstream effectors of Rho-kinase (Matsui *et al.* 1999), ROK $\alpha$  (RhoA-binding kinase  $\alpha$ ) or its close relative p160ROCK (ROK $\beta$ ) (reviewed by Van Aelst & D'Souza-Schorey 1997). Rho GTPase binds to these kinases and increases their activity (Amano *et al.* 1997, Leung *et al.* 1995). Activated Rho-kinase inhibits the inactivation of myosin light chain (MLC) through the inactivation of MLC phosphatase (MLCP) by phosphorylating the myosin binding subunit (MBS) of MLCP (Kimura *et al.* 1996, reviewed by Ridley, 2001). This, in turn, enhances the binding of myosin to actin filaments and subsequently enhances the formation of stress fibres (Leung *et al.* 1995, Chrzanowska-Wodnicka and Burridge 1996, Amano *et al.* 1997).

### ***1.5.3.2 Adhesion dependent Rho activation***

The regulation of RhoA activity by integrins is complicated. Integrins can either stimulate or inhibit RhoA activity depending on the cell type, engagement of specific

**Figure 1.7 Mechanisms for Rho-induced stress-fibre formation through the activation of Rho kinase**

Under the regulation of integrin dependent signalling in focal adhesion, activation of Rho leads to the activation of the downstream effector Rho kinase (Rho-K). Activation of Rho-K leads to phosphorylation of myosin light chain phosphatase resulting in the inactivation of MLCP. As MLCP is inactive, myosin light chain (MLC) will no longer be dephosphorylated as normal. Subsequently elevated levels of phosphorylated MLC would then be maintained in the cell through the action of myosin light chain kinase (MLCK). Phosphorylated myosin (containing the MLC) leads to bundling of actin filaments forming actin stress fibres. Activation of MLCK has been shown to regulated by ERK activation.

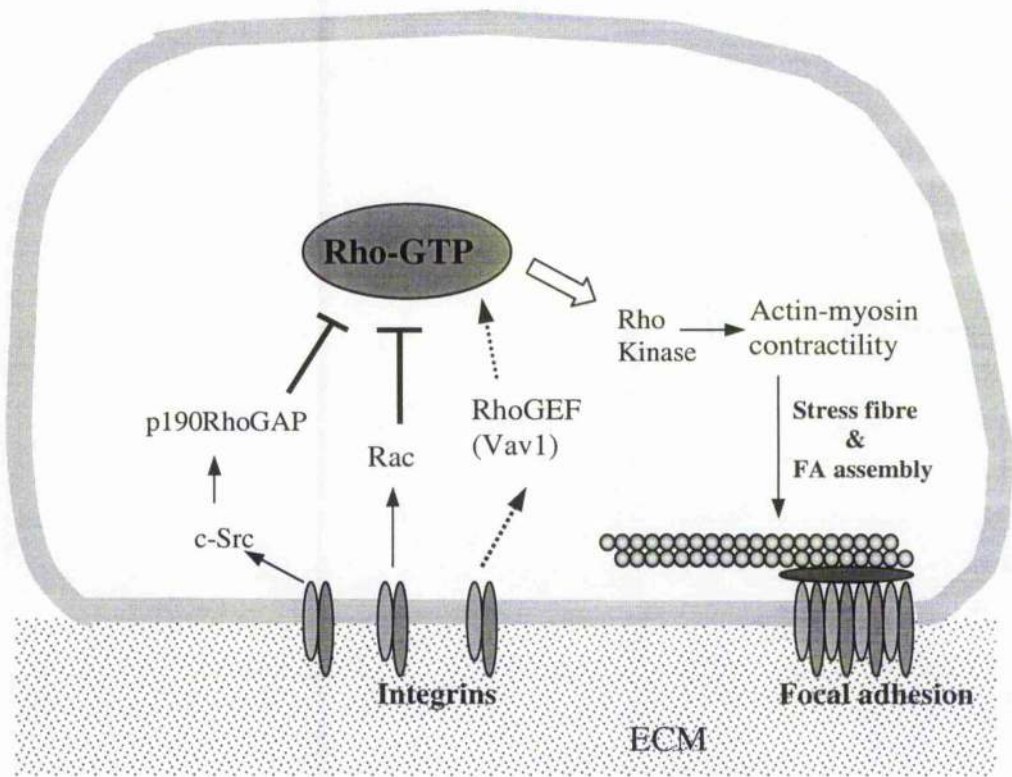




integrins, and the time course of engagement (Ren, *et al.*, 1999; O'Connor *et al.*, 2000; Arthur, *et al.*, 2000). This duality may reflect the role of integrin-mediated signals in promoting membrane extensions, a condition in which low RhoA activity is desirable, versus the role of integrins in establishing strong attachments across which tension is transmitted, for which higher Rho activity is needed. In fibroblasts, integrin engagement initially inhibits Rho activity but later activates it, correlating with the completion of cell spreading (Ren *et al.*, 1999), during which time integrin-mediated activation of Rac or Cdc42 is high (del Pozo, *et al.*, 2000; reviewed in Hall, 1998). Barry and colleagues found that addition of RGD peptides to quiescent fibroblasts stimulated focal adhesion and stress fibre assembly (Barry, *et al.*, 1996). Arthur and colleagues identified a pathway by which integrin engagement results initially in a decrease in RhoA activity (Arthur, *et al.*, 2000). It was found that incubation of fibroblasts with integrin ligands caused a rapid drop in Rho activity, but that this did not occur in cells deficient in the Src family tyrosine kinases (Src, Fyn, and Yes). c-Src has been identified to be required for this integrin-mediated drop in Rho activity (Arthur *et al.*, 2000). v-Src expression in fibroblasts has long been known to disrupt focal adhesions and stress fibres (Fincham *et al.*, 1999). Downstream from c-Src, p190RhoGAP was identified as a target that is phosphorylated and activated, in response to integrin engagement. Thus, the short-term effect of integrin engagement leads to the inhibition of Rho activity via the activation of c-Src and p190RhoGAP (Arthur *et al.*, 2000). The pathway by which integrin-mediated adhesion results in long-term activation of RhoA has not been determined. It seems likely that the initial activation of p190RhoGAP must be switched off, but whether there is an additional activation of a Rho-specific GEF remains to be elucidated. Numerous GEFs for the Rho family of GTPases have been discovered (Bishop and Hall, 2000) but little information exists concerning how these GEFs become activated by integrin signalling. One exception is Vav1, a hematopoietic GEF for Rho family GTPases. Vav1 is tyrosine phosphorylated and activated in response to integrin engagement or clustering (Gotoh, *et al.*, 1997. Miranti, *et al.*, 1998). The integrin-mediated inactivation of Rho and focal adhesion assembly is shown in figure 1.8.

**Figure 1.8 Multiple signaling pathways control focal adhesion assembly by coordinately regulating the activation of the small GTP-binding protein RhoA**

Integrins transmit both positive and negative signals to RhoA. Initially, engagement of integrins with ECM inhibits RhoA. Integrins activate p190 RhoGAP through a c-Src-dependent mechanism. Integrins also activate Rac1 or Cdc42 as the cell spreads, which can antagonize RhoA activity. As stable adhesions form, integrins activate RhoA, most likely through an integrin-dependent RhoGEF. Downstream of RhoA, actin–myosin contractility stimulates actin stress fiber formation and clustering of integrins and associated proteins to form focal adhesions. This pathway is triggered by a RhoA effector, Rho kinase.



## 1.6 Aims of the study

In addition to integrin-mediated focal adhesion signalling, growth factors receptors such as receptor tyrosine kinases (RTK) have long been known to promote the activation of the ERK cascade and mitogenesis (reviewed in Clark and Brugge, 1995). This convergence of integrin-mediated ERK signalling and RTK-mediated ERK signalling raises the possibility that integrin-mediated ERK signalling might be responsible for signalling beyond mitogenesis. Evidence supporting this aspect has been reported (Table 1.2). First, integrin activation was found to be suppressed by activation of Ras/Raf-initiated ERK pathway. The activation of ERK downstream substrate JNK is not involved in the ERK-dependent integrin inhibition, suggesting that integrin activity is regulated by a transcriptional-independent ERK activation in cytoplasm (Hughes *et al.*, 1997). Additionally, the direct association of ERKs with integrin in some tumour cells was found, implying that routes to modulate cytoskeleton organisation between integrin and cytoplasmic ERKs exist in normal cells (Ahmed *et al.*, 2002). Moreover, calpain, a protease which cleaves actin binding proteins in adhesion disassembly, has been reported to be inhibited by both integrin-mediated and EGF-dependent ERK activation (Glading *et al.*, 2000). The evidence implies that ERKs might play a role in regulating adhesion protein assembly.

An interesting finding is that active ERK2 has been shown to directly interact with and activate myosin light chain kinase (MLCK), which phosphorylates myosin light chain (MLC) subsequently enhances stress fibre and focal adhesion formation (Klemke *et al.*, 1997). Thus ERK, in addition to a role as a mitogenetic activator, could co-operate with Rho kinase, which inhibits MLCP to regulate myosin and modulate cell motility (Fig 1.7). Fincham and colleagues (Fincham *et al.*, 2000) have demonstrated that active ERKs targets to newly forming focal adhesion sites in rat embryo fibroblast (REF52) cells. The activation and targeting of ERKs is induced by the activation of v-Src protein, in response to integrin engagement. Thus, a signalling pathway has emerged which is triggered by integrin engagement followed by activation and targeting of ERK to adhesions, and subsequent activation of MLCK to regulate cytoskeletal reorganisation.

**Table 1.2 Evidence of ERK-mediated non-mitogenetic regulation**

<b>Description</b>	<b>Cell type</b>	<b>Reference</b>
Activity of MAP kinase regulates Cell motility		Stoker and Gherardi, 1991 Klemke <i>et al.</i> , 1994 Leavesley <i>et al.</i> , 1993 Yenush <i>et al.</i> , 1994
Activation of integrin is inhibited by the activation of ERK cascade.	CHO	Hughes <i>et al.</i> , 1997
MLCK is activated by active ERKs	COS-7	Klemke <i>et al.</i> , 1997
ERKs inhibit protease Calpain	NR-6 (mouse fibroblast)	Glading <i>et al.</i> , 2000 Glading <i>et al.</i> , 2001
Blocking of integrin-mediated ERK activation inhibits the migration of cells.	COS-7	Klemke <i>et al.</i> , 1997
ERK directly associates with integrin	WiDr, HT29, SW480 (human colon cancer cell line)	Ahmed <i>et al.</i> , 2002
Active ERK localise at newly formed adhesion in leading edge of the cell.	REF52	Fincham <i>et al.</i> , 2000

Previous work has shown that  $\alpha$ -dystroglycan co-localised at focal adhesion sites with active ERK (Spence, *et al.*, 2003a). As mentioned above, dystroglycan has been considered to be a signalling molecule playing a role in regulating cell adhesion and cytoskeleton reorganisation in non-muscle cells. Dystroglycan is an ECM laminin receptor and has been shown to associate with Grb2-Sos and FAK, and could be able to trigger Ras-mediated ERK activation. If engagement of dystroglycan activates Grb2-Sos and activates the ERK cascade, it is possible that dystroglycan plays a role in ERK-dependent adhesion and mediates actin stress fibres reorganisation through the activation of ERK and MLCK. To date, however, the study of relationship between cytoplasmic ERK and dystroglycan has not been reported. Therefore, this study aimed to investigate the role of dystroglycan in cell adhesion-mediated signalling with particular emphasis on the role of the ERK cascade.

**Chapter 2**  
**Methods and materials**

## **2.1 Materials**

### **2.1.1 Chemicals, reagents and Kits**

Appendix I

### **2.1.2 Media and general buffers**

Appendix II

### **2.1.3 Plasmid and clones**

Appendix III

### **2.1.4 Cell lines**

Appendix IV

### **2.1.5 Antisera**

Appendix V

### **2.1.6 Oligos**

Appendix VI

## **2.2 Molecular biology methods**

### **2.2.1 Bacterial strain**

*E. coli* strain DH5 $\alpha$  was used for all cloning, amplification and propagation of plasmid DNA in this study. Genotype of DH5 $\alpha$  is: F',  $\phi$ 80 $\Delta$ lacZ $\Delta$ M15,  $\Delta$  (*lacZYA-argF*)U169, *deoR*, *recA1*, *endA1*, *hsdR17*(*r<sup>k</sup>*, *mk<sup>+</sup>*), *phoA*, *supE44*,  $\lambda$ , *thi-1*, *gyrA96*, *relA1*. DH5 $\alpha$  culture in the stationary phase was suspended in 50% sterilised glycerol solution at the ratio of 3:2 and stored at  $-80^{\circ}\text{C}$  until needed.



### **2.2.2 Growth of bacteria**

DH5 $\alpha$  was grown at 37°C in sterilised 2x YT liquid medium or on sterilised 2x YT solid medium. To maintain selection for plasmid DNA, transformed DH5 $\alpha$  was grown in 2x YT liquid medium or 2x YT solid medium containing ampicillin (25 $\mu$ g/ml) or kanamycin (30 $\mu$ g/ml).

### **2.2.3 Transformation of DH5 $\alpha$**

#### ***2.2.3.1 preparation of calcium competent cells***

DH5 $\alpha$  was transferred from a frozen stock, streaked and incubated at 37°C on 2x YT solid medium for overnight. A single colony from this culture was transferred to 5ml 2x YT liquid medium and incubated at 37°C for overnight. 100 $\mu$ l of this culture was transferred to 100 ml 2x YT liquid medium and incubated at 37°C until the OD<sub>600</sub> value reached to 0.6. This culture was then centrifuged at 4°C for 20 minutes at 2500xg and the supernatant discarded. The cell pellet was resuspended in 10 ml of 100mM calcium chloride solution and on ice for at least 45 minutes. These competent cells were used fresh or aliquoted into Eppendorf tubes (100 $\mu$ l aliquots) and stored at -80°C.

#### ***2.2.3.2 Transformation of calcium competent cells***

90 $\mu$ l of calcium competent cells were thawed on ice, and mixed with the 10  $\mu$ l DNA to be transformed. The mixture was then incubated on ice for 30 minutes, heat shocked at 42°C for 2 minutes and transferred into 0.9ml 2x YT liquid medium. The cells were allowed to recover for 30 minutes at 37°C before being spread onto 2x YT solid medium supplemented with ampicillin or kanamycin. To isolate single colonies, these cells were incubated at 37°C for 16 hours overnight.

## **2.2.4 Preparation of plasmid DNA**

### ***2.2.4.1 Small-scale preparation of plasmid DNA by spin column***

Plasmid DNA was prepared using QIAprep Miniprep kit, following the manufacturers' guidelines. DNA was extracted from 3ml *E. coli* culture, resuspended in 50µl of distilled water and stored at -20°C.

### ***2.2.4.2 Large-scale preparation of plasmid DNA for transfection***

Large scale DNA for transfection was prepared using QIAprep Midiprep kit, following the manufacturers' guideline. DNA was extracted from 50ml *E. coli* culture, resuspended in 300µl of distilled water and stored at -20°C.

## **2.2.5 Spectrophotometric quantification of DNA**

The concentration of DNA was determined by measuring the absorption of 100 times diluted DNA solution at 260nm for DNA or 280nm for RNA using Heλiosy spectrophotometer (Unicam) and Ultra-micro cuvette (Sigma-Aldrich). For double-stranded DNA, an OD260 value of 0.1 represents a DNA concentration of approximately 50µg/ml. For determination of the quality of plasmid DNA, both OD260 and OD280 value were detected. A value of OD260/ OD280 >1.5 meant that the quality of the batch of DNA purification was sufficient for mammalian cell transfection (section 2.3.2).

## **2.2.6 Restriction digestion of DNA**

Restriction enzymes were purchased from Boehringer Mannheim, or New England Labs. For SalI and SmaI double digestion, the required quantity of DNA was mixed with 5 units of SalI in Y+/TANGO (Fermantas) buffer at 2x concentration, and was incubated at 37°C for 2 hours. The enzyme activity of SalI was then terminated by heating to 65°C for 20 minutes. After cooling down to room temperature, distilled water was added to the mixture until Y+/TANGO buffer reached to 1x concentration. 5 units of SmaI was then added into the mixture and incubated at 25°C for 3-5 hours until it was used for ligation. For other digestions, requisite quantity of DNA was digested in

10-20 $\mu$ l volumes containing appropriate buffers at 1x concentration and restriction enzyme at 1-5 units. These mixtures were incubated at the recommended temperature following the guideline and the digestions were examined by using agarose gel electrophoresis (section 2.2.7).

### **2.2.7 Agarose gel electrophoresis**

Agarose gel electrophoresis of DNA fragments was performed with 0.8% (W/V) agarose gel by using EM-100 Mini Gel Unit (Cambridge). Gels were prepared by melting appropriate amount of agarose in 0.5x TBE buffer and adding ethidium bromide to a final concentration of 0.5  $\mu$ l/ml. Samples to be analysed were mixed with agarose gel loading buffer and directly loaded into the gel. The gels were placed in 0.5x TBE buffer in the gel running chamber and typically run at 100V for 20-30 minutes. HyperLadder I (Bioline), size range from 200-10000bp, was used as the size marker.

## **2.3 Cell culture**

### **2.3.1 Growth of cell lines**

REF52 and COS7 cells were maintained in DMEM media supplemented with 10% FBS in 5% CO<sub>2</sub> atmosphere at 37°C in 75T flasks. Confluent cells were passaged using 0.25% trypsin solution and reseeded at a dilution of 1:4 for REF52 cells or 1:10 for COS7 cells. Primary culture of utrophin null and the utrophin wild type of mouse embryo fibroblast were cultured in DMEM media supplemented with 10% FBS in 5% CO<sub>2</sub> atmosphere at 37°C in 75T flask. For utrophin knockout primary cultures of rat embryonic fibroblasts, cells were kept in the same condition as above and used for transfection within 10 days.

### **2.3.2 Transfection and cotransfection**

Expression of plasmid DNA in mammalian cells were carried out by using Lipofectamine<sup>TM</sup> reagent, following the manufacturers' guidelines. Cells were seeded in tissue culture dishes or flasks and allowed to spread and grow at 37°C in DMEM supplement with 10% FBS and 5% CO<sub>2</sub> overnight (less than 24 hour) until 80-95%

confluent. For transfection, the appropriate amount of DNA was mixed with lipofectamine reagent in OPTIMEM serum free medium and incubated at room temperature for 20 minutes. At this time, the cells were washed 2-3 times with OPTIMEM; and the DNA-lipofectamine mixtures were added immediately to the cells. The cells were then incubated at 37°C for 5 hours to overnight until required. The same protocol but with reduced concentration of DNA were used for cotransfection. The conditions for transfection or cotransfection of each construct to each cell line are in appendix VIII.

### **2.3.3 Harvesting cells in RIPA buffer**

Cells were washed gently 2-3 times in cold PBS before being harvested in ice-cold RIPA buffer including 1 mM sodium orthovanadate, 100nM Calyculin A, 1mM PMSF, 10µM TPCK, 10µM Leupeptin, 1mM Pepstain, 10µg/ml Aprotinin, and 10µg/ml Benzamidine. These cells were lysed on ice (or at 4°C) for 30 minutes. The lysate was then collected by cell scraper, centrifuged for 15 minutes at 18000xg. The supernatant was used fresh or stored at -80°C until needed.

### **2.3.4 EGF treatment**

For the assay of activation of ERK, the cells on the dishes were washed 3 times with DMEM and then incubated at 37°C in DMEM supplemented with 20ng/ml EGF at 5% CO<sub>2</sub> for 1 hour.

### **2.3.5 UO126 treatment**

For the assay of inhibition of ERK, 10µM UO126, the ERK inhibitor, were added to the EGF treated or untreated cells and incubated at 37°C in DMEM at 5% CO<sub>2</sub> for further 30 minutes.

## **2.4 Protein Biochemistry methods**

#### **2.4.1 Quantification of protein concentration**

The protein concentration in cell extracts was quantified using MicroBCA protein quantification kit (Pierce), following the manufacturers' guidelines. A series of BSA solutions were prepared by diluting 2mg/ml BSA stock in distilled water to give a dilution series ranging from 20-200µg/ml. 2ml working reagent was added to each 1000µl of standard solution and incubated at 65°C for 1 hour. The OD<sub>562</sub> of each sample was measured and the values were used to plot a graph of BSA concentration versus OD<sub>562</sub>. Protein samples were treated in the same manner and the concentration was interpolated from the standard plot.

#### **2.4.2 SDS polyacrylamide gel electrophoresis (SDS-PAGE)**

SDS-polyacrylamide gels were run using the Mini-proteanII protein electrophoresis system (BioRad). The 10% separating gel solution was prepared and poured between two set of glass plates and allowed to polymerise at room temperature for 20-30 minutes followed by addition of the 5% stacking gel solution (1.66 ml 30% polyacrylamide solution, 2.5 ml stacking gel buffer, 5.76ml distilled water, 40µl TEMED, 120µl 10% APS) and a comb was inserted into the top of the gel. After the polymerisation was complete, the comb was gently taken out and the wells were washed with distilled water. The gel assembled was placed in the electrophoresis apparatus and the chamber and the tank were filled with 1x SDS-PAGE running buffer. Protein samples were mixed with an equal volume of 2x SDS loading buffer, boiled for 2 minutes and loaded onto the gels. Pre-stained broad range protein marker (NEB; size range 6.5-175 KDa) was used as the size marker. The gel was run for 20-30 minutes at 50V until the sample dye reached the interface of stacking gel and separating gel; then, the running voltage was increased to 100V for further 1.5-2 hour until the sample dye completely left the gel.

#### **2.4.3 Immunoprecipitation**

Cell extracts harvested in RIPA buffer (section 2.3.3) were quantified using MicroBCA assay (section 2.4.1). At this time, protein A Sepharose beads (50% slurry in RIPA buffer) was added to the sample at a final dilution of 1:10 and incubated at 4°C for 1

hour on a roller to reduce non-specific binding. The protein A Sepharose beads were removed by centrifugation at 18000xg for 30 seconds, and the supernatants were incubated with appropriate primary antibodies at 4°C for 2 hours on a roller. 50µl of Protein A Sepharose (50% slurry in RIPA buffer) was then added into each of cell extract and incubated at 4°C for a further 1 hour on a roller. Following the primary antibodies and protein A Sepharose interaction, the cell extracts were centrifuged at 4°C for 30 seconds at 18000xg, and the supernatant was removed. The protein A Sepharose beads were resuspended in ice-cold appropriate buffer and centrifuged as above; the wash was repeated for 3 times. After washing, the beads were used for SDS gel electrophoresis by adding SDS loading buffer, or used for other biochemical assay.

#### **2.4.4 Western blotting**

Proteins were electrophoretically transferred from the SDS-polyacrylamide gel to PVDF membrane using Trans-Blot cell transfer system (BioRad). The transfer was performed in CAPS/methanol transfer buffer and blotted at 4 °C for 1hour at 400mA.

#### **2.4.5 Antibody binding and detection (Alkaline phosphatase development)**

After protein transfer was complete, PVDF membrane was blocked in 5% skim milk powder in TBST buffer (V/W) for 30 minutes and then incubated overnight at 4°C with appropriately diluted primary antibodies in skimmed milk/TBST (see above) buffer on a roller. For the washing, the membrane was rinsed 3 times and washed 3 times (5 minutes for each wash) in TBST buffer. The appropriately diluted AP-conjugated secondary antibody (see Appendix V) was then added to the membrane in TBST buffer and incubated for 1 hour at room temperature. After the interaction, the membrane was washed 3 times (5 minutes for each wash) in TBST buffer; the membrane was then developed in AP buffer containing 0.4mM NBT and 0.4mM BCIP.

#### **2.4.6 Development of the expression of AP-dystroglycan construct**

AP-dystroglycan transfected cells were rinsed twice in PBS and fixed for 5 minutes at room temperature in PBS containing 3.7% formaldehyde. The cells were washed 3 times in PBS and treated with PBS containing 0.1% Triton X100 for 1 minute. The

buffer was then removed, and the cells were washed 3-5 times in PBS. After washing, the overexpressed proteins in the cells were detected using AP buffer containing 0.4mM NBT and 0.4mM BCIP, gently shaking at room temperature until the purple colour on the dishes was recognisable.

## **2.5 Protein immunofluorescence assay**

### **2.5.1 Immunofluorescent staining of transfected cells**

The transfected cells on coverslips were fixed at room temperature for 5 minutes in PBS containing 3.7% formaldehyde, washed 3 times in PBS and treated for 1 minute with PBS containing 0.1% of Triton-X100. After washing 3 times with PBS, the coverslips with cells were blocked at room temperature for 30 minutes in IFA blocking buffer and incubated at room temperature for 3 hours in IFA blocking buffer containing appropriately diluted primary antibodies (see Appendix V). The coverslips were washed 3 times before interacting with IFA blocking buffer containing appropriately diluted fluorescence-conjugated secondary antibodies and incubated at room temperature for 1-1.5 hours. After the interaction, the coverslips with cells were washed 3-5 times in PBS and sealed with mounting medium (Vector) on glass microscope slides.

### **2.5.2 Actin morphology**

To detect the morphology of actin filaments, the transfected or untransfected cells on coverslips were incubated at room temperature for 45 minutes in blocking buffer containing 1:1000 diluted Rhodamine-phalloidin (TRITC, Sigma). The coverslips were washed 3 times in PBS before being sealed as above.

### **2.5.3 Fluorescent microscopy**

The glass microslides with cell on the coverslips were viewed on Olympus BX60 fluorescent microscope equipped for epifluorescence and with IPLab (Scanalytics) image capturing software. Immersion oil (Olympus) was used on the coverslips for oil lens.

## 2.6 Construction of dystroglycan mutants

### 2.6.1 PCR mutagenesis

Sequences of dystroglycan or dystroglycan deletion mutants for cloning were generated by using a PCR mutagenesis technique. The PCR reaction mixture for 5 reactions were prepared as follow:

For 5 reaction	$\mu$ l
Distilled water	79.5
10x PCR buffer	10
12.5mM dNTPs	2
Forward primer (100 pmol/ $\mu$ l)	2
Reverse primer (100 pmol/ $\mu$ l)	2
Template plasmid (50ng/ $\mu$ l)	0.5
Taq polymerase	1
50mM MgCl <sub>2</sub>	3
	100

mDG-1 plasmid encoding full-length mouse dystroglycan was used as the template for generating full-length dystroglycan-GFP ( $\alpha\beta$ DG-GFP) construct. The construct  $\alpha\beta$ DG-GFP was then used as the template for constructing of dystroglycan deletion mutants. The reaction mixture was aliquoted into PCR reaction tubes and the reactions were carried out in a Biometra Personal Cycler (Whatman) with appropriate running conditions (appendix VII). The sequences of extracellular  $\beta$ -dystroglycan ( $\alpha\beta$ DG $\Delta\epsilon\beta$ ) or  $\alpha$ -dystroglycan deletion ( $\alpha\beta$ DG $\Delta\alpha$ ) mutants were generated by using overlap extension site directed mutagenesis. Two double-stranded DNA fragments containing sequence overlapping to each other were generated respectively by two pairs of primers (P1 and P2) in the first round of PCR reaction. The two products containing overlapping sequence generated from first round of PCR were then purified from agarose gel (section 2.2.7) and used as templates for second round PCR.



### 2.6.2 Purification of PCR products

The PCR products were excised from agarose gels as above (section 2.2.7). QIAquick gel extract spin kit was used to extract the DNA fragment from the agarose gels following the manufacturers' guidelines. The eluted DNA fragments were resuspended in 30 $\mu$ l distilled water and digested with the appropriate restriction enzyme (section 2.2.6). After the digestion, these DNA fragments were purified again in the same manner before being used for ligation.

### 2.6.3 Ligation of DNA

Vector and insert DNA fragments digested with appropriate restriction enzymes were mixed at a molar ratio 1:3 in 8 $\mu$ l of distilled water. The ligation of DNA fragments was carried out using Rapid Ligation Kit (Roche), following the manufacturers' guidelines. 20 $\mu$ l of ligation was used directly for transformation of calcium competent cells (section 2.2.3).

### 2.6.4 Colony screening by PCR

Single colonies containing recombinant DNA were screened by colony PCR. The PCR reaction mixture was prepared as follows;

<u>For 5 reaction</u>	<u><math>\mu</math>l</u>
Distilled water	80
10x PCR buffer	10
12.5mM dNTPs	2
Forward primer (100 pmol/ $\mu$ l)	2
Reverse primer (100 pmol/ $\mu$ l)	2
Taq polymerase	1
<u>50mM MgCl<sub>2</sub></u>	<u>3</u>
	100

20 $\mu$ l of the mixture was aliquoted into each PCR reaction tube, and several tubes of 2xYT liquid medium (3ml/tube) containing appropriate antibiotics were also prepared.

Single colonies were picked from the 2x YT solid medium plates by sterilised toothpicks; the cells were resuspended both in tubes with PCR reaction mixture and in tubes with 2XYT medium. The PCR reactions, 94°C 1 minute, 65°C 1 minute, 72°C 1 minute were run for 30 cycles; the PCR products were analysed by agarose gel electrophoresis to identify the containing plasmids. After the recombinant plasmids were selected, colonies carrying recombinant plasmid in the 2x YT liquid medium tubes were incubated at 37°C for overnight to amplify the plasmid.

## **2.7 Cell Adhesion assay**

### **2.7.1 Coating of coverslips**

Extracellular matrix proteins fibronectin, laminin or poly-L-lysine, were diluted in distilled water at the appropriate concentration and 100µl added to each sterilised 13mm glass coverslip. These coverslips were oven dried at 50°C for 1 hour until all the liquid was evaporated, and then were transferred to 24 well culture dishes. After washing 5 times in distilled water, these coverslips were airdried at room temperature for 1-2 hours until required. If not used fresh, the coated coverslips were stored at 4°C overnight.

### **2.7.2 Adhesion time course of transfected REF52**

Lipofectamine<sup>TM</sup> transfected REF52 cells (section 2.3.2) were trypsinized from tissue culture flasks or dishes and resuspended in DMEM medium in absence of serum. The suspended cells were washed once and diluted to the appropriate concentration in DMEM. These cells were then seeded onto matrix-coated coverslips in 24 well culture dishes and were incubated in 37°C incubator at 5% CO<sub>2</sub>. For the adhesion time course, 4 coverslips with cells were collected and fixed for microscopy (section 2.5.1 and 2.5.3) at each time point.

### **2.7.3 Substrate dependent assay of dystroglycan transfected REF52**

13 mm coverslips coated with 1µg/ml of fibronectin, poly-L lysine or laminin were placed in 24 well culture dishes as above (section 2.7.1). Dystroglycan or dystroglycan

mutant transfected cells were trypsinized and resuspended in DMEM in absent of serum. Resuspended cells were seeded onto coverslips in each well (approximately  $1 \times 10^6$ ) and incubated at  $37^\circ\text{C}$  for 3 hours. The coverslips were collected and fixed for microscopy (section 2.5.1 and 2.5.3).

## **2.8 ERK kinase activity assay**

### **2.8.1 Preparation of ERK kinase assay sample**

YFP-ERK construct was transfected into REF52 cells on  $100\text{mm}^2$  tissue culture dishes (approximately  $5 \times 10^6$  cells per dish) following the procedure in section 2.3.2. The transfected cells were incubated at  $37^\circ\text{C}$ , 5%  $\text{CO}_2$  overnight in DMEM supplemented with 10% FBS, and were washed 3 times with DMEM to remove the serum. The cells were then incubated in at  $37^\circ\text{C}$  in DMEM in the presence of EGF or UO126 (see section 2.3.4 and 2.3.5). After the treatment, the cells were gently washed 3 times with PBS and lysed on ice for 30 minutes in  $400\mu\text{l}/\text{dish}$  MAPK lysis buffer, supplemented with  $200\text{mM}$   $\beta$ -glycerophosphate,  $0.5\text{ mM}$  DTT and  $1\text{mM}$  orthovanadate. The cell lysates were collected by cell scraper and stored at  $-80^\circ\text{C}$  until required.

### **2.8.2 Myelin Basic Protein (MBP) ERK kinase activity assay**

In order to identified the expressed YFP-ERK from the endogeneous ERK, the cell lysates were immunoprecipitated with anti-GFP antibodies as above (section 2.4.3); MAPK washing buffer was used for the first and second of the Protein A Sepharose bead washes. After the washing was complete, the beads were washed twice in MAPK kinase buffer containing  $10\text{mM}$   $\beta$ -glycerophosphate,  $2\text{mM}$  DTT and  $0.5\text{mM}$  orthovanadate. At this time, the kinase mix containing  $170\mu\text{l}$  kinase buffer,  $10\mu\text{l}$  myelin basic protein and  $10\mu\text{l}$  cold ATP was prepared.  $10\mu\text{Ci}$   $[^{32}\text{P}]\text{-ATP}$  was added to the kinase mix in radiation hot room.  $25\mu\text{l}$  of this kinase mix was added to each protein A beads sample and the mixtures were incubated at  $30^\circ\text{C}$  for 20 minutes. After the incubation, the samples were centrifuged for 1 minute at  $18000\text{xg}$  and  $10\text{ ml}$  of supernatant from each sample was spotted on each  $3 \times 3\text{ cm}^2$  of P81 paper. The P81

paper squares with samples were immediately dropped into 0.5% phosphoric acid and washed three times for 5 minutes. After washing, the P81 paper squares were briefly rinsed with acetone and airdried for 20-30 minutes. The value of P32 was detected by using LS6500 Multi-purpose Scintillation Counter (Beckman).

**Chapter 3**  
**Expression of YFP -ERK construct in REF52 cells**

## 3.1 Introduction

### 3.1.1 ERK cascade

The transmission of extracellular signals into intracellular responses is a complex process that often involves the activities of mitogen-activated protein (MAP) kinases. Extracellular signal-regulated kinase (ERK) cascade, which is activated by the interaction of membrane receptors with the ECM, is one of the most important MAP kinase signalling cascades responsible for transmission of extracellular signals into intracellular responses (Nashida and Gotoh, 1993). ERK1 and ERK2 are proteins of 44 and 42 kDa that are 85% identical overall (reviewed in Boulton *et al.*, 1991) which are believed to have overlapping signalling capability and are also referred to as ERK1/2 or p44<sup>ERK1</sup> /p42<sup>ERK2</sup> (Morino *et al.*, 1995). ERKs are proline-directed serine-threonine kinases, which contain a T-E-Y (Thr-Gly-Tyr) sequence. The activation of ERKs refers to the dual phosphorylation of threonine and tyrosine (Tp-E-Yp) residues of its T-E-Y motif in response to diverse extracellular stimuli (reviewed in Cobb and Goldsmith, 2000). The activation of ERK1/2 involves a three kinase cascade consisting of Raf (MEKK or MAPKKK) which activates a MEK (MAPKK), which then stimulates a phosphorylation-dependent increase in the activation of ERK. Upon activation, ERK1/2, which is activated in the cytoplasm, translocates immediately to the nucleus and phosphorylates a variety of intracellular targets including transcription factors and transcriptional adaptor proteins, which regulate the expression of genes essential for cell proliferation, survival and growth (reviewed in Cyert, 2001). In mitogenesis, the translocation of ERKs to the nucleus is required for cell cycle progression and cell differentiation (Brunet *et al.*, 1999; Robinson *et al.*, 1998).

In addition to being activated through integrin-mediated focal adhesion signalling (section 1.5.2), the growth factor-induced ERK cascade is the major ERK signalling pathway that modulates cell proliferation and survival. The ERK cascade can be activated by soluble growth factors that interact with receptor tyrosine kinases (RTKs) including neuronal growth factor (NGF), epithelial growth factor (EGF) and platelet

derived growth factor (PDGF) (reviewed in Clark and Brugge, 1995). The signalling pathway from RTK to ERK1/2 is well studied (Fig 3.1) (reviewed in Pawson and Scott, 1997; Pearson *et al.*, 2001; Hunter, 1995). Ligand binding to RTKs stimulates the dimerisation of RTK subunits and increases its tyrosine kinase activity. Activation of RTKs leads to the autophosphorylation of its cytoplasmic domain, creating a motif that can be recognised by SH2 domain of Grb2 adaptor protein. The guanine nucleotide exchange factor (GEF) Son of Sevenless (SOS) protein, which interact with the SH3 domain of Grb2 then becomes engaged with the complex and induces Ras to exchange the GDP for GTP. GTP-liganded Ras is targeted to many effectors, including Raf. Ras binding to Raf results in a conformation change in Raf that localises it to the plasma membrane and increases its kinase activity to activate MEK-ERK cascade.

### 3.1.2 Aim of the experiment

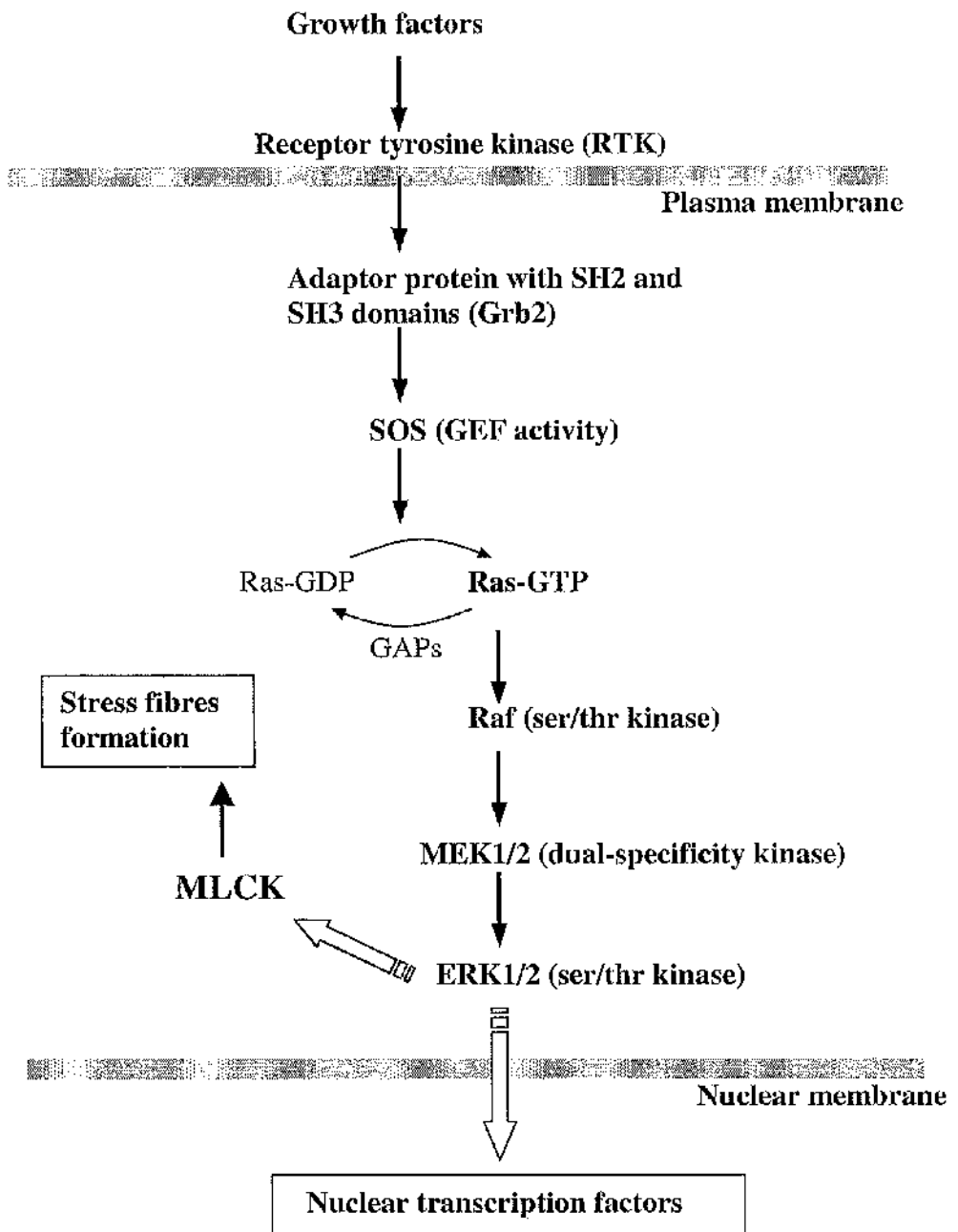
To determine whether dystroglycan plays a role in focal adhesion signalling and MLCK-induced actin stress fibre formation, mediated by activation of ERK, the first approach was to visualise the expression and localisation of ERK and dystroglycan during focal adhesion formation. Two fluorescent protein tagged constructs were made for this propose: YFP-ERK, a N-terminal yellow fluorescent protein-tagged p44<sup>ERK1</sup> / p42<sup>ERK2</sup> and  $\alpha\beta$ DG-GFP, a C-terminal GFP-tagged full-length dystroglycan. The constructs were expressed in REF52 cells. REF52 cells are an anchorage-dependent rat embryonic fibroblast cell, which spread rapidly and give rise to flat cells with prominent focal adhesions. They are widely used as a model for studying focal adhesion formation (Belkin and Smalheiser, 1996). We used the YFP-ERK construct to observe the localisation of ERK in focal adhesions and for further studies on the relationship between dystroglycan and ERK-dependent cytoskeleton reorganisation in the cytoplasm.

The expression and localisation of YFP-ERK in REF52 cells was determined by fluorescence microscopy. UO126 (C<sub>18</sub>H<sub>16</sub>N<sub>6</sub>S<sub>2</sub>), which is a chemically synthesised organic compound that inhibits MEK1/2, was used to examine the biological activity of overexpressed YFP-ERK in the cells. Since MEK1/2 is the only direct activator

### **Figure 3.1 RTK induced ERK cascade in mammalian cells**

Receptor tyrosine kinase (RTK) induced ERK cascade in mammalian cells. Binding of the growth factors leads to the dimerisation of RTK and autophosphorylation of the cytoplasmic domain of RTK. Phosphorylation of RTK creates a motif that can be recognised by SH2 domain of Grb2 followed by activation of SOS, which associates with Grb2 via the SH3 domain. Activated SOS acts as a Ras GEF that induces the exchange of Ras-GDP to Ras-GTP, the active form of Ras. The membrane associated Ras-GTP is then able to bind to the N-terminal of Raf, leading to the membrane localisation and a conformation change in Raf. The conformation change of Raf-1 also leads to the increase of its kinase activity to MEK1/2 that phosphorylates the serine/threonine residue of MEK1/2. Active MEK1/2 subsequently phosphorylates the T-E-Y motif of ERK1/2. The active ERK1/2 can translocate to the nucleus followed by activation of its substrates including transcription factors and other transcription-related kinases to promote relevant gene transcription and regulate the survival events of the cell. Activation of ERK in cytoplasm has also been shown to induce the activation of MLCK and play a role in enhancing the formation of actin stress fibres.





identified for ERK1/2, UO126 is sufficient to inhibit the activation of ERK1/2 in the cascade (Davies *et al.*, 2000). The effect of treating the cells with UO126 on the translocation of YFP-ERK was observed in REF52 cells; the activity of YFP-ERK was then determined by using western blotting and MBP-ERK activity assay. Finally, the activation of YFP-ERK at focal adhesion sites in REF52 cells was determined by immunofluorescence staining of the YFP-ERK expressing cells using an anti-talin antibody. The expression and localisation of  $\alpha\beta$ DG-GFP in REF52 cells are examined and discussed in chapter 4.

## 3.2 Results

### 3.2.1 Expression of YFP-ERK in REF52

A YFP-ERK construct was made by subcloning the p44<sup>ERK1</sup> cDNA into pRESYFP mammalian cell expression vector. To examine the expression of the construct and the localisation of the YFP-ERK fusion protein in focal adhesions, the YFP-ERK construct was transfected into REF52 cells. By counting the YFP positive cells by microscopy, the transfection efficiency of YFP-ERK construct or pRESYFP empty vector in REF52 cells was determined to be 25-30% or 40% on average, respectively. In the transfection of YFP-ERK, but not pRESYFP, large numbers of cell were found rounded, lysed and floating in the culture medium after the standard transfection procedure, revealing that the transfection and expression of YFP-ERK might be lethal to the REF52 cells.

The expression of YFP-ERK in REF52 is shown in figure 3.2. A relatively high amount of YFP-ERK protein is concentrated at the nuclear region rather than distributed in the cytoplasm (Fig 3.2 A). In contrast, the expression of YFP was distributed all around the cell body while higher concentration at nuclear region was still recognisable (Fig 3.2 B). The activation of ERK has been shown to occur in the cytoplasm followed by ERK translocating to nucleus for mitogenetic signalling (reviewed in Pouyssegur et al., 2002). The highly concentrated nuclear localisation of YFP-ERK which is consistent with what has been shown in the immunostaining of endogeneous active ERK indicates that the biological activity of the overexpressed YFP-tagged ERK might not be altered.

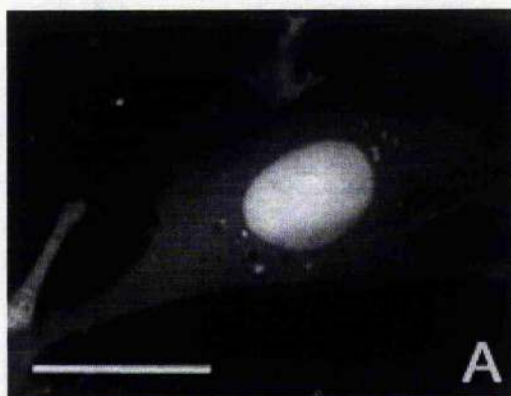
### 3.2.2 Western blotting assay of YFP-ERK activity

The expression and activity of YFP-ERK in REF52 cells was further determined by using western blotting. As shown in figure 3.3, the expression of YFP-ERK was detected by either anti-total ERK antibodies or anti-GFP antibody, and UO126 treatment has no effect on the expression of YFP-ERK in REF52 cells (Fig 3.3 A and B, upper panels). The expression of endogeneous ERK1 and ERK2 were unaffected by expression of either YFP-ERK or pRESYFP whether UO126 is present or not (Fig 3.3 A, lower panel). The activity of YFP-ERK was determined by an anti-phospho ERK antibody,

**Figure 3.2 Overexpression of YFP-ERK construct in REF52 cells**

YFP-ERK (2 $\mu$ g/ $\mu$ l) or pRESYFP empty vector (2 $\mu$ g/ $\mu$ l) were transfected into REF52 cells plated on glass coverslips using the standard transfection procedure. The transfected cells were incubated overnight and fixed with 3.7% formaldehyde. YFP-ERK expressed in REF52 cells was clearly concentrated in nucleus (A). The YFP expressed in REF52 cells was distributed all around the cell body, including the nucleus (B). Scale bar= 25 $\mu$ m.

**YFP-ERK**



**pRESYFP**

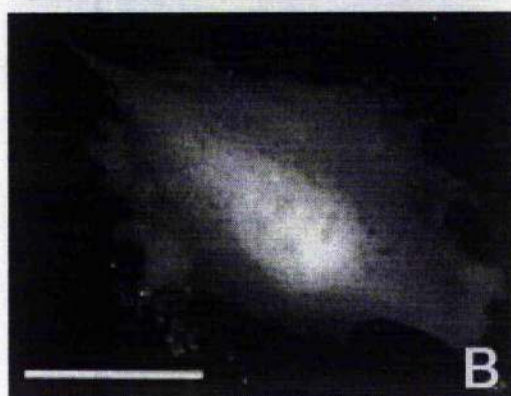
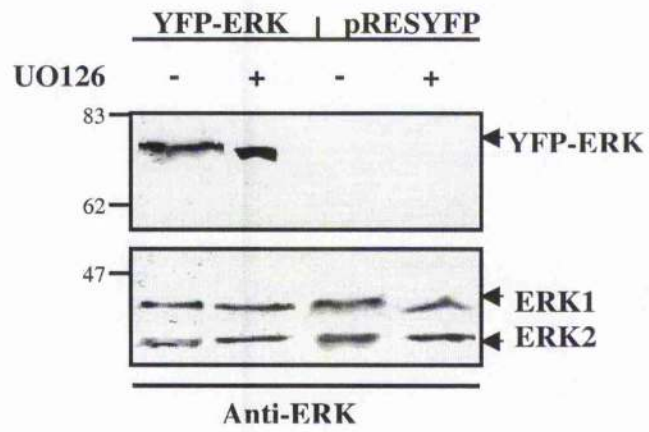


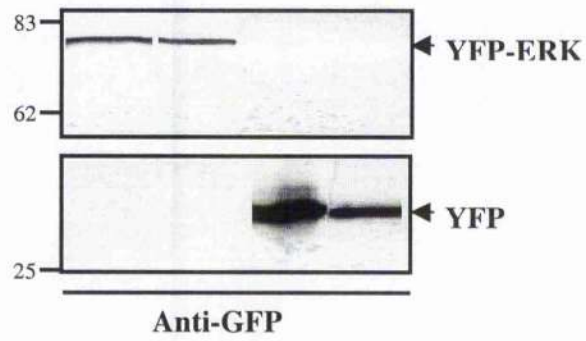
### **Figure 3.3 Expression and inhibition YFP-ERK in REF52 cells**

YFP-ERK (2 $\mu$ g/ $\mu$ l) or pRESYFP (2 $\mu$ g/ $\mu$ l) transfected REF52 cells with or without UO126 treatment were washed 3 times with PBS buffer lysed in SDS loading buffer. The expression and activity of YFP-ERK were detected by western blot with anti-ERK (A), anti-GFP (B) or anti-phospho ERK (C) antibodies, the dilution of primary antibodies in all cases are 1:1000. The expression of YFP-ERK was detected by anti-ERK or anti-GFP and showed no difference on UO126 treatment (**upper panel, A and B**). Expression of endogenous ERK1 and ERK2 were constant in the absence or presence of UO126 (**lower panel, A**). The activation of YFP-ERK and endogenous ERK1 and ERK2 were detected by anti-phospho-ERK, all active forms of ERKs were completely inhibited by UO126 treatment (**upper panel C**). For empty vector expression control, YFP expression was detected by anti-GFP antibodies (**lower panel, B**). Expression of ERK1 and ERK2 were constant (**lower panel A**) and the activity of ERK was inhibited by UO126 (**lower panel C**).

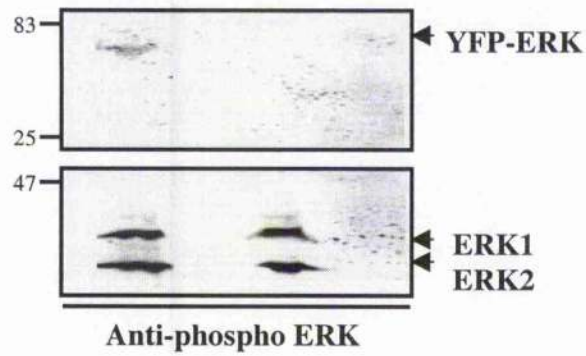
**A**



**B**



**C**



which only recognises the active form of ERK (Fig 3.3 C). Compared with the total expression of YFP-ERK detected by anti total ERK (Fig 3.3 A, upper panel), in the same amount of protein loading, only a small amount of YFP-ERK fusion protein was detected as activated. This activity of YFP-ERK (Fig 3.3 C upper panel), as well as endogenous ERK1 and ERK2 (Fig 3.3 C lower panel), is completely inhibited in the presence of UO126. These results suggested that firstly, the expression and activation of endogenous ERK1 and ERK2 is not affected by the expression of YFP-ERK. Secondly, part of the expressed YFP-ERK was activated and this activity was inhibited by UO126. Finally, UO126 treatment does not inhibit the expression but does inhibit the activation of YFP-ERK.

### **3.2.3 Effects of UO126 on YFP-ERK in REF52 cells**

To further examine the biological activity of the overexpressed YFP-ERK, localisation of inactivated YFP-ERK was observed in the presence of UO126. As shown in figure 3.4, UO126 treatment had no effect on the cells expressing YFP. YFP was distributed around the cell body and in the nucleus in the presence or absence of UO126 (Fig 3.4 A and C). In contrast, UO126 treatment led to a loss of nuclear localisation of YFP-ERK. By comparison with the UO126 untreated YFP-ERK transfected cells, where most overexpressed protein was concentrated in the nuclear region (Fig 3.4 E), no or very little YFP-ERK was found localised in the nuclear region in the transfected cells treated with UO126 (Fig 3.4 G, solid arrow). More YFP-ERK was distributed in the cytoplasm rather than concentrated in the nuclear region in the present of UO126. These results suggested that the inhibition of the ERK activity of YFP-ERK prevents YFP-ERK from its nuclear translocation. Thus, YFP-ERK was expressed with biological activity in the REF52 cells. UO126 treatment has no significant effect on YFP, suggesting that the translocation of YFP-ERK was caused by the inhibition of ERK activation rather than an effect on the YFP.

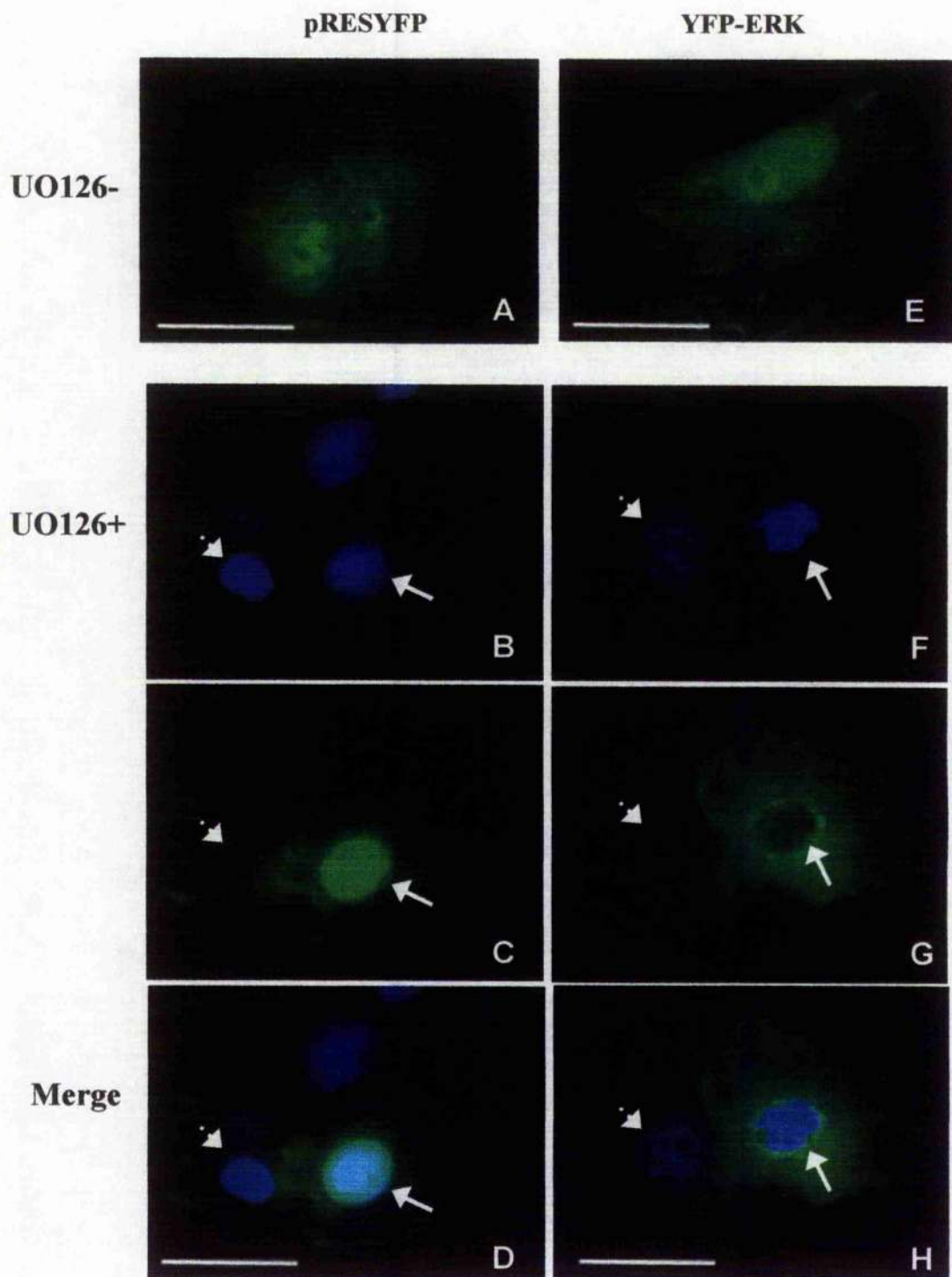
### **3.2.4 MBP kinase activity assay of YFP-ERK**

To further determine whether the biological activity of YFP-ERK was altered, the upstream pathway that activates YFP-ERK was examined. The serum-starved YFP-ERK



**Figure 3.4 UO126 treatment of YFP-MAPK overexpressed REF52 cells**

REF52 cells plated on glass coverslips were transfected with pRESYFP empty vector (2 $\mu$ g/ $\mu$ l) or YFP-ERK (2 $\mu$ g/ $\mu$ l) following the standard transfection procedure. The transfected cells were incubated in DMEM containing 50 $\mu$ M UO126 at 37°C for 30 min and fixed with 3.7% formaldehyde. The coverslips were sealed with mounting media (Vector), and the nucleus was stained as blue. Nuclear morphology of pRESYFP and YFP-ERK transfected cells in the presence of UO126 are shown in **B and F**. Compared with the untreated cells (**A**), treatment of UO126 in pRESYFP transfected cells showed no effect on the localisation of YFP (**C**). In YFP-ERK transfected cells, nuclear localisation of YFP-ERK was seen in UO126 untreated cells (**E**); treatment of UO126 led to loss of the nuclear localisation of YFP-ERK, YFP-ERK was distributed in cytoplasm (**G**). The merged image showed that in YFP-ERK transfected cells, the nuclear region is completely dark in the presence of UO126 (**H**), and the localisation of YFP was not affected by the treatment of UO126 (**D**). Dashed arrows point to the untransfected, and solid arrows points to the transfected cells. Scale bar =25 $\mu$ m



transfected REF52 cells were plated on fibronectin or treated with EGF to examine whether ERK activity of YFP-ERK can be triggered by integrin engagement or RTK activation. As shown in figure 3.5, cells replated on fibronectin or treated with EGF showed significantly higher ERK activity (Fig 3.5, FN and EGF) than control cells plated on uncoated (Fig3.5, CON) or poly-L-lysine coated (Fig3.5, PLL) culture dishes. The activity of YFP-ERK was reduced nearly to the background level by treatment of UO126 (Fig 3.5, FN+UO and EGF+UO), indicating that the YFP-ERK has its ERK activity, which is sensitive to UO126. This result suggested that the ERK activity of YFP-ERK could be stimulated by either integrin-mediated and growth factor-initiated signalling events. The activation of YFP-ERK triggered by EGF receptor is stronger than that induced by integrin, revealing the characteristics of overexpressed YFP-ERK is consistent with wild type or endogenous ERK (Morino *et al.*, 1995).

### 3.2.5 Adhesion time course

The ERK activity of YFP-ERK fusion protein was sufficient to be detected by immunoblotting and MBP activity assay. However, to study the role of ERK in the cytoplasm, the visualisation of YFP-ERK in adhesion sites is required. In the YFP-ERK transfected cells, the overexpressed YFP-ERK was diffuse all over the cell body and no adhesion-like structure could be recognised (Fig 3.2 A). The formation of focal adhesions and the activation of ERK has been determined in REF52 cells (Fincham *et al.*, 2000). The YFP-ERK here has been determined to be a functional ERK. Thus, lack of visualisation of adhesion structures in the YFP-ERK transfected REF52 cells might be because the adhesion sites were difficult to recognise when YFP-ERK protein was expressed at very high levels and diffuse all over the cell body in the REF52 cells.

To address to this question, the YFP-ERK transfected REF52 cells were replated onto laminin coated glass coverslips and the change in localisation of YFP-ERK was monitored during cell adherence over 1-16 hours. As shown in figure 3.6 D, YFP-ERK transfected cells 16 hours after the transfection procedures; the nuclear localisation of YFP-ERK suggested that it was activated. In this state, no or very little adhesion was

### **Figure 3.5 MBP-ERK activity assay in YFP-ERK transfected REF52 cells**

REF52 cells were transfected with YFP-ERK (2 $\mu$ g/ $\mu$ l) following the standard procedure. The transfected cells were incubated overnight and resuspended in DMEM in absent of serum. These transfected cells were replated on uncoated (**CON**), 10 $\mu$ g/ml poly-L-lysine coated (**PLL**) or 10 $\mu$ g/ml fibronectin coated (**FN**) culture dishes and incubated at 37 $^{\circ}$ C for 2.5 hr. For EGF treatment, 20ng/ml EGF was added to the cells at the first hour replated on uncoated culture dish and the cells were then incubated at 37  $^{\circ}$ C for a further 1.5 hours (**EGF**). For UO126 treatment, 50 $\mu$ M UO126 was added to the cells replated on uncoated (**CON+UO**), FN coated (**FN+UO**) or to EGF treated (**EGF+UO**) cells and incubated at 37  $^{\circ}$ C for a further 30 minutes. The ERK kinase activity of YFP-ERK in cells plated on FN (**FN**) and treated with EGF (**EGF**) is significantly higher than in the control cells. The ERK activity of YFP-ERK is reduced nearly to the background as a result of UO126 treatment (**CON+UO**, **FN+UO** and **EGF+UO**). Kinase assays were carried out in triplicate for each sample. The assay was repeated twice in different transfections. Data shown are the mean +SD.

**ERK activity assay in YFP-ERK transfected REF52 cells**

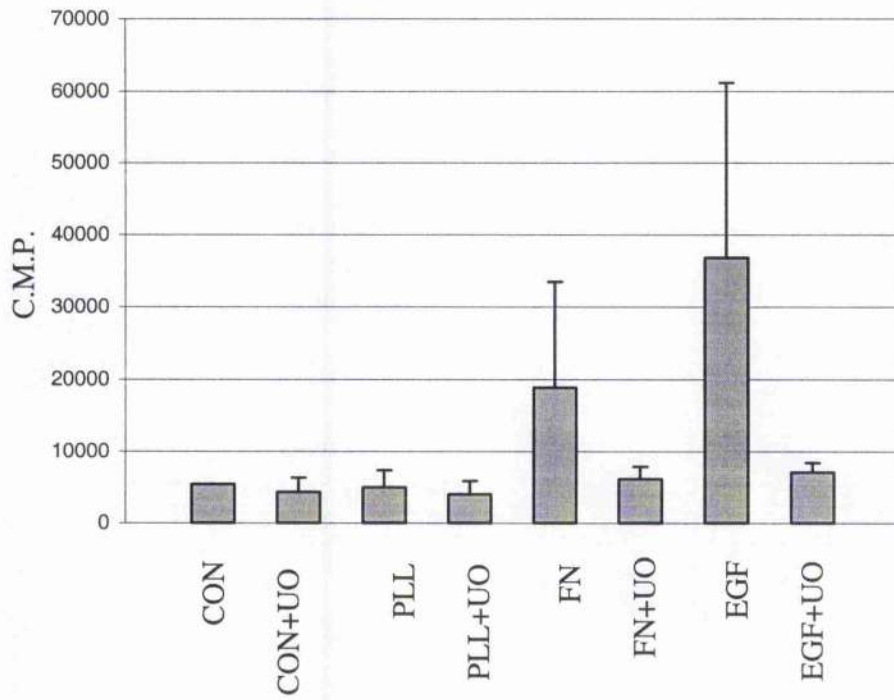
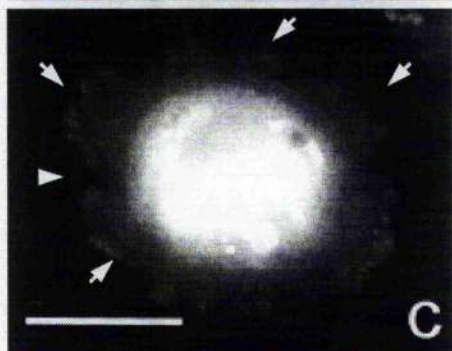
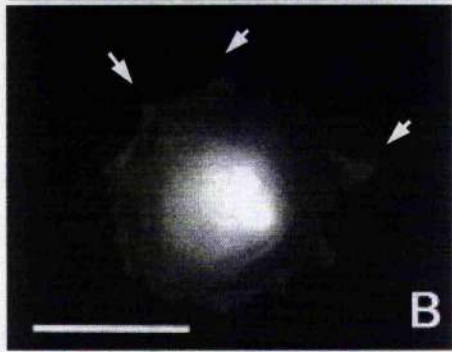
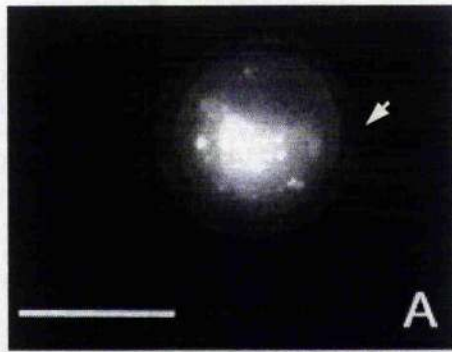


**Figure 3.6 Adhesion timecourse of YFP-ERK transfected REF52 cells**

YFP-ERK (2 $\mu$ g/ml) were transfected into REF52 cells following the standard procedure. The transfected cells incubated overnight were replated onto laminin-coated coverslips and incubated at 37°C for 4 hour in DMEM (A-C) or incubated at 37 for 16 hours in DMEM with 10% FBS (D). The coverslips incubated in serum free DMEM were fixed after 1, 2 and 4 hours during spreading and the coverslips incubated in serum containing DMEM were collected at 16 hours. The coverslips were fixed with 3.7% formaldehyde. After 1 hour, transfected cells had attached to the laminin. Some lamellipodia-like structures had started to form at the cell periphery (**A arrow**). YFP-ERK based adhesion-like structures appeared after 2 hours (**B arrows**). The numbers of these structures are increased to maximal levels after 4 hours (**C arrows**). YFP-ERK was distributed all over the cell and no adhesion structure could be recognised after 16hr incubation (**D**). The scale bar = 25 $\mu$ m



found in the well-spread transfected cells. However, adhesion-like structures are found during cell spreading (Fig A-C). One hour after spreading, some membrane ruffling and lamellipodia-like structures are formed in the cell periphery (Fig 3.6 A, arrows). Adhesion-like structures were found after 2 hours (Fig 3.6 B arrows), and the number of these structures maximised after 4 hours (Fig 3.6 C, arrows). The time-lapse images of the translocation of YFP-ERK revealed that YFP-ERK does localise at the adhesion-like site during cell spreading. However, after 4 hours when the cell gradually came to a well-spread state, active and inactive YFP-ERK were present all over the cell, and the specific YFP-ERK-based adhesion-like structures were no longer recognisable.

### **3.2.6 Localisation of ERK at focal adhesion sites in REF 52 cells**

To further examine the adhesion structures formed in the REF52 cells expressing YFP-ERK during spreading, the YFP-ERK expressing cells were costained with anti-talin, which is a focal adhesion structure protein widely used as a marker of focal adhesion (Belkin and Smalheiser, 1996). As shown in figure 3.7, the YFP-ERK-based adhesion-like structures in REF 52 cells (Fig 3.7 A, arrows) were recognised by anti-talin antibody as well (Fig 3.7 B arrows). The merged image of the adhesion site revealed that the YFP-ERK was not completely colocalised with talin at focal adhesion site (Fig 3.7 C, box). The closer examination of this structure in the merged image showed that YFP-ERK is closer to the plasma membrane to talin staining, an overlap of approximately 1 $\mu$ m was seen between YFP-ERK and talin (Fig 3.7 D), revealing that YFP-ERK localises at the tip of adhesion-like structures. It has been shown by immunostaining that active ERK is localised at the tip of talin-based focal adhesion sites in the newly forming leading edge in REF52 (Fincham, *et al.*, 2000). This staining pattern of talin and YFP-ERK is similar to that has been shown by Fincham and colleagues. However, these adhesion-like structures produced by YFP-ERK in REF52 cells do not appear to be typical adhesion structures. Therefore, it is necessary to determine whether YFP-ERK localised at the adhesion-like structure is expressed in an active form.

### **3.2.7 Activity of ERK at focal adhesion sites in REF52**

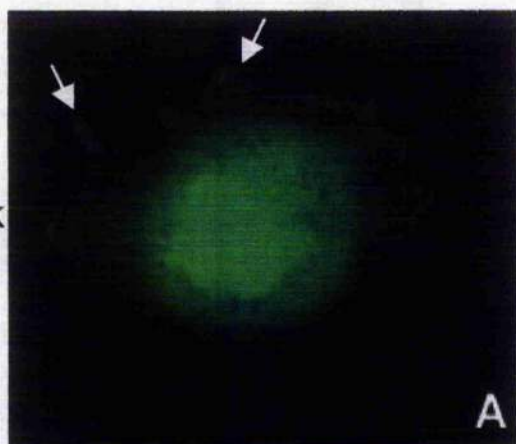
In an attempt to use the YFP-ERK construct to study dystroglycan signalling, a method



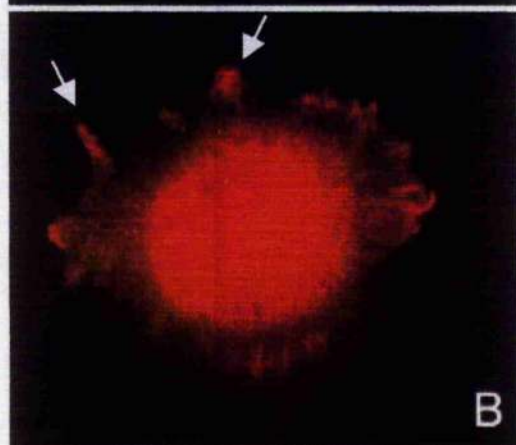
**Figure 3.7 Colocalisation of YFP-ERK and talin in the adhesion sites in REF52 cells**

YFP-ERK (2 $\mu$ g/ml) was transfected into REF52 cells following the standard procedure. The transfected cells were replated onto laminin-coated coverslips and incubated at 37°C for 4 hour in DMEM (A-C). The coverslips were fixed with 3.7% formaldehyde and stained with anti-talin [(Sigma) at 1:1000]. At the fourth hour of cell spreading, YFP-ERK based adhesion structures were found most in one side of the cell (A arrows). These structures were stained by anti-talin antibody as well (B arrows). The merged image shows the localisation of YFP-ERK and talin are very close (C arrows). The magnified image showed that the YFP-ERK was not completely colocalised with talin (D). The scale bars =25  $\mu$ m in C and =5  $\mu$ m in D.

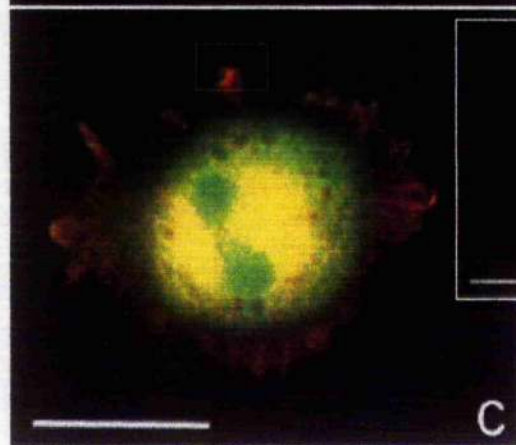
**YFP-ERK**



**Talin**



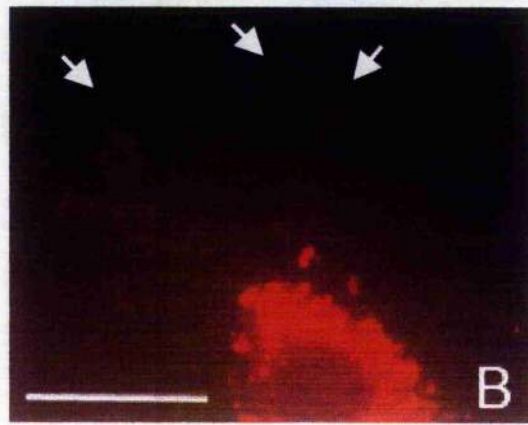
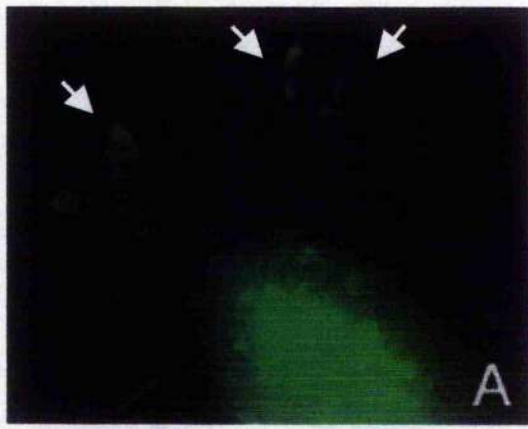
**Merge**



to determine the activation of YFP-ERK in the adhesion sites is necessary. The anti-phospho ERK (NEB9105), which has shown to be very efficient for immunofluorescent staining of the active ERK, was used to detect the activation of YFP-ERK in adhesion sites. As shown in figure 3.7, however, the staining of anti-phospho ERK at the adhesion sites in YFP-ERK transfected REF52 cells was very weak (Fig 3.8 B, arrows) while YFP-ERK is forming relatively clear adhesion-like structure in the cell periphery (Fig 3.8 A, arrows). This result suggested that either the antibody we were using might not be sufficient to detect the phosphorylation of the activity of YFP-ERK *in vivo* by immunofluorescent staining, or the YFP-ERK might not be activated at these adhesion-like sites.

**Figure 3.8 Phospho-specific ERK antiserum staining of focal adhesions in YFP-ERK transfected REF52 cells**

YFP-ERK (2 $\mu$ g/ml) was transfected into REF52 cells following the standard procedure. The transfected cells were replated onto laminin-coated coverslips and incubated at 37°C for 4 hour in DMEM (A-C). The coverslips were fixed with 3.7% formaldehyde and stained with anti-pY ERK [(NEB) at 1:100]. At the fourth hour of spreading, YFP-ERK was localised at the adhesion sites in the cells (**arrows, A**). Extremely weak phospho-ERK was stained at the same adhesion sites (**arrows, B**). The scale bars =25 $\mu$ m



### 3.3 Discussion

To investigate whether dystroglycan is involved in the integrin-mediated ERK-dependent activation of MLCK, YFP-tagged ERK was constructed and expressed in REF52 cells. The ERK kinase activity assay of YFP-ERK which were carried out by using UO126 inhibition, western blotting assay and MBP-ERK kinase activity assay has shown that YFP-ERK is expressed as a functional ERK in REF52 cells. The localisation of YFP-ERK was clearly visible in the REF52 cells. Compared with the localisation of YFP, YFP-ERK was more concentrated at the nucleus, indicating the YFP-ERK is an active kinase. Additionally, the MBP ERK activity assay showed that both EGF and fibronectin could induce the activation of YFP-ERK, indicating that the activity of YFP-ERK is upregulated by either integrin-mediated or RTK-induced pathway. Together this suggested that the recombinant YFP-ERK in REF52 cells behaves like the wild type ERKs. Thus, the YFP-ERK construct could successfully produce an YFP-tagged functional ERK in REF52 cells.

#### 3.3.1 Regulation of expression and activation of YFP-ERK

On western blotting, most endogenous ERK1/2 in REF 52 cells was detected as the active form (Fig 3.3 A lower panel and C lower panel). However, compared with the total expression of YFP-ERK, only a small amount of YFP-ERK is activated (Fig 3.3 A upper panel and C upper panel). This result revealed that despite overexpression of YFP-ERK in the REF52 cells, only a constant amount of ERK was activated, implying a feed-back regulation might exist between ERK and its upstream regulators to control the activation of ERK. ERK is an important signalling molecule that enhances the cell adhesion, proliferation and survival signalling events, overexpression of ERK appeared to be lethal to the cells (section 3.2.1). Thus, a mechanism that regulates active ERK at a constant level in cells might be necessary. It has been shown that activation of integrin was suppressed by the activation of Ras-induced ERK cascade (Hughes *et al.*, 1997), supporting the idea that a negative regulation of ERK by its upstream regulator might be able to maintain the active ERK in a constant level. Additionally, a series of scaffold proteins of ERK cascade mediators was identified in yeast (reviewed in Pryciak, 2001).

In mammalian cells, scaffold protein MP-1 (MEK Partner-1) binds specifically to MEK-1 and ERK-1 to form a protein complex that enhances the activation of ERK1/2 and its downstream signalling (Schaeffer *et al.*, 1998). KSR-1 (Kinase Suppressor of Ras) was shown to bind MEK and ERK (Therrien, *et al.*, 1996). Activation of Ras has been shown to lead to the conformational activation of Raf, thereby recruiting KSR-1 along with MEK and ERK to the membrane region (Yu *et al.*, 1998). Overexpression of KSR inhibited ERK-dependent biological effects (Cacace *et al.*, 1999). Such a dose-dependent reversal of effect is typical for a scaffold protein that can only assemble its target protein when present in an appropriate stoichiometric ratio, but disperses the signalling complexes when overexpressed (Walter, 2000). Thus, although the regulation mechanism of MP-1 and KSR remains unclear, it is likely that the constant amount of activation of ERK is regulated by the interaction of ERK cascade mediators with scaffold proteins.

### **3.3.2 Translocation of YFP-ERK**

Initially, YFP-ERK was constructed to visualise the activation of YFP-ERK at focal adhesion sites. However, in REF52 cells, no YFP-ERK based-adhesion was found until the transfected cells were replated onto laminin. The time-lapse experiment showed that YFP-ERK-based adhesion-like structures were forming during 1-4 hours after replating. Interestingly, the result also showed that very little YFP-ERK was localised in the nuclear region during this period, indicating that activation of YFP-ERK for cytoplasmic function might be taking place earlier than that for mitogenesis during the cell spreading. It has been shown that the adhesion dependent activation of ERK was continually maintained at a constant level within few hours after cell spreading whereas the mitogen-dependent ERK activation increased rapidly and decreased to a level nearly equal to background levels within minutes (Pouyssegur *et al.*, 2002). Thus, the YFP-ERK expressed in REF52 cells in 1-4 hour during spreading might not be involved in the mitogenesis but involved in cytoplasmic focal adhesion signalling regulation in the first 4 hours after the replating.

YFP-ERK accumulates in the nucleus as a result of long-term expression (Fig 3.2 A). Figure 3.2 A clearly showed that YFP-ERK is localised in the nucleus as a long-term effect of expression of YFP-ERK. In serum-starved NIH 3T3 cells, the nuclear accumulation of active ERK was increased maximally within 10 minutes after serum stimulation, and the nuclear accumulation of ERK was reduced gradually within 2 hours until the ERK accumulation level in the nucleus was reduced nearly equal to the background, indicating the ERK activation for mitogenesis takes place within 10 minutes after stimulation. However, under the same conditions, total ERK started to translocate to the nucleus within 10 minutes and continued to accumulate, reducing the maximal level after 3 hours (reviewed in Pouyssegur *et al.*, 2002). This nuclear accumulation of ERK remained at a high level for 6 hours. These ERK translocation studies suggested that both active and inactive ERK are able to translocate to the nucleus; the translocation of ERK to the nucleus might be in an ERK activation-independent manner. In this study, we therefore do not know if the YFP-ERK localised at the nucleus is either the active or inactive form of ERK. The activation of YFP-ERK could not be determined by its translocation to nucleus.

### **3.3.3 Localisation of YFP-ERK at focal adhesion sites**

The YFP-ERK-based adhesion-like structures formed during spreading were not completely colocalised with talin. The staining pattern of talin with YFP-ERK in the adhesion-like structures was similar to that shown by Fincham and colleagues (Fincham *et al.*, 2000). However, no active YFP-ERK was found using anti-phospho ERK antibody at the adhesion sites by immunofluorescent staining. The western blot activity assay of YFP-ERK and endogenous ERK showed that most of the endogenous ERK in REF52 cells was active while only a very small amount of YFP-ERK, which was expressed in a fairly high level, was active (Fig 3.3). This suggested that the overexpression of YFP-ERK in the REF52 cells, MEK, the direct activator of ERK, might tend to interact with endogenous ERK rather than the highly expressed recombinant YFP-ERK. Therefore, despite the high expression, only a little of YFP-ERK could be activated in the ERK cascade. This might explain the failure of the phospho-ERK staining at YFP-ERK based adhesion sites.



Additionally, the distribution and morphology of YFP-ERK-based adhesion structures do not seem like the typical focal adhesion structures although some of them are colocalised with talin. Moreover, perhaps due to the strong expression and lack of the control by other signalling molecules, the YFP-ERK tends to diffuse throughout the whole cell body and make the adhesion-like structures become difficult to distinguish. Initially, YFP-ERK was constructed in an attempt to visualise the localisation of active ERK in the cytoplasmic compartment and for the further study of dystroglycan and MLCK dependent actin regulation. Unfortunately, these disadvantages suggested that YFP-ERK might not be a perfect tool for these studies. However, due to the visible nuclear translocation and the biological activity, the YFP-ERK construct still could be a useful tool for studying of the activation and translocation of ERK in mitogenesis.

**Chapter4**  
**Expression of GFP-tagged dystroglycan and dystroglycan functional**  
**domain deletion mutants**

## 4.1 Introduction

In order to investigate the relationship between dystroglycan and ERK at focal adhesion sites, YFP-ERK and dystroglycan-GFP expression vectors were constructed. As shown in chapter 3, YFP-ERK was poorly localised at focal adhesion sites, revealing that the YFP-ERK construct might not be useful for the study of localisation of ERK at focal adhesions and the further study of dystroglycan signalling. Here, the dystroglycan-GFP ( $\alpha\beta$ DG-GFP) was constructed and expressed in REF52 cells. The expression of  $\alpha\beta$ DG-GFP, however, surprisingly greatly altered the organisation of the cytoskeleton resulting in the formation many microspikes in REF52 cells, indicating that dystroglycan may act as a mediator of filopodia formation. Thus, the work has shifted to this interesting topic: the function of dystroglycan in the formation of microspikes. First of all, it was determined that the filopodia formation and the filopodia phenotype is in response to the expression of dystroglycan. Then, a series of GFP-tagged dystroglycan functional domain deletion mutants were constructed and expressed in REF52 cells to determine which functional domains of dystroglycan are responsible for the filopodia formation. The filopodia phenotype induced by each dystroglycan mutant construct was observed. Finally, the dystroglycan dependent cytoskeleton reorganisation signalling will be examined and discussed in chapter 5.

## 4.2 Result

### 4.2.1 Construction of GFP-tagged dystroglycan and functional domain deletion mutants

$\alpha\beta$ -dystroglycan is expressed as 859 a.a. propeptide in cells. This propeptide undergoes post-translational modification to generate mature  $\alpha$ - and  $\beta$ -dystroglycan, and the mature  $\alpha$  and  $\beta$ -dystroglycan are presented on the plasma membrane. Functional domains on dystroglycan have been determined (fig1.2) (Ibraghimov-Beskrovnaya *et al.*, 1992). In this study,  $\alpha/\beta$ dystroglycan is delineated as 5 functional domains: N-terminal signal sequence (SS; 1-28a.a),  $\alpha$ -dystroglycan ( $\alpha$ ; 29-653a.a), extracellular domain of  $\beta$ -dystroglycan (c $\beta$ ; 654-750a.a), transmembrane domain of  $\beta$ -dystroglycan (TM; 751-774) and cytoplasmic domain of  $\beta$ -dystroglycan (c $\beta$ ; 775-893) (Fig 4.1A). Full-length mouse dystroglycan cDNA (2679 bp.) was subcloned between the SalI and SmaI sites in the pEGFP mammalian expression vector. GFP was conjugated at the C-terminus of the dystroglycan. For construction of GFP-tagged dystroglycan functional domain deletion mutants see figure 4.1 B.

### 4.2.2 Examination of GFP-tagged dystroglycan construct ( $\alpha\beta$ DG-GFP) in REF52 cells

#### 4.2.2.1 Expression of $\alpha\beta$ DG-GFP in REF52 cells

The concentration of  $\alpha\beta$ DG-GFP (1.8  $\mu$ g/ml) used for transfection was modified for REF52 cells to achieve the highest transfection efficiency and the lowest cell death. The transfection efficiency of  $\alpha\beta$ DG-GFP obtained in REF52 cells was 15-20 % on average. Compared with the cells expressing GFP empty vector that showed a very smooth cell periphery (Fig 4.2 A), the cells expressing  $\alpha\beta$ DG-GFP presented many long and thin microspikes throughout the plasma membrane (Fig4.2 C-E). These microspikes also presented on cell surface (Fig 4.2 C, arrows). Some of these microspikes were clustered together forming a crown-like structure (Fig 4.2.D arrows). Transfection of  $\alpha\beta$ DG-GFP construct has altered certain signalling events leading to this morphology change.

**Figure 4.1 Construction of dystroglycan-GFP and dystroglycan functional domain deletion mutants**

(A), Dystroglycan has five distinct functional domains. From N-terminus; **SP**: N-terminal signal peptide, 1-28 a.a.;  **$\alpha$** :  $\alpha$  dystroglycan, 29–653 a.a.; **e $\beta$** : extracellular domain of  $\beta$ -dystroglycan, 654-750 a.a.; **TM**: transmembrane domain of  $\beta$  dystroglycan, 751-774 a.a.; **c $\beta$** : cytoplasmic domain of  $\beta$ -dystroglycan, 775-893 a.a. (B), The GFP-tagged dystroglycan and dystroglycan functional domain deletion mutants. GFP (220a.a) is conjugated at the C-terminal of dystroglycan or dystroglycan mutants.  **$\alpha\beta$ DG-GFP**: Full-length  $\alpha$ - and  $\beta$ -dystroglycan (893a.a).  **$\alpha\beta\Delta$ c $\beta$ DG-GFP**:  $\beta$ -dystroglycan cytoplasmic domain (c $\beta$ ; 121a.a) deletion mutant. **c $\beta$ DG-GFP**: GFP-tagged 121a.a  $\beta$ -dystroglycan cytoplasmic domain.  **$\beta$ DG-GFP**: GFP-tagged full-length  $\beta$ -dystroglycan (242a.a).  **$\alpha\beta\Delta\alpha$ DG-GFP**:  $\alpha$ -dystroglycan (625a.a) deletion mutant; full-length  $\beta$ -dystroglycan is directly fused at the C-terminal of signal peptide (SP, 29a.a).  **$\alpha\beta\Delta$ e $\beta$ DG-GFP**:  $\beta$ -dystroglycan extracellular domain (97a.a) deletion mutant.  **$\alpha$ DG-GFP**: GFP-tagged full-length  $\beta$ -dystroglycan deletion mutant;  $\alpha$ -dystroglycan with its N-terminal SP sequence were fused at the N-terminal of GFP. All deletion mutants were cloned between SalI and SmaI sites in pEGFP (N-3) vector. An extra alanine was added at the C-terminal end to accommodate the SmaI restriction site.

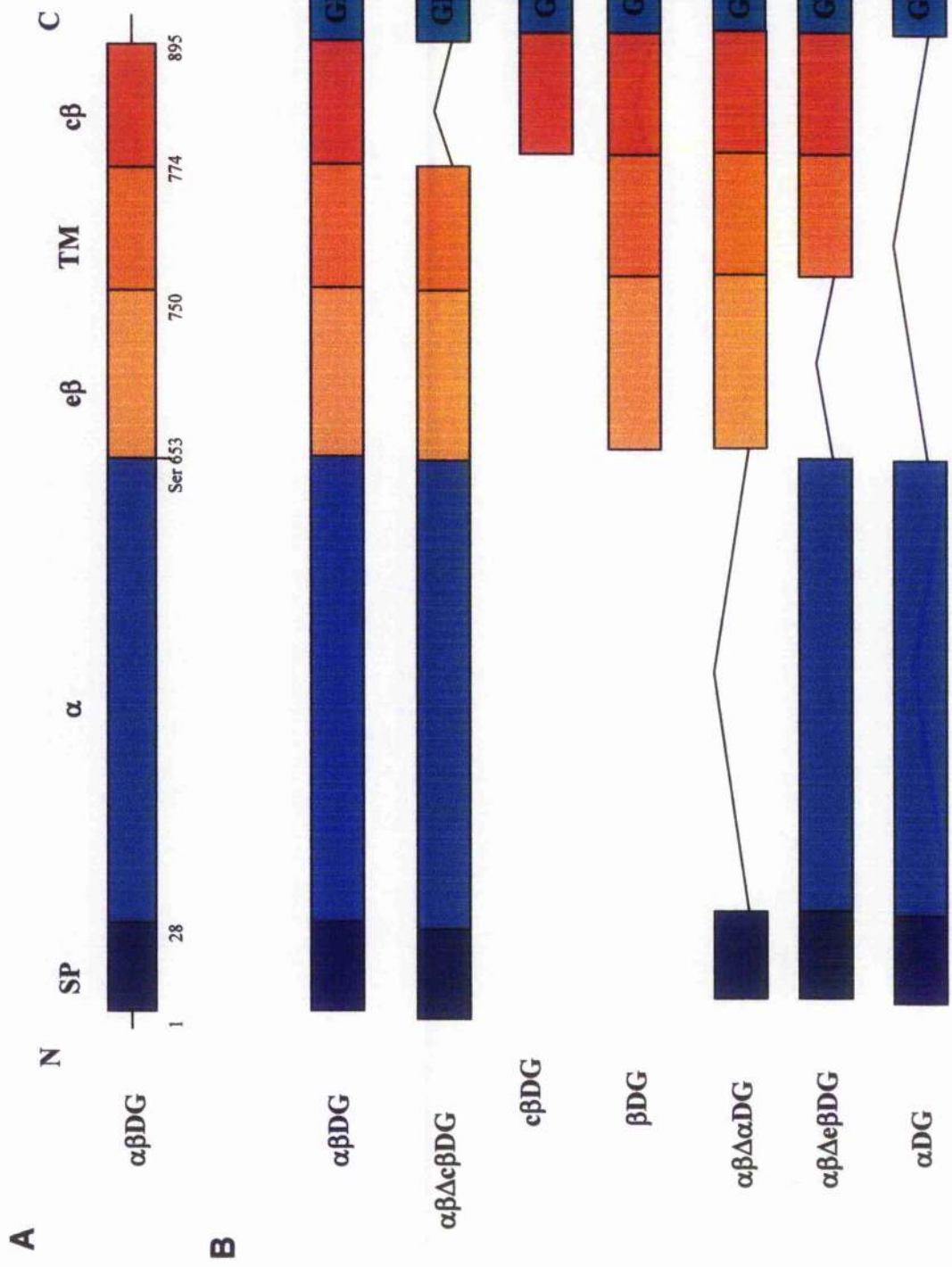
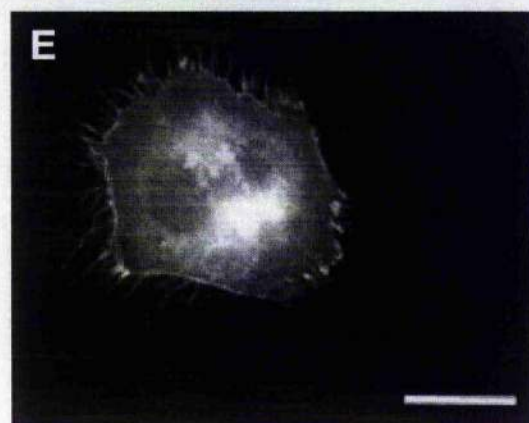
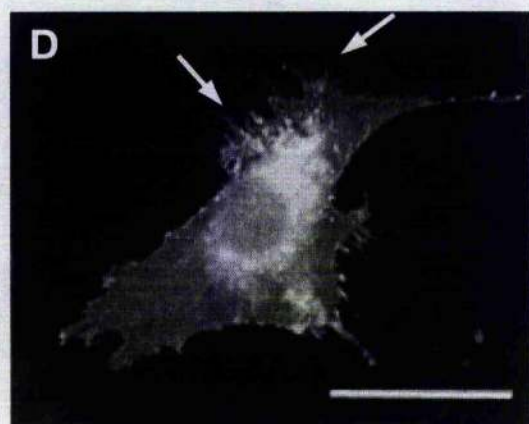
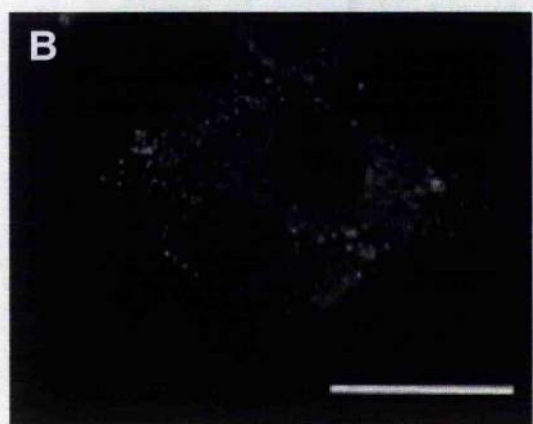
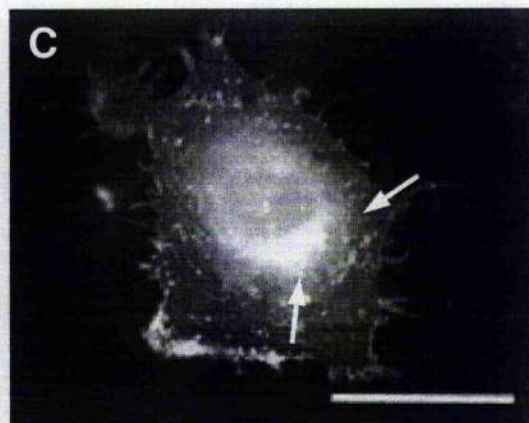
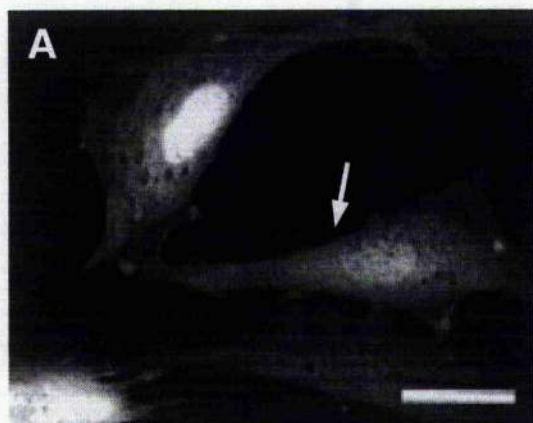


**Figure 4.2 Expression of DG-GFP construct in REF52 cells**

REF52 cells were transfected with  $\alpha\beta$ DG-GFP (1.8 $\mu$ g/ml) construct (**C-E**), or pEGFP empty GFP vector (**A**); or the negative control, which was treated with equal amounts of lipofectamine as transfected cells but with no DNA (**B**). The transfected cells on glass coverslips were incubated at 37°C overnight after the standard transfection procedure. The coverslips with cells were fixed with 3.7% formaldehyde. Many long and thin microspikes were found in the cells transfected with  $\alpha\beta$ DG-GFP (**C-E**). These microspikes also distributed on the surface (**C**, **arrows**) of the cells. Some of these microspikes were clustered as a crown-like structure (**D**, **arrows**). The pEGFP empty vector (2 $\mu$ g/ml) transfected cells showed typical GFP expression and nuclear accumulation, cell body diffusion (**A**) and smooth cell periphery (**A**, **arrow**). No fluorescence localisation was identified in the negative control except for the background autofluorescence from the lipofectamine transfection reagent (**B**). Scale bar=25 $\mu$ m





This unexpected change of morphology in  $\alpha\beta$ DG-GFP transfected cells has raised several questions. First, what are these microspikes present in  $\alpha\beta$ DG-GFP transfected cells, and do these structures correspond to actin rearrangement? Second, which factor in  $\alpha\beta$ DG-GFP transfected cells induces the change of morphology? Does dystroglycan mediate the formation of these microspikes? Third, if it does, which functional domain of dystroglycan is responsible for the formation of microspikes? Fourth, if cytoskeleton reorganisation is involved in the formation of the microspikes, what is the signalling pathway? Do small Rho GTPases or other integrin-dependent signalling, such as ERK signalling play a role in this morphology change?

#### ***4.2.2.2 Filopodia formation of $\alpha\beta$ DG-GFP transfected REF52 cells on Laminin***

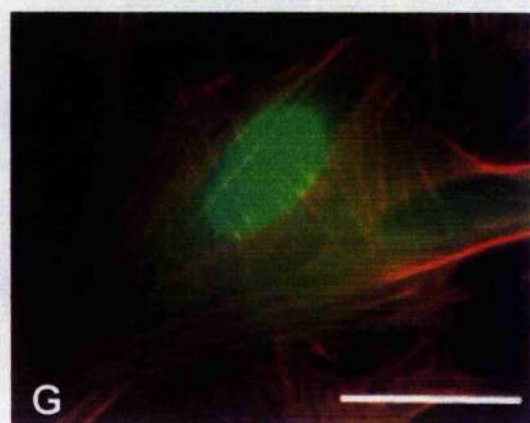
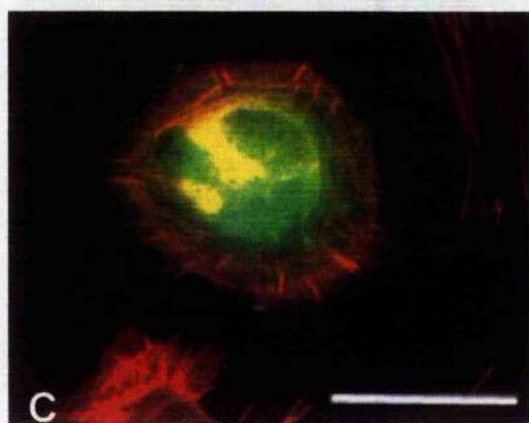
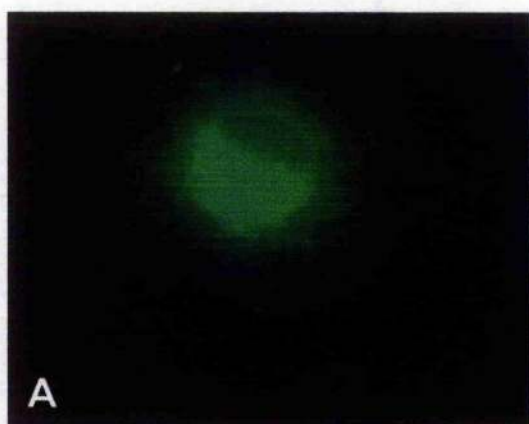
To address the question of whether the change of morphology was induced by expression of dystroglycan and to further investigate these microspikes in  $\alpha\beta$ DG-GFP transfected cells,  $\alpha\beta$ DG-GFP transfected cells were replated onto laminin, which is a substrate for dystroglycan, and the actin-containing structures stained with rhodamine-conjugated phalloidin. As shown in figure 4.3, after incubating in DMEM containing 1% FBS overnight on laminin, all the transfected cells were well spread. Numerous branching microspikes were expressed throughout the periphery of  $\alpha\beta$ DG-GFP transfected cells (Fig 4.3 A). In contrast, the pEGFP empty vector transfected cells incubated in the same conditions on laminin showed a smooth cell periphery (Fig 4.3 E). Upon actin staining, remarkable actin-rich rings were found in the cell cortex forming a doughnut-like actin structure (Fig 4.3 B). Based in the actin-rich cortex region, the actin bundles protruded outward from the cell body and extended into each microspike (Fig 4.3C). The magnification of the merged images at the microspikes (Fig 4.3 D) indicated that the microspikes present in  $\alpha\beta$ DG-GFP transfected cells are branching fibre-like actin-rich structure, a so called filopodia. Normal stress fibre actin phenotype was seen in pEGFP transfected REF52 cells (Fig 4.3 F), as well as that in untransfected REF52 cells (data not shown), revealing the ring-like and the filopodia actin phenotype might be induced by expression of dystroglycan.

**Figure 4.3 Expression of  $\alpha\beta$  DG-GFP in REF52 on laminin**

$\alpha\beta$  DG-GFP (1.8 $\mu$ g/ml) or pEGFP (2 $\mu$ g/ml) empty vector transfected REF52 cells were replated on to laminin (2 $\mu$ g/ml) coated coverslips and incubated in DMEM containing 1% FBS at 37°C for overnight. Cells were fixed with 3.7% formaldehyde and stained with rhodamine-phalloidin [(Sigma) at 1:1000]. Plenty of branching microspikes were expressed in the periphery of  $\alpha\beta$  DG-GFP transfected cells (A). Remarkable ring-like actin rich structures were present in the cell cortex region in  $\alpha\beta$ DG-GFP transfected cells (B), while stress fibre actin phenotype was found in pEGFP empty vector transfected cells (E and F). The merged image show that the microspikes expressed in  $\alpha\beta$ DG-GFP transfected cells are actin-rich structures (C). In the magnified images (D), these actin filament, based in the ring-like structure in cortex, extended into each branch of the microspike and are expressed throughout the cell body. These structures are very like filopodia. The filopodia structure was not seen in pEGFP transfected cells (E-G). The scale bars in D = 5 $\mu$ m. Others =25 $\mu$ m.

$\alpha\beta$ DG-GFP

pEGFP



Compared with the  $\alpha\beta$ DG-GFP transfected cells shown in figure 4.2 C-E, no significant increase in filopodia number was observed in the pEGFP transfected cells replated on laminin. However, the morphology of filopodia present in  $\alpha\beta$ DG-GFP transfected cells was more organised both in size and in length, implying that in the  $\alpha\beta$ DG-GFP transfected cells, laminin engagement might play a role in the arrangement of the filopodia. To further examine whether the formation of filopodia resulted from the expression of dystroglycan, the filopodia formation was monitored in  $\alpha\beta$ DG-GFP or pEGFP empty vector transfected cells replated on laminin. The number of cells with filopodia was counted at 1, 3, 5, and 7 hours; the cells presenting more than 30 microspikes were counted as filopodia positive. As shown in figure 4.4, after one hour of spreading, nearly 82% of  $\alpha\beta$ DG-GFP transfected cells were filopodia positive (Fig 4.4, blue circles), while only half the number of pEGFP transfected cells were filopodia positive (Fig 4.4, red square). However, in the pEGFP transfected cells, the number of filopodia positive cells increased to 70%, which was very close to  $\alpha\beta$ DG-GFP transfected cells, at the third hour, this number dropped dramatically until less than 10% at 7 hours (Fig 4.4, red curve). In contrast, the number of filopodia positive cells in  $\alpha\beta$ DG-GFP transfected cells was almost constant between 79-80% during the 7 hours (Fig 4.4, blue curve), suggesting that expression of  $\alpha\beta$ DG-GFP leads to the formation of filopodia, which are normally present within the first 3 hours of cell spreading. Thus, the filopodia formation did indeed result from the expression of dystroglycan, not from GFP.

#### **4.2.2.3 Examination of utrophin in $\alpha\beta$ DG-GFP transfected REF52 cells**

In non-muscle cells, utrophin is the molecule that directly interacts with dystroglycan and connects it to actin filaments (Ervasti and Campbell, 1993; Winder *et al.*, 1995). Phosphorylation of the  $\beta$ -dystroglycan cytoplasmic tail leads to the reduction of binding affinity between utrophin and  $\beta$ -dystroglycan (James *et al.*, 2000). Therefore, utrophin is possibly a mediator of dystroglycan-dependent filopodia formation. In an attempt to determine whether utrophin is a mediator of dystroglycan-dependent filopodia formation, we first examined the utrophin expression in  $\alpha\beta$ DG-GFP transfected cells. As shown on the western blot in figure 4.5, an approximately 70KDa GFP-tagged  $\beta$ DG was

**Figure 4.4 Quantification of the filopodia formation in  $\alpha\beta$ DG-GFP transfected cells on laminin**

Monitoring the formation of filopodia in  $\alpha\beta$ DG-GFP or pEGFP transfected REF52 cells, the transfected cells were replated onto laminin (2 $\mu$ g/ml) coated coverslips and incubated at 37°C in DMEM. Coverslips with cells were fixed after one, three, five and seven hours; and the number of cell with filopodia (more than 30 filopodia) was counted. In  $\alpha\beta$ DG-GFP transfected cells, the number of filopodia positive cells is steady between 79-82% within the 7 hours (blue curve), while the pEGFP transfected cells (red curve) reached 72% by the 3rd hour and then quickly dropped down until less then 10%. The counting was repeated twice at each time point in two transfections. Data are means  $\pm$  SD.

Formation of filopodia on laminin induced by expression of  $\alpha\beta$ DG-GFP

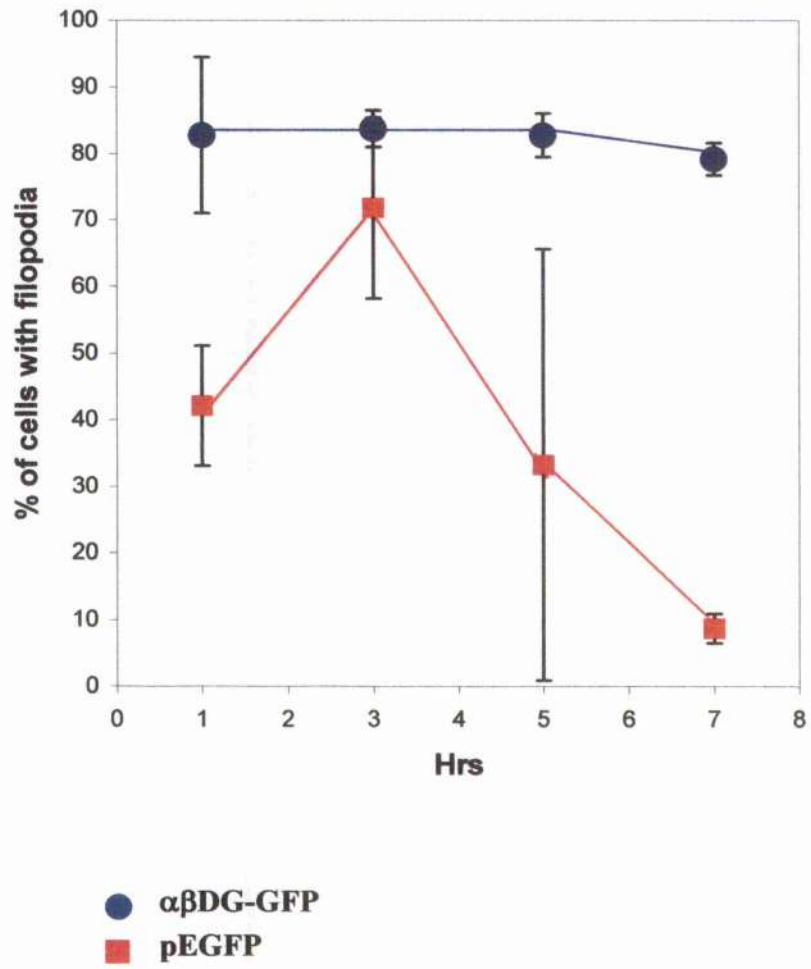
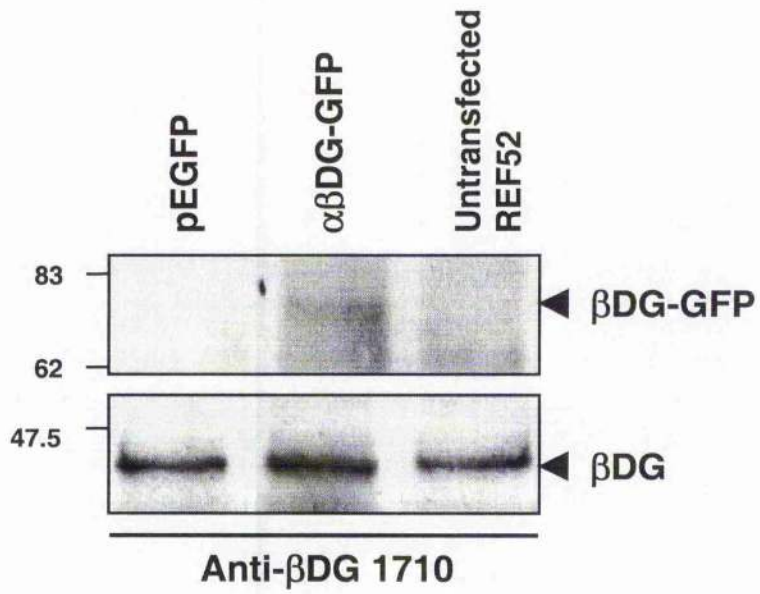


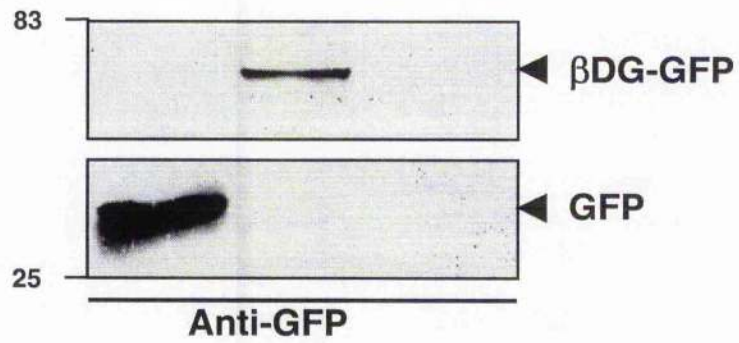
**Figure 4.5 Expression of utrophin in dystroglycan overexpressed REF52 cells**

Western blotting of  $\alpha\beta$ DG-GFP, pEGFP empty vector transfected and untransfected REF52 cells. Cell lysates were blotted with anti  $\beta$ DG antibody ( $\beta$ DG-1710) at the concentration of 1:1000, anti-GFP antibody at the concentration of 1:1000, or anti C-terminus utrophin (Rab6) at the concentration of 1:10000. Overexpression of  $\alpha\beta$ DG-GFP or GFP protein did not alter the expression of 43KDa endogenous  $\beta$ DG, which was detected by anti  $\beta$ DG-1710 antibody (**A lower panel**). 70KDa  $\beta$ DG-GFP fusion protein was detected by anti- $\beta$ DG (**A, upper panel**) or anti-GFP antibody in  $\alpha\beta$ DG-GFP transfected cells (**B upper panel**). Utrophin expression (**C**), is not affected by overexpression of  $\alpha\beta$  DG-GFP or pEGFP.

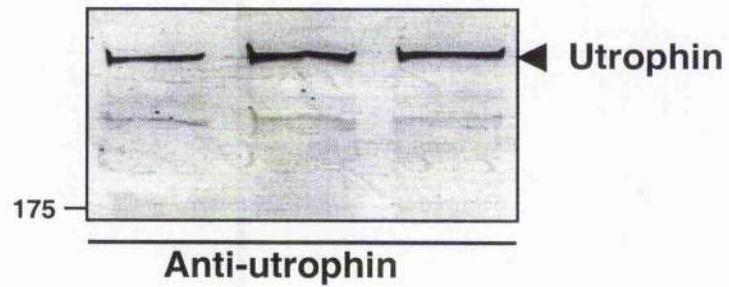
**A**



**B**



**C**





detected by anti GFP antibody (Fig 4.5 A upper panel) or anti  $\beta$ DG 1710 antibody (Fig 4.5 B upper panel) in  $\alpha\beta$ GD-GFP transfected cells. However, expression level of utrophin was not affected by overexpression of  $\alpha\beta$ GD-GFP or GFP (Fig 4.5 C), revealing that utrophin expression is not regulated by overexpression of dystroglycan.

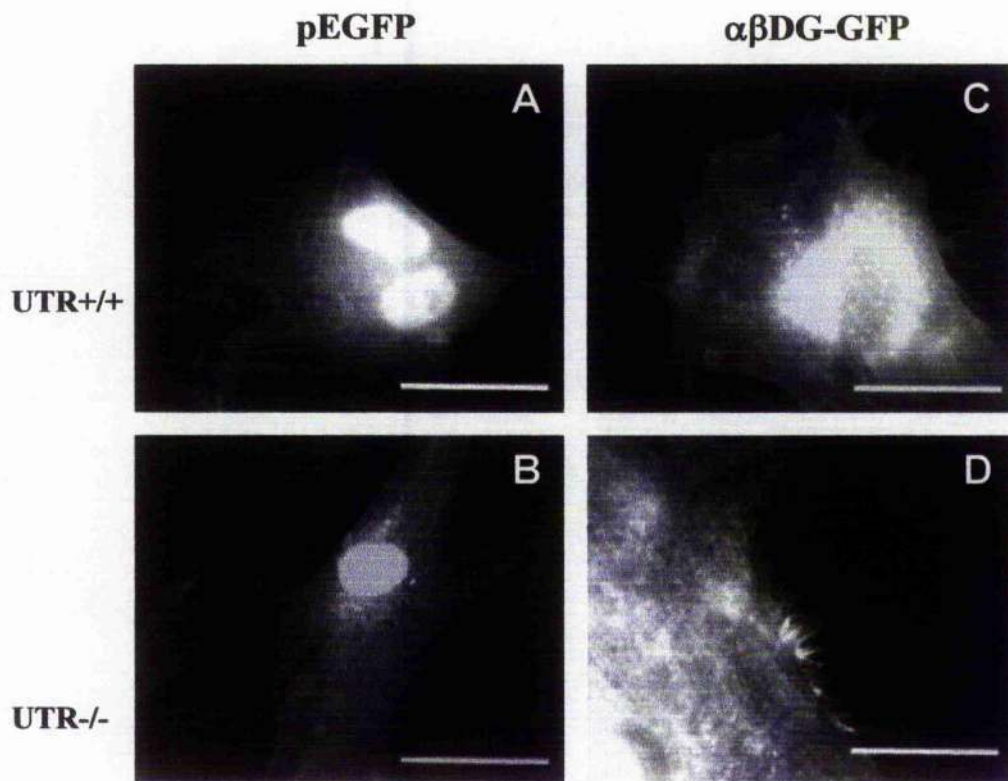
To further determine the role of utrophin in dystroglycan-dependent filopodia formation, we transfected  $\alpha\beta$ DG-GFP construct into utrophin-knockout mouse embryonic fibroblast primary culture. As shown in figure 4.6, the filopodia phenotype was present in  $\alpha\beta$ DG-GFP transfected utrophin knockout mouse embryonic primary culture (Fig 4.6 D), as well as the wild type mouse embryonic primary culture (Fig 4.6 C), indicating that utrophin might not be involved in the dystroglycan-dependent filopodia formation. Transfection of GFP empty vector did not cause the formation of filopodia whether in utrophin knockout or wild type cells (Fig 4.6, A and B), suggesting that dystroglycan is responsible for the formation of filopodia. At the same time, the effect of dystroglycan in utrophin wild type and knockout cells was measured by counting the number of cells presenting filopodia phenotype (Fig 4.6 E). No significant difference in dystroglycan-dependent filopodia formation was seen between utrophin wild type and knockout cells (Fig 4.6 E, green columns), indicating that the defect in utrophin expression has no influence on the dystroglycan-dependent filopodia formation. Therefore, despite linking dystroglycan physically to the cytoskeleton, utrophin is not a mediator of dystroglycan dependent filopodia formation, nor required for it.

#### **4.2.3 Expression of c $\beta$ deletion mutant construct ( $\alpha\beta\Delta$ c $\beta$ -GFP) in REF52 cells**

In the experiments above, expression of dystroglycan has been shown to induce the formation of filopodia. Experiments were carried out to further determine which functional domain of dystroglycan was responsible for the filopodia formation signalling. Since the cytoplasmic domain of  $\beta$ -dystroglycan has been shown to associate with cytoskeleton related signalling molecules (section 1.4), it is the best candidate domain that may mediate the signalling events of dystroglycan-dependent filopodia formation. In an attempt to determine the role of  $\beta$ -dystroglycan cytoplasmic domain in

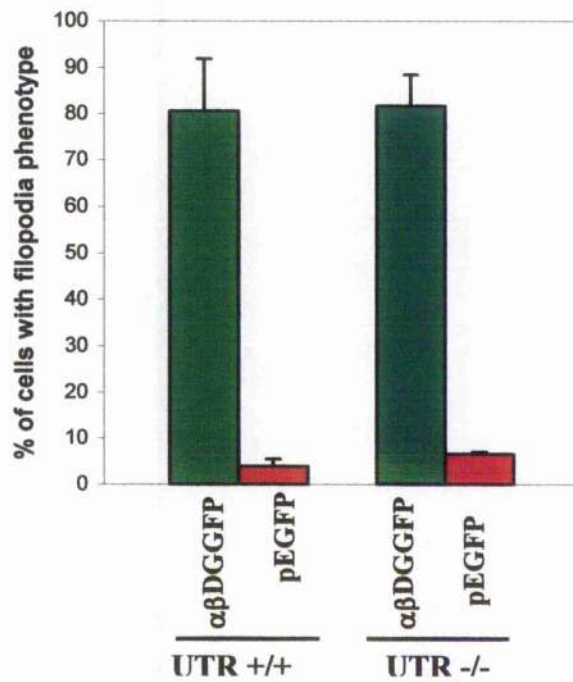
#### **Figure 4.6 Expression of dystroglycan GFP in utrophin null cells**

Utrophin wild type or utrophin knockout mouse embryo fibroblast primary culture were transfected with  $\alpha\beta$ DG-GFP (1.8 $\mu$ g/ml) (**C and D**) or pEGFP (2 $\mu$ g/ml) (**A and B**). The cells were transfected on glass coverslips and then incubated at 37°C overnight after the transfection procedure. Coverslips with cells were fixed with 3.7% formaldehyde. The cells with more than 30 microspikes were identified as filopodia positive. In cells transfected with  $\alpha\beta$ DG-GFP, the filopodia phenotype was present in utrophin wild type (**C**) as well as in utrophin knockout cells (**D**); both utrophin wild type and knockout cells showed fairly high number of filopodia positive cells (80% and 82%) (**E, green columns**). The transfection of pEGFP did not induce the formation of filopodia in utrophin wild type or knockout cells (**A**) with less than 10 % of utrophin wild type or knockout cells with the filopodia phenotype (**E, red columns**). The counting was repeated twice in two different transfections. Data are mean + SD. The scale bars= 25 $\mu$ m.



**E**

**Filopodia formation in utrophin knock-out cells transfected with  $\alpha\beta$ DG-GFP**



dystroglycan- dependent filopodia formation, the construct of GFP-tagged  $\beta$  dystroglycan cytoplasmic domain deletion mutant ( $\alpha\beta\Delta c\beta$ -GFP) was expressed in REF52 cells. As shown in figure 4.7 A and B, most of the  $\alpha\beta\Delta c\beta$ -GFP transfected cells plated on glass coverslips had a smooth cell periphery. Replating the transfected cells on laminin, revealed no significant induction of filopodia (Fig 4.7 C). Instead of the ring-like actin structure, fairly high number of actin stress fibres, as has been shown in pEGFP transfected cells (Fig 4.3 F), was present in  $\alpha\beta\Delta c\beta$ -GFP transfected cells (Fig 4.7 D). Therefore, the dystroglycan dependent filopodia formation appeared to be inhibited by the absence the cytoplasmic domain of  $\beta$ -dystroglycan.

#### **4.2.4 Substrate effects on dystroglycan dependent filopodia formation**

Since adhesion dependent tyrosine phosphorylation of dystroglycan has been reported to regulate the affinity between  $\beta$ -dystroglycan and the utrophin WW domain (James, et al., 2000), adhesion dependent signalling might be involved in the dystroglycan dependent cytoskeleton reorganisation. Additionally, *in vivo* formation of filopodia is induced by integrin mediated Cdc42 activation (Kozma *et al.*, 1995). Therefore, despite utrophin not mediating the dystroglycan-dependent filopodia formation, it is possible that integrin dependent or adhesion dependent signalling is involved in the dystroglycan dependent filopodia formation. To determine whether integrin is required for dystroglycan dependent filopodia formation, we replated the transfected cells onto fibronectin, which is a ligand for integrin, or poly-L-lysine, which prevents integrin from activation, and monitored the morphology change in  $\alpha\beta$ DG-GFP or  $\alpha\beta\Delta c\beta$ -GFP transfected cells. As shown in figure 4.8 A, after incubation in serum free DMEM for 4 hours, filopodia phenotype was present in  $\alpha\beta$ DG-GFP transfected cells plated on laminin (Fig 4.8 A), as well as on fibronectin (Fig 4.8 B), while the cells were not spread on poly-l-lysine (Fig 4.8 C) or uncoated glass control (Fig 4.8 D). In contrast, whether plating on laminin or fibronectin, the filopodial phenotype was not induced by expression of GFP in the cells (Fig 4.8 E and F).

**Figure 4.7 Expression of  $\beta$  dystroglycan cytoplasmic domain deletion mutant.**

**$\alpha\beta\Delta c\beta$ -GFP**

$\alpha\beta\Delta c\beta$ -GFP (1.8 $\mu$ g/ml) was transfected into REF52 cells plated on glass coverslips following the standard transfection procedure (A and B). The  $\alpha\beta\Delta c\beta$ -GFP transfected cells were replated onto laminin coated coverslips and incubated in DMEM containing 1%FBS at 37 °C overnight (C). The cells were fixed with 3.7% formaldehyde, and the cells replated on laminin were further stained with rhodamine-phalloidin [(Sigma) at 1:1000]. Expression of  $\alpha\beta\Delta c\beta$ -GFP did not induce the formation of a filopodial phenotype in REF52 cells (A and B). The  $\alpha\beta\Delta c\beta$ -GFP transfected cells replated on laminin showed no induction of filopodia either (C). Stress fibre actin phenotype was present in the  $\alpha\beta\Delta c\beta$ -GFP transfected cells (D). (E), merged image of  $\alpha\beta\Delta c\beta$ -GFP and actin. Scale bar= 25 $\mu$ m

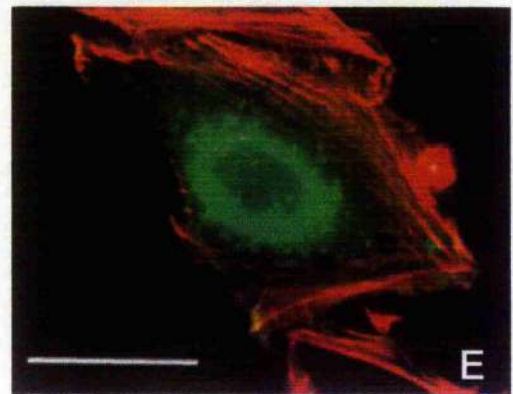
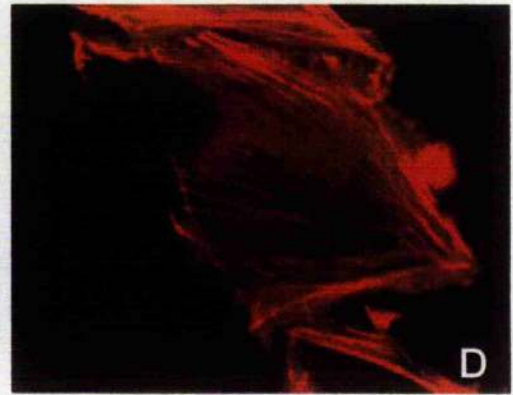
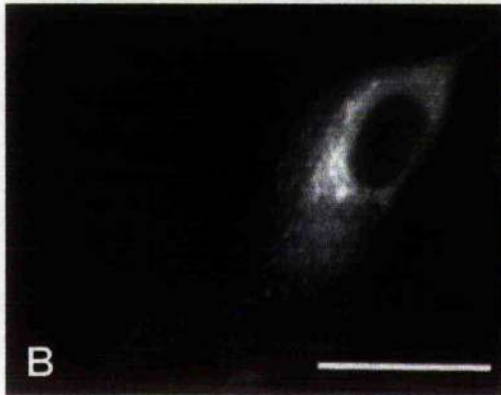
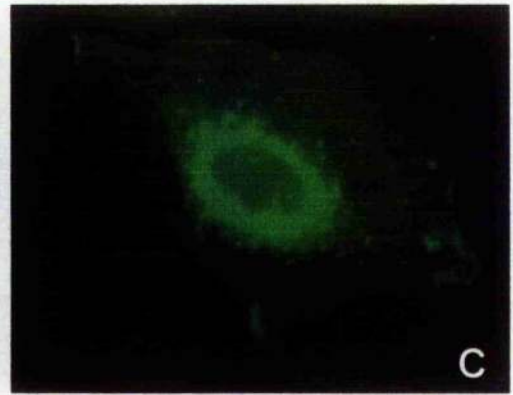
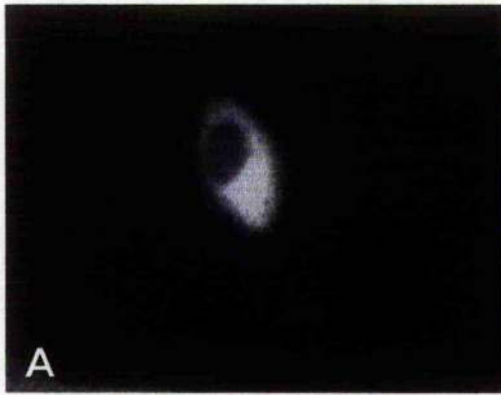


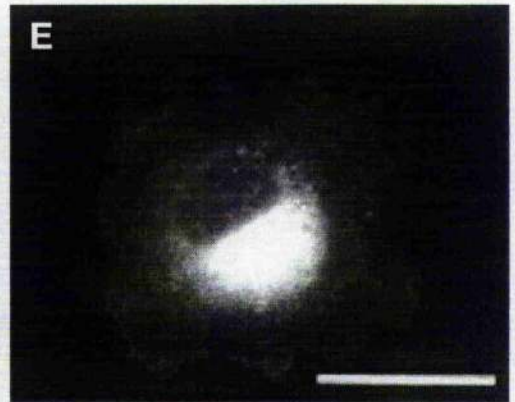
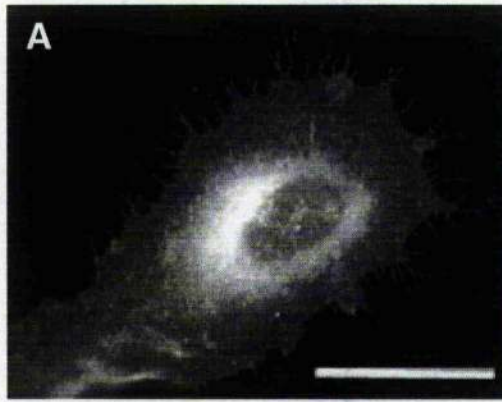
**Figure 4.8 Formation of filopodia in  $\alpha\beta$ DG-GFP transfected cells on extracellular substrates**

REF52 cells transfected with  $\alpha\beta$ DG-GFP (1.8 $\mu$ g/ml) or pEGFP (2.0 $\mu$ g/ml) were replated onto glass coverslips or glass coverslips coated with laminin (2 $\mu$ g/ml), fibronectin (2 $\mu$ g/ml) or poly-L-lysine (2 $\mu$ g/ml) and incubated at 37°C in serum free DMEM for 5 hours. The coverslips with cells were fixed with 3.7% formaldehyde.  $\alpha\beta$ DG-GFP transfected cells can spread well on laminin or fibronectin and present a filopodia phenotype (**A and B**). Whether on laminin or fibronectin,  $\alpha\beta\Delta c\beta$ -GFP transfected cells can also spread well, but no induction of filopodia phenotype was found (**E and F**). Whether transfected with  $\alpha\beta$ DG-GFP or  $\alpha\beta\Delta c\beta$ -GFP, cells were unable to spread on poly-L-Lysine (**C and G**) or on uncoated glass coverslips (**D and H**) in the absence of serum. The scale bar=25 $\mu$ m.

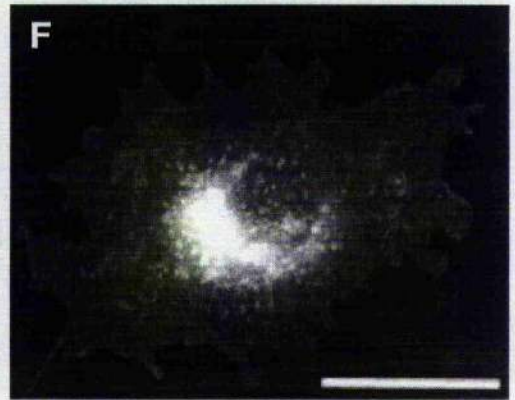
$\alpha\beta$ DG-GFP

pEGFP

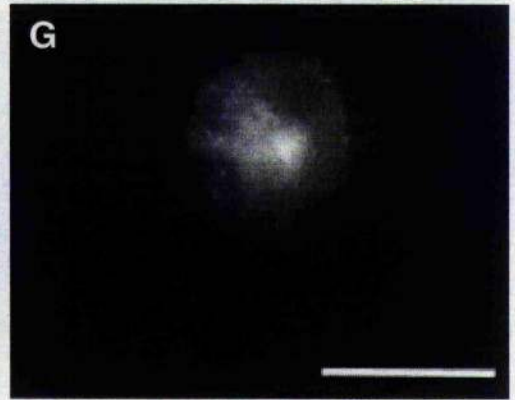
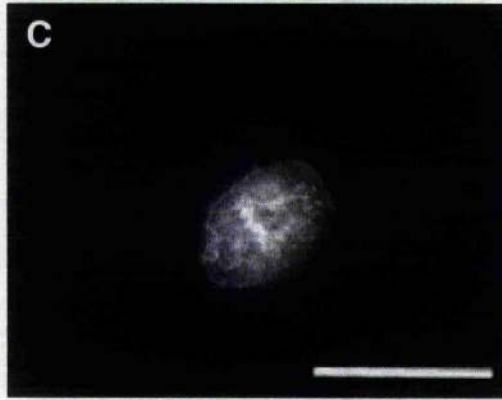
LN



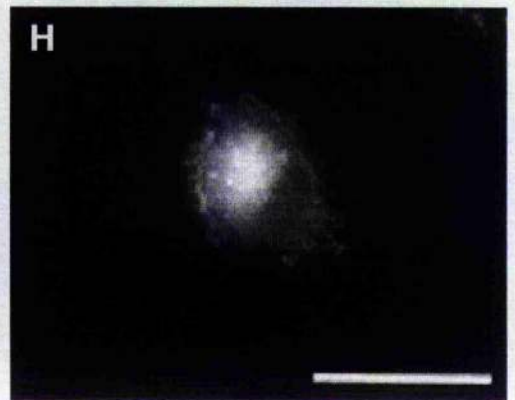
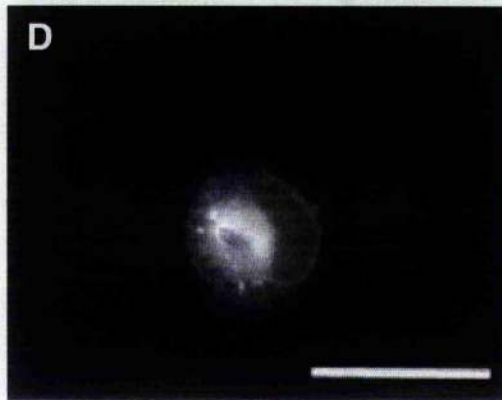
FN



PLL



GLA





Counting the number of filopodia phenotype positive cells on the substrates reveals a similarly high percentage of filopodia positive cells (70% and 68%) in  $\alpha\beta$ DG-GFP transfected cells plated on laminin and on fibronectin (Fig 4.9, green columns). The formation of filopodia was reduced in  $\alpha\beta\Delta c\beta$ -GFP transfected cells, and the percentage of filopodia positive cells in  $\alpha\beta\Delta c\beta$ -GFP transfected cells on laminin and on fibronectin was very similar (22% and 21%); (Fig 4.9, red columns). Therefore, the dystroglycan dependent filopodia formation appeared not to be specific for laminin engagement to dystroglycan; fibronectin can induce the dystroglycan dependent filopodia formation as well. The disruption of integrin engagement inhibited the formation of filopodia (Fig 4.8 PLL and GLA). Since both laminin and fibronectin are extracellular ligands of integrins, the dystroglycan dependent filopodia formation, which was considered to be mediating cytoskeleton reorganisation signalling via its cytoplasmic domain, seems more likely to be dependent on integrin-mediated cell adhesion instead of dystroglycan-laminin engagement. Thus, more evidence supporting  $\beta$ -dystroglycan cytoplasmic domain mediates the formation of filopodia is required.

Additionally, compared with approximately 70% of  $\alpha\beta$ DG-GFP transfected cell presenting a filopodia phenotype,  $\alpha\beta\Delta c\beta$ -GFP transfected cells showed a significant reduction of filopodia formation (Fig 4.8, LN). Obviously, the  $\beta$ -dystroglycan cytoplasmic domain plays an important role in the dystroglycan dependent filopodia formation. However, it could not be ruled out that approximate 20% of  $\alpha\beta\Delta c\beta$ -GFP transfected cells still are expressing more the 30 microspikes. It is likely that in addition to  $\beta$ -dystroglycan cytoplasmic domain, other factors may participate in dystroglycan-dependent filopodia formation as well.

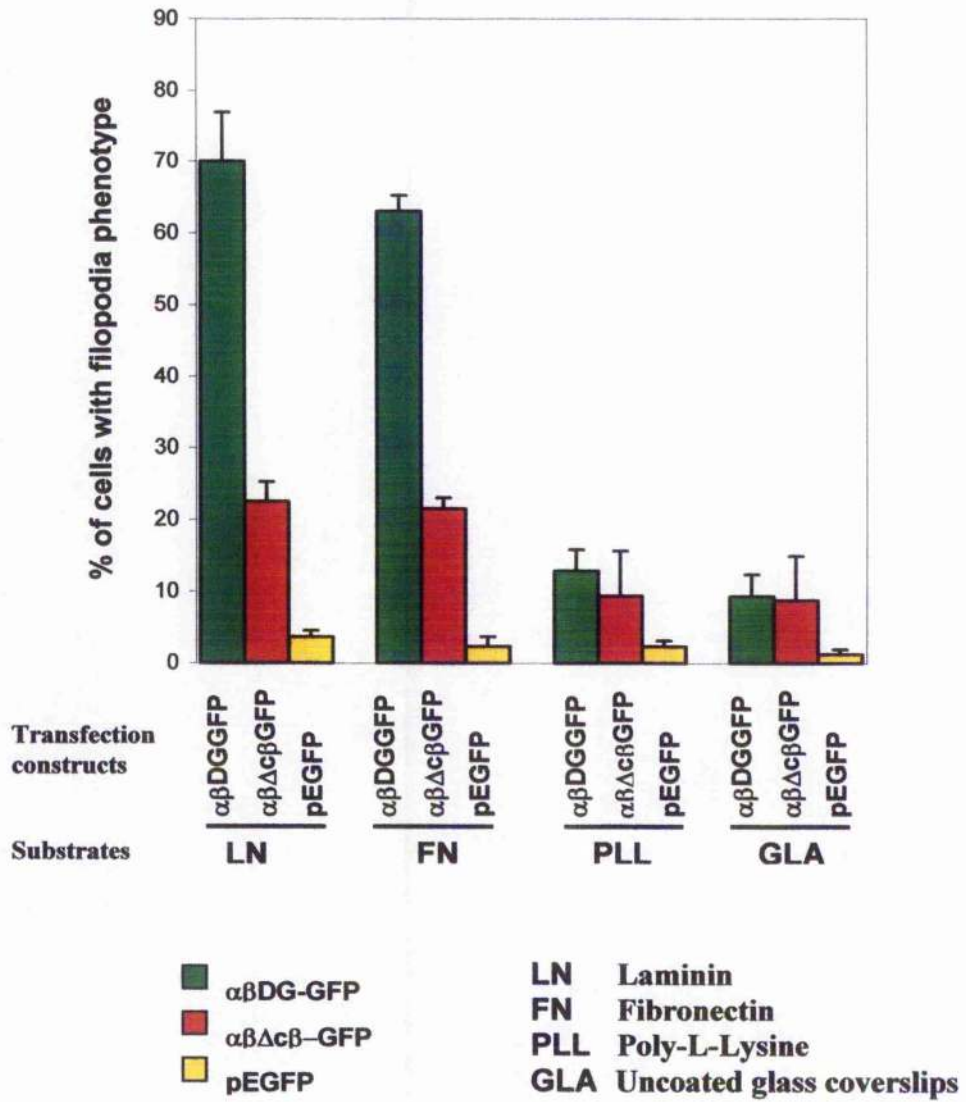
#### **4.2.5 Expression of c $\beta$ dystroglycan construct (c $\beta$ DG-GFP) in REF52 cells**

To further examine how  $\beta$ -dystroglycan mediates the formation of filopodia, GFP-tagged  $\beta$ -dystroglycan cytoplasmic domain alone was transfected into REF52 to see if it can induce the formation of filopodia. Interestingly, while the expression of  $\alpha\beta\Delta c\beta$ -GFP has shown that  $\beta$ -dystroglycan cytoplasmic domain is required for the formation of the

#### **Figure 4.9 Substrate effects on dystroglycan mutants transfected cells**

REF52 cells transfected with  $\alpha\beta$ DG-GFP (1.8 $\mu$ g/ml), pEGFP (2.0 $\mu$ g/ml) or  $\alpha\beta\Delta c\beta$ -GFP (2.0 $\mu$ g/ml) were replated onto glass coverslips or glass coverslips coated with laminin (2 $\mu$ g/ml), fibronectin (2 $\mu$ g/ml) or poly-L-lysine (2 $\mu$ g/ml) and incubated at 37°C in serum free DMEM for 5 hours. The coverslips with cells were fixed with 3.7% formaldehyde. Cells with more than 30 microspikes are identified as filopodia positive. Nearly 70% of cells transfected with  $\alpha\beta$ DG-GFP had a filopodia phenotype on laminin (**LN green column**), and similar number (68%) was present on fibronectin (**FN green column**). On poly-L-lysine (**PLL green column**) or on uncoated glass coverslips (**GLA green column**),  $\alpha\beta$ DG-GFP transfected cells were unable to spread and less than 10% of cells were filopodia positive. In  $\alpha\beta\Delta c\beta$ -GFP transfected cells, number of filopodia positive cells was reduced to approximately 20% on laminin (**LN red columns**) and on fibronectin (**FN red columns**).  $\alpha\beta\Delta c\beta$ -GFP transfected cells were unable to spread on poly-L-lysine or on uncoated glass coverslips, and less than 10% of cells were determined as filopodia positive (**PLL and GLA, red columns**). Less than 5% of pEGFP empty vector transfected cells presented filopodia (**yellow columns**). The counting(100-200 cells) was repeated for 4 times in each transfection. Data are mean +SD (n=4).

**Substrate effects on filopodia formation in  $\alpha\beta$ GD-GFP and on  $\alpha\beta\Delta c\beta$ -GFP transfected REF52**



filopodia phenotype, c $\beta$ -GFP, which contains only the cytoplasmic domain of  $\beta$ -dystroglycan, was insufficient to induce the filopodia phenotype (Fig 4.10 A and B). The c $\beta$ -GFP in the cells localised not only in the cytoplasm but also at the nuclear region; in fact, the major pool of overexpressed c $\beta$ -GFP appeared to be in the nuclear region. Interestingly, no particular nuclear signal sequence on  $\beta$ -dystroglycan, has been reported, the nuclear import of c $\beta$  might be caused by the transporting of its GFP tag. Replating the c $\beta$ -GFP transfected cells on laminin did not induce any formation of filopodia phenotype (Fig 4.10 C). A normal actin stress fibre phenotype was found in the transfected cells (Fig 4.10 D and E).

The unexpected result that c $\beta$ -GFP is insufficient to induced the formation of filopodia raised two possibilities: first, despite the cytoplasmic domain of  $\beta$ -dystroglycan mediating the formation of filopodia, contribution from other dystroglycan functional domains must be required for the  $\beta$ -dystroglycan cytoplasmic domain to interact with cytoskeleton reorganisation signalling molecules. Second, since c $\beta$ -GFP localised to the nuclear region, it may have failed to induce any formation of filopodia. It is likely that correct localisation of dystroglycan is important for dystroglycan to act as a mediator for filopodia formation.

#### 4.2.6 Expression of $\beta$ dystroglycan ( $\beta$ DG-GFP) construct in REF52 cells

If contributions from other functional domains are necessary for the  $\beta$ DG-dystroglycan cytoplasmic domain to mediate the formation of filopodia, which functional domain on dystroglycan would it be? In an attempt to determine which domain of dystroglycan is required, several dystroglycan functional domain deletion mutants were constructed. First, GFP tagged full-length  $\beta$ -dystroglycan ( $\beta$ DG -GFP), which lacks  $\alpha$ -dystroglycan and the N-terminal signal peptide, was expressed in REF52 cells.

As shown in figure 4.11, relatively high amounts of  $\beta$ DG -GFP still localised to the nuclear region and did not induce the formation of filopodia (Fig 4.11 A and B). Compared with the expression of c $\beta$ DG -GFP shown in figure 4.10,  $\beta$ DG -GFP was

**Figure 4.10 Expression of dystroglycan cytoplasmic domain c $\beta$ -GFP**

c $\beta$ -GFP (1.8 $\mu$ g/ml) was transfected into REF52 cells plated on glass coverslips following the transfection procedure and incubated at 37 °C overnight (**A-B**). The c $\beta$ -GFP transfected cells were subsequently replated onto laminin (1 $\mu$ g/ml) coated coverslips and incubated in DMEM containing 1% FBS at 37 °C overnight (**C-E**). The cells were fixed with 3.7% formaldehyde and cells replated on laminin were further stained with rhodamine-phalloidin [(Sigma) at 1:1000]. Expression of c $\beta$ -GFP in REF52 cells did not induce filopodia formation, the overexpressed c $\beta$ -GFP was concentrated mainly in the nucleus and slightly less in the perinuclear region (**A and B**). Filopodia phenotype was not found in c $\beta$ -GFP transfected cells plated on laminin either (**C**). Stress fibre actin phenotype was present in c $\beta$ -GFP transfected cells (**D**). (**E**), the merged image of c $\beta$ -GFP (green) and actin (red). Scale bar=25 $\mu$ m

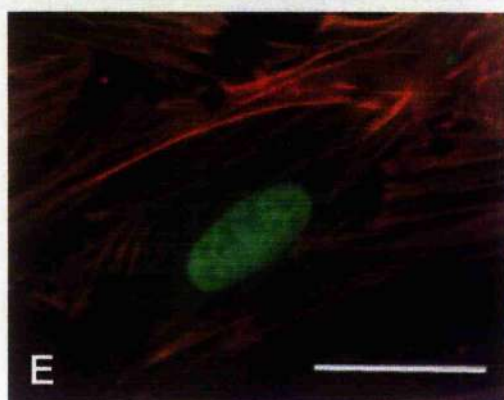
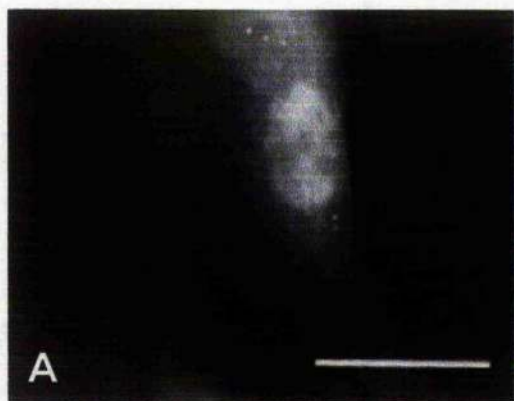
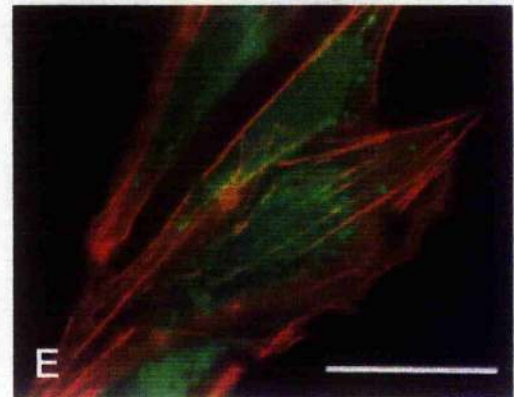
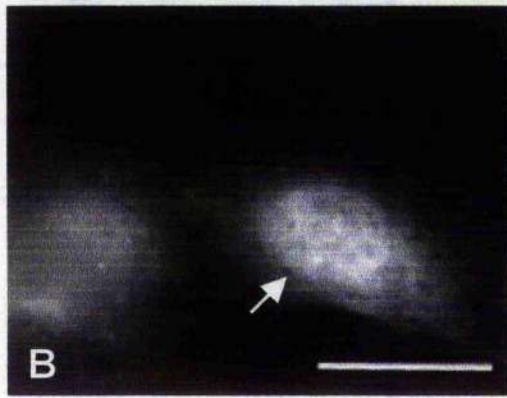
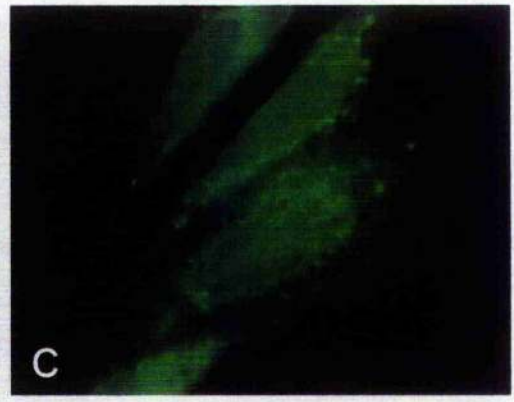


**Figure 4.11 Expression of  $\beta$  dystroglycan,  $\beta$ DG-GFP, in REF52 cells**

REF52 cells plated on glass coverslips were transfected with  $\beta$ DG-GFP (1.8 $\mu$ g/ml). Following the transfection procedure, they were incubated at 37°C overnight (**A-B**). The  $\beta$ DG-GFP transfected cells were subsequently replated on laminin (2 $\mu$ g/ml) coated coverslips and incubated in DMEM containing 1% FBS at 37 °C overnight (**C-E**). The coverslips were fixed with 3.7% formaldehyde.  $\beta$ DG-GFP transfected cells replated on laminin were stained with rhodamine-phalloidin [(Sigma) at 1:1000]. Expression of  $\beta$ DG-GFP did not induce the formation of filopodia, the  $\beta$ DG-GFP concentrated mainly in the nuclear region and diffused around the perinuclear region (**A and B arrows**); very little of  $\beta$ DG-GFP was found in other regions of the cytoplasm. Replating the  $\beta$ DG-GFP transfected cells onto laminin did not induce the formation of filopodia (**C**). Actin stress fibre phenotype was present in  $\beta$ DG-GFP transfected cells (**D**), (**E**). The merged image of  $\beta$ DG-GFP (green) and actin (red). Scale bar=25 $\mu$ m.





localised both in perinuclear and cytoplasmic region of the cells. Again, replating the  $\beta$ DG-GFP transfected cells onto laminin did not induce filopodia formation (Fig 4.11 C) or alter the stress fibre actin phenotype (Fig 4.11 D and E). Thus, even with extracellular and transmembrane domains of  $\beta$ -dystroglycan, the cytoplasmic domain still failed to mediate the formation of filopodia, suggesting the extracellular and transmembrane domains of  $\beta$ -dystroglycan might be insufficient to contribute cytoplasmic domain to mediate the formation of filopodia.

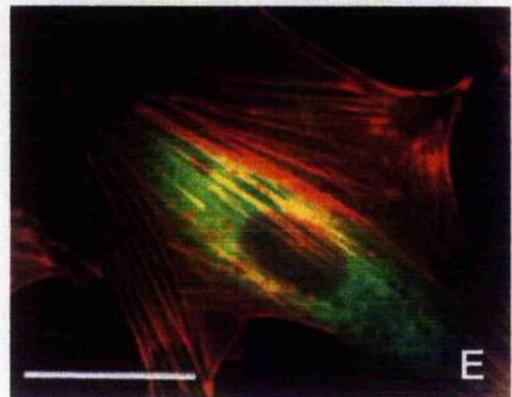
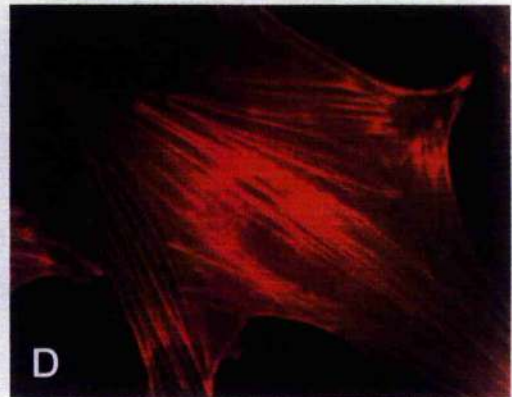
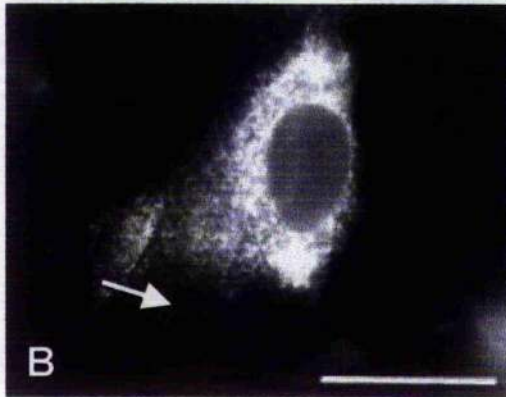
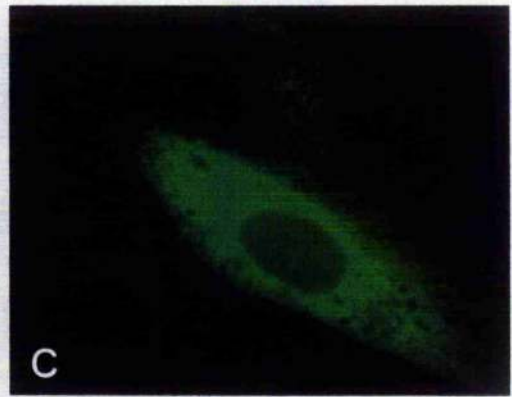
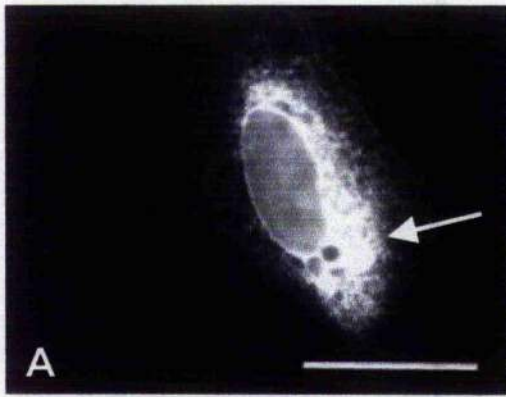
#### **4.2.7 Expression of $\alpha$ -dystroglycan deletion mutant construct ( $\alpha\beta\Delta\alpha$ DG-GFP) in REF52 cells**

With its extracellular domain,  $\beta$ DG-GFP still localised to the nuclear region and was unable to induce the formation of filopodia, indicating that the additional domain required to mediate the formation of filopodia might not lie in  $\beta$ -dystroglycan.  $c\beta$ DG-GFP and  $\beta$ DG-GFP showed an unusual nuclear localisation, implying that the translocation of  $c\beta$ DG-GFP or  $\beta$ DG-GFP might be altered in the absence of  $\alpha$ -dystroglycan or the N-terminal signal peptide. Thus, the additional domain required to mediate the formation of filopodia is more likely lie in  $\alpha$ -dystroglycan or in the N-terminal signal peptide, and these two domains might be involved in the trafficking of dystroglycan to plasma membrane.

To determine whether the N-terminal signal peptide is required for dystroglycan dependent filopodia formation, we constructed the  $\alpha$ -dystroglycan functional domain deletion mutant ( $\alpha\beta\Delta\alpha$  DG-GFP), in which the N-terminal signal peptide (1-28a.a) was fused to the N-terminal of  $\beta$ -dystroglycan-GFP. As shown in figure 4.12, expression of  $\alpha\beta\Delta\alpha$  DG-GFP did not induce the formation of filopodia (Fig 4.12 A and B). Filopodia formation and actin reorganisation was not found in the  $\alpha\beta\Delta\alpha$  DG-GFP transfected cells replated on laminin either (Fig 4.12 C and D). The stress fibre phenotype was present in  $\alpha\beta\Delta\alpha$  DG-GFP transfected cells (Fig 4.12 D and E).

**Figure 4.12 Expression of dystroglycan  $\alpha$  subunit deletion mutant  $\Delta\alpha$ -GFP**

REF52 cells plated on glass coverslips were transfected with  $\alpha\beta\Delta\alpha$ DG-GFP (1.8 $\mu$ g/ml) following the transfection procedure cells and incubated at 37°C overnight (**A and B**). The  $\alpha\beta\Delta\alpha$ DG-GFP transfected cells were subsequently replated onto laminin coated glass coverslips and incubated in DMEM containing 1% FBS at 37°C overnight (**C**). The coverslips with cells were fixed with 3.7% formaldehyde.  $\alpha\beta\Delta\alpha$ DG-GFP transfected cells were further stained with rhodamine-phalloidin [(Sigma) at 1:1000]. Filopodia phenotype was not present in  $\alpha\beta\Delta\alpha$ DG-GFP transfected cells (**A and B**). The  $\alpha\beta\Delta\alpha$ DG-GFP localised mainly in the perinuclear region (**A arrow**), and a lot of vesicle-like grains distributed around the cytoplasm (**B arrow**). Replating the  $\alpha\beta\Delta\alpha$ DG-GFP transfected cells on laminin did not induce the formation of filopodia (**C**) or the reorganisation of actin filament; actin stress fibre phenotype was found in the cells (**E**). (**D**), the merged image of  $\alpha\beta\Delta\alpha$ DG-GFP (green) and actin (red). Scale bar = 25 $\mu$ m



The localisation of  $\alpha\beta\Delta\alpha$  DG-GFP is very different from that found in the expression of  $c\beta$ DG-GFP or  $\beta$ DG-GFP. The  $\alpha\beta\Delta\alpha$  DG-GFP was mainly localised in the perinuclear region instead of in the nucleus (Fig 4.11A, arrow). Additionally, high levels of  $\alpha\beta\Delta\alpha$  DG-GFP staining were toward in the cytoplasm forming a vesicle-like structures (Fig 4.11 B, arrow). Since the N-terminal signal peptide is predicted to direct dystroglycan to the ER lumen and to be cleaved off as soon as the  $\alpha\beta$ -dystroglycan precursor is elongated through the ER membrane (Fig 4.16), the possible impact of the N-terminal SP for dystroglycan- dependent filopodia formation could be to regulate dystroglycan trafficking instead of to regulation of dystroglycan signal transduction. The vesicle-like structures of  $\alpha\beta\Delta\alpha$  DG-GFP distributed in the perinuclear region demonstrates that  $\alpha\beta\Delta\alpha$  DG-GFP is still maintained in the submembrane system such as ER, Golgi, and transporting vesicles. Despite the ER-Golgi or post-Golgi processing and transporting of dystroglycan, these results suggest that although the N-terminal SP peptide is required to direct dystroglycan to its exocytotic route away from the nucleus, it is still insufficient for  $\beta$ -dystroglycan to mediate the formation of filopodia. Thus, both  $\alpha$ -dystroglycan and the N-terminal SP domain might be necessary for dystroglycan-dependent filopodia formation.

Together the results shown in section 4.2.5 to 4.2.7, suggested that  $c\beta$  alone is insufficient to mediate the dystroglycan dependent filopodia formation;  $e\beta$ , TM, or dystroglycan N-terminal SP is not the domain required for  $c\beta$  to mediate the formation of filopodia either. Thus,  $\alpha$ -dystroglycan is the suspected functional domain that contributes to  $\beta$ -dystroglycan cytoplasmic domain to mediate the formation of filopodia. Inconsistently, however, the results in section 4.2.4 showed that  $\alpha$ -dystroglycan-laminin engagement is not necessary for dystroglycan-dependent filopodia formation. The explanation for the phenomenon is that while  $\alpha$ -dystroglycan might be unnecessary for dystroglycan signal transduction, it plays a crucial role in the biosynthesis of the dystroglycan propeptide, especially in the protein transporting and localisation pathways.

#### 4.2.8 Expression of $\alpha\beta$ dystroglycan deletion mutant ( $\alpha\beta\Delta\epsilon\beta$ -GFP) in REF52 cells

To examine the hypothesis above and determine the role of  $\alpha$ -dystroglycan in dystroglycan dependent filopodia formation, a  $\beta$ -dystroglycan extracellular domain deletion mutant ( $\alpha\beta\Delta\epsilon\beta$ -GFP) was constructed and expressed in REF52 cells. Very interestingly, the expression of  $\alpha\beta\Delta\epsilon\beta$ -GFP showed that the filopodia phenotype was restored (Fig 4.13 A and B). The morphology of the  $\alpha\beta\Delta\epsilon\beta$ -GFP transfected cells was very similar to that of  $\alpha\beta$ DG-GFP transfected cells; hundreds of filopodia were expressed throughout the cell surface. Replating the  $\alpha\beta\Delta\epsilon\beta$ -GFP transfected cells on laminin, produced a clear filopodia phenotype (Fig 4.13 C) with reduced numbers of stress fibres observed (Fig 4.13 D).

As a control,  $\alpha$ DG-GFP, which composes of  $\alpha$ -dystroglycan and its N-terminal signal sequence, was constructed and expressed in REF52 cells. The expression of  $\alpha$ DG-GFP in REF52 cells is weaker than the other dystroglycan mutant constructs in the experiment. As shown in figure 4.14 A-C, the expression of  $\alpha$ DG-GFP did not induce any filopodia formation in the REF52 cells, revealing that  $\alpha$ -dystroglycan is insufficient to induce the formation of filopodia. Thus, in the  $\alpha\beta\Delta\epsilon\beta$ -GFP, the cytoplasmic domain of  $\beta$ -dystroglycan instead of  $\alpha$ -dystroglycan is responsible for induction of the formation of filopodia.

However, as shown in section 4.2.5 to 4.2.7, the dystroglycan mutants without the  $\alpha$  subunit localised to the nucleus or the submembrane system in the cytoplasm and failed to mediate the formation of filopodia. Therefore, supporting our hypothesis,  $\alpha$ -dystroglycan is indeed necessary for dystroglycan dependent filopodia formation; but instead of participating in the cytoskeleton reorganisation signalling events,  $\alpha$  dystroglycan probably plays a crucial role in the post-translational modification and targeting of dystroglycan to its membrane location.

**Figure 4.13 Expression of  $\beta$ -dystroglycan extracellular domain deletion mutant,  $\Delta\epsilon\beta$ DG-GFP, in REF52 cells**

REF52 cells plated on glass coverslips were transfected with  $\alpha\beta\Delta\epsilon\beta$ DG-GFP (1.8 $\mu$ g/ml), following the transfection procedure and cells were subsequently incubated at 37°C overnight (**A and B**). The  $\alpha\beta\Delta\epsilon\beta$ DG-GFP transfected cells were replated onto laminin (2  $\mu$ g/ml) coated glass coverslips and incubated in DMEM containing 1% FBS at 37°C overnight (**C**). The coverslips with cells were fixed with 3.7% formaldehyde.  $\alpha\beta\Delta\epsilon\beta$ DG-GFP transfected cells plated on laminin were further stained with rhodamine-phalloidin [(Sigma) at 1:1000]. Filopodia phenotype was present at the cell periphery (**A, arrow**) and on the surface (**B, arrow**) in the cells expressing  $\Delta\epsilon\beta$ DG-GFP. Filopodia phenotype (**C**) and reduced number of stress fibre (**D**) were found in the  $\Delta\epsilon\beta$ DG-GFP transfected cells replated on laminin. (**E**), The merged image of  $\Delta\epsilon\beta$ DG-GFP (green) and actin (red). Scale bar = 25 $\mu$ m

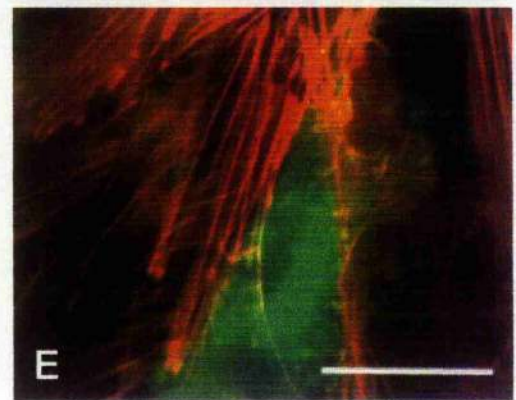
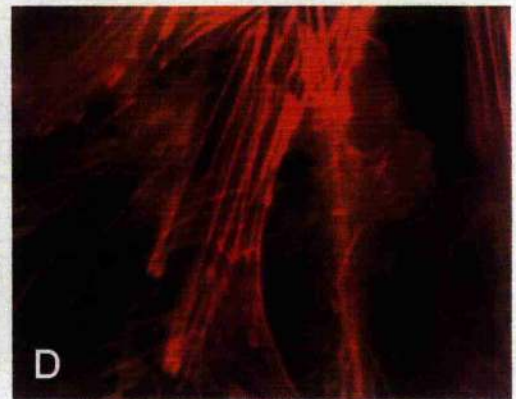
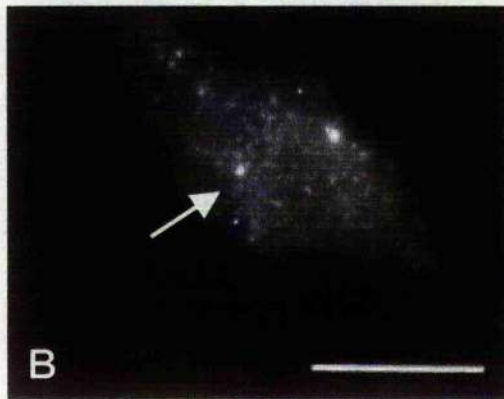
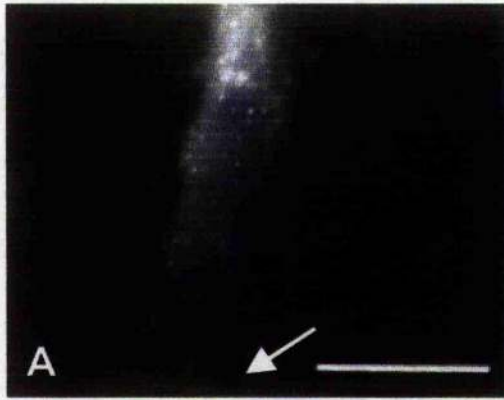
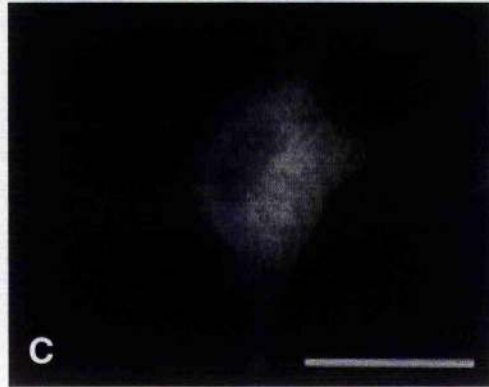
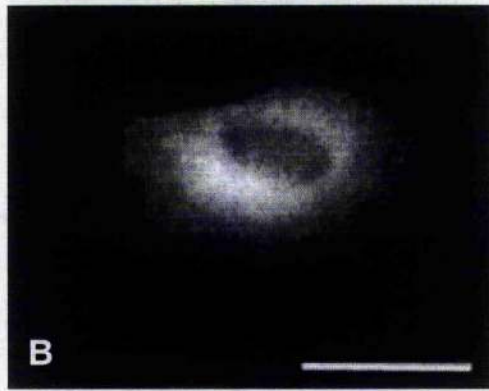
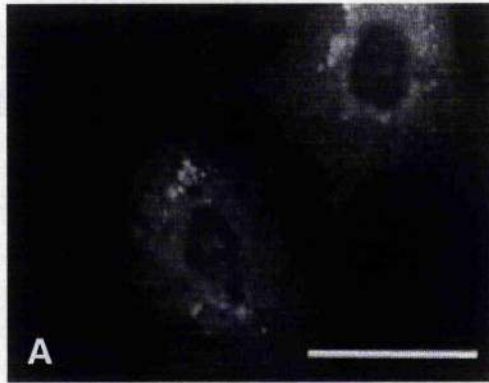


**Figure 4.14 Expression of  $\alpha$ DG-GFP in REF 52 cells**

REF52 cells plated on glass coverslips were transfected with  $\alpha$ DG-GFP (1.8 $\mu$ g/ml) following the transfection procedure and they were subsequently incubated at 37 $^{\circ}$ C overnight (A-B). The  $\beta$ DG-GFP transfected cells were replated on laminin (2 $\mu$ g/ml) coated coverslips and incubated in DMEM containing 1% FBS at 37  $^{\circ}$ C overnight (C-E). The coverslips were fixed with 3.7% formaldehyde. Expression of  $\alpha$ DG-GFP did not induce the formation of filopodia. The fluorescent level of the  $\alpha$ DG-GFP was low, and the  $\alpha$ DG-GFP protein diffused all around the cells. No significant localisation of  $\alpha$ DG-GFP was seen in the cells. Scale bar=25 $\mu$ m.





#### **4.2.9 Expression of alkaline phosphatase conjugated $\beta$ -dystroglycan (AP- $\beta$ DG) construct in REF52 cells**

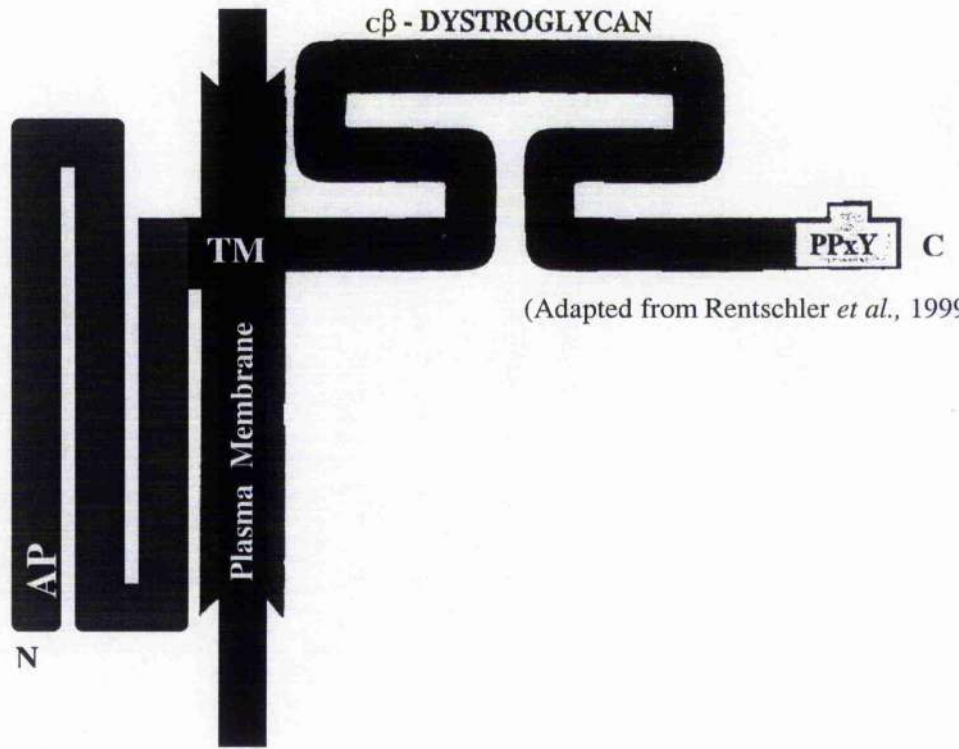
As shown in the results, defects in  $\alpha$ -dystroglycan disrupt the formation of filopodia due to the loss of localisation of the  $\beta$ -dystroglycan cytoplasmic domain. Therefore, the localisation of dystroglycan seems to play a critical role in the formation of filopodia. Dystroglycan is a transmembrane protein; to determine whether the membrane localisation is crucial for  $\beta$ -dystroglycan cytoplasmic domain to mediate the formation of filopodia, an alkaline phosphatase conjugated  $\beta$ -dystroglycan (AP- $\beta$ DG) construct was expressed in REF52 cells. The AP- $\beta$ DG construct expresses a fusion protein of alkaline phosphatase (AP) conjugated to the N-terminal of  $\beta$ -dystroglycan transmembrane and cytoplasmic domain (Rentschler *et al.*, 1999). Since AP is a secreted protein that undergoes the exocytotic sorting from the Golgi and is released from the plasma membrane, the conjugation of the  $\beta$ -dystroglycan transmembrane and cytoplasmic domain could maintain the AP on the plasma membrane surface with  $\beta$ -dystroglycan cytoplasmic domain at the intracellular region proximal to the membrane (Fig 4.15 A). Thus the AP- $\beta$ DG fusion protein is predicted to mimic the localisation of the cytoplasmic domain of  $\beta$ -dystroglycan in the plasma membrane region but without  $\alpha$ -dystroglycan. The expression of AP- $\beta$ DG can be detected by standard AP development (section 2.2.1.11).

As shown in figure 4.15 B, REF52 cells expressing AP- $\beta$ DG showed similar morphology to the expressing  $\alpha\beta$ DG-GFP; many thin and long filopodia were found extended around the cell surface (Fig 4.15 B, arrows), suggesting that filopodia formation signalling in the AP- $\beta$ DG transfected cells was activated due to the membrane localisation of  $\beta$ -dystroglycan cytoplasmic domain. Despite of the loss of function of  $\alpha$ - and  $\epsilon\beta$ -dystroglycan,  $\beta$ -dystroglycan cytoplasmic domain can still mediate the formation of filopodia. This finding suggests that it is the membrane localisation of  $\beta$ -dystroglycan that is crucial for the  $\beta$ -dystroglycan cytoplasmic domain to mediate filopodia formation.  $\alpha$ -dystroglycan, which appeared to be necessary for dystroglycan dependent filopodia formation, is involved in targeting  $\beta$ -dystroglycan to its membrane localisation. In fact,

**Figure 4.15 Expression of alkaline phosphatase tagged  $\beta$ -dystroglycan construct (AP- $\beta$ DG) in REF52 cells**

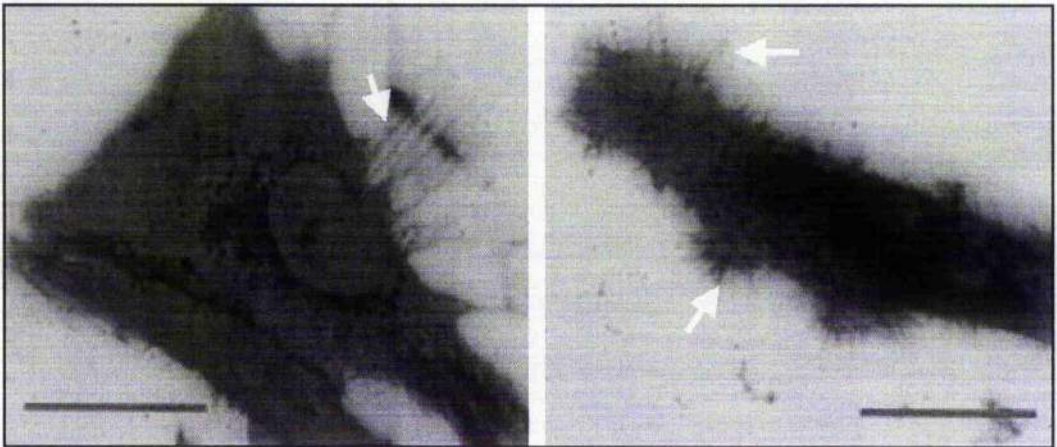
(A) A model of AP- $\beta$ DG and its localisation to the plasma membrane. Alkaline phosphatase (AP) was conjugated to the N-terminal of  $\beta$  dystroglycan transmembrane domain (TM) and cytoplasmic domain. The  $\beta$ -dystroglycan transmembrane domain maintains the AP on the plasma membrane surface, allowing  $\beta$ -dystroglycan cytoplasmic domain to localise to the proximal membrane region. AP- $\beta$ DG (2 $\mu$ g/ml) was transfected into REF52 cells on glass coverslips. The coverslips with cells were fixed with 3.7% formaldehyde and treated with 0.1% Triton X-100 in PBS, and then developed in AP buffer containing 0.4mM NBT and 0.4mM BCIP. Filopodia phenotype was present in the cells transfected with AP- $\beta$ DG (B). The distribution of filopodia is all around the cell (B, arrows). Scale bar=25 $\mu$ m

A



(Adapted from Rentschler *et al.*, 1999)

B



with its membrane localisation,  $\beta$ -dystroglycan cytoplasmic domain can mediate the formation of filopodia independently of  $\alpha$ -dystroglycan or the extracellular domain of  $\beta$ -dystroglycan.

A summary of expression, localisation and filopodia phenotype induction of the dystroglycan mutant constructs is shown in table 4.1

**Table 4.1 Localisation and filopodia formation of GFP-tagged dystroglycan and dystroglycan mutants transfected REF 52**

Constructs	Approximate size of the protein expressed in Cos7 cells	Descriptions of expression	Protein localisation	Filopodia phenotype
pEGFP	27KDa	EGFP tagged mammalian cell expression vector	Nucleus and Cytoplasm	-
$\alpha\beta$ DG-GFP	80KDa	Full-length $\alpha\beta$ dystroglycan	Plasma membrane	+
$\alpha\beta\Delta c\beta$ DG-GFP	55KDa	Dystroglycan $c\beta$ deletion mutant	Plasma membrane	-
$c\beta$ DG-GFP	30KDa	Dystroglycan $c\beta$ domain alone	Mainly in nucleus and diffused in cytoplasm	-
$\beta$ DG-GFP	ND*	Dystroglycan full-length $\beta$ alone	Mainly in nucleus and concentrated in perinuclear region	-
$\alpha\beta\Delta\alpha$ DG-GFP	ND*	Dystroglycan $\alpha$ domain deletion mutant	Mainly in perinuclear region and vesicle-like grains in cytoplasm	-
$\alpha\beta\Delta c\beta$ DG-GFP	ND*	Dystroglycan $e\beta$ domain deletion mutant	Plasma membrane	+
$\alpha$ DG-GFP	ND*	Dystroglycan full-length $\beta$ deletion mutant	Cytoplasm	-
AP- $\beta$ DG	ND*	Alkaline phosphatase conjugated $\beta$ dystroglycan (TM+ $c\beta$ )	Plasma membrane	+

\*ND=Unidentified

### 4.3 Discussion

The  $\alpha\beta$ DG-GFP construct was made initially to investigate the relation between ERK and dystroglycan. However, the dramatic actin phenotype in the  $\alpha\beta$ DG-GFP transfected cells implied that dystroglycan might play a role in cytoskeletal reorganisation, which ERK might be not directly involved in. The microspikes present in  $\alpha\beta$ DG-GFP transfected cells were identified as filopodia. To date dystroglycan-dependent filopodia formation signalling has not been reported. Therefore, the interest shifted to the study of dystroglycan-dependent filopodia formation and associated signalling. First, the cytoplasmic domain of  $\beta$ -dystroglycan was determined to be responsible for the formation of filopodia. Additionally, integrin signalling was shown to be involved in the dystroglycan dependent filopodia formation. The interaction of dystroglycan PPPY motif and utrophin WW domain appeared to have no effect on the dystroglycan dependent filopodia formation. Moreover, different dystroglycan functional domain deletion mutants led to differing localisations of dystroglycan, but only dystroglycan localised to the plasma membrane is able to mediate the formation of filopodia (Table 4.1). Therefore, the spatial localisation might be very important for  $\beta$ -dystroglycan to carry out its biological function. The other functional domains of dystroglycan, during post-translational modification or post-Golgi sorting, could contribute to  $\beta$ -dystroglycan function as targeting it to its membrane localisation.

#### 4.3.1 Spatial importance for $\beta$ -dystroglycan cytoplasmic domain in induction of filopodia formation

The formation of filopodia induced by expression of  $\alpha\beta$ DG-GFP was significantly greater than induced by the expression of  $\beta$ -dystroglycan cytoplasmic domain deletion mutant ( $\alpha\beta\Delta$ c $\beta$ DG-GFP), suggesting that the  $\beta$ -dystroglycan cytoplasmic domain is an important mediator of dystroglycan-dependent filopodia formation. This result was perhaps not too surprising since the cytoplasmic domain of  $\beta$ -dystroglycan has long been considered to be associated with signalling molecules and regarded as a potential mediator of cytoskeleton reorganisation (Yang *et al.*, 1995; Henry and Campbell, 1996;

Winder, 2001). However, the result of c $\beta$ DG-GFP expression showed that despite being an important mediator for dystroglycan-dependent filopodia formation,  $\beta$ -dystroglycan cytoplasmic domain on its own is insufficient to induce filopodia formation. Expression of c $\beta$ DG-GFP,  $\beta$ DG-GFP or  $\alpha\beta\Delta\alpha$ DG-GFP which all lack  $\alpha$ -dystroglycan were unable to induce the formation of filopodia, whereas the filopodia phenotype was restored in the cell expressing  $\alpha\beta\Delta\epsilon\beta$ DG-GFP construct, indicating that  $\alpha$ -dystroglycan, is as important as  $\beta$ -dystroglycan cytoplasmic domain inducing dystroglycan dependent filopodia formation. However, as dystroglycan-dependent filopodia formation appeared to be induced by fibronectin,  $\alpha$ -dystroglycan seemed to be unnecessary for the dystroglycan-dependent filopodia formation.

The explanation of why  $\alpha$ -dystroglycan plays an inconsistent role in the dystroglycan dependent filopodia formation could be that  $\alpha$ -dystroglycan is required for the dystroglycan propeptide to complete the post-translational modification and consequently localise dystroglycan to the plasma membrane. Membrane localisation would be crucial for dystroglycan to mediate the formation of filopodia. This hypothesis is strongly supported by the expression of AP- $\beta$ DG that mimics the localisation of the endogenous  $\alpha\beta$ -dystroglycan heterodimer on the plasma membrane. Although the  $\alpha$  subunit is deleted, the  $\beta$ -dystroglycan cytoplasmic domain of AP- $\beta$ DG was localised to the intracellular proximal membrane region, and could mediate the formation of filopodia. This suggested that  $\alpha$ -dystroglycan, or  $\alpha$ -dystroglycan-laminin engagement, is not necessary for  $\beta$ -dystroglycan cytoplasmic domain to mediate the formation of filopodia; it is the membrane localisation that allows  $\beta$ -dystroglycan cytoplasmic domain to mediate the formation of filopodia. The role of  $\alpha$ -dystroglycan in the dystroglycan dependent filopodia formation is to target dystroglycan to the membrane localisation.

In previous studies of dystroglycan function, a great deal of effort was placed on the study of  $\alpha$ -dystroglycan. Dystroglycan is thought to be a laminin receptor which might stimulate cell adhesion and cytoskeletal organisation signalling (Ervasti and Campbell, 1991; reviewed in Durbeej et al., 1998a). The results here show strong evidence that  $\beta$ -



dystroglycan is able to mediate the cytoskeletal organisation signalling, independent of  $\alpha$ -dystroglycan. In this case,  $\alpha$ -dystroglycan is required for  $\beta$ -dystroglycan targeting to the plasma membrane instead of transmitting extracellular signalling to stimulate  $\beta$ -dystroglycan dependent filopodia formation.

These results show that the plasma membrane localisation is required for  $\beta$ -dystroglycan to act as a mediator for filopodia formation. It may reflect a possible biological role of  $\beta$ -dystroglycan cytoplasmic domain in the formation of filopodia. During the formation of actin-based membrane protrusions or filopodia, a variety of essential molecules including Rho GTPases, Arp2/3 complex, N-WASP, actin, etc., are recruited or accumulated in the membrane cortex (reviewed in Mullins et al., 1998) (Chapter 5) The results here show that integrin-mediated adhesion signalling was also required for the dystroglycan-dependent filopodia formation signalling, suggesting that crosstalk between integrins and cytoplasmic domain of  $\beta$ -dystroglycan might be very important for dystroglycan to mediate filopodia formation. Therefore, the membrane localisation of  $\beta$ -dystroglycan cytoplasmic domain could allow dystroglycan to interact with membrane signalling molecules, including crosstalk with integrins, and to act as a mediator of actin filopodia formation. The molecular basis of filopodia formation and the mechanisms of dystroglycan in the formation of filopodia will be discussed in Chapter 5.

#### **4.3.2 Role of $\beta$ -dystroglycan C-terminal tail PPPY motif in dystroglycan dependent filopodia formation**

The results have shown that the 120 a.a. (776-893)  $\beta$ -dystroglycan cytoplasmic domain is a mediator of filopodia formation, however, which motif in the  $\beta$ -dystroglycan cytoplasmic domain is responsible for the dystroglycan-dependent filopodia formation? Several proline-rich regions, which are potential candidates for the signalling adaptor motifs, have been identified in the  $\beta$ -dystroglycan cytoplasmic domain. Of these, the PPPY motif at the very C-terminal tail of  $\beta$ -dystroglycan is the best characterised (Jung *et al.*, 1995; Rentschler *et al.*, 1999). Since the PPPY motif is the signalling motif that directly regulates the association between dystroglycan and actin cytoskeleton through

the interaction with utrophin/dystrophin WW domain (Winder, 1997), it is the PPPY motif of  $\beta$ -dystroglycan that was initially suspected to be the mediator for dystroglycan dependent filopodia formation. However, as seen in the experiments shown in section 4.2.2.3,  $\alpha\beta$ DG-GFP transfected utrophin-knockout cells clearly expressed a filopodia phenotype, suggesting that utrophin might not be a mediator of  $\beta$ -dystroglycan cytoplasmic domain dependent filopodia formation. Therefore, the PPPY-WW interaction might not be involved in the dystroglycan dependent filopodia formation. However, since integrin dependent adhesion, which leads to the tyrosine phosphorylation at Y892 of PPPY motif, might be involved in the dystroglycan dependent filopodia formation signalling, the PPPY motif might still be involved in dystroglycan-dependent filopodia formation.

In addition to the WW domain, the N-terminal SH3 domain of Grb2 SH2 (Yang *et al.*, 1995; Jung *et al.*, 1995) and caveolin were also shown to associate with the PPPY motif of  $\beta$ -dystroglycan. Interestingly, WW, Grb2 and caveolin are all molecules which compete for the PPPY motif (Rosso *et al.*, 2000; Sotgia *et al.*, 1999) (section 1.4). The tyrosine phosphorylation of Y892 of PPPY appears to play an important role in regulating the binding of these competitors. Tyrosine phosphorylation at Y892 has been shown to lead to the reduction in its binding affinity to the WW domain (Ilsley *et al.*, 2001) and recruitment of SH2 containing molecules (Sotgia *et al.*, 2001). Caveolin appeared to bind PPPY motif in an Y892 phosphorylation independent manner (Sotgia *et al.*, 2001) however, the interaction with caveolin inhibits phosphorylation at Y892 (Sotgia *et al.*, 2003). Therefore, the precise role of this regulation is still elusive. While evolutionarily unrelated, the Grb2 SH3 domain shows a striking structural similarity to the WW domain (Yu, *et al.*, 1994; Feng *et al.*, 1994; Lim *et al.*, 1994) and it also interacts with the PPPY motif of  $\beta$ -dystroglycan (Jung *et al.*, 1995). Grb2, which associates with the PPPY motif, has been shown to associate with FAK via its SH2 domain (Cavaldesi *et al.*, 1999), to date, however, Grb2-FAK mediated dystroglycan signalling events have not been reported, and it has also not yet been determined whether the binding of Grb2 is regulated by the Y892 phosphorylation of the PPPY motif. The role of Grb2 in  $\beta$ -dystroglycan signalling is still elusive. It has been shown

that tyrosine phosphorylation at Y892 of  $\beta$ -dystroglycan led to the recruitment of SH2 containing proteins (Sotgia *et al.*, 2001). Therefore, Grb2 might still be a potential adaptor for dystroglycan to couple to other signalling pathways.

#### **4.3.3 Dystroglycan functional domains in its post-translational processing**

As mentioned above, the results have shown that in order to induce filopodia formation,  $\beta$ -dystroglycan localised to the plasma membrane is able to mediate the signalling independent of  $\alpha$ -dystroglycan-laminin interaction. However,  $\alpha$ -dystroglycan is required for  $\beta$ -dystroglycan to target to its membrane localisation. This interesting finding implies that the interaction of dystroglycan  $\alpha$ - and  $\beta$ - subunit during biosynthesis, perhaps during the post-translational processing, plays an important role in leading dystroglycan to its membrane localisation. Dystroglycan is encoded by a single mRNA and translated to a 97 KDa  $\alpha\beta$ -dystroglycan propeptide (Ibraghimov-Beskrovnaya *et al.*, 1992). This propeptide undergoes post-translational modification, including glycosylation at several sites and proteolytic cleavage at Ser 653, to generate mature  $\alpha$ - and  $\beta$ - dystroglycan subunits (Ervasti and Campbell, 1993) (section 1.2). It has been shown that level of both  $\alpha$ - and  $\beta$ -dystroglycan were greatly reduced on the muscle membrane of dystrophin gene deficient *mdx* mice or DMD patients while the mRNA for dystroglycan propeptide was still expressed at normal levels (Ibraghimov-Beskrovnaya *et al.*, 1992), suggesting the reduction of dystroglycan in DMD patients or *mdx* mice is in response to a defect in posttranslational modification instead of the transcription of dystroglycan. Thus the proper presence of dystroglycan at the plasma membrane might be modulated by its posttranslational modification.

##### **4.3.3.1 Glycosylation of dystroglycan in biosynthesis**

Dystroglycan is a highly glycosylated protein with both O-linked and N-linked glycoconjugation (Ibraghimov-Beskrovnaya *et al.*, 1992). To date, the structure of the glycoconjugation and the role of glycosylation in dystroglycan function are still poorly understood. The O-linked glycosylation with large amounts of sialic acid present on amino acid residues 318-484, forms a region of mucin-like structure on  $\alpha$ -dystroglycan

(Ibraghimov-Beskrovnaya *et al.*, 1992). Chemical deglycosylation that removes all glycosylation on dystroglycan causes the loss of binding of dystroglycan to laminin, while removal of N-linked glycosylation of dystroglycan did not affect on laminin binding activity of dystroglycan (Ervasti and Campbell, 1993), suggesting that O-linked sugars on  $\alpha$ -dystroglycan are responsible for its laminin binding activity. The O-linked glycans of  $\alpha$ -dystroglycan has been identified in bovine peripheral nerve as an O-mannosyl linkage, which is rarely expressed in other mammalian proteins (Chiba *et al.*, 1997). An O-mannosyl structure, Neu5Ac( $\alpha$ 2-3)Glc( $\beta$ 1-4)GlcNAc( $\beta$ 1-2)Man-Ser/Thr, isolated from dystroglycan has been proposed to be required for laminin binding, however, this a poor inhibitor of the binding of dystroglycan to laminin, suggesting that on  $\alpha$ -dystroglycan, it is not the main structure for laminin binding (Chiba *et al.*, 1997). Sialic acid has been reported to inhibit laminin binding to  $\alpha$ -dystroglycan in bovine peripheral nerve at a very low concentration and might be critical for laminin binding (Yamada *et al.*, 1996a). However, enzymatic removal from skeletal muscle dystroglycan has no effect on laminin binding (Ervasti *et al.*, 1997). Furthermore, dystroglycan from brain and cardiac muscle has decreased terminal sialoglycosylation compared to skeletal muscle dystroglycan but dystroglycan from all three tissues binds tightly to laminin (Ervasti *et al.*, 1997). Therefore, although it is well accepted that glycoconjugates are important for ligand binding, the hypothesis that specific glycoconjugates on dystroglycan are involved directly in ligand binding is still controversial.

While O-linked glycoconjugates of  $\alpha$ -dystroglycan have been accepted to be involved in the binding of laminin, the function of the N-linked glycoconjugates on dystroglycan are uncertain. Treatment with N-glycanases that completely removed all N-linked oligosaccharides did not alter the binding activity of dystroglycan to laminin suggesting N-linked sugars are not required for ligand binding (Ervasti and Campbell, 1993). Unlike O-linked glycosylation, structures of N-linked glycosylation in cells are more diverse. Removal of N-linked glycoconjugates by treatment of PNGaseF or blocking the synthesis of N-linked glycosylation by using tunicamycin has no effect on the proteolytic cleavage at Ser653 of dystroglycan propeptide to from  $\alpha$  and  $\beta$  subunits, suggesting that the N-linked oligosaccharides not required for the proteolytic cleavage of

dystroglycan precursor peptide (Holt *et al.*, 2000). Interestingly, while the N-linked sugar chains might not be involved in the proteolytic cleavage event, blocking N-linked glycosylation inhibits the trafficking of  $\beta$  dystroglycan. In the presence of tunicamycin,  $\beta$ -dystroglycan was accumulated in perinuclear region instead of localising in peripheral cell membrane (Holt *et al.*, 2000). Thus, N-linked oligosaccharides on dystroglycan might play an important role in directing dystroglycan to its membrane localisation.

Four potential N-glycosylation sites have been identified on dystroglycan, three of them are on  $\alpha$  (Asn-141, Asn-641 and Asn-649) subunits and the other one (Asn-661) is on a  $\beta$ -subunit; none of their structures have been identified, the function of these N-linked glycoconjugates is also unclear. The results presented here showed that the formation of filopodia in cells is not altered in cells expressing  $\beta$ -dystroglycan extracellular domain deletion mutant ( $\alpha\beta\Delta\epsilon\beta$ -GFP) or AP-tagged  $\beta$ -dystroglycan (AP- $\beta$ DG) lacking the  $\beta$ -dystroglycan extracellular domain, suggesting that  $\beta$ -dystroglycan extracellular domain containing its N-linked sugar chain, is not required for dystroglycan targeting to plasma membrane. The other two N-linked glycoconjugates which are very close to each other are located at the C-terminal end of  $\alpha$ -dystroglycan (Asn-641 and Asn-649). It is likely that these two N-linked sugar chains might be involved in regulation of binding affinity between dystroglycan  $\alpha$  and  $\beta$  subunits. However, a recent study has determined that the amino acid sequence 550-585 on  $\alpha$ -dystroglycan is sufficient for binding to the extracellular domain of  $\beta$ -dystroglycan (Bozzi *et al.*, 2001). Therefore, the N-linked oligosaccharide at Asn-641 and Asn-649 might not directly affect the binding of  $\alpha$ - and  $\beta$ - dystroglycan subunits.

N-linked sugar chains on  $\alpha$  and  $\beta$  dystroglycan have been shown to be unnecessary for proteolytic cleavage but are required for the proper localisation of  $\beta$ -dystroglycan (Holt *et al.*, 2000), raising a possibility that the N-linked glycoconjugates of dystroglycan play a role in dystroglycan submembrane trafficking. Since all the dystroglycan deletion mutants lacking the  $\alpha$ -subunit cannot induce the formation of filopodia due to the unsuccessful targeting to plasma membrane, this suggests that  $\alpha$ -dystroglycan is

required for dystroglycan targeting to plasma membrane, and it is very likely the N-linked glycoconjugates on  $\alpha$ -dystroglycan play an important role in dystroglycan trafficking and membrane localisation.

#### **4.3.3.2 Hypothesis for dystroglycan trafficking**

The processing and maturation of dystroglycan is still elusive. However, recent studies of Fukuyama congenital muscular dystrophy (FCMD), congenital muscular dystrophy type 1C (MDC1C) and Muscle-Eye-Brain (MEB) disease have provided some clues. FCMD is one of the congenital muscular dystrophies (CMD), which is caused by the mutation in the gene encoding fukutin (Kondo-Iida, *et al.*, 1999). FCMD patients suffer congenital muscular dystrophy with mental retardation and neuronal migration defects (Fukuyama *et al.*, 1981). The muscle biopsies have shown that the glycosylation of  $\alpha$ -dystroglycan on the muscle membrane of FCMD patients was greatly reduced (Hayashi *et al.*, 2001). Laminin binding activity of dystroglycan on FCMD muscle membrane was greatly reduced as well (Cote *et al.*, 2002; Cohn *et al.*, 2002), indicating that O-linked glycoconjugates on  $\alpha$ -dystroglycan which are responsible for laminin LG domain binding, are affected by the abnormality in fukutin. Similar levels of  $\alpha$ -dystroglycan reduction and loss of laminin binding ability were also found in the muscle membrane of an MEB patient (Chiba *et al.*, 1997). MEB is an autosomal recessive disorder characterised by congenital muscular dystrophy, ocular abnormalities, and brain malformation (Santavuori *et al.*, 1989). Recently, MEB has been shown to be caused by mutation in the protein peptide-O-mannosyl-GlcNac transferase (POMGnT1) (Yoshida *et al.*, 2001). Therefore, the reduction of  $\alpha$ -dystroglycan in muscle membrane, which causing MEB or FCMD, might result from the defect in O-linked glycosyltransferases and failure of the processing the O-linked glycoconjugates on  $\alpha$ -dystroglycan. Interestingly, while there was a greatly reduced level of glycosylated  $\alpha$ -dystroglycan, the normal level of  $\beta$ -dystroglycan localised on plasma membrane was still found in FCMD or MEB muscles (Michele *et al.*, 2002), suggesting that the expression or localisation of  $\beta$ -dystroglycan is not affected by the abnormalities of O-linked glycosylation of  $\alpha$ -dystroglycan. The membrane targeting of  $\beta$ -dystroglycan might be unaffected by the O-linked glycoconjugates on  $\alpha$ -dystroglycan.

The function of fukutin in FCMD is unknown. However, a homologue for fukutin, fukutin related protein (FKRP), which was identified in MDC1C, has been studied very recently (Aravind, *et al.*, 1999; Brockington *et al.*, 2001; Esapa *et al.*, 2002). MDC1C is caused by mutation in FKRP; patients with MDC1C have severe muscular dystrophy as well. A reduction in glycosylated  $\alpha$ -dystroglycan has been found in MDC1C patients, revealing that the FKRP might be involved in the glycosylation and maturation of dystroglycan (Brockington *et al.*, 2001). The primary sequence showed that both FKRP and fukutin are possibly glycosyltransferases (Aravind, *et al.*, 1999). More recently, FKRP has been shown to target to the Golgi apparatus by its N-terminal transmembrane domain, and directly affects the glycosylation of dystroglycan in CHO cells (Esapa *et al.*, 2002). 60KDa and a 90KDa  $\alpha$ -dystroglycan isoforms were detected in cells coexpressing FKRP and chick dystroglycan (ChDG) while the 160KDa mature  $\alpha$ -dystroglycan was detected in cells expressing ChDG alone, indicating glycosylation of  $\alpha$ -dystroglycan is affected by FKRP (Esapa *et al.*, 2002). Interestingly, the western blotting of  $\beta$ -dystroglycan in the ChDG and FKRP coexpressing cells showed that  $\beta$ -dystroglycan was also reduced from mature 43KDa to an approximately 41KDa isoform, indicating the N-linked glycosylation on  $\beta$ -dystroglycan is also affected by FKRP. Additionally, FKRP mutants which are unable to target to the Golgi apparatus did not appear to affect the glycosylation of  $\alpha$ - and  $\beta$ -dystroglycan, demonstrating that FKRP is a Golgi associated protein that directly alters the glycosylation of  $\alpha$ - and  $\beta$ -dystroglycan in the subcellular state (Esapa *et al.*, 2002).

These findings raise several ideas for the post-translational processing of dystroglycan. First, during trafficking, full-length  $\alpha$ -dystroglycan and the extracellular domain of  $\beta$ -dystroglycan are presumably localised at the ER lumen or Golgi lumen while the cytoplasmic domain is at the surface of ER or Golgi membrane. Therefore the glycosylation modifications of  $\alpha$ -dystroglycan and extracellular domain of  $\beta$ -dystroglycan can take place in the ER or Golgi lumen. Second, since glycosylated reduction of  $\alpha$ -dystroglycan in MDC1C results from mutations in the *FKRP* gene, the expression of FKRP is expected to restore the glycosylation of  $\alpha$ -dystroglycan. However,

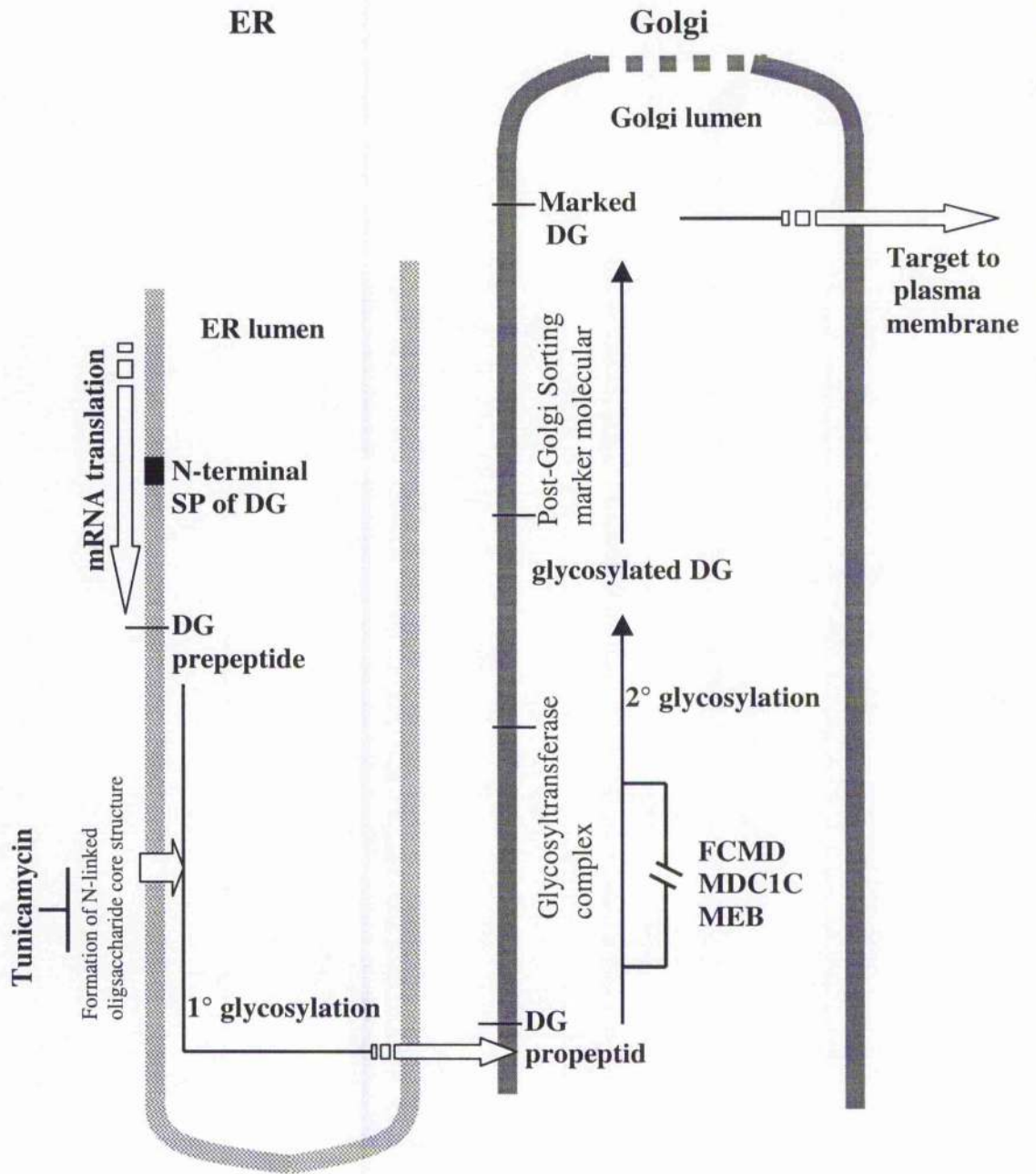
the coexpression of FKRP and dystroglycan subsequently reduced the glycosylation of  $\alpha$ -dystroglycan, implying that FKRP might not be the only Golgi associated protein that modulates the glycosylation of dystroglycan. Several glycosyltransferases on the Golgi membrane which might have opposing function to FKRP, might be involved in the glycosylation of dystroglycan. Since increasing numbers of gene encoding glycosyltransferases or homology to glycosyltransferases are found to be mutated resulting in the reduction of a dystroglycan glycosylation (Michele and Campbell, 2003), the glycosylation of dystroglycan might be catalysed by a group of glycosyltransferases, perhaps forming a protein complex on the Golgi membrane. Finally, it has been shown that O-linked glycosylation on  $\alpha$ -dystroglycan has no effect on trafficking of dystroglycan but N-linked glycosylation has (Holt *et al.*, 2000), and our results showed that  $\alpha$ -dystroglycan is necessary for  $\beta$ -dystroglycan targeting to the plasma membrane. Thus, the N-linked glycosylation on  $\alpha$ -dystroglycan seem to play a role in dystroglycan trafficking. The hypothesis of posttranslational route of dystroglycan is shown in figure 4.14

Altogether, in this chapter, it has been found that expression of dystroglycan dramatically induces the formation of actin-rich filopodia phenotype in REF52 cells, suggesting a novel role for dystroglycan triggering actin filopodia formation. The functional domain of dystroglycan responsible for the formation of filopodia is located in the cytoplasmic domain of  $\beta$ -dystroglycan. However, the PPPY motif of  $\beta$ -dystroglycan, which is responsible for the regulation of WW domain, Grb2, and caveolin binding, might not be a direct mediator for dystroglycan-dependent filopodia formation.  $\beta$ -dystroglycan with proper plasma membrane localisation can mediate the formation of filopodia independent of  $\alpha$ -dystroglycan, suggesting that  $\beta$ -dystroglycan can undergo intracellular regulation which is not directly affected by  $\alpha$ -dystroglycan-laminin interaction. Integrin dependent adhesion signalling is involved in the dystroglycan dependent filopodia formation, implying crosstalk between integrin and dystroglycan.



#### **Figure 4.16 Model of posttranslational modification route of dystroglycan**

Dystroglycan propeptide is translated from single mRNA by ribosomes on rough endoplasmic reticulum (ER). The N-terminal signal peptide (SP) which directs dystroglycan prepeptide to the ER lumen is cleaved and then digested in the ER membrane. Dystroglycan propeptide is translated as a transmembrane peptide with  $\alpha$ -dystroglycan and extracellular  $\beta$  dystroglycan in the lumen and cytoplasmic  $\beta$ -dystroglycan on the ER surface. The **DG propeptide** undergoes the primary glycosylation (**1<sup>o</sup> glycosylation**) adding the N-linked oligosaccharides core, and then transports to **Golgi** membrane. Treatment with **tunicamycin** inhibits the activity of UDP-N-acetylglucosamine glycosyltransferases and blocks formation of N-linked oligosaccharide cores consequently disrupts the N-linked glycosylation and trafficking of dystroglycan. In the Golgi lumen, by interacting with a series of membrane associated **glycosyltransferases** which might act as a protein complex,  $\alpha$ -dystroglycan and extracellular  $\beta$ -dystroglycan undergo secondary glycosylation (**2<sup>o</sup> glycosylation**) that adds O-linked oligosaccharides and modifies the N-linked oligosaccharides to dystroglycan. Biosynthesis of  $\alpha$ -dystroglycan in **FCMD, MDC1C** or **MEB** patients has a defect in secondary glycosylation; however these defects might not directly affect the exocytosis of dystroglycan. A structure in dystroglycan resulting from secondary glycosylation could be recognised by certain molecules in the Golgi and “label” the dystroglycan. The labeled dystroglycan could be sorted to vesicles and targeted to the membrane by exocytosis.



The spatial importance of the membrane localisation for  $\beta$ -dystroglycan acting as a mediator for filopodia formation implies that during the formation of filopodia,  $\beta$ -dystroglycan might be required for other membrane associated molecules to promote the reorganisation of actin cytoskeleton. Finally, despite  $\alpha$ -dystroglycan not being directly required to regulate the dystroglycan-dependent filopodia formation signalling, it is required for  $\beta$ -dystroglycan targeting to the plasma membrane, suggesting  $\alpha$ -dystroglycan might play an important role in the subcellular trafficking and posttranslational sorting of dystroglycan.

**Chapter 5**  
**Dystroglycan dependent activation of Rho GTPases and the  
organisation of the actin cytoskeleton**

## 5.1 Introduction

### 5.1.1 Cdc42 dependent actin dynamics of the cell cortex

As shown in chapter 4, the actin cytoskeleton was significantly altered by introducing a  $\alpha\beta$ DG-GFP construct into REF52 cells, suggesting dystroglycan is involved in cytoskeleton reorganisation in cells. In mammalian cells, cell locomotion, cell adhesion and spreading, cell polarity, cell movement and wound healing, have all been shown to depend greatly on the organisation of the actin cytoskeleton. The RhoGTPases Rho, Rac and Cdc42 are known to be responsible for the formation of specific actin cytoskeletal structures (reviewed in Hall, 1998) (Fig 1.6 B). Since dystroglycan was initially suspected to regulate the actin cytoskeleton through adhesion signalling, it was initially presumed to be involved in Rho and Rho-dependent stress fibre formation (section 1.5.3). However, the expression of  $\alpha\beta$ DG-GFP induced a clear actin-based filopodia morphology change in REF52 cells which is very similar to that induced in constitutively activated Cdc42 construct transfected cells (Fig 1.6 B, b and Fig 4.3 C). This striking similarity of actin morphology caused by  $\alpha\beta$ DG-GFP strongly implied that activation of Cdc42 might be involved in the dystroglycan dependent filopodia formation.

Cdc42, a member of small Rho GTPase family, was originally detected in the yeast *Saccharomyces cerevisiae* as a mutation that caused defects in budding and cell polarity (Johnson and Pringle, 1990). The studies in yeast suggested that Cdc42 might play a role in cell polarity through an effect on the actin cytoskeleton (Reviews in Herskowitz, 1995). A human homologue of Cdc42 was also identified (Hart *et al.*, 1991). Microinjection of mammalian Cdc42 into fibroblasts revealed a distinct signalling pathway linking plasma membrane receptors to actin cytoskeleton organisation. While both Rac and Cdc42 happened to be involved in the formation of actin rich membrane protrusions (Luo, *et al.*, 1994), expression of Cdc42Hs has been shown to trigger the formation of actin-rich filopodia protrusions at the cell periphery followed by the formation of lamellipodia and membrane ruffling (Kozma *et al.*, 1995). It is suggested

that Cdc42 could be directly responsible for the formation of filopodia which then leads to the activation of Rac.

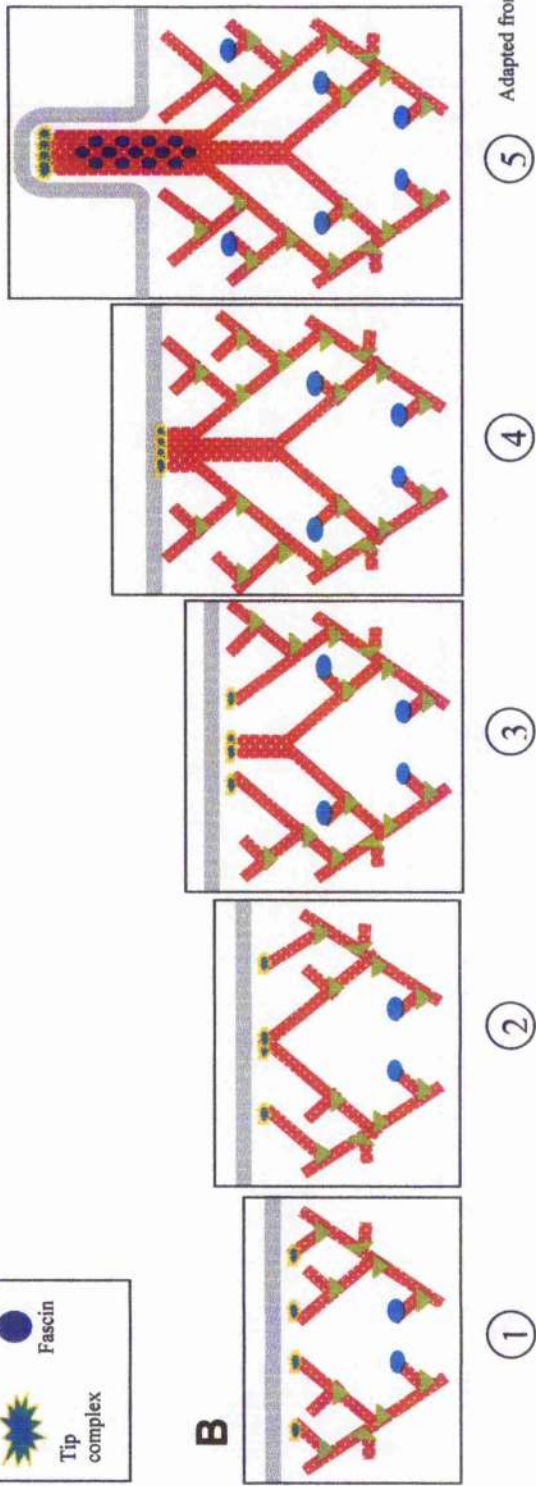
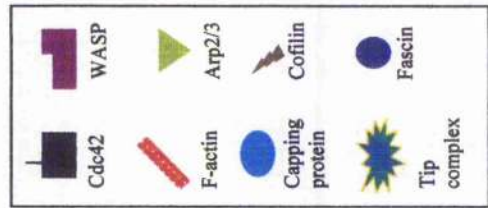
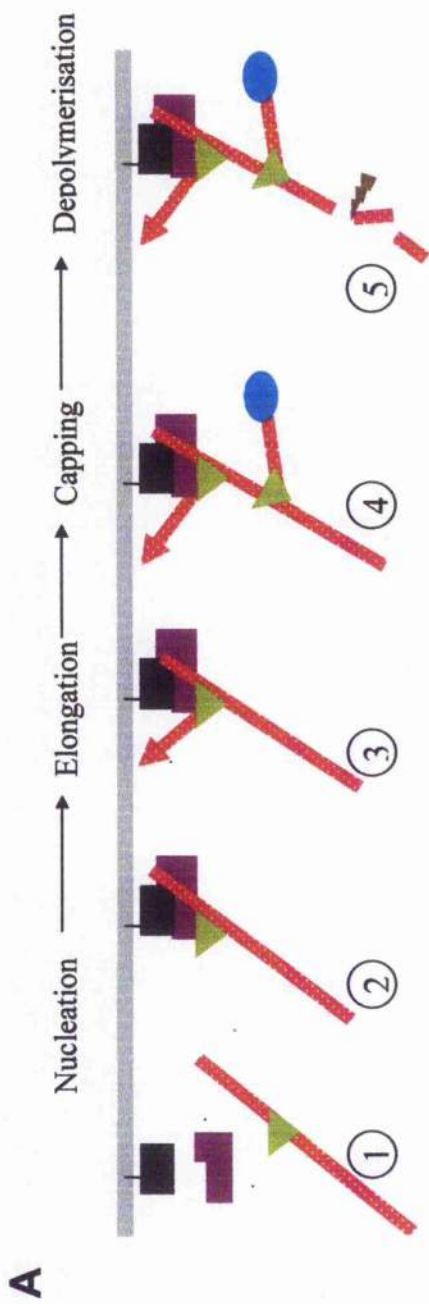
### 5.1.2 Model of Cdc42 dependent filopodia formation

Both filopodia and lamellipodia actin structures have been shown to drive formation of actin-rich membrane protrusion at the cell periphery (reviewed in Pollard *et al.*, 2000). Polymerisation and organisation of actin filaments in protrusions are regulated by Rac or Cdc42 are highly dynamic. Studies of actin organisation at the leading edge of mammalian cells have suggested a Cdc42 dependent pathway in the cell cortex which is mediated by actin binding protein profilin/cofilin, Arp2/3 and WASPs, leading to the formation of dendritic network in actin-based protrusions (Pollard *et al.*, 2000). Since filopodial protrusion was found to be a process based on the lamellipodia meshwork, it was thought to occur by the mechanism which was originally proposed for both lamellipodia and filopodia (Pollard *et al.*, 2000). However, recent studies into filopodia formation suggested that the formation of filopodia, might be initiated by organisation and parallel bundling of the dendritic meshwork of lamellipodia instead of direct elongation of actin filaments from the dendritic meshwork (Svitkina *et al.*, 2003).

In lamellipodia, which are broad, flat protrusions, actin filaments form a branched network (Svitkina *et al.*, 1997; Svitkina and Borisy, 1999). The current model for lamellipodial dynamics (Borisy and Svitkina, 2000; Pollard *et al.*, 2000) suggests a branched actin filament array consists of repeated cycles of dendritic nucleation, elongation, capping, and depolymerization of filaments (Fig 5.1 A). Dendritic nucleation is mediated by the Arp2/3 complex, which is activated by members of WASP family proteins (WASP, N-WASP and SCAR)(reviewed in Higgs and Pollard, 2001). Both WASP and N-WASP has been identified as downstream effectors of active Cdc42 (Symons *et al.*, 1996; Miki *et al.*, 1996) while SCAR was identified as an effector of active Rac (Machesky, *et al.*, 1998). During nucleation, membrane associated Cdc42-GTP recruits and activates WASP. Activation of WASP leads to the recruitment and activation of the Arp2/3 complex, which binds to the side of actin filaments, and triggers the elongation of actin filaments from the Arp2/3 complex side,

**Figure 5.1 Model of Cdc42-dependent lamellipodia formation and filopodia organisation**

(A), The current model for lamellipodial dynamics is a repeated cycle of dendritic nucleation, elongation, capping, and depolymerisation of filaments. During nucleation, membrane associated Cdc42-GTP recruits and activates WASP and Arp2/3 complex, targeting actin filaments to the plasma membrane (1). Activation of Arp2/3 complex stimulates the elongation of branched actin filaments from the Arp2/3 binding site at an angle of  $70^\circ$  (2). The growing filament pushes the membrane forward (3). When a filament elongates beyond the efficient length for pushing, the growth of the actin filament is terminated by capping protein (4). Cofilin binding to F-actin leads to the depolymerisation of the actin filament (5). (B), Formation of filopodia is initiated by organisation of the lamellipodia meshwork. In the organisation to form filopodia, elongation of some barbed ends in the meshwork is terminated by capping protein, but other barbed ends are continuously elongated by binding with a complex of molecules (tip complex) (1). Then, with the elongation initiated from the Arp2/3 complex, these barbed ends drift during elongation and collide with each other (2-4). Finally, converged filaments with linked barbed ends continue to elongate together and the multimeric filopodial tip complex initiates filament cross-linking by recruiting and/or activating fascin (5), which bundles the actin filaments as they continuously elongate and push the filopodia forward.





forming an actin filament branch (Machesky and Insall, 1998; Rohatgi *et al.*, 1999; Takenawa and Miki, 2001). During a period of elongation after nucleation, the filament pushes the membrane. When a filament elongates beyond the efficient length for pushing, the growth of the actin filament is thought to be terminated by capping protein (reviewed in Cooper and Schafer, 2000). Depolymerization is assisted by proteins of the ADF/cofilin family (reviewed in Bamburg, 1999). The actin disassociated by cofilin binding is recycled to form new actin filaments. By the polymerisation and depolymerisation of the actin filament, the membrane can be pushed forward.

Filopodia, are thin cellular processes with long and parallel actin filaments which are organized into tight bundles. Other cellular structures, such as retraction fibres, and microvilli are related to them (Small, 1988; Lewis and Bridgman, 1992; Small *et al.*, 2002). Filopodia structure is found to be processed based on the lamellipodia meshwork and was initially considered to be regulated by the same mechanism as that of the formation of lamellipodia. However, the Arp2/3 complex, which initiates the branching of actin filaments in the lamellipodia meshwork, is absent from established filopodia (Svitkina and Borisy, 1999). Additionally, some proteins, including Ena/VASP proteins (Janier *et al.*, 1999), N-WASP, CR16 (Ho *et al.*, 2001), myosin X (Berg and Cheney, 2002), talin (DePasquale and Izzard, 1991), syndapin I (Qualmann and Kelly, 2000), Abl interactor proteins (Stradal *et al.*, 2001), and Vav (Kranewitter *et al.*, 2001) were found enriched in filopodia tips, and a cross-linking protein, fascin was found to mediate actin filament bundling in filopodia (reviewed in Bartles, 2000; Kureishy *et al.*, 2002), suggesting these proteins might be involved in filopodia formation. The role of most of these proteins remains largely unknown with the exception of Ena/VASP proteins. In lamellipodia, Ena/VASP has been shown to bind barbed ends of actin filaments and protect them from being capped at the leading edge of lamellipodia, which results in formation of longer filaments within the lamellipodial dendritic network (Bear *et al.*, 2002). These data suggest that Ena/VASP proteins that are enriched at filopodial tips may mediate continuous elongation of filopodial actin filaments. In accordance with these studies, Svitkina and colleagues have recently examined the dynamics of Arp2/3 complex, Ena/VASP and fascin in filopodia in B16F1

mouse melanoma cells and established a model for filopodia initiation from lamellipodia meshwork (Svitkina *et al.*, 2003).

According to this model (Fig 5.1B), a lamellipodial network is formed by Arp2/3-mediated dendritic nucleation. Firstly, elongation of some barbed ends in the network is terminated by capping protein, but other barbed ends acquire a privileged status by binding a complex of molecules (tip complex) that allows them to elongate continuously. Ena/VASP proteins are likely members of the tip complex. Then, with the elongation initiated from Arp2/3 complex, privileged barbed ends drift laterally during elongation and collide with each other. Finally, converged filaments with linked barbed ends continue to elongate together and the multimeric filopodial tip complex initiates filament cross-linking by recruiting and/or activating fascin, which bundles the actin filaments as they continuously elongate and push the filopodia forward. In the nascent filopodium, the filopodial tip complex retains its functions of promoting coordinated filament elongation and bundling, as well as fusion with other filopodia.

### 5.1.3 Cdc42 activity assay in $\alpha\beta$ DG-GFP transfected cells

To investigate the potential role of Cdc42 in dystroglycan dependent filopodia formation, initially, Rho GTPase activity pull-down assay (Benard, *et al.*, 1999) was planned to be used to determine the activity of Cdc42 in dystroglycan transfected cells. To carry out this assay, a very high number of  $\alpha\beta$ DG-GFP transfected cells is necessary. However, neither by using G418 selection, nor by using different types of transfection procedure was it possible to achieve a transfection efficiency of  $\alpha\beta$ DG-GFP in REF52 cells greater than 25%. By using FACS sorting system to select the  $\alpha\beta$ DG-GFP in transfected REF52 cells, less than 5% of GFP positive cells were collected. These numbers of cells were insufficient to come out a Rho GTPase activity assay. Therefore,  $\alpha\beta$ DG-GFP and REF52 cells was not a useful system for determining the relationship between dystroglycan and Rho GTPases by using Rho GTPase activity assay. Despite the insufficiency for Rho GTPases activity assay, the post transfectorial morphology changes of cytoskeleton were very clear in  $\alpha\beta$ DG-GFP transfected REF52.

Thus, the cotransfection of dominant negative or constitutively activated mutants of Rho GTPases could be used in  $\alpha\beta$ DG expressing REF52 cells for the study of activation of Rho GTPase. By cotransfecting Rho GTPase mutant constructs that block or activate the Rho, Rac or Cdc42 pathway in  $\alpha\beta$ DG-GFP transfected REF52 cells, it was possible to observe the changes in filopodia formation.

## 5.2 Results

### 5.2.1 Morphological similarity of V12Cdc42 transfected cells with $\alpha\beta$ DG-GFP transfected cells

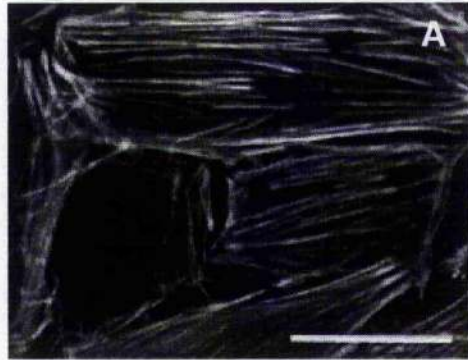
The constitutively activated constructs of Rho GTPases, V14Rho, V12Rac or V12Cdc42, were expressed in REF52 cells. Transfectants with the constitutively activated constructs showed the expected Rho, Rac or Cdc42 activated actin phenotype. Compared with the untransfected cells (Fig 5.2 A) the cells expressing V14Rho had a significantly increased number of stress fibres (Fig 5.2 B, arrow). The cells expressing V14Rac presented lamellipodia at the cell periphery (Fig 5.2 C, arrows). Introducing V12Cdc42 into REF52 cells led to the formation of a ring-like actin structure in the cell cortex (Fig 5.2 D dashed arrow) and, based on this ring-like actin structure, numerous actin filopodia bundles were present throughout the cells (Fig 5.2 D solid arrow). This actin filopodia morphology was strikingly similar with that seen in  $\alpha\beta$ DG-GFP transfected REF52 (Fig 5.2 E). Therefore, activation of Cdc42, more likely than activation of Rho or Rac, might be a consequence of overexpression of  $\alpha\beta$ DG-GFP in REF52 cells.

### 5.2.2 Effects of coexpression of dominant negative Rho GTPases constructs on $\alpha\beta$ DG-GFP transfected REF52 cells

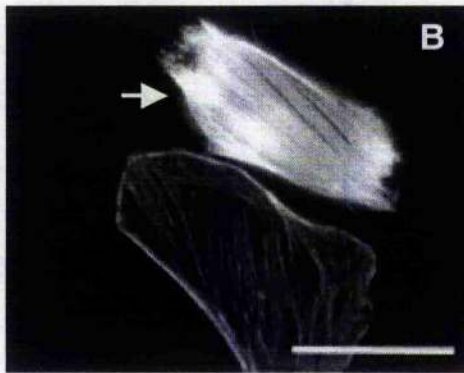
To further examine the role of Cdc42 in dystroglycan dependent filopodia formation, the dominant negative Rho GTPase constructs N14Rho, N12Rac or N17Cdc42 were coexpressed with  $\alpha\beta$ DG-GFP in REF52 cells. As shown in figure 5.4, the filopodial phenotype induced by expression of  $\alpha\beta$ DG-GFP in REF52 cells was not significantly affected by coexpressing N14Rho (Fig 5.3 A and B) or N12Rac (Fig 5.3 C and D). However, the cells cotransfected with N17Cdc42 and  $\alpha\beta$ DG-GFP showed a smooth periphery and presented no filopodia (Fig 5.3 E and F), suggesting disruption of Cdc42 activation might be able to inhibit the dystroglycan dependent filopodia formation. Quantification of the effect on the N17Cdc42 on dystroglycan dependent filopodia formation is shown in figure 5.4. Compared with the control cells coexpressing  $\alpha\beta$ DG-

**Figure 5.2 Actin phenotypes of constitutively Rho GTPases constructs transfected cells and  $\alpha\beta$ DG-GFP transfected cells**

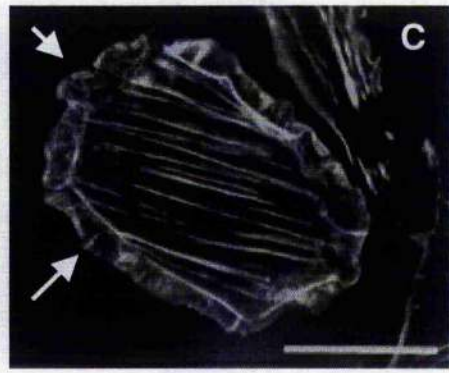
REF52 cells incubated on glass coverslips were transfected with constitutively activated, V12Rac (2 $\mu$ g/ml), V14Rho (2 $\mu$ g/ml) or V12Cdc42 (2 $\mu$ g/ml) by using lipofectamine following the standard procedure. The untransfected control cells were treated following the same procedure but without adding DNA to the lipofectamine reagent. The coverslips with transfected or untransfected cells were incubated at 37°C overnight and fixed with 3.7% formaldehyde, and then stained with rhodamine- phalloidin [(Sigma) at 1:1000]. The untransfected REF52 cells showed a normal actin stress fibres actin phenotype (**A**). A significant increase in the number of stress fibre was found in the V14Rho expressing cells (**B**, **arrow**), and formation of lamellipodia was induced by expression of V12Rac (**C**, **arrows**). REF52 cells transfected with V12Cdc42 presented a ring like actin structure in the cortical region (**D**, **dotted arrow**) and filopodia were visible (**D**, **solid arrow**). These actin structures were very similar to those found in  $\alpha\beta$ DG-GFP transfected REF52 cells (**E**). Scale bar= 25 $\mu$ m.



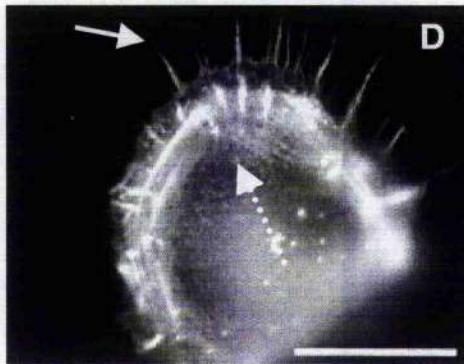
V14Rho



V12Rac



V12Cdc42



$\alpha\beta$ DG-GFP

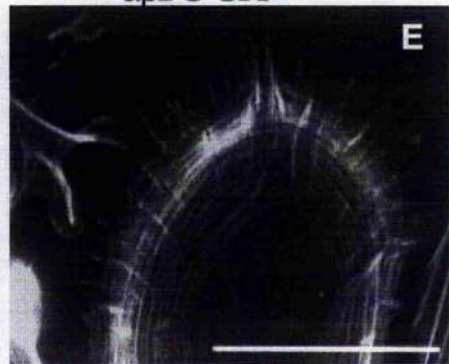


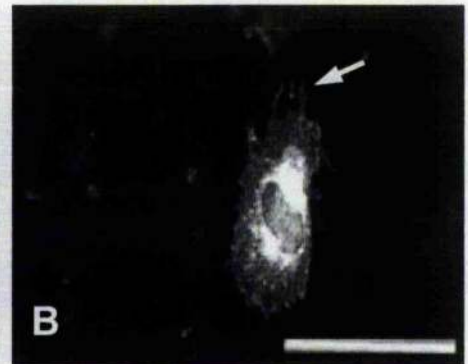
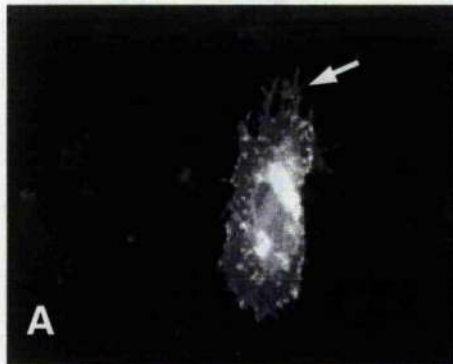
**Figure 5.3 Coexpressing  $\alpha\beta$ DG-GFP with dominant negative Rho GTPase constructs in REF52 cells**

REF52 cells incubated on glass coverslips were cotransfected with  $\alpha\beta$ DG-GFP (1 $\mu$ g/ml) and either, c-Myc-tagged N12Rac (1 $\mu$ g/ml), N14Rho (1 $\mu$ g/ml) or N17Cdc42 (1 $\mu$ g/ml), by using lipofectamine following the standard procedure. The coverslips with transfected cells were fixed with 3.7% formaldehyde and treated with PBS containing 0.1% Triton X100, and then stained with anti c-Myc antibody [(Santa Cruz) 1:100]. The images of cells expressing  $\alpha\beta$ DG-GFP (**A, C and E**) and stained with anti c-Myc (**B, D and F**) were captured. The coexpression of N14Rho (**A and B**) or N12Rac (**C and D**) in  $\alpha\beta$ DG-GFP transfected cells did not appear to affect the dystroglycan dependent filopodia formation (**A and B, arrows; C and D arrows**); the cotransfected cells presented filopodia on the cell periphery and cell surface. The cells coexpressing  $\alpha\beta$ DG-GFP and N17Cdc42 were very smooth in the cell periphery (**E and F**); no filopodia were produced in these cotransfected cells.

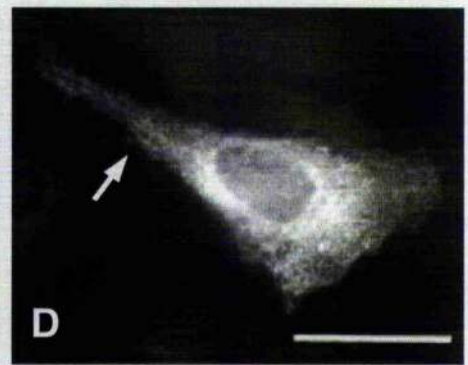
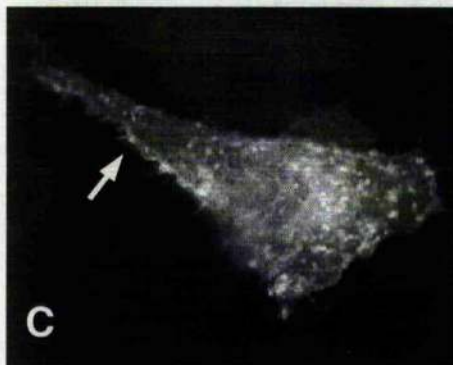
$\alpha\beta$ DG-GFP

c-Myc

N14Rac



N12Rho



N17Cdc42

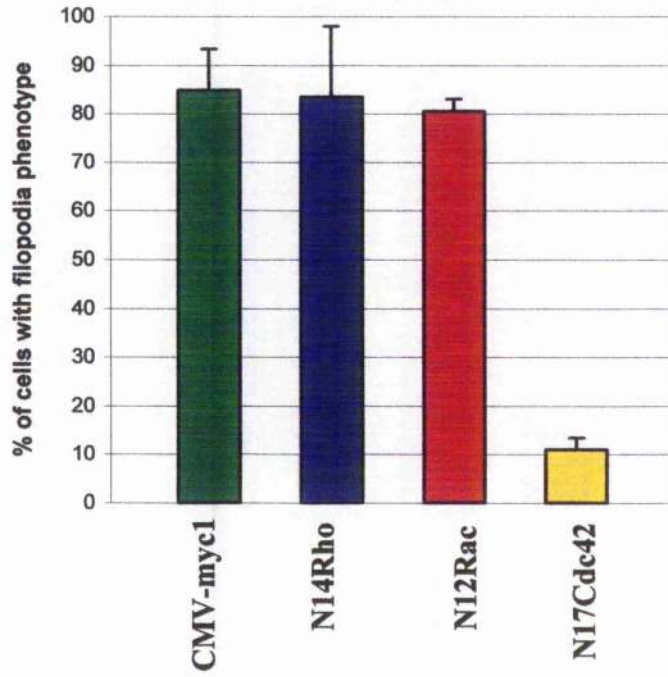




**Figure 5.4 Quantification of the effect of dominant negative Rho GTPase constructs coexpressing with  $\alpha\beta$ DG-GFP with in REF52 cells**

REF52 cells incubated on glass coverslips were cotransfected with  $\alpha\beta$ DG-GFP (1 $\mu$ g/ml) and either CMV-myc1 plasmid (1 $\mu$ g/ml), c-Myc-tagged N12Rac (1 $\mu$ g/ml), N14Rho (1 $\mu$ g/ml) or N17Cdc42 (1 $\mu$ g/ml), by using lipofectamine following the standard procedure. The coverslips with transfected cells were fixed with 3.7% formaldehyde and treated with PBS containing 0.1% Triton X100, and then stained with anti c-Myc antibody [(Santa Cruz) 1:100]. The costained cells presenting more than 30 microspikes were identified as filopodia positive cells. Compared with the control cells coexpressing  $\alpha\beta$ DG-GFP with CMV-myc1 of which 84.9% are filopodia positive, (**green column**), the number of filopodia positive cells in N12Rac (**blue column**) or N14Rho (**red column**) coexpressing cells were not changed significantly. However, the number of filopodia positive cells coexpressing N14Cdc42 dropped to 12% (**yellow column**), by comparison. The counting (100-200 cotransfected cells) was repeated twice in two different transfections. Data are mean  $\pm$  SD.

**Effect of dominant negative Rho GTPases  
cotransfection on  $\alpha\beta$ DG transfected  
REF52 cells**



GFP with empty vector CMV-myc1 (Fig 5.4, green column), the coexpression of  $\alpha\beta$ DG-GFP with N14Rho (Fig 5.4, blue column) or N12Rac (Fig 5.4, red column) had no significant effect on the formation of filopodia. However, the filopodia formation was reduced by coexpressing  $\alpha\beta$ DG-GFP with N17Cdc42 (Fig 5.4, yellow column). While blocking the activation of Rac or Rho did not alter the dystroglycan dependent filopodia formation, the disruption of Cdc42 activation largely reduced the dystroglycan dependent filopodia formation. Therefore, Cdc42 activation might be, at least partly, required for dystroglycan dependent filopodia formation.

### **5.2.3 Coexpression of constitutively activated Cdc42 construct and $\alpha\beta\Delta$ c $\beta$ DG-GFP in REF52 cells**

The results in section 4.2.3 and 4.2.9 have shown that cytoplasmic domain of dystroglycan is responsible for the  $\alpha\beta$ DG-dependent filopodia formation. To examine whether cytoplasmic domain of dystroglycan could mediate the dystroglycan dependent Cdc42 activation inducing filopodia formation, constitutively activated V12Cdc42 construct was coexpressed with dystroglycan mutant  $\alpha\beta\Delta$ c $\beta$ DG-GFP in REF52 cells. Expression of  $\alpha\beta\Delta$ c $\beta$ DG-GFP mutant has been determined to disrupt the formation of filopodia due to the lack of the  $\beta$ -dystroglycan cytoplasmic domain (see section 4.2.3). As shown in figure 5.5, filopodia phenotype was present in V12Cdc42 transfected REF52 cells (Fig 5.5 A and B). However, cells coexpressing  $\alpha\beta\Delta$ c $\beta$ DG-GFP and V12Cdc42 had a very smooth cell periphery (Fig 5.5 C and D), indicating that V12Cdc42 induced filopodia formation might be interrupted by the expression of  $\alpha\beta\Delta$ c $\beta$ DG-GFP. Quantification of the effect of  $\alpha\beta\Delta$ c $\beta$ DG-GFP on V12Cdc42 induced filopodia formation is shown in figure 5.6. Compared with the V12Cdc42 transfected REF52 cells (Fig 5.6, red column) 77% of which are filopodia positive, the number of filopodia positive cells in  $\alpha\beta\Delta$ c $\beta$ DG-GFP and V12Cdc42 cotransfection dropped down to approximately 14% (Fig 5.6, yellow column). These results showed that the activation of Cdc42 leading to the formation of filopodia was inhibited by coexpressing dystroglycan lacking the cytoplasmic domain. Therefore, in dystroglycan dependent filopodia formation, the  $\beta$ -dystroglycan cytoplasmic domain appeared to be required for

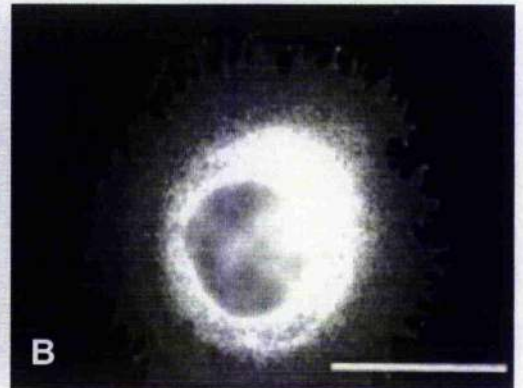
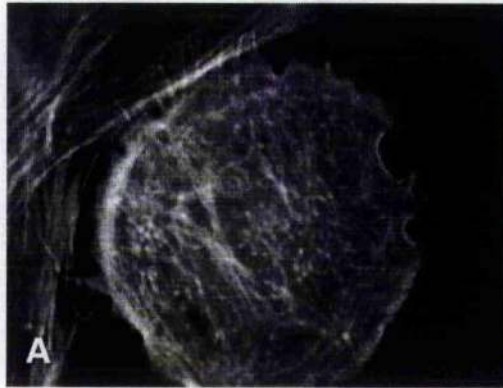
**Figure 5.5 Coexpression of constitutively activated Cdc42 construct with dystroglycan mutants**

REF52 cells incubated on glass coverslips were cotransfected with c-Myc-tagged V12Cdc42 (1 $\mu$ g/ml) with  $\alpha\beta\Delta c\beta$ DG-GFP (1 $\mu$ g/ml) or c $\beta$ DG-GFP (1 $\mu$ g/ml). For the control, REF cells incubated on glass coverslips were transfected with V12Cdc42 (1 $\mu$ g/ml). The transfection or cotransfection was carried out by using lipofectamine following the standard procedure. Transfected or cotransfected cells were fixed with 3.7% formaldehyde and treated with PBS containing 0.1% Triton X100, and then stained with anti c-Myc antibody [(Santa Cruz) 1:100] or rhodamine-phalloidin [(Sigma) at 1:1000]. Filopodia phenotype was presented in V12Cdc42 transfected cells in both actin and c-Myc staining (**A and B**). Coexpression of  $\alpha\beta\Delta c\beta$ DG-GFP with V12Cdc42 in REF52 cells did not induce the formation of filopodia; the cotransfected cells were smooth at the periphery (**C and D**). Coexpressing of c $\beta$ DG-GFP with V12Cdc42 did not induce the formation of filopodia either; the cotransfected cells were also smooth at the periphery (**E and F**). Scale bar=25 $\mu$ m.

Actin

c-myc

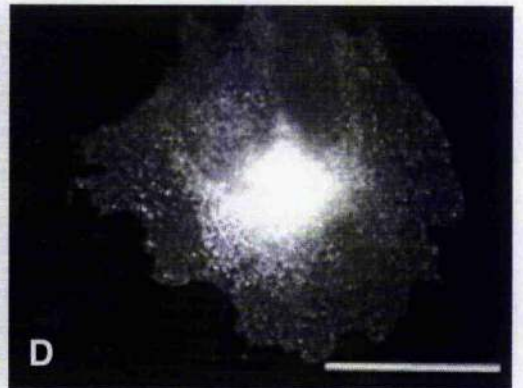
V12Cdc42



GFP

c-myc

V12Cdc42  
 $\alpha\beta\Delta\epsilon\beta$ DG-GFP



V12Cdc42  
c $\beta$ DG-GFP

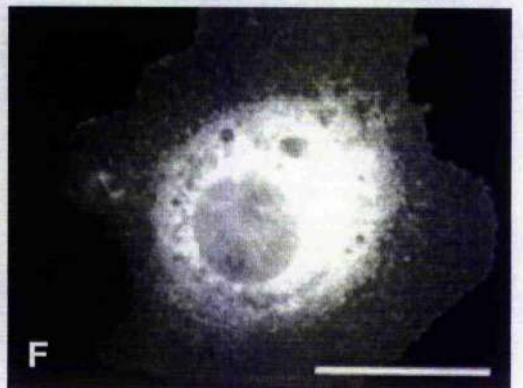
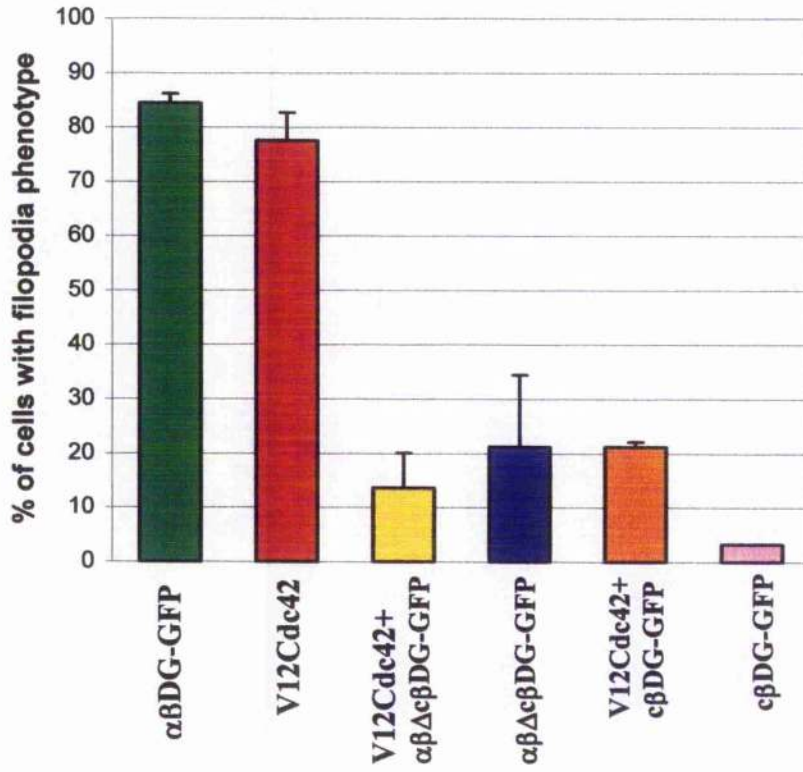


**Figure 5.6 Quantification of the coexpression of constitutively activated Cdc42 construct with dystroglycan mutants**

REF52 cells incubated on glass coverslips were cotransfected with c-Myc-tagged V12Cdc42 (1 $\mu$ g/ml) with  $\alpha\beta\Delta c\beta$ DG-GFP (1 $\mu$ g/ml) or c $\beta$ DG-GFP (1 $\mu$ g/ml). For the control, REF cells incubated on glass coverslips were transfected with  $\alpha\beta$ DG-GFP (1 $\mu$ g/ml), V12Cdc42 (1 $\mu$ g/ml),  $\alpha\beta\Delta c\beta$ DG-GFP (1 $\mu$ g/ml) or c $\beta$ DG-GFP (1 $\mu$ g/ml). The transfection or cotransfection was carried out by using lipofectamine following the standard procedure. Transfected or cotransfected cells were fixed with 3.7% formaldehyde and treated with PBS containing 0.1% Triton X100, and then stained with anti c-Myc antibody [(Santa Cruz) 1:100] or rhodamine-phalloidin [(Sigma) at 1:1000]. The cotransfected cells presenting more than 30 microspikes were identified as filopodia phenotype positive cells. REF52 cells expressing V12Cdc42 or  $\alpha\beta$ DG-GFP present filopodia at a high percentage approximately 80% (**green and red columns**). The number of filopodia positive cells was reduced to approximately 14% by coexpressing  $\alpha\beta\Delta c\beta$ DG-GFP (**yellow column**), or approximately 21% by coexpressing c $\beta$ DG-GFP (**orange column**) with V12Cdc42. The control cells expressing  $\alpha\beta\Delta c\beta$ DG-GFP (blue column) or c $\beta$ DG-GFP (pink column) alone were 21% and 3% filopodia positive, respectively. The counting (100-200 cotransfected cells) was repeated at least twice in different transfections. Data are mean  $\pm$  SD.

**Cotransfection of V12Cdc42 with dystroglycan mutants in REF52 cells**



the Cdc42 dependent filopodia formation, and might play a role in upregulating the activation of Cdc42 or downregulating Cdc42 downstream effectors.

#### **5.2.4 Coexpression of constitutively activated Cdc42 construct and $\alpha\beta$ DG-GFP in REF52 cells**

To further examine the relationship between the  $\beta$ -dystroglycan cytoplasmic domain and Cdc42, the  $c\beta$ DG-GFP construct was coexpressed with V12Cdc42 in REF52 cells.  $c\beta$ DG-GFP mutant was determined to be defective in mediating the formation of filopodia due to the improper localisation of  $\beta$ -dystroglycan cytoplasmic domain (see section 4.2.5). As shown in figure 5.5 E and F, the cell coexpressing  $c\beta$ -GFP and V12Cdc42 did not present a filopodia phenotype. Quantification of the effect  $c\beta$ DG-GFP on V12Cdc42 induced filopodia formation is shown in figure 5.6. Compared with that of V12Cdc42 transfected REF52 cells (Fig 5.6, red column), the filopodia formation was significantly inhibited by coexpressing  $c\beta$ -GFP with V12Cdc42 (Fig 5.6, orange column), suggesting that plasma membrane localisation is crucial for  $\beta$ -dystroglycan to stimulate Cdc42-dependent filopodia formation.

Together these results have shown that the active Cdc42 appeared to be a mediator of dystroglycan-dependent filopodia formation and might itself be regulated by dystroglycan. The cytoplasmic domain of  $\beta$ -dystroglycan is responsible for mediating Cdc42 dependent filopodia formation, and the membrane localisation of  $\beta$ -dystroglycan cytoplasmic domain is critical for the stimulation of Cdc42-dependent filopodia formation. Since Cdc42-dependent filopodia formation was significantly inhibited by coexpression of  $\alpha\beta\Delta c\beta$ DG-GFP, the  $\alpha\beta\Delta c\beta$ DG-GFP construct could be used as an dominant negative dystroglycan construct for other studies of dystroglycan in the future.

#### **5.2.5 Focal adhesions in $\alpha\beta$ DG-GFP transfected cells**

Rho is one of the well-studied members of Rho GTPases. Activation of Rho leads to increasing number of stress fibres and assembly of focal adhesion complex (section



1.5.3). In this work, Rho was initially suspected to be a mediator for dystroglycan signalling that regulates focal adhesion assembly and actin stress fibre formation. However, here activation of Cdc42 and formation of actin filopodia rather than Rho activation and stress fibre formation appeared to be regulated by dystroglycan. The activation of Rho has been shown to be inhibited by activation of Cdc42 (Arthur and Burridge, 2001; Ren *et al.*, 1999; Hall, 1998). To examine whether focal adhesion formation is affected by dystroglycan signalling, the  $\alpha\beta$ DG-GFP transfected cells were stained with anti-talin antibody. As shown in figure 5.7, in the  $\alpha\beta$ DG-GFP transfected REF52 cells (Fig 5.7 D), the focal adhesion plaques were found distributed around the cells (Fig 5.7 E), and no particular colocalisation of focal adhesions with  $\alpha\beta$ DG-GFP was observed (Fig 5.7 F). There was no significant difference in distribution of talin staining between  $\alpha\beta$ DG-GFP (Fig 5.7 E) and pEGFP empty vector transfected cells (Fig 5.7 B). However, in some cells expressing very high levels of  $\alpha\beta$ DG-GFP (Fig 5.7G dashed arrow), talin-containing focal adhesions appeared to be absent (Fig 5.7H, dashed arrow), implying that Rho dependent focal adhesion formation might be inhibited in this state. This interesting finding revealed that focal adhesion formation in REF52 cells might be reduced by high-level overexpression of  $\alpha\beta$ DG-GFP, indirectly supporting the suggestion that Cdc42 is activated in the REF52 cells due to the expression of dystroglycan. However, since only cells expressing a very high-level of  $\alpha\beta$ DG-GFP had reduced talin staining, Rho dependent focal adhesion formation signalling might not normally be inhibited by dystroglycan.

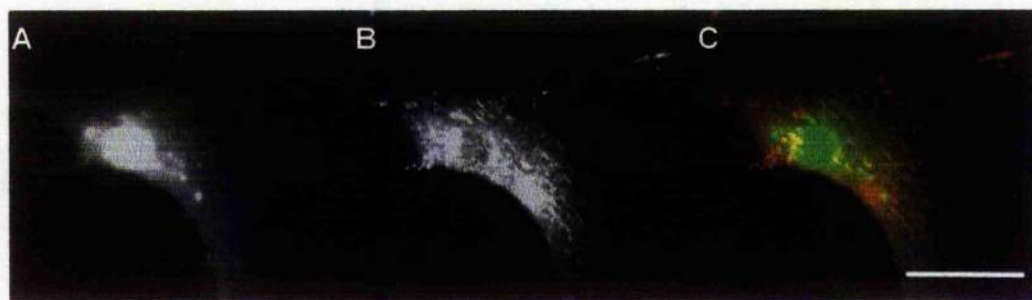
**Figure 5.7 Immunostaining of talin in  $\alpha\beta$ DG-GFP transfected REF52 cells**

REF52 cells transfected with  $\alpha\beta$ DG-GFP or pEGFP were replated on laminin coated coverslips and incubated in DMEM containing 1% FBS at 37 °C overnight. The coverslips with cells were fixed with 3.7% formaldehyde and stained with anti-talin [(Sigma) at 1:1000]. The filopodia phenotype was seen in  $\alpha\beta$ DG-GFP transfected cells (D) but not in pEGFP transfected cells (A). Talin adhesion plaques were distributed around the  $\alpha\beta$ DG-GFP transfected cells (E), however, in the merged image, no particular colocalisation of  $\alpha\beta$ DG-GFP with talin was seen (F). Similar distribution of adhesion plaques was present in pEGFP transfected cells (B), and no remarkable colocalisation of GFP with adhesions were seen either (C). In the same transfection of  $\alpha\beta$ DG-GFP, some transfected cells with high expression level of  $\alpha\beta$ DG-GFP (G) showed little staining with anti-talin antibodies (H). The merged image showed that no adhesion sites were present in the cell expressing very high level of  $\alpha\beta$ DG-GFP (I). The dashed arrows point to  $\alpha\beta$ DG-GFP transfected cells, solid arrows to  $\alpha\beta$ DG-GFP untransfected cells. The scale bars=25 $\mu$ m.

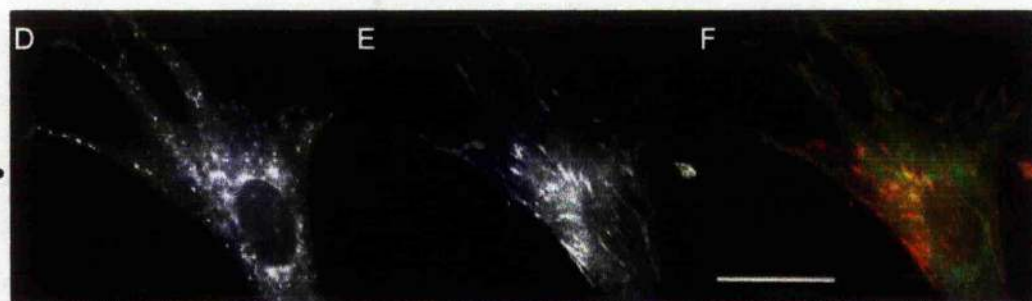
$\alpha\beta$ DG-GFP

Talin

Merge



$\alpha\beta$ DG-GFP



## 5.3 Discussion

### 5.3.1 Cdc42 mediates dystroglycan in dependent filopodia formation

Expression of  $\alpha\beta$ DG-GFP in REF52 cells has been shown to lead to the reorganisation of the actin cytoskeleton resulting in the formation of actin-rich ring-like structures at the cell cortex and filopodia on the cell surface. In this chapter, it has been determined that both the actin-rich ring-like structure and the filopodia are typical actin phenotypes induced by Cdc42 activation in REF52 cells. The coexpression of dominant negative Cdc42, but not Rho or Rac, with  $\alpha\beta$ DG-GFP led to a significant reduction in dystroglycan-dependent filopodia formation, suggesting that activation of Cdc42, instead of Rho or Rac, might be required for the dystroglycan-dependent filopodia formation in REF52 cells. Coexpression of  $\alpha\beta\Delta$ c $\beta$ DG-GFP with constitutively activated V12Cdc42 disrupted the formation of filopodia mediated by Cdc42 activation, indicating that the cytoplasmic domain of  $\beta$ -dystroglycan is required for the Cdc42 dependent filopodia formation. In the studies in chapter 4, membrane localisation of  $\beta$ -dystroglycan was determined to be crucial for downstream filopodia formation. A similar and consistent result was revealed here also. Coexpression of c $\beta$ DG-GFP with V12Cdc42 significantly inhibited the Cdc42-induced filopodia formation, suggesting that the cytoplasmic domain of dystroglycan, with its proper membrane localisation, might be necessary for Cdc42-dependent filopodia formation.

Since a Cdc42 activity assay in this work was not feasible, it was not possible to determine whether activation of Cdc42 is upregulated or downregulated by the cytoplasmic domain of dystroglycan. However, significant inhibition of the filopodia formation was a consequence of either disruption of Cdc42 activation or disruption of dystroglycan functional domain, implying that dystroglycan and Cdc42 could regulate each other in the formation of filopodia. Since no direct association between Cdc42 and dystroglycan has ever been determined, this finding implied that other mediators are responsible for the regulation between dystroglycan and Cdc42. In vivo activation of Cdc42 resulting from GDP-GTP exchange has been determined to be triggered only by GEFs (reviewed in Bishop and Hall, 2000). Thus, dystroglycan could upregulate Cdc42

through activation of Cdc42 specific GEFs. All GEFs are identified as plasma membrane associated proteins (Cerione and Zheng, 1996). Interestingly, plasma membrane localisation was determined to be necessary for dystroglycan to mediate Cdc42-induced filopodia formation. This finding implies a situation where dystroglycan regulates Cdc42 GEFs at the plasma membrane followed by activation of Cdc42 and the formation of filopodia.

### 5.3.2 Mediators between dystroglycan and Cdc42

The PPPY motif in the C-terminal tail of dystroglycan has been identified as a signalling mediator that associates with WW, Grb2 or caveolin (section 1.4). However, it has been shown previously that expression of dystroglycan could induce the formation of filopodia independent of utrophin. This raised the possibility that  $\beta$ -dystroglycan itself might regulate Cdc42-mediated filopodia formation through other protein binding motifs. Sequence analysis of dystroglycan has shown that dystroglycan has no significant homology with any other protein in data base (Ibraghimov-Beskrovnaya *et al.*, 1992) except for a recent study, which has shown that  $\alpha$ -dystroglycan contains two cadherin-like domains (Dickens, *et al.*, 2002).

However, examining the amino acid sequence of cytoplasmic  $\beta$ -dystroglycan by eye, a small positively charged juxtamembrane region, referring to amino acid sequence RKKRK, was revealed (Fig 5.8). Similar positively charged juxtamembrane regions have been found in CD44, CD43, ICAM and L-selectin (Fig 5.8), and identified as the binding regions for ERM (ezrin-radixin-moesin) family proteins. ERM family proteins have been shown to be concentrated in actin rich membrane protrusions e.g. microvilli and filopodia, in many cell types (Berryman *et al.*, 1993; Amnieva and Furthmayr, 1995; Yonemura *et al.*, 1999), and have been identified as crosslinkers between plasma membrane proteins and actin filaments (reviewed in Tsukita and Yonemura, 1995). This interesting finding revealed that ERM family proteins might be involved in dystroglycan dependent filopodia formation signalling. Indeed, in a more recent study that further examines the relationship between dystroglycan and ezrin, a member of ERM protein family,  $\beta$ -dystroglycan was found to colocalise with ezrin in microvilli

**Figure 5.8 The sequence of dystroglycan juxtamembrane region and ezrin association sequence in the membrane protein**

The domain organisation of dystroglycan, SP,  $\alpha$ ,  $e\beta$ , TM, and  $c\beta$  see figure 4.1. The amino acid sequence of dystroglycan 776-782, is a positively charged juxtamembrane region, which is predicted to bind ezrin. A similar positively charged juxtamembrane region is present in the ERM associated transmembrane proteins, including CD44, CD43, ICAM-1, and L-selectin (Heiska *et al.*, 1998; Legg and Isacke 1998; Yonemura *et al.*, 1998; Ivetic *et al.*, 2002), and has been identified as the binding region recognised by ERM proteins.



Dystroglycan

RKKRKGKLTTLDQA

CD44

RRRCGQKKKLVING

CD43

RQRQKRRTGALTLS

ICAM-1

RQRKIKKYRLQQAQ

L-selectin

RRLKKGKKSQERMD

structures in JEG-3 cells as well as in REF52 cells (Spence *et al.*, 2003 b). Both coimmunoprecipitation and  $\beta$ -dystroglycan-GST pull-down assay have indicated that ezrin might directly associate with  $\beta$ -dystroglycan. Furthermore, expression of the dystroglycan construct mutated at RKKRK, which is the predicted ezrin binding region, led to a significant reduction of actin rich protrusion in the cells, indicating that RKKRK motif of dystroglycan is necessary for regulation of actin rich membrane protrusions. Thus, dystroglycan might be involved in the organisation of the actin cytoskeleton and formation of membrane protrusions by interacting with ezrin through its RKKRK motif. Ezrin is therefore a novel molecule identified to bind to the RKKRK motif in the cytoplasmic domain of dystroglycan.

Ezrin contains a N-terminal globular domain followed by a  $\alpha$ -helical region, a short proline-rich linker and a charged C-terminal domain. The membrane protein binding activity is localised in the N-terminal FERM domain while the F-actin binding activity is localised in a C-terminal 15 aa. F-actin binding sequence (Pearson *et al.*, 2000). *In vivo*, ERM proteins undergo a conformational activation process and cycle between cytosol and plasma membrane compartments. In cytosol, ezrin has been found to form head-to tail autoinhibitory inactive structure (Berryman *et al.*, 1995). Once activated, the binding affinity between N-terminal and C-terminal of ezrin is reduced by its phosphorylation at Ser567, thereby releasing both FERM domain and F-actin binding domain and allowing ezrin to associate with F-actin and target to the membrane protein (Gary and Brcstcher, 1995). In a fractionation assay in Swiss 3T3 cells expressing  $\alpha\beta$ DG-GFP, ezrin was found concentrated in the actin containing triton-insoluble fraction associating with F-actin instead of in the soluble cytoplasm fraction (Spence *et al.*, 2003b), suggesting that expression of dystroglycan induces the activation of ezrin. Additionally, disruption of dystroglycan binding to ezrin led to a significant reduction of dystroglycan-dependent membrane protrusions, indicating that ezrin could mediate the dystroglycan-dependent cytoskeleton organisation.

Interestingly, it was shown that the  $\beta$ -dystroglycan-dependent activation of ezrin was greatly inhibited by coexpression with N17Cdc42, suggesting that ezrin activation and



targeting to dystroglycan may be under the control of Cdc42 activity (Spence *et al.*, 2003b). Expression a dominant negative construct of P21 associated kinase (PAK), a downstream effector for Cdc42, in  $\alpha\beta$ DG-GFP expressing Swiss 3T3 cells inhibited the activation of ezrin, revealing that PAK might play a role in the activation of ezrin. In the same Swiss 3T3 cell line expressing  $\alpha\beta$ DG-GFP, coexpression of dominant negative PAK mutant, which has a defective in Cdc42 binding site, also led to a reduction in ezrin activation, suggesting that both Cdc42 and PAK are mediators for dystroglycan to induce the activation of ezrin (Spence *et al.*, 2003b). Thus, the activation of ezrin triggered by Cdc42 could be mediated by PAK.

Together, active ezrin could be recognised by the RKKRK motif and target F-actin to dystroglycan. The interaction of dystroglycan and ezrin appeared to be necessary for completing the dystroglycan-dependent filopodia formation. Active ezrin has been shown to act as a crosslinker between actin filaments and membrane proteins, however, the precise signalling function of ezrin is still unclear. The studies here implied that in dystroglycan-dependent filopodia formation, active ezrin might play a role in both mediating the formation of membrane protrusion and providing a physical linkage between dystroglycan and actin filaments. This also indicates the importance of the proper membrane localisation of dystroglycan cytoplasmic domain in the formation of filopodia not only for triggering the activation of Cdc42 but also for being recognised by active ezrin and forming the physical link to F-actin.

In accordance with these findings, a possible signalling pathway for actin cytoskeleton organisation triggered by dystroglycan is shown in figure 5.9. Expression of dystroglycan leads to the activation of Cdc42. Activation of Cdc42 triggered by dystroglycan leads to filopodia formation through two routes. First, activation of Cdc42 leads to the activation of WASP/Arp2/3 complex and promotes actin polymerisation, thereby forming an actin filaments meshwork in the cortex and initiates filopodia formation. Second, in regulating the formation of actin-based filopodia or microvilli, activation of Cdc42 triggered by dystroglycan could also lead to the activation of ezrin by PAK. Integrin engagement is also required for dystroglycan dependent filopodia

formation and crosstalk between integrin and dystroglycan might also play a role in dystroglycan-dependent filopodia formation. It has been identified in many studies that integrin engagement leads to the activation of Cdc42 and the downstream induction of filopodia (Price *et al.*, 1998; reviewed in Schoenwaelder and Burridge, 1999). Therefore, integrin engagement could also be able to trigger the Cdc42-PAK-ezrin pathway and target ezrin to dystroglycan.

Finally, previous work using yeast two hybrid assay revealed that actin interacts with  $\beta$ -dystroglycan (Ilseley, 2001). Further work resolving the interaction between actin and  $\beta$ -dystroglycan showed that purified  $\beta$  dystroglycan was co-sedimentated with F-actin at low-speed in the pellet fraction, indicating that  $\beta$ -dystroglycan might associate with actin filaments directly. Additionally, both the falling-ball assay and electron microscopy images have shown that single actin filaments were bundled in the presence of  $\beta$ -dystroglycan. These results suggested that *in vitro*,  $\beta$ -dystroglycan might associate with F-actin and promote the bundling of F-actin (Chen *et al.*, 2003). This interesting finding implied that  $\beta$ -dystroglycan might act as an actin binding protein that recruits F-actin to the cortical region where the actin polymerisation to form filopodia or microvilli is taking place (Fig 5.9 dashed arrow). The hypothesis for the mechanism of dystroglycan-dependent filopodia or microvilli formation is shown in figure 5.10.

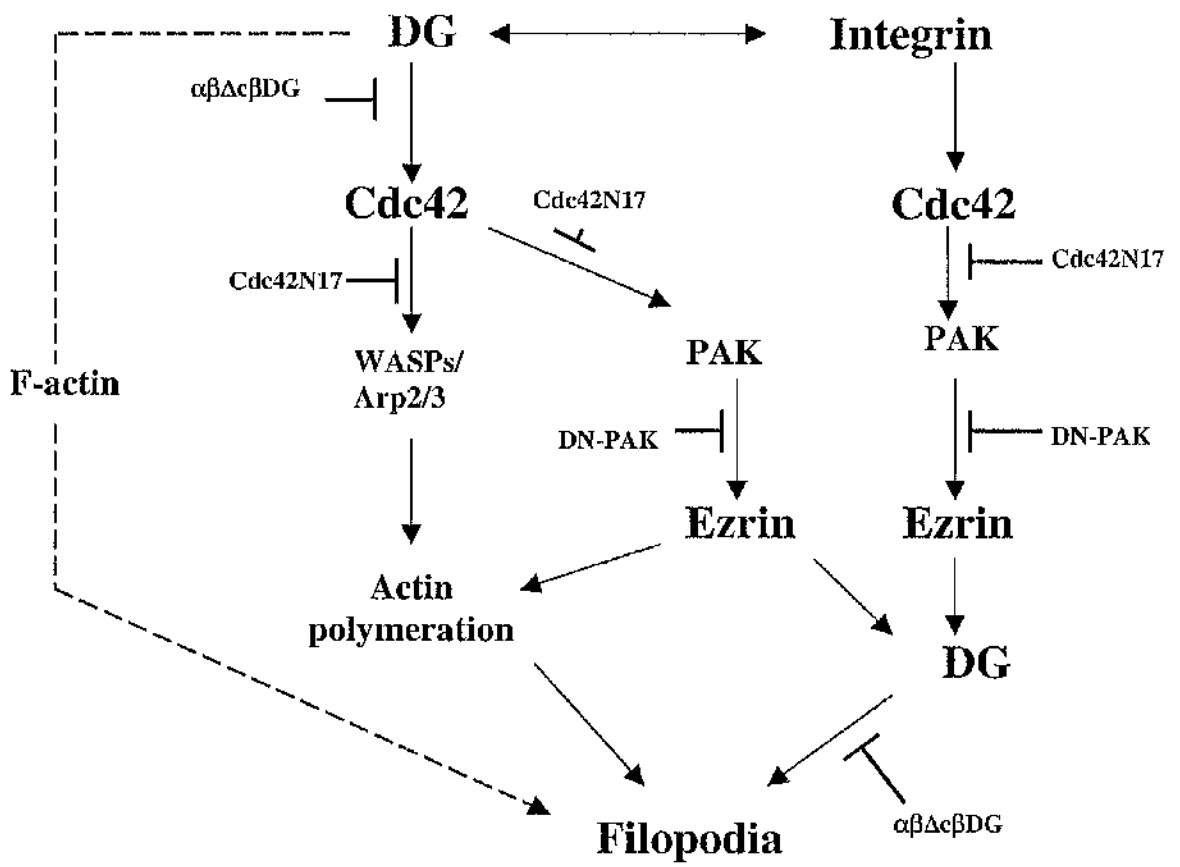
### **5.3.3 Regulation of dystroglycan dependent filopodia formation through the mediators**

#### **5.3.3.1 Role of PAK**

As mentioned above, the activation of ezrin regulated by Cdc42 is mediated by PAK. Whether PAK is involved in the activation of moesin or radixin has not been reported. However, Rac/Cdc42 dependent activation of PAK has been shown to induce the phosphorylation of merlin, which is identified as a member of ERM protein family, at its residue S518 and is involved in the regulation of cell proliferation (Xiao, *et al.*, 2002). Since PAK is a multi-functional-domain protein, a variety of molecules, including some which might be important for regulating cytoskeleton dynamics, have been shown to interact with different binding regions of PAK (reviewed in Bokoch,

**Figure 5.9 Signalling of dystroglycan induced formation of membrane protrusions**

Dystroglycan localised at the plasma membrane is able to trigger the activation of Cdc42. The activation of Cdc42 leads to the activation of WASP/Arp2/3 thereby promoting the polymerisation of actin filaments and inducing the formation of filopodia at the leading edge of cells. However, activation of Cdc42 triggered by dystroglycan also leads to the activation of ezrin mediated by PAK. Active ezrin interacting with F-actin could be targeted to dystroglycan, leading to the aggregation and polymerisation of filopodia or microvilli. This pathway was interrupted by expression of dominant negative Cdc42 (N17Cdc42) or dominant negative PAK constructs (DN-PAK). Integrin signalling is required for dystroglycan dependent filopodia formation. Crosstalk between integrin and dystroglycan might be involved in the dystroglycan-dependent filopodia formation. Integrin is also an upregulator of Cdc42 and might be able to trigger the activation of ezrin through Cdc42 and PAK, thereby converging on the dystroglycan signalling pathway. Additionally, F-actin was found to directly associate with  $\beta$ -dystroglycan; a direct modulation of actin filament by dystroglycan might exist (dashed arrow).



2003). Myosin light chain kinase (MLCK) was found to be phosphorylated by PAK (Sanders *et al.*, 1999). The phosphorylation of MLCK leads to the activation of its kinase activity and induces the phosphorylation of myosin light chain (MLC), thereby promoting the actin-myosin interaction resulting in formation of actin stress fibres (Fig 1.7). Thus, by regulating the activation of PAK, activation of Cdc42 appeared to induce the formation of stress fibres. Recently, PAK interacting exchange factor (PIX), which is a family of newly identified PAK binding proteins, was found to contain a DH/ PH domain, which was identified as a GEF functional domain for GDP/GTP exchange, suggesting that PIX might have GEF activity (reviewed in Hoffman and Cerione, 2002). It has been shown that the activity of PAK and the level of Cdc42-GDP were enhanced by PIX directly binding to PAK, suggesting that by binding to PAK, PIX might be able to act as a GEF for activation of Cdc42 and is involved in the formation of membrane protrusion (reviewed in Daniels and Bokoch, 1999). Therefore, PAK could be an upregulator for activation of Cdc42 as well.

Additionally, PAK activation was found to lead to the activation of LIM kinase (Edwards *et al.*, 1999). LIM kinase contains two LIM domains, which are protein interaction motifs found in proteins commonly associated with the cytoskeleton (Carrier, 1998). It has been shown that active LIM kinase was sufficient to trigger the phosphorylation of cofilin (Arber, *et al.*, 1998; Yang *et al.*, 1998). Phosphorylation of cofilin reduces its severing activity and results in an inhibition of F-actin depolymerisation. Thus, the actin polymerisation in leading edge could be regulated by Cdc42 or Rac through the activation of PAK. Altogether, activation of PAK appears to be an important key for various actin organisation pathways. The finding that PAK is involved in the dystroglycan dependent filopodia formation implies that dystroglycan, in addition to triggering the Cdc42-PAK-ezrin pathway, might be involved in a complicated network mediated by multifunctional PAK.

#### **5.3.3.2 Role of ezrin**

In addition to interacting with membrane proteins, active ezrin has also been shown to bind and disassociate RhoGDI from GDP bound Rho GTPases (Takahashi *et al.*, 1997)

(Fig 1.6A). In the cytoplasm, RhoGDI is found bound to the switch domains of Cdc42 leading to the inhibition of both GDP dissociation and GTP hydrolysis (reviewed in Hoffman and Cerione 2001). Binding of ERM proteins with RhoGDI reduces the binding affinity of RhoGDI to Cdc42-GDP, resulting in dissociation of RhoGDI from Cdc42 and the recovery of GDP/GTP exchange ability of Cdc42 (Takahashi, *et al.*, 1997). The molecular mechanism of ERM protein binding induced disassociation of RhoGDI from Cdc42 is still unknown. Since N-terminal FERM domain of ERM proteins has been shown to be sufficient to dissociate RhoGDI from Rho GTPases (Takahashi, *et al.*, 1997), the conformational activation of ERM might be required for its binding to RhoGDI. Thus, by modulating the disassociation of RhoGDI from Cdc42, activation of ezrin appears to play a role in upregulating gross Cdc42 activity (reviewed in Louvet-Vallee, 2000).

Activation of ezrin has also been shown to be regulated by RhoA (Mackay *et al.*, 1997; Shaw *et al.*, 1998), Rho kinase (Matsui *et al.*, 1999), and protein kinase C (PKC) (Ng *et al.*, 2001; Pietromomaco *et al.*, 1998). Activation of RhoA in Swiss 3T3 cells induced the activation of ERM proteins followed by recruitment of ERM to plasma membrane structures (Mackay *et al.*, 1997; Shaw *et al.*, 1998). Activation of Rho kinase, a downstream effector of RhoA, was found to lead to the phosphorylation of ERM proteins at a carboxy-terminal threonine (Matsui *et al.*, 1999). Thus, Rho dependent signalling appears to regulate the activation of ezrin and is involved in formation of the membrane protrusions, while activation of Rho-dependent signalling has also been described as inducing the formation of stress fibres and being inhibited by the activation of Cdc42.

PKC- $\alpha$  and PKC- $\theta$  have been shown to stimulate the conformational change and activation of ERM proteins as well (Ng *et al.*, 2001; Pietromomaco *et al.*, 1998). CD44 is an integral cell membrane glycoprotein with a postulated role in matrix adhesion lymphocyte activation (reviewed in Haynes *et al.*, 1991). Legg and colleagues have recently demonstrated that PKC stimulated the CD44-ezrin interaction as a consequence of Ser325 and Ser291 in the cytoplasmic tail of CD44 being phosphorylated (Legg *et al.*,

2002).. This study showed that activation of PKC led to dephosphorylation of Ser325 and phosphorylation of Ser 291 on CD44, resulting in the decrease of the binding affinity between ezrin and CD44. Additionally, they also suggested that the phosphorylation of CD44 cytoplasmic tail at Ser291, which is adjacent to its positively charged juxtamembrane region, might interfere with the charge of this juxtamembrane region and reduce the binding affinity of CD44 to ezrin.

This interesting finding raised the possibility that the binding affinity of ERM proteins to their membrane targets could be regulated by their phosphorylation.  $\beta$ -dystroglycan contains several potential tyrosine phosphorylation sites, and the binding affinity of  $\beta$ -dystroglycan to WW domain has been shown to be regulated by a phosphorylation-dependent conformational change of its PPPY motif in the C-terminal end (James *et al.*, 2000; Haung, *et al.*, 2000; Ilsley *et al.*, 2002). Thus, conformational changes triggered by tyrosine phosphorylation seem to play an important role for  $\beta$ -dystroglycan in regulating its affinity for its binding partners. In accordance with these, it is possible that the binding affinity of  $\beta$ -dystroglycan RKKRK domain to ezrin could be regulated in a phosphorylation-dependent manner, which might alter the charge or conformation of RKKRK domain and modulate the dystroglycan-ezrin-Cdc42 dependent formation of membrane protrusions.

#### **5.3.4 Role of dystroglycan in adhesion and filopodia formation**

In this work, a novel pathway of dystroglycan stimulated Cdc42-PAK-ezrin activation is suggested. The active ezrin targets to the RKKRK sequence, a positively charged juxtamembrane region in the  $\beta$ -dystroglycan cytoplasmic tail, required to induce the actin-based microvilli or filopodia formation. Thus, dystroglycan seems to stimulate a signalling cycle that activates Cdc42, PAK, and ezrin in turn, and transmits the signal back to dystroglycan. This signalling cycle can induce the filopodia formation through the activation of WASP/Arp2/3 and activation of ezrin (Fig 5.10).

As mentioned above, formation of filopodia is now considered to be initiated from the organisation and parallel bundling of a lamellipodial meshwork (Svitkina *et al.*, 2003)

**Figure 5.10 Hypothesis of the regulation of dystroglycan-dependent filopodia formation**

$\beta$ -dystroglycan triggers a signalling cycle that, in turn, activates Cdc42, PAK, ezrin and triggering ezrin to interact with  $\beta$ -dystroglycan. In the signalling cycle, activation of Cdc42 triggered by dystroglycan causes formation of membrane protrusions through activation of WASP/Arp2/3 complex or through activation of ezrin.  $\beta$ -dystroglycan localised to the plasma membrane enhances the filopodia bundling by recruitment of ezrin-F-actin or by direct interaction and bundling of F-actin. Activation of PAK in the signalling cycle might inhibit actin depolymerisation by activation of LIM kinase, which phosphorylates cofilin. Activation of PAK might also regulate the activation of Cdc42 through PIX, which acts as a Cdc42GEF. Activation of PAK induces the activation of MLCK, which is responsible for enhancing the assembly of focal adhesions and actin stress fibre formation. Activation MLCK is induced by ERK as well. Therefore, dystroglycan inhibits ERK activation could reduced the activation of MLCK thereby inhibiting the focal adhesions assembly and stress fibre formation. Together, by this signalling cycle, dystroglycan can induce the formation of membrane protrusions, filopodia bundling and inhibit the focal adhesions formation and stress fibre formation.



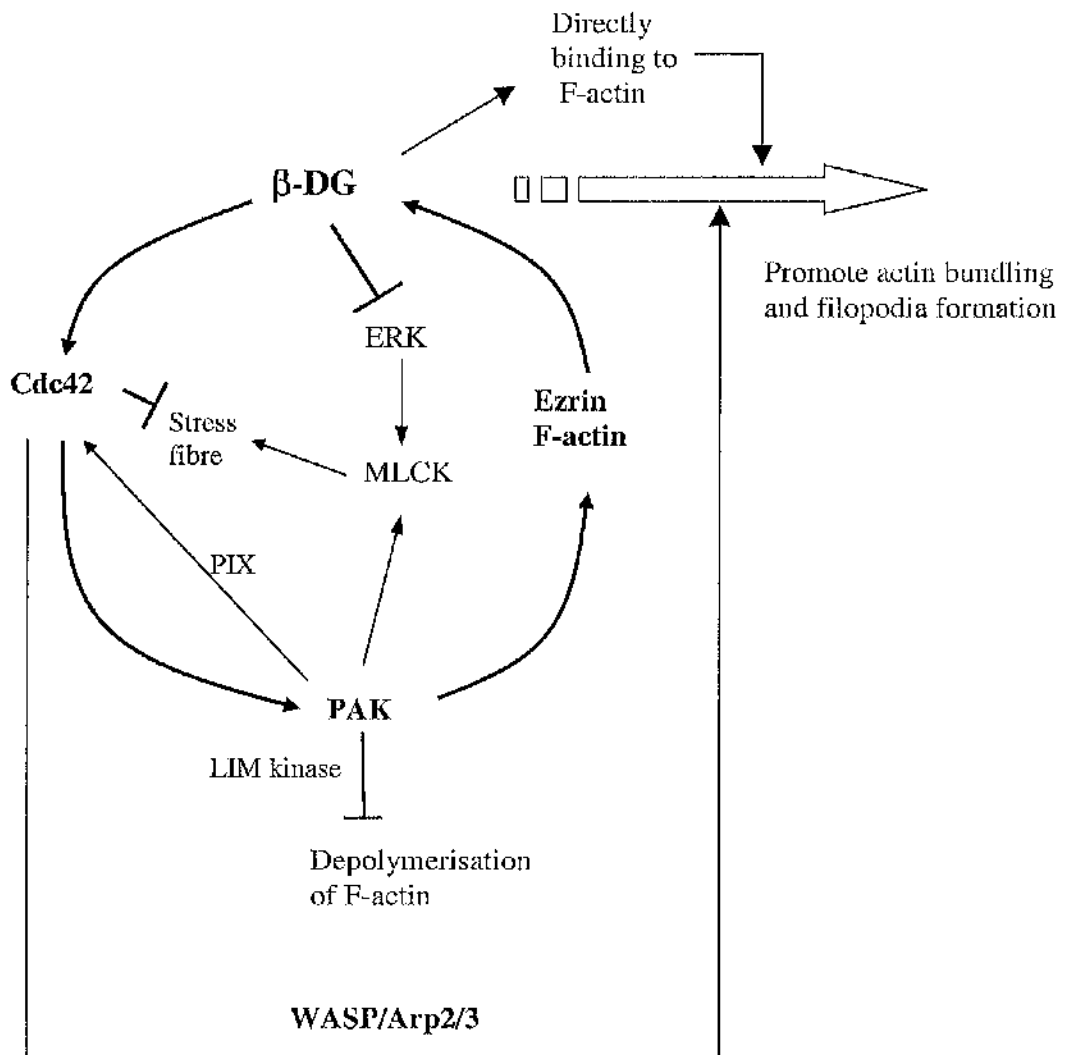


(Fig 5.1). Activation of ezrin recruits F-actin to dystroglycan, implying that dystroglycan plays a role in actin organisation by regulating ezrin. Additionally, the finding that dystroglycan directly interacts with actin and promotes F-actin bundling also strongly implies that dystroglycan is a transmembrane receptor which mediates the bundling of actin during the formation of filopodia from the lamellipodia meshwork. Supporting this idea, it has been shown that activation of Cdc42 promotes the formation of a IRSp53: Mena complex, which induces the formation of filopodia (Krugmann *et al.*, 2001). IRSp53 is a SH3 domain-containing scaffold protein, which is conformationally activated by Cdc42 (Govind *et al.*, 2001). Mena is a member of Ena/VASP family which has been shown to localised at the tip of established filopodia structure (Krugmann *et al.*, 2001). This finding revealed that the activation of Cdc42 might be involved in not only the nucleation and actin branching in lamellipodia extension, but also the organisation of filopodia formation. Dystroglycan, which regulates Cdc42 activation, ezrin activation, and promotes F-actin bundling, might play a role in the organisation of the initiation or bundling of filopodia.

In this work, the PPPY motif in the C-terminal of  $\beta$ -dystroglycan was initially suspected to be a mediator of the regulation for dystroglycan-dependent filopodia. Ezrin was later identified as a substrate for  $\beta$ -dystroglycan interaction via the RKKRK motif and mediating dystroglycan-dependent filopodia formation (Spance *et al.*, 2003b). Thus, the dystroglycan dependent filopodia formation appeared to be regulated in a PPPY motif independent manner. In Src activated transform cells, dystroglycan PPPY motif has been shown to be phosphorylated at Y892 (Sotgia *et al.*, 2001). This Y892 phosphorylation has been shown to lead to the reduction of the binding affinity between PPPY motif and WW domain, and the recruitment of SH2 containing protein including Fyn, Csk, Nck, and SHC (Sotgia *et al.*, 2001). The role of these SH2 containing proteins in dystroglycan signalling is unknown. Since activation of Src causes the assembly of focal adhesion complex followed by activation of ERK cascade, and PPPY motif has been shown to bind Grb2, which is also a mediator of ERK cascade (section 1.4), dystroglycan seemed to play a role in regulating focal adhesion formation through the phosphorylation of PPPY motif. However, a very recent study has shown that  $\beta$ -

dystroglycan phosphorylated at Y892 was localised to intracellular vesicles, revealing that dystroglycan with Y892 phosphorylation at PPPY motif does not target to focal adhesions (Sotgia *et al.*, 2003). Thus, the regulation role of PPPY in focal adhesion assembly or ERK cascade activation is controversial.

In fibroblasts, focal adhesion assembly and actin stress fibre formation are consequences of Rho or Rho kinase activation (section 1.7). Activation of Rho has been shown to be inhibited by integrin-induced activation of P190GAP mediated by activation of Src (Arthur and Burridge, 2001; Ren *et al.*, 1999) (Fig 1.7). Integrin engagement appeared to inhibit Rho activity in the protrusion formation stage (2 hour and more) and suppresses the downstream focal adhesion complex and actin stress fibre formation (Arthur and Burridge, 2001; Ren *et al.*, 1999). Activation of Cdc42 induced by integrin engagement has been found to be mediated by activation of Src and inhibits the activity of Rho (Hall, 1998). Therefore, during the filopodia formation stage, activation of Cdc42 can induce lamellipodia and filopodia formation and, at the same time, inhibit the activation of Rho and the downstream focal adhesion assembly and actin stress fibre formation. Thus, dystroglycan might indirectly play a role in suppressing Rho activation and inhibit the focal adhesion/stress fibre formation. The result shown in figure 5.7 supports this idea. However, activation of PAK, which is the Cdc42 downstream effector, has been determined as an activator of MLCK enhancing the formation of stress fibres (Sanders *et al.*, 1999). It seems activation of Cdc42 can also be involved in inducing stress fibre formation.

Since dystroglycan has been identified as being involved in the Cdc42 dependent filopodia formation, the inconsistent role of Cdc42 in both inducing stress fibres and filopodia formation might be regulated in a dystroglycan-dependent manner. Ferletta and colleagues have very recently demonstrated that in two types of epithelial cells, ERK activity, which is activated by engagement of integrin  $\alpha 6 \beta 1$  to laminin 10/11, is suppressed by the interaction of dystroglycan with laminin10/11, suggesting an opposing role of integrin and dystroglycan in regulating ERK activity (Ferletta *et al.*, 2003). Active ERK has been shown to function as an activator for MLCK to enhance

the formation of focal adhesion and stress fibres (Klemke *et al.*, 1997). Therefore, dystroglycan, which is involved in the inhibition of ERK activity, may also reduce the activation of MLCK and inhibit the formation of focal adhesion and actin stress fibres formation. Thus, the stress fibre formation through MLCK might be enhanced by Cdc42 and PAK activation and regulated by dystroglycan (Fig 5.10).

Altogether, dystroglycan is identified as a regulator for Cdc42 and downstream membrane protrusion formation. A dystroglycan-dependent signalling cycle of  $\beta$ -dystroglycan-Cdc42-PAK-ezrin- $\beta$ -dystroglycan was identified to regulate the formation of membrane protrusions. Activation of Cdc42 triggered by dystroglycan localised in the plasma membrane can either induce the membrane protrusions by activating WASP/Arp2/3 complex or organise filopodia bundling by recruiting ezrin-F actin or directly interacting with and bundling F-actin. This signalling cycle can also inhibit the focal adhesion assembly and stress fibre formation through the regulation of MLCK. ERK activation of MLCK was initially proposed to be mediated by dystroglycan signalling that could enhance the formation of focal adhesion and stress fibre formation. However, the dystroglycan dependent signalling cycle has shown that the possible role of dystroglycan in adhesion is to inhibit the formation of focal adhesion and stress fibre and induce actin rich membrane protrusions.

**Chapter 6**  
**Summary**

Dystroglycan, which is a membrane laminin receptor containing  $\alpha$  and  $\beta$  subunits linking the extracellular matrix to the cytoskeleton, has been identified as playing a role in maintaining the stability of muscle cells. Dystroglycan is expressed in non-muscle cells associating with actin filaments via dystrophin/utrophin isoforms, and interacting with laminin.

$\alpha$ -dystroglycan, which interacts with the extracellular laminin or LG domain containing ligands, has been identified to be necessary for cell adhesion dependent events such as morphogenesis, myelinogenesis and embryogenesis, indicating that dystroglycan plays a role in regulating cell adhesion signalling. Considering the signalling mediated by dystroglycan, it has been shown that  $\beta$ -dystroglycan interacts with Grb2 SH3 domain, caveolin, and the utrophin/dystrophin WW domain via its C-terminal PPPY motif. The binding of these appeared to be regulated in a PPPY motif phosphorylation dependent manner. Some SH2 containing proteins including Fyn, Csk, Nck, SHC, and v-Src have been shown to be recruited to the PPPY motif in response to the tyrosine phosphorylation in the PPPY motif. Therefore, dystroglycan PPPY motif might play a role in mediating the signalling which regulates adhesion and cytoskeleton organisation. Additionally, it has shown that dystroglycan was colocalised with the structural proteins in focal adhesions and active ERK has also been demonstrated to be localised to focal adhesions. Previous work showed that dystroglycan is colocalised with ERK at focal adhesion site. These all suggested that dystroglycan signalling might be involved in the regulation of focal adhesion and actin stress fibre formation.

To investigate the relationship between dystroglycan and ERK, the first approach was to visualise the localisation of ERK or dystroglycan. Fluorescent protein tagged ERK (YFP-ERK), and dystroglycan ( $\alpha\beta$ DG-GFP) expression plasmids were constructed and expressed in REF52 cells. YFP-ERK expressed in REF52 cells was determined to be a functional ERK that can be regulated by integrin-mediated or RTK-mediated signalling and inhibited by UO126. However, examining the localisation, YFP-ERK seemed not to be found in a typical focal adhesion structures. Additionally, ERK activity was not detected at the adhesion-like structures formed by YFP-ERK. Therefore, YFP-ERK

construct might not be useful for the further study of investigating the relationship between dystroglycan and ERK.

The expression of dystroglycan-GFP construct on the other hand led to dramatic actin reorganisation, resulting in filopodia formation in REF52. This interesting finding shifted the work into the study of the role of dystroglycan signalling in the regulation of actin filopodia. The functional domain of dystroglycan which is responsible for the dystroglycan filopodia formation signalling was determined to be the C-terminal cytoplasmic domain of  $\beta$ -dystroglycan. The dystroglycan-dependent filopodia formation is induced by either fibronectin or laminin, and inhibited by poly L lysine, indicating that integrin-dependent signalling might be required for the dystroglycan dependent filopodia formation. Dystroglycan deletion mutants with defects in  $\alpha$ -dystroglycan failed to induce the formation of filopodia, implying  $\alpha$ -dystroglycan is required for the dystroglycan dependent filopodia formation. However, expressing an AP $\beta$ -DG construct,  $\beta$ -dystroglycan with its proper membrane localisation was sufficient to induce the formation of filopodia, suggesting that  $\beta$ -dystroglycan regulates the formation of filopodia in a  $\alpha$ -dystroglycan independent manner. Since the dystroglycan functional domain deletion mutants lacking  $\alpha$ -dystroglycan showed a nuclear or intracellular vesicle localisation,  $\alpha$ -dystroglycan appeared to play an important role in the regulation of dystroglycan trafficking and targeting  $\beta$ -dystroglycan to the plasma membrane.

The dystroglycan-induced actin filopodia formation is very similar to a Cdc42-induced filopodia phenotype. By coexpressing constitutively activated or dominant negative constructs of Rho GTPases with dystroglycan or dystroglycan mutants, Cdc42 was identified as a mediator for dystroglycan dependent filopodia formation. The membrane localisation is necessary for  $\beta$ -dystroglycan in mediating Cdc42 dependent filopodia formation as well, indicating that  $\beta$ -dystroglycan-dependent Cdc42 activation might regulate the filopodia formation signalling taking place in the plasma membrane region. This idea is supported by the finding that ezrin is activated by Cdc42-induced activation

of PAK. Active ezrin can recognise RKKRK motif of  $\beta$ -dystroglycan with proper plasma membrane localisation, and target F-actin to dystroglycan. Thus a signalling cycle of dystroglycan-Cdc42-PAK-ezrin-dystroglycan was identified. This signalling cycle might be regulated in dystroglycan PPPY motif independent manner. Additionally,  $\beta$ -dystroglycan has been shown to directly associate with actin and promote the bundling of actin filaments. Thus, with active ezrin that targets F-actin to  $\beta$ -dystroglycan, according to the current model of filopodia formation,  $\beta$ -dystroglycan might play an important role in organisation and bundling filopodia from the actin dendritic network through the signalling cycle. Finally, in this work, ERK activated MLCK was initially presumed to mediate the dystroglycan signalling that could enhance the formation of focal adhesion and stress fibre formation. However, a recent study has shown that dystroglycan activation leads to the reduction of ERK activity. Therefore, instead of enhancing formation of focal adhesion and stress fibre formation, dystroglycan and dystroglycan-dependent signalling cycle appears to play a role in reducing the activity of ERK and MLCK thereby inhibiting focal adhesion and stress fibre formation.

Altogether, dystroglycan dependent signalling, which was initially predicted to regulate focal adhesion and actin stress fibre formation, has been identified to regulate formation of actin-rich membrane protrusions and filopodia formation. A novel signalling cycle of dystroglycan-Cdc42-PAK-ezrin-dystroglycan has been determined to be responsible for the dystroglycan-dependent filopodia formation. By triggering this signalling cycle, dystroglycan might be able to induce the formation of membrane protrusions and, at the same time, inhibit focal adhesion and stress fibre formation.



## Appendices

## **Appendix I Chemicals, reagents and Kits**

The chemicals, reagents and kits used were obtained from following suppliers

### ***Amersham-Pharmacia Biotech UK Ltd., Buckinghamshire, UK***

[32P]-ATP

### ***BDH Ltd., Lutterworth, UK***

NaCl, MgCl<sub>2</sub>, Sodium deoxycholate, Na<sub>2</sub> HPO<sub>4</sub>, KH<sub>2</sub> PO<sub>4</sub>, Phosphoric Acid

### ***Fisher Scientific UK Ltd., Loughborough, Leicestershire, UK***

Glycine, EGTA, Sodium Dodecyl Sulphate (SDS), KCl, Hepes, NaF, MgCl<sub>2</sub>, Boric Acid

### ***Gibco BRL, Life Technologies Ltd., Paisley, UK***

Lipofectamine™ reagent, Laminin, Fibronectin, epithelial growth factor (EGF), Fetal Bovine Serum (FBS)

### ***Iwaki, Scitech Dicision, Asahi, Japan***

25T, 75T and 175 T tissue culture flasks, 24 well tissue culture culture plates, 100mm tissue culture dishes.

### ***Promega UK Ltd., Southampton, UK***

UO126

### ***Pierce, Perbio Science UK Ltd., Cheshire, UK***

MicroBCA

### ***Qiagen, Crawley West Sussex, UK,***

QIAprep miniprep kit, QIAprep midiprep kit, QIAquick gel extraction kit

***Roche Molecular Biochemicals/Boehringer-Mannheim, Germany***

Rapid DNA ligation kit

***Schleicher & Schuell, Dassel, Germany***

Polyvinylidene Difluoride (PVDF) transfermembrane

***Severn Biotech Ltd., Worcestershire, UK***

30% polyacrylamide solution

***Sigma-Aldrich Company Ltd., Poole, Dorset, UK***

Ethylenediamine Tetra-Acetic Acid (EDTA), Ethidium bromide, Ampicillin, Kanamycin, Protein A Sepharose, Heparin, Poly-L-lysine, Bovine Serum Albumin (BSA), Tris-base, Bromophenol blue, Triton X-100, Ethylene Glycol-bis Tetra-Acetic Acid (EGTA), Tween-20, 3-(Cyclohexylamino)-1-Propane Sulphonic Acid (CAPS), Sodium azide, Nitro Blue Tetrazolium (NBT), 5-bromo-4-chloro-3-indolyl phosphate (BCIP), Tetramethylethylenediamine (TEMED), Ammonium persulfate (APS), Rhodamine-Phalloidin.

***Vector Laboratories Ltd., Peterborough, UK***

VECTASHIELD Mounting medium

## **Appendix II Media and general buffers**

### ***2 X YT liquid medium***

1.6% Tryptone (W/V), 1% Yeast extract (W/V), 0.5% NaCl (W/V) in 1L distilled water

### ***2 X YT solid medium***

0.64% Tryptone (W/V), 0.4% Yeast extract (W/V), 0.2% NaCl (W/V), 0.8% agar (W/V) in 400 ml distilled water

### ***Dulbecco's Modified Eagle Medium (DMEM)***

Gibco BRL

### ***OPTIMEM***

Gibco BRL

### ***TBE buffer (5X)***

54g Tris base, 27.5g Boric acid, 50ml 0.2M EDTA in 1L distilled water, pH = 8.0

### ***Agarose gel loading buffer***

30% Glycerol (V/V) and 0.25% Bromophenol (W/V) Blue in 0.5 X TBE buffer

### ***2 X SDS gel loading buffer***

100mM Tris, 200mM DTT, 4% SDS, 0.2% Bromophenol Blue, 20% glycerol, pH = 6.8

### ***Caps/methanol transblot buffer***

10mM CAPS [3-(Cyclohexylamino)-1-propansulfonsyre] in 20% methanol, pH=11

### ***TBST***

20mM Tris-HCl, 0.15M NaCl, 0.5% Tween20, pH= 7.5

### ***AP buffer***

100mM NaCl, 5mM MgCl<sub>2</sub>, 100mM Tris, pH= 9.5

### ***Separating gel buffer***

1.5mM Tris-base, 0.4% SDS, pH=8.8

***Stacking gel buffer***

0.5mM Tris-base, 0.4% SDS, pH=6.8

***10xSDS gel running buffer***

0.25 M Tris-base, 1.92 M Glycine, 10% SDS in 5L water

***IFA blocking buffer***

1% FBS (V/V) and 1% BSA (V/W) in PBS

***Permeant buffer***

0.1% TritonX-100 in PBS

***RIPA buffer***

50mM Tris-HCl pH7.5, 150mM NaCl, 1mM EDTA, 1mM EGTA, 1% Triton X-100, 0.5% Sodium deoxycholate, 0.1% SDS, 1mM Azide

***PBS (10X)***

80g NaCl, 2g KCl, 11.5g Na<sub>2</sub>HPO<sub>4</sub>•7H<sub>2</sub>O, 2g KH<sub>2</sub>PO<sub>4</sub> in 1L distilled water

***MAPK lysis buffer***

25mM Hepes, 0.3M NaCl, 1.5mM MgCl<sub>2</sub>, 0.2mM EDTA, pH=7.4

***MAPK Wash buffer***

20mM Hepes, 50mM NaCl, 2.5mM MgCl<sub>2</sub>, 0.1mM EDTA, pH=7.4

***MAPK kinase buffer***

20mM Hepes, 0.5mM NaF, 7.5mM MgCl<sub>2</sub>, 0.2mM EDTA, pH=7.4

## Appendix III Plasmids and clones

### (A) Plasmids used in this work

Names	Features	Source
PRESYFP-C1	Mammalian expression vector with yellow fluorescent protein (YFP) tag sequence. Multiple cloning site allowed fusion to be made at C-terminus of YFP. CMV promoter, SV40 and fl ori, Kan <sup>R</sup> and Neo <sup>R</sup> .	J. Pines (Chambridge)
PEGFP-N3	Mammalian expression vector with green fluorescent protein (GFP) tag sequence. Multiple cloning sites allowed fusion to be made at N-terminus of GFP. CMV promoter, SV40 and fl ori, Kan <sup>R</sup> and Neo <sup>R</sup> .	Clontech

### (B) Clones used in this work

Names	Features	Source/Reference
YFP-ERK	P44 MAPK sequence cloned into EcoRI site of pRES-YFP vector.	This work
$\alpha\beta$ DG-GFP	Full-length dystroglycan cloned into Sall and SmaI sites of pEGFP vector.	This work
$\alpha\beta$ DG $\Delta$ c $\beta$ -GFP	Dystroglycan cytoplasmic deletion mutant sequence cloned at the Sall and SmaI site of pEGFP vector.	This work
C $\beta$ -GFP	Cytoplasmic $\beta$ -dystroglycan sequence cloned at the Sall and SmaI site of pEGFP vector.	This work
$\alpha\beta$ DG $\Delta$ e $\beta$ -GFP	Dystroglycan extracellular $\beta$ domain deletion mutant cloned at the Sall and SmaI site of pEGFP vector.	This work
$\alpha\beta$ DG $\Delta$ a-GFP	Dystroglycan a subunit deletion mutant sequence cloned at the Sall and SmaI site of pEGFP vector.	This work

$\alpha$ DG-GFP	$\alpha$ -dystroglycan sequence cloned at the Sall and SmaI site of pEGFP vector.	This work
HA/P44 <sup>MAPK</sup>	P44 MAPK sequenced cloned into EcoRI site of pCDNAI/Neo. Kan <sup>R</sup>	Meloche et al., 1992
mDG-1	Full-length of mouse dystroglycan cDNA sequence (DAG-1) cloned between EcoRI and BstXI sites in pCDNAII. Kan <sup>R</sup>	D.J. Blake (Oxford)
AP- $\beta$ DG	Full-length $\beta$ -dystroglycan with an alkaline phosphatase sequence cloned into HindIII and EcoRI site of PCAGGS vector. Amp <sup>R</sup> .	Rentschler, S. <i>et al.</i> , 1999
N17Cdc42	Dominant negative Cdc42 sequence cloned into CMVneo-myc-1 at the BamHI and NheI sites. Amp <sup>R</sup>	A.Hall (London)
V12Cdc42	Constitutively activated Cdc42 sequence cloned into CMVneo-myc1 at the BamHI and NheI sites. Amp <sup>R</sup>	A.Hall (London)
N17 Rac	Dominant negative Rac sequence cloned into CMVneo-myc-1 at the BamHI and NheI sites. Amp <sup>R</sup>	A.Hall (London)
V12 Rac	Constitutively activated Rac sequence cloned into CMVneo-myc-1 at the BamHI and NheI sites. Amp <sup>R</sup>	A.Hall (London)
N19 Rho	Dominant negative Rho sequence cloned into CMVneo-myc-1 at the BamHI and NheI sites. Amp <sup>R</sup>	A.Hall (London)
V14Rho	Constitutively activated Rho sequence cloned into CMVneo-myc-1 at the BamHI and NheI sites. Amp <sup>R</sup>	A.Hall (London)

## Appendix IV Cell lines

### Cells used in this work

Cells	Features	Source
REF52	Rat embryo fibroblast cell line	D. Helfman
COS7	Human epithelial cell line	M. Frame (Glasgow)
Utrophin +/+ and Utrophin -/-	Primary culture of mouse embryo fibroblasts	K. Davies



## Appendix V Antibodies

### (A) Primary antibodies used in this work

Antibody names	Direct against	Dilution for Western blot and [IF]	Source / Reference
Total ERK* ∞ (NEB 9102)	Whole molecule	1:1000 [-]	New England Biolabs
Phospho-ERK (NEB 9105) φ °	Thr202/ Tyr204	1:1000 [1:100]	New England Biolabs
GFP ∃ ∞	Whole molecule	1:1000 [-]	F. Barr (Glasgow)
Talin φ °	Chicken talin, clone 8d4	- [1:1000]	Sigma-Aldrich
Poly-βDG* ∞ 1710	β-dystroglycan 15 a-a peptide of extreme C-terminus	1:1000 [-]	Ilisley <i>et al.</i> , 2001
c-myc φ °	Amino acids 408-439 within the carboxy terminal domain of c-Myc of human origin	- [1:100]	Santa Cruz
Rab6* ∞	C-terminus of human utrophin (3204-3343)	1:1000 [-]	Winder, <i>et al.</i> , 1995

\*Rabbit  
φ Mouse  
∃ Sheep

° monoclonal antibodies  
∞ polyclonal antibodies

**(B) Secondary antibodies used in this work**

Antibody names	Direct against	Conjugate	Raised in	Dilution for Western blot and [IF]	Source
Anti-mouse IgG	$\gamma$ -chain	AP	Goat	1:10000 [-]	Sigma-Aldrich
Anti-rabbit IgG	Whole molecule	AP	Goat	1:10000 [-]	Sigma-Aldrich
Anti-sheep IgG	Whole molecule	AP	Donkey	1:10000 [-]	Sigma-Aldrich
Anti-mouse IgG	Whole molecule	TR	Horse	- [1:1000]	Vector
Anti-mouse IgG	Whole molecule	FITC	Horse	- [1:1000]	Vector

AP: Alkaline phosphatase

TR: Texas-red

FITC: Fluorescein

## Appendix VI PCR Primers

### Oligonucleotides used in this work

Oligos	Function	Sequence 5'-3'
$\alpha$ DG5	Full-length dystroglycan primer with Sall site	TTG GTC GAC ATG TCT GTG GAC AAC TGG CTA
$\beta$ DG3	Full-length dystroglycan primer with SmaI site	GCT TCC CGG GGC AGG GGG AAC ATA CGG AGG
Trans $\beta$ 5	Dystroglycan $\alpha$ subunit and extracellular $\beta$ domain deletion mutant primer with Sall site	GCT TCC CGG GGC ATA GCA GAT CAT AGC AAT
$c\beta$ DG5-Tyr	$\beta$ -dystroglycan cytoplasmic domain primer with Sall site	TTG GTC GAC TAT CGC AAG AAG AGG AAG GGC
$e\beta$ DG5	Full-length $\beta$ -dystroglycan primer with Sall site	TTG TGC GAC GGC TCT ATC GTG TGT GAA TGG
ss $\alpha$ 5	Dystroglycan signal sequence primer for $\alpha$ dystroglycan deletion mutant. 10 bases overlaps with 3' end of $\beta$ -dystroglycan	TGT TGG TCC ATT CCA CGA TAG AAG CCA CAG CCA CAG
sse $\beta$ 3	$\beta$ -dystroglycan extracellular domain primer for $\alpha$ dystroglycan deletion mutant; 10 bases overlaps with 5' end of dystroglycan signal sequence	TCT ATC GTG TGT GAA TGG
ss $\alpha$ TM5	$\alpha$ -dystroglycan primer for extracellular $\beta$ domain deletion mutant. 10 bases overlaps with 3' end of $\beta$ transmembrane domain	TGG GAT AAC GGT GTG CAG AGA GCC CCG AGT GAT
TM3	$\beta$ -dystroglycan transmembrane domain primer for extracellular $\beta$ domain deletion mutant. 10 bases overlaps with 5' end of $\alpha$ dystroglycan	CTG CAC ACC GTT ATC CCA
$\alpha$ DG5X	$\alpha$ -dystroglycan primer with Sall site	GCT TCC CGG GGC GCC CCG ATG GAT GTT CTG

## Appendix VII PCR reaction conditions

### Primers and PCR reaction conditions of dystroglycan functional domain deletion mutants

Mutants	Primers	Condition of PCR reaction
$\alpha\beta$ DG-GFP	$\alpha$ DG5	1) 95°C 1minute, 2) 95°C 1 minute, 3) 55°C 1 minute, 4) 72°C 3minutes and 30 seconds. 2)- 4) repeat for 30 cycles
	$\beta$ DG3	
$\alpha\beta$ DG $\Delta$ $\beta$ -GFP	$\alpha$ DG5	1) 95°C 1minute, 2) 95°C 1 minute, 3) 60°C 1 minute, 4) 72°C 3 minutes. 2) – 4) repeat for 30 cycles
	Trans $\beta$ 5	
C $\beta$ -GFP	C $\beta$ DG5-Tyr	1) 95°C 1minute, 2) 95°C 1 minute, 3) 65°C 1 minute, 4) 72°C 2 minute 2)-4) repeat for 30 cycles
	$\beta$ DG3	
$\alpha\beta$ DG $\Delta$ $\alpha$ -GFP	P1 $\alpha$ DG5* <sup>Ⓞ</sup>	First Round P1 95°C 1minute, 95°C 1 minute, 65°C 1 minute, 72°C 2 minute .2-4 repeat for 30 cycles P2 95°C 1minute, 95°C 1 minute, 65°C 1 minute, 72°C 2 minute 2-4 repeat for 30 cycles Second round 95°C 1minute, 95°C 1 minute, 65°C 1 minute, 72°C 2 minute 2-4 repeat for 30 cycles
	P1 S $\alpha$ 5*	
	P2 S $\alpha$ $\beta$ 3*	
	P2 $\beta$ DG3* <sup>Ⓞ</sup>	
$\alpha\beta$ DG $\Delta$ $\alpha\beta$ -GFP	P1 $\alpha$ DG5* <sup>Ⓞ</sup>	First Round P1 95°C 1minute, 95°C 1 minute, 65°C 1 minute, 72°C 2 minute .2-4 repeat for 30 cycles P2 95°C 1minute, 95°C 1 minute, 65°C 1 minute, 72°C 2 minute 2-4 repeat for 30 cycles Second round 95°C 1minute, 95°C 1 minute, 65°C 1 minute, 72°C 2 minute 2-4 repeat for 30 cycles

P1 Pair 1 of primer

\* Primers for first round PCR

P2 Pair 2 of primer

Ⓞ Primers for second round PCR

## Appendix VIII Plasmid trasfection conditions

### Transfection and cotransfection conditions used in this study

	REF52	COS7	UTR <sup>+/+</sup> and UTR <sup>-/-</sup> Primary mouse embryo fibroblast
<b>YFP-ERK *</b>	<ol style="list-style-type: none"> <li>1. <math>3 \times 10^6</math> /ml; 80%</li> <li>2. 2 <math>\mu</math>g/ml</li> <li>3. 5hr; then added equal volume of growth medium</li> </ol>	-	-
<b>Dystroglycan and mutants*</b>	<ol style="list-style-type: none"> <li>1. <math>3 \times 10^6</math> /ml; 80%</li> <li>2. 1.8<math>\mu</math>g/ml</li> <li>3. 5hr; then added equal volume of growth medium</li> </ol>	<ol style="list-style-type: none"> <li>1. <math>2 \times 10^6</math> /ml; 95%</li> <li>2. 1.8<math>\mu</math>g/ml</li> <li>3. Overnight</li> </ol>	<ol style="list-style-type: none"> <li>1. <math>3 \times 10^6</math> /ml ; 80-90%</li> <li>2. 1.5<math>\mu</math>g/ml</li> <li>3. 8hr; then added equal volume of growth medium</li> </ol>
<b>AP-dystroglycan*</b>	<ol style="list-style-type: none"> <li>1. <math>3 \times 10^6</math> /ml; 80%</li> <li>2. 2.2 <math>\mu</math>g/ml</li> <li>3. 5hr; then added equal volume of growth medium</li> </ol>	-	-
<b>Cdc42 mutants*</b>	<ol style="list-style-type: none"> <li>1. <math>3 \times 10^6</math> /ml; 80%</li> <li>2. 1.5 <math>\mu</math>g/ml</li> <li>3. 5hr; then added equal volume of growth medium</li> </ol>	-	-
<b>Rac mutants *</b>	<ol style="list-style-type: none"> <li>1. <math>3 \times 10^6</math> /ml; 80%</li> <li>2. 1.5 <math>\mu</math>g/ml</li> <li>3. 5hr; then added equal volume of growth medium</li> </ol>	-	-

<b>Rho mutants*</b>	<ol style="list-style-type: none"> <li>1. <math>3 \times 10^6</math> /ml; 80%</li> <li>2. 1.5 <math>\mu</math>g/ml</li> <li>3. 5hr; then added equal volume of growth medium</li> </ol>	-	-
<b>Dystroglycan or mutants with Cdc42 mutants <sup>Φ</sup></b>	<ol style="list-style-type: none"> <li>1. <math>3 \times 10^6</math> /ml; 80%</li> <li>2. 0.9 <math>\mu</math>g/ml+ 0.9<math>\mu</math>g/ml</li> <li>3. 5hr; then added equal volume of growth medium</li> </ol>	-	-
<b>Dystroglycan or mutants with Rac mutants <sup>Φ</sup></b>	<ol style="list-style-type: none"> <li>1. <math>3 \times 10^6</math> /ml; 80%</li> <li>2. 0.9 <math>\mu</math>g/ml+ 0.9<math>\mu</math>g/ml</li> <li>3. 5hr; then added equal volume of growth medium</li> </ol>	-	-
<b>Dystroglycan or mutants with Rho mutants <sup>Φ</sup></b>	<ol style="list-style-type: none"> <li>1. <math>3 \times 10^6</math> /ml; 80%</li> <li>2. 0.9 <math>\mu</math>g/ml+ 0.9<math>\mu</math>g/ml</li> <li>3. 5hr; then added equal volume of growth medium</li> </ol>	-	-
<ol style="list-style-type: none"> <li>1. Initially seeding number; percentage of cell confluent overnight</li> <li>2. DNA concentration</li> <li>3. Transfection reaction time and condition</li> </ol> <p>* Single DNA transfection  <sup>Φ</sup> DNA cotransfection</p>			

## References

- Abe, K., Rossman, K., Liu, B. P., Ritola, K., Chiang, D., Campbell, S., Burridge, K., and Der, C.** (2000) Vav2 is an activator of Cdc42, Rac1, and RhoA. *J. Biol. Chem.* 275, 10141–10149.
- Almed, N., Niu, J., Doraby, D. J., Gu, X., Andrews, S., Meldrum, C. J., Sott, R. J., Baker, M. S., Marecadie, I. G. and Agrez, M. V.** (2002) Direct integrin  $\alpha v\beta 5$ -ERK binding implications for tumour growth. *Oncogene* 21, 1370-1380
- Amano, M., Chihara, K., Kimura, K., Fukata, Y., Nakamura, N., Matsuura, Y. and Kaibuchi, K.** (1997) Formation of actin stress fibers and focal adhesions enhanced by Rho-kinase. *Science* 275, 1308-11
- Amieva, M. R. and Furchtmayr, H.** (1995) Subcellular localization of moesin in dynamic filopodia, retraction fibers, and other structures involved in substrate exploration, attachment, and cell-cell contacts. *Exp. Cell Res.* 219, 180-196
- Andac, Z., Sasaki, T., Mann, K., Brancaccio, A., Deutzmann, R. and Timpl, R.** (1999) Analysis of heparin, alpha-dystroglycan and sulfatide binding to the G domain of the laminin alpha1 chain by site-directed mutagenesis. *J. Mol. Biol.* 287, 253-64.
- Apel, E. A., Glass, D. J., Moscoso, L. M., Yancopoulos, G. D. and Sanes, J. R.** (1997) Rapsyn is required for MuSK signalling and recruits synaptic components to a MuSK-containing scaffold. *Neuron* 18, 623-635
- Arahata, K., Ishiura, S., Ishiguro, T., Tsukahara, T., Suhara, Y., Eguchi, C., Ishihara, T., Nonaka, I., Ozawa, E. and Sugita, H.** (1988) Immunostaining of skeletal and cardiac muscle surface membrane with antibody against Duchenne muscular dystrophy peptide. *Nature* 333, 861-3.
- Aravind, L. and Koonin, E. V.** (1999) The fukutin protein family-predicted enzymes modifying cell-surface molecules. *Curr. Biol.* 9, R836–R837
- Arber, S., Barbayannis, F. A., Hanser, H., Schneider, C., Stanyon, C.A., Bernard, O. and Caroni, P.** (1998) Regulation of actin dynamics through phosphorylation of cofilin by LIM-kinase. *Nature* 393, 805-809
- Arthur, W. T., Petch, L. and Burridge, K.** (2000) Integrin engagement suppresses RhoA activity via a c-Src-dependent mechanism. *Curr. Biol* 10, 719–722.



- Arthur, W. T. and Burridge, K.** (2001) RhoA inactivation by p190RhoGAP regulates cell spreading and migration by promoting membrane protrusion and polarity. *Mol. Biol. Cell.* 12, 2711-20.
- Assoian, R. K.** (1997) Anchorage-dependent cell cycle progression. *J. Cell Sci.* 136, 1-4
- Bamburg, J. R.** (1999) Proteins of the ADF/cofilin family: essential regulators of actin dynamics. *Annu. Rev. Cell Dev. Biol.* 15,185-230.
- Barry, S. T., Flinn, M. H., Humphries, M. J., Critchley, D. R. and Ridley, A. J.** (1996) Requirement for Rho in integrin signalling. *Cell Adhes. Commun.* 4, 387-398.
- Bartles, J. R.** (2000) Parallel actin bundles and their multiple actin-bundling proteins. *Curr. Opin. Cell Biol.* 12, 72-78.
- Bear, J. E., Svitkina, T. M., Krause, M., Schafer, D. A., Loureiro, J. J., Strasser, G. A., Maly, I. V., Chaga, O. Y., Cooper, J. A., Borisy, G.G. and Gertler, F.B.** (2002) Antagonism between Fna/VASP proteins and actin filament capping regulates fibroblast motility. *Cell.* 109, 509-521.
- Belkin, A. M. and Burridge, K.** (1995a) Association of aciculin with dystrophin and utrophin. *J. Biol. Chem.* 270, 6328-6337
- Belkin, A. M. and Burridge, K.** (1995b) Localization of utrophin and aciculin at site of cell-matrix and cell-cell adhesion in culture cells. *Exp. Cell Res.* 221, 132-140
- Belkin, A. M. and Smalheiser, N. R.** (1996) Localization of cranin (dystroglycan) at site of cell-cell adhesion and recruitment to focal adhesions depends upon extracellular ligands. *Cell Adhes. Commun.* 4, 281-296
- Beltran-Valero de Bernabe, D., Currier, S., Steinbrecher, A., Celli, J., van Beusekom, E., van der Zwaag, B., Kayserili, H., Merlini, L., Chitayat, D., Dobyns, W.B., Cormand, B., Lehesjoki, A.E., Cruces, J., Voit, T., Walsh, C.A., van Bokhoven, H. and Brunner, H.G.** (2002) Mutations in the O-mannosyltransferase gene POMT1 give rise to the severe neuronal migration disorder Walker-Warburg syndrome. *Am J Hum Genet.* 71,1033-43.

- Benard, V., Bohl, B. P. and Bokoch, G. M.** (1999) Characterization of rac and cdc42 activation in chemoattractant-stimulated human neutrophils using a novel assay for active GTPases. *J. Biol. Chem.* 274, 13198-204
- Berg, J. S. and Cheney, R. E.** (2002) Myosin-X is an unconventional myosin that undergoes intrafilopodial motility. *Nat. Cell Biol.* 4, 246-250.
- Berryman, M., Franck, Z. and Bretscher, A.** (1993) Ezrin is concentrated in the apical microvilli of a wide variety of epithelial cells whereas moesin is found primarily in endothelial cells. *J. Cell Sci.* 105, 1025-43
- Bishop, A. L. and Hall, A.** (2000) Rho GTPases and their effector proteins. *Biochem. J.* 348, 241-246
- Boffi, A., Bozzi, M., Sciandra, F., Woellner, C., Bigotti, M. G., Ilari, A. and Brancaccio, A.** (2001) Plasticity of secondary structure in N-terminal region of  $\beta$ -dystroglycan. *Biochimica et Biophysica Acta* 4564, 114-121
- Bokoch, G. M.** (2003) Biology of the p21-activated kinases. *Annu. Rev. Biochem.* 72, 743-781
- Borisy, G. G., and Svitkina, T. M.** (2000) Actin machinery: pushing the envelope. *Curr. Opin. Cell Biol.* 12,104-112.
- Boulton, T.G., Nye, S. H., Robbins, D. J., Ip, N.Y., Radziejewska, E., Morgenbesser, S. D., DePinho, R. A., Panayotatos, N., Cobb, M. II. and Yancopoulos, G. D.** (1991) ERKs: A family of protein -Serine/ Theronine kinasc that are activated and tyrosin phosphorylated in response to insulin and NGF. *Cell* 65, 663-675
- Bowe, M.A., Mendis, D.B. and Fallon, J. R.** (2000) The small leucine-rich repeat proteoglycan biglycan binds to alpha-dystroglycan and is upregulated in dystrophic muscle. *J Cell Biol.* 148, 801-10.
- Bozzi, M., Veglia, G., Paci, M., Sciandra, F., Giardina, B. B. and Brancaccio, A.** (2001) A synthetic peptide corresponding to the 550-585 region of a dystroglycan binds  $\beta$ -dystroglycan as revealed by NMR spectroscopy. *FEBS Lett.* 449, 210-214
- Brancaccio, A., Schulthes, T., Gesemann, M. and Engel, J.** (1995) Electron microscopic evidence for mucin-like region in chick muscle  $\alpha$ -dystroglycan. *FEBS Lett.* 368, 139-142

- Brockington, M., Blake, D. J., Prandini, P., Brown, S. C., Torelli, S., Benson, M. A., Ponting, C. P., Estournet, B., Romero, N. B., Mercuri, E., Voit, T., Sewry, C. A., Guicheney, P., and Muntoni, F.** (2001) Mutations in the fukutin-related protein gene (FKRP) cause a form of congenital muscular dystrophy with secondary laminin alpha2 deficiency and abnormal glycosylation of alpha-dystroglycan. *Am. J. Hum. Genet.* 69,1198–1209
- Brunet, A., Roux, D., Lenormand, P., Dowd, S., Keyse, S. and Pouyssegur, J.** (1999) Nuclear translocation of p42/p44 mitogen-activated protein kinase is required for growth-factor-induced gene expression and cell cycle entry. *EMBO J.* 18, 664-674
- Bulfield, G., Siller, W. G., Weight, P. A. and Moore, K. J.** (1984) X chromosome linked muscular dystrophy (mdx) in mouse. *Proc. Natl. Acad. Sci. USA.* 81, 118-192
- Burdend, S. J.** (1998) The formation of neuromuscular synapses *Gen & Dev* 12,133–148
- Burridge, K. and Chrzanowska-Wodnicka, M.** (1996) Focal adhesions, contractility and signaling. *Annu. Rev. Cell Dev. Biol.* 12, 463–519
- Cacace, A. M., Michaud, N.R., Therrien, M., Mathes, K., Copeland, T., Rubin, G. M., Morrison, D. K.** (1999) Identification of constitutive and ras-inducible phosphorylation sites of KSR: implications for 14-3-3 binding, mitogen-activated protein kinase binding, and KSR overexpression. *Mol. Cell Biol.* 19, 229-40.
- Calvaldesi, M., Macchia, G., Barca, S., Deflippi, P., Tarone, G. and Petrucci, T. C.** (1999) Association of dystroglycan complex isolated from bovine brain synaptosomes with protein involved in signal transduction. *J. Neurochemistry* 72, 1648-1655
- Carrier, M. F.** (1998) Control of actin dynamics. *Curr Opin Cell Biol* 10, 45-51
- Cartaud, A., Countant, S., Pertucci, T. C. and Cartaud, J.** (1998) Evidence for in situ and in vitro association between  $\beta$ -dystroglycan and the subsynaptic 43KDa rapsyn protein. *J. Biol. Chem.* 273, 232-236
- Campanelli, J. T., Ronerds, S. L., Campbell, K. P. and Scheller, R. H.** (1994) A role of dystrophin-associated glycoproteins and utrophin in agrin-induced AChR clustering. *Cell* 77, 663-674
- Cerione, R. A. and Zheng, Y.** (1996) The Dbl family of oncogenes. *Curr. Opin. Cell Biol* 8, 216-222

- Chang, J., Gill, S., Settleman, J., Yu, H., Chen, J.K., Feng, S., Dalgarno, D.C., Brauer, A.W., Schreiber, S. L. and Parsons, S.** (1995) c-Src regulates the simultaneous rearrangement of actin cytoskeleton, p190RhoGAP, and p120RasGAP following epidermal growth factor stimulation. *J. Cell Biol.* 130, 355–368.
- Chen, I. H. and Sudol, M.** (1995) The WW domain of Yes-associated protein binds a proline-rich ligand that differs from the consensus established for Src homology 3 binding modules. *Proc. Natl Acad. Sci.* 92, 7819-7823
- Chen, Y-J, Spence, H. J., Cameron, L.M., Jess, T., Ilsley, J. L. and Winder, S. J.** (2003) Direct interaction of  $\beta$ -dystroglycan with F-actin. *Biochem J.* 375, 329-337
- Chiba, A., Matsumura, K., Yamada, H., Inazu, T., Simizu, T., Kusunoki, S., Kanazawai, I., Kobata, A. and Endo, T.** (1997) Structures of sialylated O-linked oligosaccharides of bovine peripheral nerve alpha-dystroglycan. The role of a novel O-mannosyl-type oligosaccharide in the binding of alpha-dystroglycan with laminin. *J. Biol. Chem* 272, 2156-2162
- Clark, E. A. and Brugge, J. S.** (1995) Integrins and signal transduction pathways: the road taken. *Science.* 268, 233-9.
- Chrzanowska-Wodnicka, M. and Burridge, K.** (1996) Rho-stimulated contractility drives the formation of stress fibers and focal adhesions. *J Cell Biol.* 133, 1403-15.
- Cobb, M. H. and Goldsmith, E. J.** (2000) Dimerisation in MAP-Kinase signalling. *Trends Biochem Sci.* 25, 7-9
- Cohn, R. D., Henry, M. D., Michele, D. E., Barresi, R., Saito, F., Moore, S. A., Flanagan, J. D., Skwarchuk, M. W., Robbins, M. E. and Mendell, J. R.** (2002) Disruption of DAG1 in differentiated skeletal muscle reveals a role for dystroglycan in muscle regeneration. *Cell* 110, 639-48
- Cote, P. D., Moukhles, H. and Carbonetto, S.** (2002) Dystroglycan is not required for localization of dystrophin, syntrophin, and neuronal nitric-oxide synthase at the sarcolemma but regulates integrin alpha 7B expression and caveolin-3 distribution. *J. Biol. Chem.* 277, 4672–4679
- Cooper, J. A. and Schafer, D. A.** (2000) Control of actin assembly and disassembly at filament ends. *Curr. Opin. Cell Biol.* 12, 97–103.

- Cyert, M. S.** (2001) The regulation of nuclear localisation during signal transduction. *J. Biol. Chem.* 276, 20805-20808
- Daniels, R.H. and Bokoch, G. M.** (1999) p21-activated protein kinase: a crucial component of morphological signaling? *Trends Biochem Sci.* 24, 350-5
- Davies, S. P., Reddy, H., Caivano, M. and Cohen, P.** (2000) Specificity and mechanism of action of some commonly used protein kinase inhibitors. *Biochem J.* 351, 95-105.
- Deconinck, A. E., Rafael, J. A., Skinner, J. J. A., Brown, S. C., Potter, A. C., Metzinger, L., Watt, D. J., Dickson, G., Tinsley, J. M. and Davies, K. E.** (1997) Utrophin-dystrophin-deficient mice as a model for Duchenne muscular dystrophy. *Cell* 90, 717-727.
- DePasquale, J. A. and Izzard, C. S.** (1991) Accumulation of talin in nodes at the edge of the lamellipodium and separate incorporation into adhesion plaques at focal contacts in fibroblasts. *J. Cell Biol.* 113, 1351-1359.
- del Pozo, M., Price, L., Alderson, N., Ren, X. and Schwartz, M.** (2000) Adhesion to the extracellular matrix regulates the coupling of the small GTPase Rac to its effector PAK. *EMBO J.* 19, 2008-2014.
- Dickens, N. J., Beatson, S. and Ponting, C. P.** (2002) Cadherin-like domains in alpha-dystroglycan, alpha/epsilon-sarcoglycan and yeast and bacterial proteins. *Curr. Biol.* 12, R197-9
- Di Stasio, E., Sciandra, F., Maras, B., Di Tommaso, F., Petrucci, T. C., Giardina, B. and Brancaccio, A.** (1999) Structural and functional analysis of the N-terminal extracellular region of beta-dystroglycan. *Biochem Biophys Res Commun.* 266, 274-8
- Dixon, A. K., Tait, T. M., Campbell, E. A., Bobrow, M., Roberts, R.G. and Freeman, T. C.** (1997) Expression of the dystrophin-related protein 2 (DRP2) transcript in the mouse. *J. Mol. Biol.* 270, 551-558.
- Durbeej, M., Larsson, E., Ibraghimov-Beskrovnyan, O., Roberds, S. L., Campbell, K. P. and Ekblom, P.** (1995) Non-muscle  $\alpha$ -dystroglycan is involved in epithelial development. *J. Cell Biol.* 130, 79-91

**Durbeej, M., Jung, D., Hjalt, T., Campbell, K. P., Ekblom, P.** (1997) Transient expression of Dp140, a product of the Duchenne muscular dystrophy locus, during kidney tubulogenesis. *Dev. Biol.* 181, 156-167

**Durbeej, M., Henry, M. D. and Campbell, K. P.** (1998a) Dystroglycan in development and disease. *Curr. Opin. Cell. Biol.* 10, 594-601

**Durbeej, M., Henry, M. D., Fletta, M., Campbell, K.P. and Ekblom, P.** (1998b) Distribution of dystroglycan in normal adult mouse tissues. *J. Histochem. Cytochem.* 46 449-457

**Edwards, D. C., Sanders, L. C., Bokoch, G. M and Gill, G. N.** (1999) Activation of LIM-kinase by Pak1 couples Rac/Cdc42 GTPase signalling to actin cytoskeletal dynamics. *Nat. Cell Biol.* 1, 253-9

**Ervasti, J. M., Ohlendieck, K., Kahl, S. D., Gaver, M. G. and Campbell, K. P.** (1990) Deficiency of a glycoprotein component of Duchenne muscular dystrophy locus. *Nature* 345, 315-319

**Ervasti, J. M. and Campbell, K. P.** (1991) Membrane organization of dystrophin-glycoprotein complex. *Cell* 66, 1121-1131

**Ervasti, J. M. and Campbell, K.P.** (1993) A role of the dystrophin glycoprotein as a transmembrane link between laminin and actin. *J. Cell Biol.* 112, 809-823

**Ervasti, J.M., Burwell, A.L. and Geissler, A. L.** (1997) Tissue-specific heterogeneity in alpha-dystroglycan sialoglycosylation. Skeletal muscle alpha-dystroglycan is a latent receptor for Vicia villosa agglutinin b4 masked by sialic acid modification. *J Biol Chem.* 272, 22315-21

**Esapa, C. T., Benson, M. A., Schroder, J. E., Martin-Rendon, E., Brockington, M., Brown, S. C., Muntoni, F., Kroger, S. and Blake, D. J.** (2002) Functional requirements for fukutin-related protein in the Golgi apparatus. *Hum Mol Genet.* 11, 3319-31

**Feng, S., Chen, J. K., Yu, H., Simon, J. A and Schreiber, S. L.** (1994) Two binding orientations for peptides to the Src SH3 domain: development of a general model for SH3-ligand interactions. *Science* 266, 1241-1247

**Ferletta, M., Kikkawa, Y., Yu, H., Talts, J. F., Durbeej, M., Sonnenberg, A., Timpl, R., Campbell, K. P., Ekblom, P. and Genersch, E.** (2003) Opposing roles of integrin alpha6A beta1

and dystroglycan in laminin-mediated extracellular signal-regulated kinase activation. *Mol Biol Cell*. 14, 2088-103

**Fincham, V. J., Chudleigh, A. and Frame, M. C.** (1999) Regulation of p190 Rho-GAP by v-Src is linked to cytoskeletal disruption during transformation. *J Cell Sci* 112, 947-56

**Fincham, V. J., James, M., Frame M. C. and Winder, S. J.** (2000) Active ERK/MAP kinase is targeted to newly forming cell-matrix adhesions by integrin engagement and v-Src. *EMBO J.* 19, 2911-2923

**Fukuyama, T. and Nakamura, M.** (1981) Blood volume determination of ischemic area with radionuclides. *Nippon Rinsho*. 39, 2529-34

**Garcia-Cardena, G., Martasek, P., Masters, B.S., Skidd, P. M., Couet, J., Li, S., Lisanti, M.P. and Sessa, W. C.** (2001) Caveolae and their coat proteins, the caveolins: from electron microscopic novelty to biological launching pad. *J Cell Physiol*. 186, 329-37

**Gary, R. and Bretscher, A.** (1995) Ezrin self-association involves binding of an N-terminal domain to a normally masked C-terminal domain that includes the F-actin binding site. *Mol Biol Cell* 6, 1061-75

**Gee, S. H., Montanaro, F., Lidenbaum, M. H. and Carbonetto, S.** (1994) Dystroglycan-  $\alpha$ , a dystrophin-associated glycoprotein is a functional agrin receptor. *Cell* 77, 675-686

**Giancotti, F.G. and Ruoslahti, E.** (1999) Integrin signaling. *Science*. 285, 1028-32.

**Glading, A., Chang, P., Lauffenburger, D. A. and Wells, A.** (2000) Epidermal growth factor receptor activation of calpain is required for fibroblast motility and occurs via an ERK/MAP kinase signalling pathway. *J. Biol. Chem.* 275, 2390-2398

**Glading, A., Uberall, F., Keyse, S. M. and Lauffenburger, D. A.** (2001) Membrane proximal ERK signalling is required for M-calpain activation downstream of epidermal growth factor receptor signalling. *J. Biol. Chem.* 276, 23341-23348

**Glass, D. J., Bowen, D. C., Radziejewski, C., Bruno, J., Stitt, T. N., Ryan, T. E., Gies, D. R., Mattsson, K., Shah, S., Burden, S. J., Valenzuela, D. M., DeChiara, T. M. and Yancopoulos, G. D.** (1996) Agrin acts via a MuSK receptor complex. *Cell* 85, 513-523

- Gorecki, D. C. and Barnard, E. A.** (1995) Specific expression of G-dystrophin (Dp71) in the brain. *Neuroreport* 6, 893-986
- Gotoh, A., Takahira, H., Geahlen, R. and Broxmeyer, H.** (1997) Cross-linking of integrins induces tyrosine phosphorylation of the proto-oncogene product Vav and the protein tyrosine kinase Syk in human factor-dependent myeloid cells. *Cell Growth Differ.* 8, 721-729
- Govind, S., Kozma, R., Monfries, C., Lim, L. and Ahmed, S.** (2001) Cdc42Hs facilitates cytoskeletal reorganization and neurite outgrowth by localizing the 58-kD insulin receptor substrate to filamentous actin. *J Cell Biol.* 152, 579-94
- Grady, R. M., Teng, H., Nichol, M. C., Cunningham, J. C., Wilkinson, R. S. and Sanes, J. R.** (1997) Skeletal and cardiac myopathies in mice lacking utrophin and dystrophin: A model for Duchenne muscular dystrophy. *Cell* 90, 729-738
- Grozdanovic, Z., Gosztanyi, G. and Gossrau, R.** (1996) Nitric oxide synthase I (NOS-I) is deficient in the sarcolemma of striated muscle fibers in patients with Duchenne muscular dystrophy, suggesting an association with dystrophin. *Acta Histochem.* 98, 61-9
- Hall, A.** (1998) RhoGTPases and the actin cytoskeleton. *Science* 279, 509-512
- Haynes, B.F., Liao, H. X. and Patton, K. L.** (1991) The transmembrane hyaluronate receptor (CD44): multiple functions, multiple forms. *Cancer Cells* 3, 347
- Harder, T. and Simons, K.** (1997) Caveolae, DIGs, and the dynamics of sphingolipid-cholesterol microdomains. *Curr. Opin. Cell Biol.* 9, 534-549
- Hart, M. J., Eva, A., Evans, T., Aaronson, S. A. and Cerione, R. A.** (1991) Catalysis of guanine nucleotide exchange on the CDC42Hs protein by the dbl oncogene product. *Nature* 354, 311-4
- Hayashi, Y. K., Ogawa, M., Tagawa, K., Noguchi, S., Ishihara, T., Nonaka, I., and Arahata, K.** (2001) Selective deficiency of alpha-dystroglycan in Fukuyama-type congenital muscular dystrophy. *Neurology* 57, 115-121
- Heiska, I., Alfthan, K., Gronholm, M., Vilja, P., Vaheri, A. and Carpen, O.** (1998) Association of ezrin with intercellular adhesion molecule-1 and -2 (ICAM-1 and ICAM-2). Regulation by phosphatidylinositol 4, 5-bisphosphate. *J Biol Chem* 273, 21893-900



- Helbling-Leclerc, A., Zhang, X., Topaloglu, H., Cruaud, C., Tesson, F., Weissenbach, J., Tome, F. M., Schwartz, K., Fardeau, M. and Tryggvason, K.** (1995) Mutations in the laminin alpha 2-chain gene (LAMA2) cause merosin-deficient congenital muscular dystrophy. *Nat Genet.* 11, 216-8
- Henry, M. D. and Campbell, K. P.** (1996) Dystroglycan: An extracellular matrix receptor link to the cytoskeleton. *Curr. Opin. Cell Biol.* 8, 625-631
- Henry, M. D. and Campbell, K. P.** (1998) A role for dystroglycan in basement membrane assembly. *Cell* 95, 859-70.
- Herskowitz, I.** (1995) MAP kinase pathway in yeast: for mating and more. *Cell* 80, 187-197
- Higgs, H. N. and Pollard, T. D.** (2001). Regulation of actin filament network formation through the ARP2/3 complex: activation by a diverse array of proteins. *Annu. Rev. Biochem.* 70, 649-676
- Ho, H. Y., Rohatgi, R., Ma, L. and Kirschner, M. W.** (2001). CR16 forms a complex with N-WASP in brain and is a novel member of a conserved proline-rich actin-binding protein family. *Proc. Natl. Acad. Sci. USA.* 98, 11306-11311
- Hoch, W.** (1999) Formation of the neuromuscular junction – Agrin and its unusual receptors. *Eur. J. Biochem* 265, 1-10
- Hoffman, E. P., Hudecki, M. S., Rosenberg, P. A., Pollina, C. M. and Kunkel, L. M.** (1988) Cell and fiber-type distribution of dystrophin. *Neuron* 1, 411-420
- Hoffman, G. R. and Cerione, R. A.** (2001) Rac inserts its way into the immune response. *Nat Immunol* 2, 194-6
- Hoffman, G.R. and Cerione, R. A.** (2002) Signaling to the Rho GTPases: networking with the DH domain. *FEBS Lett.* 513, 85-91
- Holt, K. H., Crosbie, R. H., Venzke, D. P. and Campbell, K. P.** (2000) Biosynthesis of dystroglycan: processing of precursor propeptides. *FEBS Lett.* 468, 79-83
- Howe, A. K. and Juliano, R. L.** (1998) Distinct mechanisms mediate the initial and sustained phases of integrin-mediated activation of the Raf/MEK/mitogen-activated protein kinase cascade. *J. Biol. Chem.* 273, 27268

- Howe, A. K., Aplin, A. E., Alahari, S. K. and Juliano, R. L.** (1998) Integrin signalling and cell growth control. *Curr. Opin. Cell Biol.* 10, 220-231
- Huang, X., Poy, F., Zhang, R., Joachimiak, A., Sudol, M. and Eck, M. J.** (2000) Structure of WW domain containing fragment of dystrophin in complex with  $\beta$ -dystroglycan. *Nat. Structural Biol.* 8, 634-638
- Hughes, P. E., Renshaw, M. W., Plaff, M., Forsyth, J., Keivens, V. M., Schwartz, M. A. and Ginsberg, M. H.** (1997) Suppression of integrin activation: a novel function of Ras/Raf-initiated MAP kinase pathway. *Cell* 88, 521-530
- Hunter, T.** (1995) Protein kinase and phosphatase: the Yin and Yang of protein phosphorylation and signalling *Cell* 80:225
- Hynes, R. O.** (1992) Integrins: Versatility, modulation and signalling in cell adhesion. *Cell* 69, 11-25
- Ibraghimov-Beskrovnaya, O., Ervasti, J. M., Leveille, C. J., Slaughter, C. A., Sernett, S. W. and Campbell, K. P.** (1992) Primary structure of dystrophin associated glycoproteins linking dystrophin to the extracellular matrix. *Nature* 355, 696-702
- Ibraghimov-Beskrovnaya, O., Milatovich, A., Ozcelik, T., Yang, B., Koepnick, K., Francke, U. and Campbell, K. P.** (1993) Human dystroglycan: skeletal muscle cDNA, genomic structure, origin of tissue specific isoform and chromosomal localization. *Hum. Mol. Genet.* 2, 1651-1657
- Isley, J. L.** (2001) Identification of the dystrophin-associated protein complex (DAPC) regulated by phosphorylation. PhD Thesis, University of Edinburgh pp 268
- Isley, J. L., Sudol, M. and Winder, S. J.** (2001) The interaction of dystrophin with  $\beta$  dystroglycan is regulated by tyrosine phosphorylation. *Cellular Signalling* 13, 625-632
- Isley J.L., Sudol, M. and Winder, S. J.** (2002) The WW domain: linking cell signalling to the membrane cytoskeleton. *Cell Signal.* 14,183-9.
- Inzzo, R. V.** (1998) Matrix proteoglycans: from molecular design to cellular function. *Annu. Rev. Biochem.* 67, 609-652
- Ivetic, A., Deka, J., Ridley, A. and Ager, A.** (2002) The cytoplasmic tail of L-selectin interacts with members of the Ezrin-Radixin-Moesin (ERM) family of proteins: cell activation-dependent

binding of Moesin but not Ezrin. *J Biol Chem.* 277, 2321-9

**James, M., Man, N. T., Wise, C. J., Jones, G. E. and Morris, G. E.** (1996) Utrophin-dystroglycan complex in membrane of adherent culture cells. *Cell motility and the cytoskeleton* 33, 163-174

**James M. Ervasti, A. L. Burwell, and Geissler, A. L.** (1997) Tissue-specific Heterogeneity in  $\alpha$ -dystroglycan sialoglycosylation. Skeletal muscle  $\alpha$ -dystroglycan is a latent receptor for villosa agglutinin B4 masked by sialic acid modification. *J. Biol. Chem.* 272 22315-22321

**James, M., Nuttall, A., Ilsley, J. L., Ottersbach, K., Tinsley, J. M., Sudol, M. and Winder, S. J.** (2000) Adhesion dependent tyrosine phosphorylation of  $\beta$ -dystroglycan regulates its interaction with utrophin. *J. Cell Sci.* 113, 1717-1726

**Jockusch, B. M., Bubeck, P., Giehl, K., Kroemker, M., Moschner, J., Rothkegel, M., Rudiger, M., Schluter, K., Stanke, G. and Winkler, J.** (1995) The molecular architecture of focal adhesions. *Annu Rev Cell Dev Biol.* 11, 379-416.

**Johnson, D. I. and Pringle, J. R.** (1990) Molecular characterization of CDC42, a *Saccharomyces cerevisiae* gene involved in the development of cell polarity. *J Cell Biol* 111, 143-150

**Juliano, R. L.** (2002) Signal transduction by cell adhesion receptors and the cytoskeleton: functions of integrins, cadherins, selectins, and immunoglobulin-superfamily members. *Annu Rev Pharmacol Toxicol.* 42, 283-323

**Jung, D., Yang, B., Meyer, J., Chamberlain, J. S. and Campbell, K. P.** (1995) Identification and characterisation of the dystrophin anchoring site on  $\beta$ -dystroglycan. *J. Biol. Chem.* 270, 27305-27310

**Kadoya, Y., Kadoya, K., Durbcej, M., Holmvall, K., Sorokin, I. and Ekblom, P.** (1995) Antibodies against domain E3 of laminin-1 chain integrin  $\alpha 6$  subunit perturb branching morphogenesis of submandibular gland, but by different modes. *J. Cell Biol.* 129, 521-534

**Kano, H., Kobayashi, K., Herrmann, R., Tachikawa, M., Manya, H., Nishino, I., Nonaka, I., Straub, V., Talim, B., Voit, T., Topaloglu, H., Endo, T., Yoshikawa, H. and Toda, T.** (2002) Deficiency of alpha-dystroglycan in muscle-eye-brain disease. *Biochem Biophys Res Commun.* 291, 1283-6

- Kimura, K., Ito, M., Amano, M., Chihara, K., Fukata, Y., Nakafuku, M., Yamamori, B., Feng, J., Nakano, T., Okawa, K., Iwamatsu, A. and Kaibuchi, K.** (1996) Regulation of myosin phosphatase by Rho and Rho-associated kinase (Rho-kinase). *Science* 273, 245-8.
- Klemke, R. L., Yebra, M., Bayna, E. M., and Cheresch, D. A.** (1994) Receptor tyrosine kinase signalling are required for integrin  $\alpha\beta 5$ -directed cell motility but not cell adhesion on vitronectin. *J. Cell Biol.* 127, 859-866
- Klemke, R. L., Cai, S., Giannini, A. L., Gallagher, P. J., de Lanerolle, P. and Cheresch, D. A.** (1997) Regulation of cell motility by mitogen-activated protein kinase. *J. Cell Biol.* 137, 481-492
- Kondo-Iida, E., Kobayashi, K., Watanabe, M., Sasaki, J., Kumagai, T., Koide, H., Saito, K., Osawa, M., Nakamura, Y. and Toda, T.** (1999) Novel mutations and genotype-phenotype relationships in 107 families with Fukuyama-type congenital muscular dystrophy (FCMD). *Hum Mol Genet.* 8, 2303-9
- Kozma, R., Ahmed, S., Best, A. and Lim, L.** (1995) The ras related protein Cdc42Hs and bradykinin promote formation of peripheral actin microspikes and filopodia in swiss 3T3 fibroblasts. *Mol. Cell. Biol.* 15, 1992
- Kranewitter, W. J., Danminger, C. and Gimona, M.** (2001) GEF at work: Vav in protruding filopodia. *Cell Motil. Cytoskeleton.* 49, 154-160
- Krugmann S, Jordens, I., Gevaert, K., Driessens, M., Vandekerckhove, J. and Hall, A.** (2001) Cdc42 induces filopodia by promoting the formation of an IRSp53: Mena complex. *Curr Biol.* 11, 1645-55
- Kureishy, N., Sapountzi, V., Prag, S., Anilkumar, N. and Adams, J. C.** (2002) Fascins, and their roles in cell structure and function. *Bioessays.* 24, 350-361
- Lanier, L. M., Gates, M. A., Witke, W., Menzies, A. S., Wehman, A. M., Macklis, J. D., Kwiatkowski, D., Soriano, P. and Gertler, F. B.** (1999) Mena is required for neurulation and commissure formation. *Neuron.* 22, 313-325
- Leavesley, D. I., Schwart, M. A., Rosefeld, M. and Cheresch, D. A.** (1993) Integrin  $\beta 1$  and  $\beta 3$  mediated endothelial cell migration is triggered through distinct signalling mechanisms. *J. Cell Biol.* 121, 163-170

- Legg, J. W. and Isacke, C. M.** (1998) Identification and functional analysis of the ezrin-binding site in the hyaluronan receptor, CD44. *Curr. Biol.* 8, 705-8
- Legg, J. W., Lewis, C. A., Parsons, M., Ng, T. and Isacke, C. M.** (2002) A novel PKC-regulated mechanism controls CD44 ezrin association and directional cell motility. *Nat Cell Biol.* 4, 399-407.
- Lemmon, M. A. and Ferguson, K. M** (2002) Signal-dependent membrane targeting by pleckstrin homology (PH) domains. *Biochem. J.* 350, 1-18
- Lewis, A. K., and Bridgman, P. C.** (1992) Nerve growth cone lamellipodia contain two populations of actin filaments that differ in organization and polarity. *J. Cell Biol.* 119, 1219-1243.
- Lewis, J. M., Baskaran, R., Taagepera, S., Schwartz, M. A. and Wang, Y. J.** (1996) *Proc. Natl. Acad. Sci. U.S.A.* 93, 15174
- Leung, T., Manser, E., Tan, L. and Lim, L.** (1995) A novel serine/threonine kinase binding the Ras-related RhoA GTPase which translocates the kinase to peripheral membranes. *J Biol Chem.* 270, 29051-4.
- Lim, W. A., Richards, F. M. and Fox, R. O.** (1994) Structure determination of peptide-binding orientation and sequence specificity in SH3 domains. *Nature* 372, 375-379
- Liu, B. P., and Burridge, K.** (2000) Vav2 activates Rac1, Cdc42 and RhoA downstream from growth factor receptors but not b1 integrins. *Mol. Cell. Biol.* 20, 7160-7169
- Louvet-Vallee, S.** (2000) ERM proteins: from cellular architecture to cell signaling. *Biol Cell* 92, 305-16
- Love, D. R., Hill, D. F., Dickson, G., Spurr, N. K., Byth, B. C., Marsden, R. F., Walsh, F. S., Edwards, Y. H. and Davies, K. E.** An autosomal transcript in skeletal muscle with homology to dystrophin. (1989) *Nature* 339, 28-30
- Luo L., Liao, Y. J., Jan, L. Y. and Jan, Y. N.** (1994) Distinct morphogenetic functions of similar small GTPases. *Genes Dev.* 8, 1787

- Mackay, D. J., Esch, F., Furthmayr, H. and Hall, A.** (1997) Rho- and rac-dependent assembly of focal adhesion complexes and actin filaments in permeabilized fibroblasts: an essential role for ezrin/radixin/moesin proteins. *J Cell Biol.* 138, 927-38
- Machesky L. M. and Insall, R. H.** (1998) Scar1 and the related Wiskott-Aldrich syndrome protein, WASP, regulate the actin cytoskeleton through the Arp2/3 complex. *Curr. Biol.* 8, 1347-56
- Machesky, L. M., Reeves, E., Wientjes, F., Mattheyse, F. J., Grogan, A., Totty, N. F., Burlingame, A. L., Hsuan, J. J. and Segal, A. W.** (1996) Mammalian actin-related protein 2/3 complex localizes to regions of lamellipodial protrusion and is composed of evolutionarily conserved proteins. *Biochem J.* 15, 105-12
- Mainiero, F., Murgia, C., Wary, K. K., Curatola, A. M., Pepe, A., Blunenberg, M., Westwick, J. K., Der, C. J. and Giancotti, F. G.** (1997) The coupling of alpha6beta4 integrin to Ras-MAP kinase pathways mediated by Shc controls keratinocyte proliferation. *EMBO J.* 16, 2365
- Mastumura, K., Ervasti, J. M. and Ohlendieck, K.** (1992) Association of dystrophin-related protein with dystrophin-associated protein in *mdx* mouse muscle. *Nature* 36, 588-591  
*J Cell Biol.* 140, 647-57
- Mastumura, K., Yamada, H., Fujita, S., Fukuta-Ohi, H., Tanaka, T., Campbell, K. P. and Simizu, T.** (1997) Peripheral nerve dystroglycans. Its function and potential role in the molecular pathogenesis of neuromuscular disease. *Congenital Muscular Dystrophies.* pp 267-273
- Matsui, T., Maeda, M., Doi, Y., Yonemura, S., Amano, M., Kaibuchi, K., Tsukita, S. and Tsukita, S.** (1998) Rho-kinase phosphorylates COOH-terminal threonines of ezrin/ radixin/ moesin (ERM) proteins and regulates their head-to-tail association. *J Cell Biol.* 140, 647-57
- Matsui, T., Yonemura, S., Tsukita, S. and Tsukita, S.** (1999) Activation of ERM proteins in vivo by Rho involves phosphatidylinositol 4-phosphate 5-kinase and not ROCK kinases. *Curr. Biol.* 9, 1259-62
- McNally, E. M., de Sa Moreira, E., Duggan, D. J., Bonnemann, C. G., Lisanti, M. P., Lidov, H. G., Vainzof, M., Passos-Bueno, M. R., Hoffman, E. P., Zatz, M. and Kunkel, L. M.** (1998) Caveolin-3 in muscular dystrophy. *Hum Mol Genet.* 7, 871-7

- Meier, T. and Rugg M.A.** (2000) The Role of Dystroglycan and Its Ligands in Physiology and Disease. *News Physiol Sci.* 15:255-259.
- Menke, A. and Jockusch, H.** (1991) Decrease osmotic stability of dystrophin-less muscle cells from *mdx* mouse. *Nature* 349, 69-71
- Michele, D. E. and Campbell, K. P.** (2003) Dystrophin-glycoprotein complex: post-translational processing and dystroglycan function. *Biol. Chem.* 278, 15457-15460
- Michele, D. E., Barresi, R., Kanagawa, M., Saito, F., Cohn, R. D., Satz, J. S., Dollar, J., Nishino, I., Kelley, R. L., Somer, H., Straub, V., Mathews, K. D., Moore, S. A., and Campbell, K. P.** (2002) Post-translational disruption of dystroglycan-ligand interactions in congenital muscular dystrophies. *Nature* 418, 417-421
- Miki, H., Miura, K. and Takenawa, T.** (1996) N-WASP, a novel actin-depolymerizing protein, regulates the cortical cytoskeletal rearrangement in a PIP2-dependent manner downstream of tyrosine kinases. *EMBO J.* 15, 5326-35.
- Miner, J. H., Cunningham, J. and Sanes, J. R.** (1998) Roles for laminin in embryogenesis: exencephaly, syndactyly, and placentopathy in mice lacking the laminin alpha5 chain. *J. Cell Biol.* 143,1713-1723.
- Miranti, C. K., Leng, L., Maschberger, P., Brugge, J. S. and Shattil, S. J.** (1998) Identification of a novel integrin signaling pathway involving the kinase Syk and the guanine nucleotide exchange factor Vav1. *Curr. Biol.* 8, 1289-1299.
- Miyamoto, S., Teramoto, H., Coso, O. A., Gutkind, J. S., Burbelo, P. D., Akiyama and Yamada, K. M.** (1995) Integrin function: Molecular hierarchies of cytoskeletal and signalling molecules. *J. Cell Biol.* 131, 791-805
- Moore, S., Selfors, L., Fredericks, J., Breit, T., Fujikawa, K., Alt, F., Brugge, J. and Swat, W.** (2000) Vav family proteins couple to diverse cell surface receptors. *Mol. Cell. Biol.* 20, 6364-6373.
- Morino, N., Mimura, T., Hamasaki, K., Tube, K., Ueki, K., Kikuchi, K., Takehara, K., Kadowaki, T., Yazaki Y. and Nojima, Y.** (1995) Matrix/ Integrin interaction activates the mitogen- activated protein kinase, P44 ERK1 and P42 ERK2. *J. Biol. Chem.* 270, 296-273

- Mullins R. D., Heuser, J. A. and Pollard, T. D.** (1998) The interaction of Arp2/3 complex with actin: nucleation, high affinity pointed end capping, and formation of branching networks of filaments. *Proc Natl Acad Sci U S A* 95: 6181-6
- Nigro, V., de Sa Moreira, E., Piluso, G., Vainzoli, M., Belsito, A., Politano, L., Puca, A. A., Passos-Bueno, M.R. and Zatz, M.** (1996) Autosomal recessive limb-girdle muscular dystrophy, LGMD2F, is caused by a mutation in the delta-sarcoglycan gene. *Nat Genet.* 14, 195-8.
- Nashida, E. and Gotoh, Y.** (1993) The MAP kinase cascade is essential for diverse diverse signal transduction pathways. *Trends. Biochem Sci.* 18, 128-130
- Ng, T., Parsons, M., Hughes, W.E., Monypenny, J., Zicha, D., Gautreau, A., Arpin, M., Gschmeissner, S., Verveer, P. J., Bastiaens, P. I. and Parker, P. J.** (2001) Ezrin is a downstream effector of trafficking PKC-integrin complexes involved in the control of cell motility. *EMBO J.* 20, 2723-41
- Nobes, C. D. and Hall, A.** (1994) Regulation and function of the Rho subfamily of small GTPases. *Curr. Opin. Genet. Dev.* 4, 77
- O'Connor, K., Ngynen, B. and Mercurio, A.** (2000) RhoA function in lamellae formation and migration is regulated by the  $\alpha 6 \beta 4$  integrin and cAMP metabolism. *J. Cell Biol.* 148, 253-258.
- Pandey, A., Podtelejnikov, A., Blagoev, B., Bustelo, X., Mann, M. and Lodish, H.** (2000) Analysis of receptor signaling pathways by mass spectrometry: Identification of Vav-2 as a substrate of the epidermal and platelet-derived growth factor receptors. *Proc. Natl. Acad. Sci. USA* 97, 179-184
- Pawson, T. and Scott, J. D.** (1997) Signalling through scaffold anchoring and adaptor proteins. *Science* 278, 2075
- Pearson, M. A., Reczek, D., Bretscher, A. and Karplus, P. A.** (2000) Structure of the ERM protein moesin reveals the FERM domain fold masked by an extended actin binding tail domain. *Cell.* 101, 259-70
- Pearson, G., Robinson, F., Gibson, T. B., Xu, B-E, Karadikar, M. and Cobb, M. H.** (2001) Mitogen-Activated Protein (MAP) Kinase Pathways: Regulation and Physiological Function. *Endocr. Rev.* 22, 153-183



- Pietromonaco, S. F., Simons, P. C., Altman, A. and Elias, L.** (1998) Protein kinase C-theta phosphorylation of moesin in the actin-binding sequence. *J Biol Chem* 273, 7594-603
- Pollard, T.D., Blanchoin, L. and Mullins, R. D.** (2000) Molecular mechanisms controlling actin filament dynamics in nonmuscle cells. *Annu. Rev. Biophys. Biomol. Struct.* 29, 545-576
- Pouyssegur, J., Volmat, V. and Lenormand, P.** (2002) Fidelity and spatio-temporal control in MAP kinase (ERKs) signalling. *Biochem Pharmacol.* 64, 755-63
- Pozzi, A., Wary, K. K., Giancotti, F. G. and Gardner, H. A.** (1998) Integrin alphabeta1 mediates a unique collagen-dependent proliferation pathway in vivo. *J. Cell Biol.* 142, 587-598
- Price L.S, Leng, J., Schwartz, M. A. and Bokoch, G. M.** (1998) Activation of Rac and Cdc42 by integrins mediates cell spreading. *Mol Biol Cell* 9, 1863-71
- Pryciak, P. M.** (2001) MAP kinases bite back. *Dev Cell* 1, 449-51
- Qualmann, B. and Kelly, R. B.** (2000) Syndapin isoforms participate in receptor mediated endocytosis and actin organization. *J. Cell Biol.* 148, 1047-1062
- Rambukkana, A, Yamada, H., Zanazzi, G., Mathus, T., Salzer, J.L., Yurchenco, P.D., Campbell, K.P. and Fischetti, V. A.** (1998) Role of  $\alpha$ -dystroglycan as a Schwann cell receptor for *Mycobacterium leprae*. *Science* 282, 2076-2079
- Ren, X., Kiosses, W. and Schwartz, M.** (1999) Regulation of the small GTP-binding protein Rho by cell adhesion and the cytoskeleton. *EMBO J.* 18, 578-585
- Renshaw, M. W., Ren, X and Schwartz, M.A.** (1997) Growth factor activation of MAP kinase requires cell adhesion. *EMBO J.* 16, 5592-5599
- Rentschler, S., Linn, H., Deininger, K., Bedford, M. T., Expanel, X. and Sudol, M.** (1999) The WW domain of dystrophin required EF-hands region to interact with  $\beta$ -dystroglycan. *J. Biol. Chem.* 380, 431-422
- Richardson, A. and Parsons, J. T.** (1996) A mechanism for regulation of the adhesion-associated proteintyrosine kinase pp125FAK. *Nature.* 380, 538-40
- Ridley, A. J.** (2001) Rho family proteins: coordinating cell responses. *Trends Cell Biol.* 11, 471-7

- Ridley, A. L. and Hall, A.** (1992) The small GTP binding protein Rho regulates the assembly of focal adhesions and actin stress fibers in response to growth factors. *Cell* 70, 389
- Ridley, A. L., Peterson, H. F., Johnston, C. L., Diekmann, D. and Hall, A.** (1992) The small GTP-binding protein Rac regulates growth factor-induced membrane ruffling. *Cell* 70, 401
- Roberds, S. L., Ervasti, J. M., Anderson, R. D., Ohlendieck, K., Kahl, S. D., Zoloto, D. and Campbell, K. P.** (1993) Distribution of dystroglycan-glycoprotein complex in the cardiomyopathic hamster. *J. Biol. Chem.* 268, 11496-11499
- Robinsin, M. J., Stippec, S.A., Goldsmith, E., White, M. A. and Cobb, M. H.** (1998) A constitutively active and nuclear form of MAP kinase ERK2 is sufficient for neurite outgrowth and cell transformation. *Curr. Biol.* 8: 1141-1150
- Rohatgi, R., Ma, L., Miki, H., Lopez, M., Kirchhausen, T., Takenawa, T. and Kirschner, M. W.** (1999) The interaction between N-WASP and the Arp2/3 complex links Cdc42-dependent signals to actin assembly. *Cell.* 97, 221-231
- Ruegg, M. A. and Bixby, J. L.** (1997) Agrin orchestrates synaptic differentiation at three vertebrate neuromuscular junction. *Trends. Neurosci.* 21, 22-27
- Ruoslahti, E. and Reed, J. C.** (1994) Anchorage dependence, integrins, and apoptosis. *Cell* 77, 477-8
- Russo, K., Staio, E. D., Macchia, G. Rosa, G. Brancaccio, A. and Petrucci, T. C.** (2000) Characterization of  $\beta$  dystroglycan -Growth factor receptor 2 (Grb2) interaction. *Biochem. Biophys. Res. Comm.* 274, 93-98
- Ruoslahti, E.** (1991) Integrin. *J. Clin Invest.* 87, 1-5
- Ruoslahti, E.** (1996) RGD and other recognition sequences for integrins. *Annu. Rev. Cell Dev. Biol.* 12, 697-715
- Sadoullet-Puccio, H. M. and Kunkel, L. M.** (1996) Dystrophin and its isoforms. *Brain Patholog* 6, 25-35

**Sanders, L. C., Matsumura, F., Bokoch, G. M., de Lancrolle, P.** (1999) Inhibition of myosin light chain kinase by p21-activated kinase. *Science* 283, 2083-5

**Santavuori, P., Somer, H., Sainio, K., Rapola, J., Kruus, S., Nikitin, T., Ketonen, L. and Leisti, J.** (1989) Muscle-eye-brain disease (MEB) *Brain Dev.* 11, 147-53.

**Schaeffer, H. J., Catling, A.D., Eblen, S.T., Collier, L.S., Krauss, A., Weber, M. J.** (1998) MP1: a MEK binding partner that enhances enzymatic activation of the MAP kinase cascade. *Science.* 281, 1668-71

**Schaller, M. D.** (2001) Biochemical signals and biological responses elicited by the focal adhesion kinase. *Biochim Biophys Acta.* 1540, 1-21

**Schaller, M. D., Hildebrand, J. D., Shannon, J. D., Fox, J. W., Vines, R. R. and Parsons, J. T.** (1994) Autophosphorylation of the focal adhesion kinase, pp125FAK, directs SH2-dependent binding of pp60src. *Mol. Cell. Biol.* 14, 1680

**Schlaepfer, D. D., Hanks, S. K., Hunter, T., van der Geer, P.** (1994) Integrin-mediated signal transduction linked to Ras pathway by GRB2 binding to focal adhesion kinase. *Nature* 372, 786

**Schlaepfer, D. D., Broome, M. A. and Hunter, T.** (1997) Fibronectin-stimulated signaling from a focal adhesion kinase-c-Src complex: involvement of the Grb2, p130cas, and Nck adaptor proteins. *Mol. Cell. Biol.* 17, 1702

**Schlegel, A. and Lisanti, M. P.** (1997) Dissecting the interaction between nitric oxide synthase (NOS) and caveolin. Functional significance of the NOS caveolin binding domain in vivo. *J. Biol. Chem.* 272, 25437-40

**Schoenwaelder, S. M. and Burridge, K.** (1999) Bidirectional signalling between the cytoskeleton and integrins. *Curr. Opin Cell. Biol.* 11, 274-286

**Schofield, J. N., Gorecki, D. C., Blake, D. J., Davies, K. and Edward, Y. H.** (1995) Dystroglycan mRNA expression during normal and mdx mouse embryogenesis: a comparison with utrophin and the apo-dystrophin. *Dev. Dyn.* 204, 178-185

**Schubel, K., Movilla, N., Rosa, J. and Bustelo, X.** (1998) Phosphorylation-dependent and constitutive activation of Rho proteins by wild-type and oncogenic Vav-2. *EMBO J.* 16, 6608-6621

- Schwartz, M. A.** (1997) Integrin, oncogenes and anchorage independence. *J. Cell. Biol.* 139, 575-578
- Schwartz, M and Shattil, S.** (2000). Signaling networks linking integrins and Rho family GTPases. *Trends Biochem. Sci.* 25, 388-391.
- Shaw, R. J., Henry, M., Solomon, F. and Jacks, T.** (1998) RhoA-dependent phosphorylation and relocalization of ERM proteins into apical membrane/actin protrusions in fibroblasts. *Mol Biol Cell.* 9, 403-19
- Sherman, D. L., Fabrizi, C., Gillespie, C. S. and Brophy, P. J.** (2001) Specific disruption of a Schwann cell dystrophin-related protein complex in a demyelinating neuropathy. *Neuron* 30, 677-87
- Sicinski, P., Geng, Y., Ryder-Cook, A. S., Barnard, E. A., Darlison, M. G. and Barnard, P. J.** (1989) The molecular basis of muscular dystrophy in the *mdx* mouse: a point mutation. *Science.* 244, 1578-80
- Small, J. V.** (1988) The actin cytoskeleton. *Electron Microsc. Rev.* 1, 155-174
- Small, J. V., Stradal, T., Vignat, E. and Rottner, K.** (2002) The lamellipodium: where motility begins. *Trends Cell Biol.* 12, 112-120
- Sorokin, L. M., Conzelmann, S., Ekblom, P., Battaglia, C., Aumailley, M. and Timpl, R.** (1992) Monoclonal antibodies against laminin A chain fragment E3 and their effects on binding to cells and proteoglycan and on kidney development. *Exp. Cell Res.* 210, 521-543
- Sotgia F, Lee, J. K., Das, K., Bedford, M., Petrucci, T. C., Macioce, P., Sargiacomo, M., Bricarelli, F. D., Minetti, C., Sudol, M. and Lisanti, M. P.** (2000) Caveolin-3 directly interacts with the C-terminal tail of beta -dystroglycan. identification of a central WW-like domain within caveolin family members. *J Biol Chem.* 275, 38048-58
- Sotgia, F., Lee, II., Bedford, M. T., Petrucci, T., Sudol, M. and Lisanti, M. P.** (2001) Tyrosine phosphorylation of beta-dystroglycan at its WW domain binding motif, PPxY, recruits SH2 domain containing proteins. *Biochemistry* 40, 14585-92
- Sotgia, F., Bonuccelli, G., Bedford, M., Brancaccio, A., Mayer, U., Wilson, M.T., Campos-Gonzalez, R., Brooks, J. W., Sudol, M. and Lisanti, M. P.** (2003) Localization of phospho-beta-dystroglycan (pY892) to an intracellular vesicular compartment in cultured cells and skeletal

muscle fibers in vivo. *Biochemistry* 42, 7110-23

**Spence, H. J., Chen, Y-J and Winder, S. J.** (2002) Muscular dystrophies, the cytoskeleton and cell adhesion *BioEssays* 24, 542-55

**Spence, H. J., James, M. and Winder, S. J.** (2003a) Dystroglycan, a scaffold for ERK MAP kinase cascade. *EMBO Reports* (submitted).

**Spence, H. J., Chen, Y-J., Suila, H., Carpon, O. and Winder, S. J.** (2003b) Ezrin-dependent regulation of the actin cytoskeleton by  $\beta$ -dystroglycan. *J. Cell Sci.* (in preparation)

**Stoker, M. and Gherardi, E.** (1991). Regulation of cell movement: the motogenic cytokines. *Biochim Biophys Acta.* 1072, 81-102

**Stradal, T., Courtney, K. D. Rottner, K. Habne, P. Small, J. V. and Pendergast. A. M.** (2001). The Abl interactor proteins localize to sites of actin polymerization at the tips of lamellipodia and filopodia. *Curr. Biol.* 11, 891-895

**Sudol, M.** (1996) The WW module competes with the SH3 domain? *Trends Biochem Sci.* 21, 161-163

**Sugiyama, J., Brown, D. U. and Hall, Z. W.** (1994) Dystroglycan binds nerve and muscle cell. *Neuron* 13, 103-115

**Suzuki, A., Yoshida, M., Hayashi, K., Mizuno, Y. and Ozawa, E.** (1994) Molecular organisation at the glycoprotein-complex binding site of utrophin: three utrophin associated proteins bind directly to the carboxyl terminal portion of dystrophin. *Eur. J. Biochem.* 220, 283-292

**Svitkina, T. M. and Borisy, G. G.** (1999) Arp2/3 complex and actin depolymerizing factor/cofilin in dendritic organization and treadmilling of actin filament array in lamellipodia. *J. Cell Biol.* 145, 1009-1026

**Svitkina, T.M., Verkhovsky, A.B., McQuade, K.M. and Borisy, G.G.** (1997) Analysis of the actin-myosin II system in fish epidermal keratocytes: mechanism of cell body translocation. *J. Cell Biol.* 139, 397-415

**Svitkina, T. M., Bulanova, E. A., Chaga, O. Y., Vignjevic, D. M., Kojima, S-I., Vasilieva, J. M. and Borisy, G. G.** (2003) Mechanism of filopodia initiation by reorganization of a dendritic

network. *J. Cell. Biol.* 160, 409-421

**Symons, M., Derry, J. M., Karlak, B., Jiang, S., Lemahieu, V., McCormick, F., Francke, U. and Abo, A.** (1996) Wiskott-Aldrich syndrome protein, a novel effector for the GTPase CDC42Hs, is implicated in actin polymerization. *Cell*. 84, 723-34

**Takahashi, K., Sasaki, T. Mamoto, A. Takaiashi, K. Kameyama, T. Tsukita, Sa., Tsukita, Sh. and Takia, Y.** (1997). Direct association of the Rho-GDP disassociation inhibitors with ezrin/ radixin/ moesin initiates the activation of the Rho small G proteins. *J. Biol. Chem* 272, 23371-5

**Takenawa, T. and Miki, H.** (2001) WASP and WAVE family proteins: key molecules for rapid rearrangement of cortical actin filaments and cell movement. *J. Cell Sci.* 114, 1801-9.

**Takai, Y., Sasaki, T., Tanaka, K. and Nakanishi, H.** (1995) Rho as a regulator of the cytoskeleton. *Trends Biochem Sci.* 20, 227

**Tian, M., Jacobsen, C., Gee, S. H., Campbell, K. P. Carbonetto, S. and Jucker, M.** (1996) Dystroglycan in the cerebellum is a laminin  $\alpha 2$  chain binding protein at the glial-vascular interface and is expressed in Purkinje cells. *Eur. Neurosci.* 8, 2739-2747

**Therrien, M., Michaud, N. R., Rubin, G. M., Morrison, D. K.** (1996) KSR modulates signal propagation within the MAPK cascade. *Genes Dev.* 10, 2684-95

**Tisi, D., Talts, J.F., Timpl, R. and Hohenester, E.** (2000) Structure of laminin G-like domain pair of laminin  $\alpha$ -2 chain harboring binding site for  $\alpha$  dystroglycan and heparin. *EMBO J.* 19, 1432-1440

**Tsukita, S. and Yonemura, S.** (1995) Cortical actin organization: lessons from ERM (ezrin/radixin/moesin) proteins. *J. Biol. Chem.* 274, 34507-10

**Turner, C. E.** (2000) Paxillin and focal adhesion signalling. *Nat. Cell Biol.* 2, E231-E236

**Van Aelst, L. and Sousa-Schorey, C. D** (1997). Rho GTPases and signaling networks. *Genes Dev.* 11, 2295-2322

**Vuori, K., Hirai, H., Aizawa, S. and Ruoslahti, E.** (1996) Introduction of p130CAS signaling complex formation upon integrin-mediated cell adhesion: a role for Src family kinases. *Mol. Cell. Biol.* 16, 2606

- Walter, K.** (2000) Meaningful relationships: the regulation of the Ras, Raf/MEK/ERK pathway by protein interactions. *Biochem J.* 351, 289-305
- Wary, K. K., Mainiero, F., Isakoff, S. J., Marcantonio, E. E. and Giancotti, F. G.** (1996) The adaptor protein Shc couples a class of integrins to the control of cell cycle progression. *Cell* 87, 733-745
- Wary K. K., Mariotti, A., Zurzolo, C. and Giancotti, F. G.** (1998) A requirement for caveolin-1 and associated kinase Fyn in integrin signaling and anchorage-dependent cell growth. *Cell.* 94, 625-34
- Wei, Y., Yang, X., Liu, Q., Wilkins, J. A. and Chapman, H. A.** (1999) A role for caveolin and the urokinase receptor in integrin-mediated adhesion and signaling. *J Cell Biol.* 144, 1285-94
- Williamson, R. A., Henry, M. D., Daniels, K. J., Hrstka, R. F., Lee, J.C., Sunada, Y., Ibraghimov-Beskrovnyaya, O. and Campbell, K. P.** (1997) Dystroglycan is essential for early embryonic development: disruption of Reichert's membrane in Dag1-null mice. *Hum. Mol. Genet.* 6, 831-841
- Williamson, R. A., and Campbell, K. P.** (2002) Disruption of DAG1 in differentiated skeletal muscle reveals a role for dystroglycan in muscle regeneration. *Cell* 110, 639
- Winder, S.J., Hemmings, L., Maciver, S.k., Bolton, S.J., Tinsley, J.M., Davids, K.E., Critchley, D.R. and Kendrick-Jones J.** (1995). Utrophin actin binding domain: analysis of actin binding and cellular targeting. *J. Cell. Sci.* 108, 633-71
- Winder, S. J.** (1997) The membrane-cytoskeleton interface: The role of dystrophin and utrophin. *J. Mus. Res. Cell Mot.* 18, 11-13
- Winder, S. J.** (2001) The complexities of dystroglycan. *Trends Biochem Sci.* 26, 118-124
- Xiao, G. H., Beeser, A., Chernoff, J. and Testa, J. R.** (2002) p21-activated kinase links Rac/Cdc42 signaling to merlin. *J. Biol. Chem.* 277, 883-6
- Yamada, H., Simizu, T., Tanaka, T., Campbell, K. P. and Matsumura, K.** (1994) Dystroglycan is a binding protein of laminin and merosin in peripheral nerve. *FEBS Lett.* 352, 49-53

- Yamada, H., Chiba, A., Endo, T., Kobata, A., Anderson, L. V., Hori, H., Fukuta-Ohi, H., Kanazawai, I., Campbell, K. P., Simizu, T. and Matsumura, K.** (1996a) Characterization of dystroglycan-laminin interaction in peripheral nerve. *J. Neurochem.* 66, 1518-1524
- Yamada, H., Denzer, A. J., Hori, H., Anderson, L. V. B., Fujita, S., Fukuta-Ohi, H., Shimizu, T., Ruegg, M. A. and Matsumura, K.** (1996b) Dystroglycan is a dual receptor for agrin and laminin 2 in Schwann's cell membrane. *J. Biol. Chem.* 271, 23418-23423
- Yamakita, Y., Totsukawa, G., Yamashiro, S., Fry, D., Zhang, X., Hanks, S.K., Matsumura, F.** (1999) Dissociation of FAK/p130(CAS)/c-Src complex during mitosis: role of mitosis-specific serine phosphorylation of FAK. *J. Cell Biol.* 144, 315.
- Yang, B., Jung, D., Motto, D., Meryer, J., Koretzky, G. and Campbell, K.P.** (1995) SH3 Domain mediated interaction of dystroglycan and Grb2. *J. Biol. Chem.* 270 11711-11714
- Yang, N., Higuchi, O., Ohashi, K., Nagata, K., Wada, A., Kangawa, K., Nishida, E. and Mizuno, K.** (1998) Cofilin phosphorylation by LIM-kinase 1 and its role in Rac-mediated actin reorganization. *Nature* 393, 809-12
- Yenush, L., Kundra, V., White, M. F. and Zetter, B. R.** (1994) Functional domains of the insulin receptor responsible for chemo-toxic signalling. *J. Biol. Chem.* 269,100-104
- Yonemura, S., Tsukita, S. and Tsukita, S.** (1999) Direct involvement of ezrin/radixin/moesin (ERM)-binding membrane proteins in the organization of microvilli in collaboration with activated ERM proteins. *J. Cell Biol.* 145, 1497-50
- Yoshida, A., Kobayashi, K., Manya, H., Taniguchi, K., Kano, H., Mizuno, M., Inazu, T., Mitsubashi, H., Takahashi, S., Takeuchi, M., Herrmann, R., Straub, V., Talim, B., Voit, T., Topaloglu, H., Toda, T., and Endo, T.** (2001) Muscular dystrophy and neuronal migration disorder caused by mutations in a glycosyltransferase, POMGnT1. *Dev. Cell* 1, 717-724
- Yu, H., Chen, J. K., Feng, S., Dalgarno, D. C., Brauer, A. W., Schreiber, S. L.** (1994) Structure basis for binding of proline-rich peptides to SH3 domains. *Cell* 76, 933-945
- Yu, W., Fantl, W. J., Harrowe, G., Williams, L. T.** (1998) Regulation of the MAP kinase pathway by mammalian Ksr through direct interaction with MEK and ERK. *Curr Biol.* 8, 56-64